

UNIVERSITÉ DE NANTES
UFR SCIENCES ET TECHNIQUES

ÉCOLE DOCTORALE
SCIENCES POUR L'INGÉNIEUR, GÉOSCIENCES, ARCHITECTURE

Année 2010

**Contribution for sustainable management of reinforced
concrete structures subjected to chloride penetration**

THÈSE DE DOCTORAT

Discipline : Sciences de l'Ingénieur

Spécialité : Génie Civil

*Présentée
et soutenue publiquement par*

Emilio BASTIDAS-ARTEAGA

Le 1^{er} septembre 2010, devant le jury ci-dessous :

Rapporteurs : M. Frederic DUPRAT, Maître de Conférences, HDR, INSA de Toulouse
M. Michael H. FABER, Professeur, ETH Zurich

Président : M. Denys BREYSSE, Professeur, Université de Bordeaux

Examinateurs : M. Philippe BRESSOLETTE, Maître de Conférences, Université Blaise Pascal
M. Alaa CHATEAUNEUF, Professeur, Université Blaise Pascal

M. Franck SCHOEFS, Professeur, Université de Nantes

Invités : M. Bruno CAPRA, Docteur, Société OXAND
M. Alan O'CONNOR, Senior Lecturer, Trinity College Dublin

Directeurs de thèse : M. Franck SCHOEFS et M. Alaa CHATEAUNEUF

*A Dieu,
à mes grand-parents Victoria et Ezequiel,
à mes parents María Teresa et Édgar,
à ma famille et à ma chérie Elodie.*

REMERCIEMENTS

D'après le danois Hans Christian Andersen “ *la reconnaissance est la mémoire du cœur* ”. Ainsi, je voudrai exprimer, dans ces lignes, ma profonde gratitude aux personnes dont le soutien et la contribution ont été indispensables pour le bon déroulement de cette étude.

Je tiens d'abord à remercier le professeur Franck Schoefs qui a accepté de diriger cette thèse. Pendant cette période, en plus d'un encadrement scientifique exceptionnel, il m'a encouragé à explorer des différentes pistes qui m'intéressaient et il a veillé à ce que mon travail se déploie dans les meilleures conditions. Il m'a également motivé à participer à ses projets de recherche. Cette participation m'a aidé à bien prendre en main le problème. D'un point de vue personnel, je remercie Franck pour m'avoir guidé et conseillé afin de réussir mon projet professionnel.

Je tiens à exprimer mes sentiments de gratitude au professeur Alaa Chateauneuf qui a également contribué à la direction de cette étude. Sa rigueur scientifique et ses discussions ont été essentielles pour le bon avancement de ma thèse. Sur le plan personnel, je garde un très beau souvenir de son accueil lors de mon arrivé en France et de mon séjour à Clermont-Ferrand.

Je suis très reconnaissant à messieurs Frédéric Duprat et Michael Havbro Faber pour m'avoir fait le grand honneur de rapporter cette thèse. Ses discussions et critiques constructives, basées sur leur expertise et leurs expériences, m'ont permis d'élargir mon éventail de perspectives pour mes futures recherches. Ces discussions ont été enrichies par les commentaires des autres membres du jury messieurs Denys Breysse, Philippe Bressolette, Bruno Capra et Alan O'Connor. Je leur exprime à tous mes très sincères remerciements.

Ces dernières années, j'ai eu la chance de faire des échanges scientifiques et personnels exceptionnels pendant mes passages en Colombie, à Clermont-Ferrand et à Nantes. J'exprime donc ma profonde reconnaissance aux chercheurs qui ont contribué, par ses discussions, à mon travail : Stéphanie Bonnet, Géraldine Vilain, Mauricio Sánchez-Silva, Philippe Bressolette et Abdelhafid Khelidj.

L'ambiance chaleureuse au sein de notre équipe et des projets de recherche m'a servi de grande motivation pour atteindre mes objectifs. Je tiens donc à exprimer ma profonde gratitude à tous les membres de notre équipe et du département de physique pour les discussions, les encouragements, et surtout, pour tous les bons moments que nous avons partagés.

Cette thèse a été cofinancée dans le cadre du projet MAREO et par la société OXAND. Je tiens ainsi à remercier ce soutien financier qui m'a permis d'avancer dans les meilleures conditions.

L'encouragement et l'amour que m'ont donné ma famille et ma chérie Elodie ont été les moteurs qui m'ont poussé pour que ce travail voit le jour. Je tiens donc à exprimer ma vive reconnaissance pour être toujours là lorsque j'ai besoin d'eux.

SUMMARY

Nowadays, multiple constraints imposed by economic, social and environmental considerations undergo maintenance planning optimization into a major challenge to designers, owners and users of infrastructure. This study focuses on the management of reinforced concrete (RC) structures placed in marine atmospheres. Under these exposure conditions, chloride penetration generates corrosion of the reinforcing bars reducing the RC durability. Therefore, modeling the deterioration process as well as the maintenance actions carried out during the operational life becomes paramount for the formulation of a sustainable maintenance strategy.

The main objective of this thesis is to develop a new methodology for optimizing the performance of maintenance strategies for corroding RC structures. Contrary to classical management of infrastructure that is mainly based on economic constraints, this study proposes an extension to environmental criteria in view to find sustainable maintenance solutions. The management model combines: a comprehensive model of chloride penetration, Markov processes and decision theory. The uncertainty related to material properties, model and environmental actions as well as the effect of imperfect inspections are also integrated to the model. Given that a sustainable maintenance strategy should minimize costs and environmental impact, a multi-criteria approach for decision-making is also implemented.

Several numerical examples and real case studies illustrate the aforementioned points throughout the manuscript. In general, it is concluded that the proposed methodology can be useful to improve the environmental performance and the costs of a given strategy by ensuring appropriate levels of serviceability and safety.

Keywords: Sustainability, reinforced concrete, chlorides, corrosion, reliability, maintenance.

RÉSUMÉ

A l'heure actuelle, des multiples contraintes économiques, sociales et environnementales transforment l'optimisation de la planification des travaux de maintenance en un défi majeur pour les concepteurs, les propriétaires et les utilisateurs des infrastructures. Cette étude se concentre sur la gestion des structures en béton armé placées dans des environnements marins. Dans ces conditions d'exposition, la pénétration des ions chlorure génère la corrosion des armatures en réduisant la durabilité du béton armé. Par conséquent, la modélisation des processus de dégradation ainsi que des actions de maintenance réalisées au cours de la durée de vie opérationnelle devient primordiale pour la formulation d'une stratégie de maintenance durable.

L'objectif principal de cette thèse est de développer une nouvelle méthodologie pour l'optimisation de la performance des stratégies de maintenance des structures en béton armé sujettes à la corrosion. La gestion des infrastructures est principalement basée sur des contraintes économiques. Cette étude propose une extension à des critères environnementaux pour trouver des solutions inscrites dans le cadre du développement durable. Le modèle de gestion combine : un modèle étendu de pénétration des chlorures, des processus de Markov et la théorie de la décision. L'aléa lié aux propriétés des matériaux, au modèle et aux actions environnementales ainsi que les effets des inspections imparfaites sont également intégrés au modèle. Étant donné que la stratégie de maintenance durable doit minimiser les coûts et l'impact environnemental, une approche multicritère pour la prise de décision est également mise en œuvre.

Plusieurs exemples numériques et des études de cas réels illustrent les points ci-dessus dans ce mémoire. Il est démontré que la méthode proposée peut être utile pour améliorer la performance environnementale et les coûts d'une stratégie de maintenance donnée en assurant des niveaux appropriés de service et de sûreté.

Mots-clés : Développement durable, béton armé, chlorures, corrosion, fiabilité, maintenance.

CONTENTS

Remerciements	v
Summary	vii
Résumé	ix
Contents	xi
Introduction	1
I Extended abstract in French	5
1 Résumé étendu en français	7
1.1 Introduction	7
1.1.1 Défis de la gestion des structures en béton armé soumises à la corrosion	8
1.1.2 Objectifs de recherche	8
1.2 Modèle étendu de pénétration des ions chlorure	9
1.2.1 Formulation du modèle de pénétration des ions chlorure	9
1.2.2 Solution numérique	11
1.3 Approche probabiliste pour le modèle de pénétration des chlorures	11
1.3.1 Définition des variables aléatoires de base	13
1.3.2 Modèle stochastique du climat	13
1.3.3 Modèle stochastique de la concentration des chlorures dans l'environnement	14
1.3.4 Influence des conditions climatiques sur l'initiation de la corrosion	15
1.4 Optimisation du management des structures en béton armé corrodées	16
1.4.1 Description de la stratégie de la maintenance	17
1.4.2 Approche Markovienne pour la modélisation de la pénétration des chlorures	19
1.4.3 Analyse des coûts	25
1.4.4 Exemple numérique	26
1.5 Stratégies de maintenance dans le cadre du développement durable	27
1.5.1 Gestion durable des structures vieillissantes	28
1.5.2 Durabilité des stratégies de maintenance	30
1.5.3 Prise de décision sous contraintes multi-objectifs	33
1.5.4 Cas d'étude : terminal agro-alimentaire	34
1.6 Conclusions et perspectives	38

II Core of the thesis	41
2 Requirements for management of corroding RC structures	43
2.1 Introduction	43
2.2 Life-cycle of RC structures subjected to corrosion	44
2.3 Deterioration and maintenance modeling	45
2.3.1 Failure rate function	47
2.3.2 Markov model	47
2.3.3 Stochastic process	47
2.3.4 Time-dependent reliability index	48
2.4 Framework of the proposed management strategy	49
2.4.1 Type and quality of inspection	49
2.4.2 Repair criterion	49
2.4.3 Kinematics of the deterioration process	50
2.4.4 Sustainability	51
2.5 Chloride ingress into concrete	52
2.5.1 Chloride penetration in saturated concrete	52
2.5.2 Chloride penetration in unsaturated concrete	53
2.6 Conclusions	54
3 Modeling chloride penetration into concrete	55
3.1 Introduction	55
3.2 Model of chloride ingress in unsaturated conditions	55
3.2.1 Chloride transport	56
3.2.2 Moisture diffusion	58
3.2.3 Heat transfer	61
3.3 Numerical solution of the governing equations	61
3.3.1 Model verification	64
3.4 Numerical example	65
3.4.1 Problem description	65
3.4.2 Results	67
3.5 Summary and conclusions	68
4 Stochastic modeling of chloride penetration	71
4.1 Introduction	71
4.2 Probabilistic framework for reliability analysis	72
4.2.1 Probability of corrosion initiation	73
4.3 Time-invariant random variables	73
4.3.1 Basic concepts of random variables	74
4.3.2 Definition of the random variables	75
4.4 Stochastic model for humidity and temperature	78
4.4.1 Karhunen-Loëve discretization of humidity and temperature	78
4.4.2 Effect of global warming on weather	80
4.5 Stochastic model for environmental chloride concentration	82
4.5.1 Exposure to chlorides from sea water	82
4.5.2 Exposure to chlorides from de-icing salts	82

4.6	Case study 1: Probabilistic assessment of time to corrosion initiation	83
4.6.1	Problem description	83
4.6.2	Results	84
4.7	Case study 2: Influence of global warming on corrosion initiation time	86
4.7.1	Problem description	86
4.7.2	Results	88
4.8	Conclusions	92
5	Optimal management of corroding RC structures	95
5.1	Introduction	95
5.2	Description of the strategy of maintenance	96
5.3	Markovian approach for modeling chloride ingress	98
5.3.1	Estimation of transition matrix from simulations	99
5.3.2	Selection of an appropriate Markov model	100
5.4	Probabilistic modeling of inspection/repair	102
5.4.1	Assessment of PGA and PWA	104
5.5	Simulation of inspection, repair and failure	106
5.5.1	Failure between inspections	108
5.5.2	Failure and repair at inspection years	110
5.6	Cost analysis	112
5.6.1	Inspection cost	113
5.6.2	Repair cost	113
5.6.3	Failure cost	113
5.7	Illustrative example	114
5.7.1	Problem description	114
5.7.2	Results	116
5.8	Conclusions	120
6	Sustainable decision-making for maintenance strategies	123
6.1	Introduction	123
6.2	Sustainable management of deteriorating structures	124
6.3	Sustainability of repair strategies	125
6.3.1	Cost	126
6.3.2	Waste generation	127
6.3.3	Carbon dioxide emissions	127
6.4	Decision-making under multi-objective constraints	129
6.4.1	Compromise programming	129
6.5	Case study: Agri-foodstuffs terminal	130
6.5.1	Characteristics of the repair techniques	130
6.5.2	Assessment of the repair rates	132
6.5.3	Criteria for sustainability analysis	136
6.5.4	Sustainable decision-making	138
6.6	Conclusions	142
Closure		145

A Reliability analysis	149
A.1 Time-invariant reliability analysis	149
A.2 Time-dependent reliability analysis	149
A.3 Methods for reliability assessment	150
A.3.1 Monte Carlo simulation	151
A.3.2 Latin Hypercube sampling	151
Bibliography	153

INTRODUCTION

RC deterioration due to corrosion

Chloride-induced corrosion affects significantly the operational life of reinforced concrete structures located close to the sea shore or in contact with de-icing salts. The mechanisms by which corrosion affects load carrying capacity of RC structures are: loss of reinforcement cross-section, loss of bond between steel and concrete, concrete cracking and RC delamination. RC structures are generally designed for a service life between 50 and 100 years. However, in chloride-contaminated environments many structures begin to deteriorate after 20 to 30 years (Kumar Mehta, 1997; Poupart et al., 2006; Rosquoët et al., 2006). Therefore, to guarantee optimum levels of serviceability and safety during the life-cycle, maintenance planning optimization becomes a major challenge with multiple constraints imposed by economic, social and environmental considerations.

Corrosion induced by chloride ingress is an important factor affecting the service life of RC structures and infrastructures. Nowadays, many deteriorated structures are evaluated for possible repair and continued service because they are situated where their replacement would be economically unfeasible. Bhide (1999) reports that about 173,000 bridges in the United States are structurally deficient or functionally obsolete due in part to corrosion. Thus, developing robust models for prediction and strategies for periodic inspection and maintenance plays a significant role in enabling target reliabilities to be met over a period of continued service (Clifton, 1993; Mori & Ellingwood, 1995).

Although corrosion damage rarely leads to sudden structural collapse, there are some examples of structural failure induced by corrosion in RC structures. One example is the collapse of a concrete pedestrian bridge in the year 2000 on the Motor Speedway in Charlotte, North Carolina (USA) injuring more than 100 people; the bridge has been built in 1995 and its collapse was attributed to pitting corrosion in the steel strands encased inside the concrete slabs. Another example is the case of Interstate 70 in Washington County, Pennsylvania (USA), which suffered a disruption of traffic produced by the collapse of a zone on the overpass in 2005 (Grata, 2005). The overpass, opened in 1960, serves now about 40,000 vehicles a day. Besides corrosion induced by de-icing salts, the collapse was induced by a history of trucks hitting its underside. Five people experienced minor injuries related to the incident. There are many examples where corrosion may also cause aesthetic and serviceability problems.

Regarding corrosion costs, in a study conducted by CC Technologies Laboratories Inc. (2001), it was found that the total direct cost of corrosion in the USA is close to US\$137.9 billion/yr. The industrial and infrastructure sectors which are most likely to suffer corrosion damage are shown in Table 1. These values, however, do not include indirect costs to users (delays, inconvenience, lost productivity) which can increase the total costs significantly. Note that transportation infrastructure and highway bridges produce about 37% of the total direct costs (US\$38 billion/yr). Given the size and importance of transportation infrastructures, damage costs reported (Table 1)

Table 1 — Cost of corrosion in several industrial and infrastructure sectors.

Industrial sector	Cost US\$ billion/yr
Gas and liquid transmission pipelines	7.0
Hazardous materials storage	7.0
Highway bridges	8.3
Waterways and ports	0.3
Drinking water and sewer systems	36.0
Transportation	29.7
Defense and nuclear waste storage	20.1
Production and manufacturing	17.6
Others	11.9
Total	137.9

justify research in RC corrosion-related damage process to ensure an optimal level of safety. In summary, corrosion damage is highly related to economic losses, travel delays and personal injuries in transportation infrastructure.

Challenges in management of RC corroding structures

Design or rehabilitation of construction projects are mainly based on economic feasibility analysis. However, social, environmental and economic constraints are directing design towards an integrated process oriented principally to: (1) reduce environmental impact, (2) optimize resources management, and (3) reduce waste generation. This design philosophy leads to sustainable development which is defined by the (World Commission on Environment and Development, 1987) as: “development that meets the needs of the present without compromising the ability of future generations to meet their own needs”. There are three components of sustainability: environment, economy and society. To meet its goal, sustainable development must provide a balance between these components.

Maintenance strategies are directed to ensure serviceability and safety during operational life and/or to extend life-cycle of structures. Nowadays, owners/operators have not decision-making tools to establish a maintenance strategy that minimizes costs and environmental impact. Thus, they make decisions without an overall vision of the problem.

A major challenge in management of RC corroding infrastructure is that there is no comprehensive models to assess the structural performance during the operational life. Therefore, owners/operators take corrective repair measures when visible deterioration signals appear –e.g., concrete cracking. This approach has two main problems: (1) the expenditures cannot be predicted during the life cycle, and (2) structural safety can be seriously compromised when repair is not undertaken at appropriate times.

The main objective of the agency is to ensure an optimum level of performance during the operational life. Nonetheless, for corroding RC structures, the owner/operator is usually faced up to the following questions:

1. How much chloride ingress will affect structural integrity?
2. How and when inspection and repair should be undertaken?
3. How to determine a sustainable maintenance strategy?

Concerning the first question, there are deterioration models to assess the reduction of structural lifetime produced by chloride ingress. The uncertainty of the process and the accuracy of the model will lead to correct or incorrect decisions when the structure is repaired at good or wrong times. Lifetime assessment can be improved by implementing a realistic deterioration model that considers the interaction with weather conditions as well as the uncertainties involved in the deterioration phenomenon. Since there are several uncertainties in the whole process, structural performance can also be monitored by inspections. Then, for the second question the problem lies in determining an effective method and interval of inspection. Based on both the inspection results and a given repair criterion, the owner/operator decides if repair should be undertaken. The definition of the repair criterion considers various social, environmental and economic aspects that mainly depend on the agencies' policies. As structures can be repaired by using several techniques, the third question is related to the problems of the owner/manager for choosing an optimal strategy that minimizes costs and environmental impact. Accordingly, to answer to these questions, the methodology developed in this study integrates the following aspects:

- a comprehensive probabilistic model of chloride penetration,
- the effects of inspection/repair on structural integrity, and
- the environmental impact of the inspection/repair actions.

Research objectives

The main purpose of this study is to develop a methodology for sustainable management of corroding RC structures.

The specific objectives are:

1. To provide a discussion on the advantages and the shortcomings of the methods currently available for management of corroding RC structures and to define an appropriate approach to deal with this problem.
2. To choose and to implement a comprehensive model of chloride penetration.
3. To introduce the comprehensive model of chloride penetration into an appropriate probabilistic framework to account for the uncertainties related to the deterioration phenomenon.
4. To formulate a methodology for optimizing the performance of maintenance strategies.
5. To include environmental constraints in the decision-making process to evaluate the sustainability of maintenance strategies with appropriate algorithms.

Thesis organization

This manuscript is divided into two parts. The first part (chapter 1) is an extended abstract of the thesis in French. The most relevant theory and findings are presented in this part. The second part encompasses the core of the thesis which contains five chapters. Chapter 2 describes the consequences of corrosion on safety of RC structures and presents a critical review of the state-of-the-art of management of corroding RC structures. This literature survey is used to determine an appropriate approach and to establish the needs for further research.

On the basis of the research needs identified in the literature review for the deterioration process, chapter 3 describes the formulation of the proposed model of chloride penetration. This chapter also includes a description of the adopted numerical approach and a numerical example.

Chapter 4 presents the stochastic approach for modeling chloride penetration. This chapter starts with a revision of the principles of uncertainty modeling. Afterwards, it defines the methods and the limit state functions used in reliability analysis. It concludes with the description of the proposed models for the random variables and with illustrative examples.

Taking into account the proposed deterioration model and the probabilistic framework presented in chapter 4, chapter 5 outlines the proposed approach for optimizing the management of corroding RC structures. Once the proposed method has been described and discussed, it is illustrated by a numerical example.

Finally, chapter 6 presents the proposed methodology for evaluating the sustainability of maintenance strategies as well as a tool for decision-making under multi-criteria constraints. The methodology is illustrated by an application to the maintenance of a real structure.

Part I

Extended abstract in French

CHAPTER 1

RÉSUMÉ ÉTENDU EN FRANÇAIS

N.B. : Ce résumé présente les développements et les résultats les plus importants de cette étude. Son organisation reprend celle du manuscrit en anglais (chaque section fait référence à un chapitre). Ainsi, les chapitres évoqués apportent plus de précisions et font référence aux chapitres du manuscrit en anglais.

1.1 Introduction

De nos jours, la conception ou la réhabilitation de projets de construction sont principalement basées sur l'analyse de faisabilité économique. Cependant, des contraintes sociales et environnementales, alliées à cette composante économique dirigent la conception vers un processus intégré ayant pour but de réduire l'impact environnemental, d'optimiser la gestion des ressources et de réduire la production de déchets. Cette philosophie de conception conduit à un développement durable qui est défini par la commission mondiale sur l'environnement et le développement (World Commission on Environment and Development, 1987) comme : "... un développement qui répond aux besoins du présent sans compromettre la capacité des générations futures à satisfaire leurs propres besoins... ". On compte trois composantes du développement durable : environnement, économie et société. Pour atteindre son objectif, le développement durable doit assurer un équilibre entre ces éléments.

Cette étude porte sur l'évaluation des stratégies de maintenance pour les structures en béton armé exposées aux chlorures dans le cadre du développement durable. En environnements contenant des chlorures, la durabilité du béton armé peut être réduite par la corrosion des armatures (Kumar Mehta, 1997; Poupard et al., 2006; Rosquoët et al., 2006). Par conséquent, les stratégies de maintenance sont utilisées pour garantir le bon fonctionnement et la sécurité des structures au cours de la vie opérationnelle et/ou d'étendre le cycle de vie des structures. Aujourd'hui, les propriétaires/gestionnaires n'ont pas d'outils d'aide à la décision pour mettre en place une stratégie de maintenance qui minimise les coûts et l'impact environnemental. Ainsi, ils prennent des décisions sans vision globale du problème. L'objectif principal de cette thèse est de développer une méthodologie pour évaluer les stratégies de maintenance des structures en béton armé soumises à la corrosion. Ce travail est effectué dans le cadre du projet FUI MAREO¹ avec le soutien de la société Oxand et tire partie du savoir-faire des différents acteurs liés à la gestion des structures.

¹MAintenance et REparations d'Ouvrages littoraux et fluviaux en béton : optimisation par analyse de risque

1.1.1 Défis de la gestion des structures en béton armé soumises à la corrosion

Un défi majeur dans la gestion des structures en béton armé soumises à la corrosion est qu'il n'existe pas de modèles prédictifs fiables pour évaluer la performance structurelle au cours de la durée de vie opérationnelle. Par conséquent, les propriétaires/gestionnaires doivent prendre des mesures correctives de réparation lorsque quelques signaux de dégradation sont visibles (fissuration du béton, par exemple). Cette approche conduit à deux problèmes principaux : (1) les dépenses ne peuvent pas être estimées sur l'ensemble du cycle de vie, et (2) la sécurité structurale peut être sérieusement compromise lorsque la réparation n'est pas effectuée à des moments opportuns. L'objectif principal des propriétaires/gestionnaires est d'assurer un niveau optimal de performance au cours de la durée de vie opérationnelle. Néanmoins, pour des structures en béton armé soumises à la corrosion, les propriétaires/gestionnaires sont généralement confrontés aux questions suivantes :

1. Comment la pénétration des chlorures affectera-t-elle l'intégrité structurelle ?
2. Comment et quand l'inspection et la réparation doivent-elles être entreprises ?
3. Comment déterminer une stratégie de maintenance durable ?

En ce qui concerne la première question, des modèles de dégradation sont disponibles pour évaluer la réduction de la durée de vie produite par la pénétration des chlorures. L'incertitude du phénomène de dégradation et la précision du modèle permettront de prendre de bonnes ou de mauvaises décisions lorsque la structure est réparée aux bons ou mauvais moments. L'évaluation de la durée de vie peut être améliorée par la mise en œuvre d'un modèle réaliste qui tienne compte de la dégradation due à l'interaction avec les conditions météorologiques ainsi que des incertitudes impliquées dans le phénomène de dégradation. Comme il existe plusieurs incertitudes dans l'ensemble du processus, les performances structurelles peuvent également être surveillées par des inspections. Pour la deuxième question, le problème consiste à déterminer une méthode efficace et un intervalle optimal d'inspection. En tenant compte des résultats d'inspection et d'un critère donné de réparation, le propriétaire/gestionnaire décide si la réparation doit être effectuée. La définition du critère de réparation considère différents aspects sociaux, environnementaux et économiques qui dépendent principalement des politiques des propriétaires/gestionnaires. Les structures peuvent être réparées à l'aide de plusieurs techniques. Puis, la troisième question est liée aux problèmes du propriétaire/gestionnaire pour le choix d'une technique optimale de réparation qui minimise les coûts et l'impact environnemental. En conséquence, pour répondre à ces questions, la méthodologie développée dans cette thèse intègre les aspects suivants :

- un modèle probabiliste de pénétration des chlorures,
- les effets de l'inspection et de la réparation sur la sécurité structurale, et
- l'impact environnemental des réparations.

1.1.2 Objectifs de recherche

L'objectif global de cette étude est de développer une méthodologie pour la gestion durable des structures en béton armé soumises à la pénétration des ions chlorure.

Les objectifs spécifiques sont :

1. de fournir une discussion sur les avantages et les inconvénients des méthodes actuellement disponibles pour la gestion des structures en béton armé sujettes à la corrosion et de définir l'approche la plus adaptée pour traiter ce problème ;
2. de choisir et de mettre en œuvre un modèle étendu de pénétration des chlorures ;
3. d'introduire le modèle étendu de pénétration des chlorures dans un cadre probabiliste approprié afin de prendre en considération les incertitudes liées au processus de dégradation ;
4. de proposer une méthodologie pour l'optimisation des performances des stratégies de maintenance ; et
5. d'inclure des contraintes environnementales dans le processus de prise de décision afin d'évaluer la performance des stratégies de maintenance du point de vue du développement durable.

1.2 Modèle étendu de pénétration des ions chlorure

La pénétration des ions chlorure est contrôlée par des interactions complexes entre des processus physiques et chimiques qui ont été généralement simplifiés en un problème de diffusion régi par la seconde loi de Fick. Jusqu'à présent, la plupart des études ont utilisé une solution simplifiée de la loi de Fick où la concentration en chlorures à un instant et à une position donnés est estimée par la fonction d'erreur complémentaire (Tuutti, 1982). Cette solution analytique est uniquement valable quand le coefficient apparent de diffusion des chlorures est constant dans le temps et l'espace, la concentration en chlorures dans l'environnement reste constante et le béton est saturé. Toutefois, en vertu de ces simplifications, il n'est pas possible d'envisager l'action d'autres phénomènes comme : la fixation des chlorures, les interactions entre la diffusion des ions chlorure et les conditions environnementales, la pénétration des chlorures par convection, etc. Sur la base des travaux de Saetta et al. (1993) puis de Martín-Pérez et al. (2001), les chapitres 3 et 4 présentent un modèle probabiliste étendu de pénétration des chlorures. La formulation proposée tient compte de l'interaction entre trois phénomènes : la pénétration des chlorures, la diffusion de l'humidité et le transfert de chaleur. Le processus de pénétration des ions chlorure est donc représenté par un ensemble d'équations aux dérivées partielles qui est résolu par un couplage d'éléments finis et de différences finies. Cette approche permet de prendre principalement en compte les phénomènes suivants :

- la capacité de fixation des ions chlorure ;
- la variabilité dans le temps et l'influence de la température, de l'humidité et de la concentration de chlorures dans le milieu voisin ;
- la réduction de la diffusivité des ions chlorure du béton avec l'âge, et
- le flux des ions chlorure dans des conditions de non-saturation et en deux dimensions.

1.2.1 Formulation du modèle de pénétration des ions chlorure

Cette section présente une formulation permettant de traiter le problème qui considère l'interaction entre les trois problèmes physiques : (i) pénétration des chlorures, (ii) la diffusion de l'humidité et (iii) le transfert thermique. Chaque phénomène est représenté par une équation aux dérivées

Tableau 1.1 — Correspondance entre l'équation 1.1 et les équations aux dérivées partielles.

Phénomène physique	ψ	ζ	J	J'	q'_ψ^s
Pénétration des ions chlorures	C_{fc}	1	$D_c^* \vec{\nabla} C_{fc}$	$C_{fc} D_h^* \vec{\nabla} h$	q_h^s
Diffusion de l'humidité	h	$\partial w_e / \partial h$	$D_h \vec{\nabla} h$	0	0
Transfert thermique	T	$\rho_c c_q$	$\lambda \vec{\nabla} T$	0	0

partielles (EDP). Selon Martín-Pérez et al. (2001), les équations régissant ces phénomènes peuvent être exprimées sous la forme générale suivante :

$$\zeta \frac{\partial \psi}{\partial t} = \underbrace{\text{div } J}_{\text{diffusion}} + \underbrace{\text{div } J'}_{\text{convection}} \quad (1.1)$$

où ψ représente le paramètre étudié, t est le temps et la correspondance entre ζ , J , J' et les conditions pour le phénomène physique correspondant, présenté dans le tableau 1.1.

Pour la *pénétration des chlorures*, C_{fc} représente la concentration des chlorures libres, h est l'humidité relative et D_c^* et D_h^* représentent les coefficients apparents de diffusion de chlorures et d'humidité, respectivement :

$$D_c^* = \frac{D_{c,\text{ref}} f_1(T) f_2(t) f_3(h)}{1 + (1/w_e) (\partial C_{bc}/\partial C_{fc})} \quad (1.2)$$

$$D_h^* = \frac{D_{h,\text{ref}} g_1(h) g_2(T) g_3(t_e)}{1 + (1/w_e) (\partial C_{bc}/\partial C_{fc})} \quad (1.3)$$

où $D_{c,\text{ref}}$ et $D_{h,\text{ref}}$ sont les coefficients de diffusion de référence mesurés aux conditions normales (Saetta et al., 1993), w_e est la teneur en eau évaporable et f_i et g_i sont des fonctions de correction pour tenir compte des effets de la température, de l'humidité relative, du vieillissement et du degré d'hydratation du béton. Ces fonctions sont détaillées dans le chapitre 3. Le terme $\partial C_{bc}/\partial C_{fc}$ représente la capacité de fixation du ciment qui établit un rapport entre les concentrations des chlorures libres et liés à l'équilibre (Nilsson et al., 1994). Les isothermes de Langmuir et Freundlich sont les plus utilisées pour estimer la capacité de fixation (Tang & Nilsson, 1993; Glass & Buenfeld, 2000). Glass & Buenfeld (2000) ont découvert que la capacité de fixation des ions chlorure est estimée plus précisément par l'isotherme de Langmuir (Glass & Buenfeld, 2000), par conséquent, cette isotherme est retenue dans cette étude.

Pour la *diffusion de l'humidité*, le coefficient de diffusion de l'humidité D_h est estimé en tenant compte de l'influence de l'humidité, de la température et du temps de cure –i.e., $D_h = D_{h,\text{ref}} g_1(h) g_2(T) g_3(t_e)$ (chapitre 3). Le terme $\partial w_e / \partial h$ (tableau 1.1) représente la capacité en eau qui établit un rapport entre la teneur en eau, w_e , et l'humidité relative des pores, h . Pour une température donnée, cette relation a été déterminée expérimentalement par les isothermes d'adsorption. Selon le modèle de Brunauer-Skalny-Bodor (Brunauer et al., 1969), l'isotherme d'adsorption dépend de la température, du rapport massique eau/ciment, e/c , et du temps de cure, t_e . Xi et al. (1994) ont développé des expressions empiriques de ces paramètres. Ce travail adopte le modèle de Brunauer-Skalny-Bodor pour estimer l'humidité relative.

Enfin, pour le *transfert thermique* (voir tableau 1.1), ρ_c est la masse volumique du béton, c_q est la capacité thermique spécifique du béton, λ est la conductivité thermique du béton et T est

la température à l'intérieur du béton au temps t .

Les conditions aux limites à la surface exposée du béton considèrent le flux de ψ qui traverse la surface du béton, (conditions de borne de type Robin) (Saetta et al., 1993) :

$$q_\psi^s = \underbrace{B_\psi(\psi^s - \psi_{env})}_{\text{diffusion}} + \underbrace{\psi_{env} q'_\psi}_{\text{convection}} \quad (1.4)$$

où B_ψ est le coefficient de transfert de la surface, ψ^s est la valeur de ψ à la surface exposée et ψ_{env} représente la valeur de ψ dans l'environnement. La correspondance entre l'équation 1.4 et les phénomènes physiques est également présentée dans le tableau 1.1.

1.2.2 Solution numérique

Le flux de chlorures dans le béton est estimé en résolvant simultanément le système d'équations décrit par l'équation 1.1 et tableau 1.1. Cette étude utilise la méthodologie proposée par Martín-Pérez et al. (2001), qui combine des éléments finis avec des différences finies pour estimer les variations spatiales et temporelles de C_{fc} , h et T . Pour les différences finies, la méthode de Crank-Nicolson a été adoptée.

La figure 1.1 montre la procédure pour estimer les profils de chlorures, $C_{fc}(x; t_i)$, d'humidité, $h(x; t_i)$, et de température, $T(x; t_i)$, pour le flux dans une direction (par exemple x). Pour la première itération ($i = 1$), en prenant en considération la température initiale dans le béton, $T(x; t = 0) = T_{ini}$, le profil de température est obtenu à partir de l'équation de pénétration des chlorures. Le profil d'humidité est déterminé à partir de l'équation de diffusion d'humidité en considérant l'humidité initiale dans le béton, $h(x; t = 0) = h_{ini}$, et le profil de température estimé précédemment (à savoir $T(x; t_1)$). Enfin, le profil de chlorure est calculé à partir de la relation de diffusion des ions chlorure, en tenant compte de la concentration initiale de chlorures dans le béton, $C_{fc}(x; t = 0) = C_{fc,ini}$, et des profils de température et d'humidité précédemment calculés. Pour l'itération suivante ($i = 2$), les profils obtenus à partir de $i = i - 1$ sont choisis comme nouvelles conditions initiales. Une procédure itérative est mise en œuvre pour déterminer les profils d'humidité et de chlorures parce que les coefficients de diffusion et les isothermes dépendent également des profils actuels d'humidité et de concentration en chlorures.

1.3 Approche probabiliste pour le modèle de pénétration des chlorures

Afin de prendre en compte l'ensemble des aléas présents dans le problème, le modèle de dégradation est couplé à des méthodes probabilistes pour considérer les incertitudes du processus de pénétration des ions chlorure. Trois sources d'aléa et incertitudes ont été considérées dans le problème : les propriétés du matériau, le modèle et ses paramètres et les actions environnementales. Autrement dit, la prédiction de la durée de vie des structures devrait être basée sur des modèles probabilistes et des modèles mécaniques étendus qui prennent en compte l'interaction entre plusieurs processus de dégradation de la résistance.

L'objectif principal de l'analyse de la fiabilité est d'évaluer la capacité des systèmes ou des composants de demeurer en sécurité et fonctionnels au cours de leur cycle de vie. Cette information peut être utilisée pour définir des critères pour la prise de décisions, améliorer la gestion des ressources, réaliser des études de sensibilité, etc. La fonction d'état limite ou fonction de performance sépare les résultats de *défaillance* et de *non défaillance*. Les fonctions d'état limite peuvent être

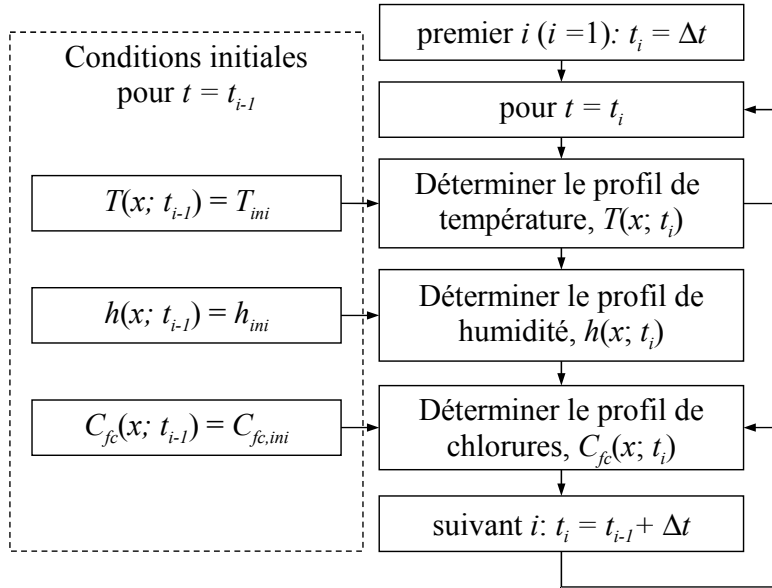


Figure 1.1 — Algorithme pour la résolution du système des équations aux dérivées partielles.

liées aux conditions structurelles suivantes :

- *état limite de service* : cette condition est accomplie lorsque les structures sont encore considérées comme utiles et sans danger même si un certain degré de dégradation a été observé. Pour le problème traité dans cette étude, l'état limite de service est lié à la *probabilité d'initiation de la corrosion*.
- *état limite ultime* : cette condition décrit l'état dans lequel la sécurité structurelle est très sérieusement affectée et peut conduire à la défaillance ou à l'effondrement. Dans le cas de corrosion provoquée par la pénétration des chlorures, la section utile de l'acier est réduite et la défaillance se produit lorsque la charge appliquée dépasse la résistance restante. L'état limite ultime est lié à la *probabilité de défaillance*.

La probabilité d'initiation de la corrosion et la probabilité de défaillance peuvent toutes deux être utiles dans l'évaluation de la durée de vie ou pour la gestion de maintenance des structures en béton armé. Cependant, la stratégie de maintenance adoptée est plus préventive que corrective, et par conséquent, dans cette étude on se limite à la probabilité d'initiation de la corrosion.

Le temps d'initiation de la corrosion, t_{ini} , se calcule généralement comme l'instant où la concentration en ions chlorures à la profondeur de l'enrobage c_t est supérieure à une valeur seuil C_{th} . Pour cet évènement, la fonction d'état limite devient :

$$g(\mathbf{x}, t) = C_{th}(\mathbf{x}) - C_{tc}(\mathbf{x}, t, c_t) \quad (1.5)$$

où \mathbf{x} est un vecteur contenant les variables aléatoires de base et $C_{tc}(\mathbf{x}; t; c_t)$ est la concentration totale en ions chlorures à la profondeur c_t et au temps t , obtenue par la résolution du système d'équations aux dérivées partielles. L'évaluation de la fonction d'état limite (équation 1.5) sert à calculer la probabilité d'initiation de la corrosion comme :

$$p_{corr}(t) = P[g(\mathbf{x}, t) \leq 0 | t] \quad (1.6)$$

Tableau 1.2 — Variables aléatoires de base.

Variable	Unité	Distribution	Moyenne	COV
$D_{c,ref}$	m^2/s	log-normale	3.0×10^{-11}	0.2
C_{th}	wt% cim	Normale	0.48	0.30
U_c	kJ/mol	beta sur [32 ; 44.6]	41.8	0.1
m		beta sur [0 ; 1]	0.15	0.3
$D_{h,ref}$	m^2/s	log-normale	3×10^{-10}	0.2
α_0		beta sur [0.025 ; 0.1]	0.05	0.2
n		beta sur [6 ; 16]	11	0.1
λ	$\text{W}/(\text{m}^\circ\text{C})$	beta sur [1.4 ; 3.6]	2.5	0.2
c_q	$\text{J}/(\text{kg}^\circ\text{C})$	beta sur [840 ; 1170]	1000	0.1
ρ_c	kg/m^3	Normale	2400	0.2

Etant donné les non-linéarités et la complexité du système d'équations aux dérivées partielles, les méthodes de simulations semblent les plus appropriées pour résoudre le problème. Pour réduire les temps de calcul, cette étude combine des simulations de Monte Carlo avec l'échantillonnage par Hypercube Latin.

1.3.1 Définition des variables aléatoires de base

La modélisation probabiliste est principalement basée sur des modèles mécaniques et sur l'introduction d'incertitudes à travers des paramètres physiques qui contrôlent le phénomène. Cette approche peut être considérée comme une modélisation physique lorsque chaque paramètre a été déterminé expérimentalement (Schoefs, 2008). Néanmoins, pour la pénétration des chlorures, des fonctions de correction ont été élaborées sur la base des principales tendances physiques des phénomènes, par exemple, les effets du vieillissement, de la température, de l'humidité, etc. Par conséquent, le choix des variables aléatoires présenté dans ce rapport est principalement basé sur un jugement d'expert.

La probabilité d'initiation de la corrosion est évaluée sur la base des modèles probabilistes présentés dans le tableau 1.2. Ces valeurs concernent les propriétés du matériau et la concentration seuil pour l'initiation de la corrosion. Les critères de sélection de ces variables sont présentés dans le chapitre 4. Ces variables aléatoires sont valables sous les hypothèses suivantes :

- les structures sont construites en béton ordinaire et sont soumises à des conditions de non-saturation ;
- les coefficients de variation (COV) des variables aléatoires sont indépendants de leur valeur moyenne.
- toutes les variables aléatoires sont indépendantes. Toutefois, cette hypothèse devrait être validée lorsque des nouvelles données expérimentales seront disponibles.

1.3.2 Modèle stochastique du climat

Afin d'améliorer les estimations du modèle de pénétration des ions chlorure, il est important de mettre en œuvre un modèle du climat qui reproduit de manière réaliste la température et l'humidité. Cette étude a utilisé des processus stochastiques pour représenter le caractère aléatoire des paramètres climatiques. Compte tenu de la simplicité de la mise en œuvre et du faible temps de calcul nécessaire, l'expansion de Karhunen-Loève a été adoptée pour modéliser le climat. Soit

$\kappa(t, \theta)$ un processus aléatoire fonction du temps t , défini sur le domaine \mathbf{D} , avec θ appartenant à l'espace des événements aléatoires, Ω ; $\kappa(t, \theta)$ devient (Ghanem & Spanos, 1991) :

$$\kappa(t, \theta) \simeq \bar{\kappa}(t) + \sum_{i=1}^{n_{KL}} \sqrt{\lambda_i} \xi_i(\theta) f_i(t) \quad (1.7)$$

où $\bar{\kappa}(t)$ est la moyenne du processus, $\xi_i(\theta)$ est un ensemble de variables aléatoires normales, n_{KL} est le nombre de termes de la discréétisation tronquée, $f_i(t)$ forment un ensemble complet de fonctions orthogonales déterministes et λ_i sont les valeurs propres de la fonction de covariance $C(t_1, t_2)$. Puisque des solutions analytiques existent pour $f_i(t)$ et λ_i quand les fonctions de covariance ont une forme exponentielle et triangulaire (Ghanem & Spanos, 1991), et que la covariance exponentielle permet de représenter un grand nombre de phénomènes, cette étude suppose que les processus de la température et de l'humidité ont ce type de covariance.

Des mesures météorologiques sur le climat annoncent des changements (augmentations) dans la température et l'humidité moyenne dans les prochaines années (IPCC, 2007). D'ailleurs, la tendance linéaire du réchauffement climatique au cours des 50 dernières années (0.13°C par décennie) montre un doublement par rapport à celle mesurée au cours des 100 dernières années (0.076°C). Sur la base de ces mesures et des différentes politiques contre le réchauffement climatique, le Groupe intergouvernemental d'experts sur le changement climatique a annoncé une augmentation de la température moyenne de 1 à 6.4°C au cours des 100 prochaines années (IPCC, 2007). Compte tenu de cette tendance, un modèle simplifié du réchauffement climatique est proposé dans cette étude. L'effet de réchauffement climatique est modélisé en supposant que l'augmentation ou la diminution de l'humidité et de la température dans les années à venir est une fonction linéaire. En plus, pour tenir compte des variations saisonnières de la température et de l'humidité, il est supposé que la moyenne du processus, $\bar{\kappa}(t)$, suit une tendance sinusoïdale :

$$\bar{\kappa}_\phi(t) = \begin{cases} \bar{\phi}(t) + \frac{\phi_{max} - \phi_{min}}{2} \sin\left(\frac{t - \lfloor t \rfloor}{1 - R(t)}\pi\right) & \text{pour les saisons chaudes ou sèches} \\ \bar{\phi}(t) - \frac{\phi_{max} - \phi_{min}}{2} \sin\left(\frac{t - \lfloor t \rfloor + R(t) - 1}{R(t)}\pi\right) & \text{pour les saisons froides ou humides} \end{cases} \quad (1.8)$$

où ϕ représente la température ou l'humidité, ϕ_{max} et ϕ_{min} sont respectivement les valeurs maximum et minimum de ϕ pendant une année, t est donné en années, R est le rapport des saisons et $\lfloor \cdot \rfloor$ représente la fonction de la partie entière par excès : $\lfloor x \rfloor = \max \{n \in \mathbb{Z} \mid n \leq x\}$.

1.3.3 Modèle stochastique de la concentration des chlorures dans l'environnement

Les ions chlorure qui pénètrent dans le béton peuvent provenir de deux sources : l'eau de mer ou les sels de dé verglaçage. Dans des environnements maritimes, la concentration en chlorures dans l'environnement dépend principalement de la proximité de la mer, d . Basé sur une étude de terrain de 1158 ponts en Australie, McGee (2000) propose une expression pour calculer la moyenne de la concentration en chlorures dans l'environnement, C_{env} . Cette expression est utilisée ici pour modéliser C_{env} comme un processus stochastique généré par des variables aléatoires log-normales indépendantes (bruit log-normal). D'après les travaux de Vu & Stewart (2000) et Duracrete (2000), le coefficient de variation de C_{env} est de 0.2.

Concernant les sels de dé verglaçage, cette étude propose un modèle qui suppose que, pendant les saisons chaudes, C_{env} est nul, alors que durant les saisons froides, il devient dépendant du temps (stochastique). Le modèle stochastique de C_{env} utilise également des variables aléatoires

Tableau 1.3 — Description des environnements étudiés.

Climat	Description	Température		Humidité	
		T_{min}	T_{max}	h_{min}	h_{max}
<i>Continental</i>	endroits situés aux latitudes moyennes loin de l'océan	-10°C	20°C	0.6	0.8
<i>Océanique</i>	structures placées aux latitudes moyennes à proximité de l'océan	5°C	25°C	0.6	0.8
<i>Tropical</i>	sites placés à des latitudes équatoriales près de l'océan	20°C	30°C	0.7	0.9

Tableau 1.4 — Paramètres retenus pour la modélisation du réchauffement climatique.

Scénario	Caractéristiques	ΔT_a	Δh_a	ΔR_a
<i>Sans Attendu</i>	le réchauffement climatique est négligé	0°C	0	0
	utilisation de sources d'énergie alternatives et fossiles, le taux de natalité suit les tendances actuelles et il n'y a pas d'utilisation importante des technologies propres	2.5°C	0.05	-0.1
<i>Pessimiste</i>	utilisation massive de sources d'énergie fossiles, la croissance de la population est appréciable et il n'y a pas de politiques visant à développer et à étendre l'utilisation de technologies propres	6.5°C	0.10	-0.2

log-normales indépendantes (pendant les saisons froides) et un COV de 0.2.

1.3.4 Influence des conditions climatiques sur l'initiation de la corrosion

L'objectif principal de cet exemple est d'étudier l'influence des conditions climatiques sur la probabilité d'initiation de la corrosion et sur la réduction de la durée de vie. Dans ce but, nous considérons une dalle ou un mur en béton armé avec une face exposée à des actions environnementales. Sachant que l'épaisseur du composant est beaucoup plus petite que ses autres dimensions, le problème est réduit au flux des chlorures en une dimension. Cependant, il est important de souligner que pour d'autres composants (par exemple, les poteaux ou les poutres) le flux des chlorures en deux dimensions accélère la probabilité d'initiation de la corrosion pour les aciers placés dans les coins. Les modèles probabilistes pour les variables aléatoires sont définis dans le tableau 1.2. La profondeur de l'enrobage suit une distribution normale tronquée à 10 mm avec les paramètres statistiques suivants : $\mu_{ct} = 50$ mm et $\text{COV}[c_t] = 0.25$.

Cette application prend en considération trois environnements dont les caractéristiques ont été définies par la latitude et par la proximité de l'océan. Le tableau 1.3 présente les valeurs retenues pour chaque cas. Pour l'environnement continental, la concentration en chlorures est $C_{max}^{env} = 14$ kg/m³, et pour les milieux marins, elle dépend de la distance de mer.

Pour tenir compte de l'effet du réchauffement climatique, trois scénarios possibles ont été définis (tableau 1.4). Les caractéristiques de ces scénarios ont été attribuées sur la base des prévisions publiées par le groupe intergouvernemental d'experts sur les changement climatique (IPCC, 2007). A notre connaissance, ce travail présente l'étude la plus complète sur ce sujet. Ces prévisions considèrent une combinaison des actions naturelles et anthropiques. Les actions naturelles concernent les changements climatiques produits principalement par l'action de l'énergie solaire et par les activités volcaniques. Les actions anthropiques comprennent l'effet des perturbations humaines sur le climat.

L'effet du type d'exposition sur la probabilité d'initiation de la corrosion est montré sur la figure 1.2a. Cette figure présente les probabilités d'initiation de la corrosion pour les environnements décrits dans le tableau 1.3 sans considérer l'action du réchauffement climatique. La concentration

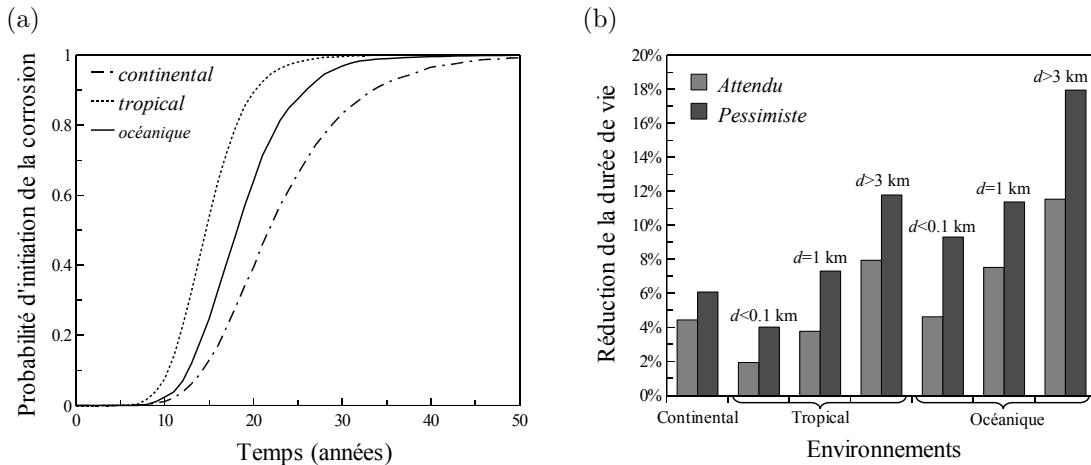


Figure 1.2 — (a) Effet du type d'exposition. (b) Réduction de la durée de vie produite par le réchauffement climatique.

de chlorure de surface pour le milieu marin (tropical ou océanique), est définie pour une distance de la mer de $d < 0.1 \text{ km}$. On observe que les plus fortes probabilités d'initiation de la corrosion correspondent à des environnements marins, en particulier, pour l'environnement tropical. Ces résultats sont expliqués par les faits que (i) des structures placées dans les milieux marins sont exposées aux chlorures tout le temps et (ii) les importantes températures et humidités accélèrent la pénétration des ions chlorure dans la matrice de béton. La différence entre les milieux continentaux et tropicaux souligne l'importance de mettre en œuvre un modèle de pénétration des chlorures qui inclut les effets environnementaux. Étant donné que la concentration en chlorures de l'environnement est la même pour les milieux marins (par exemple, tropicaux et océaniques), une analyse simplifiée conduirait aux mêmes résultats pour les deux environnements quand les considérations climatiques ne sont pas prises en compte.

La figure 1.2b montre les effets du réchauffement climatique sur la réduction de la durée de vie des structures en béton armé soumises à la pénétration des chlorures. La réduction de la durée de vie illustrée sur la figure 1.2b prend comme référence le cas où le réchauffement climatique n'a pas été considéré. Il est observé que le réchauffement climatique induit des réductions de durée de vie variant de 2 à 12% pour le scénario *attendu* et de 4 à 18% pour le scénario *pessimiste*. En comparant la réduction de la durée de vie moyenne pour tous les environnements, la plus grande influence correspond à l'environnement océanique (10,4%), suivie par celle de l'environnement tropical (6,1%) et enfin l'environnement continental (5,3%). Ces résultats justifient la mise en œuvre d'un modèle étendu de pénétration des ions chlorures afin d'adopter des actions de maintenance appropriées qui assurent des niveaux optimaux de sécurité et de fonctionnalité.

1.4 Optimisation du management des structures en béton armé corrodées

Aujourd'hui, la conception et la gestion des structures et des infrastructures doit tenir compte des aspects économiques, sociaux et environnementaux afin de réduire l'impact environnemental, d'optimiser la gestion des ressources et de diminuer la production de déchets. Cette nouvelle tendance de conception et de gestion doit également tenir compte de tous les phénomènes qui af-

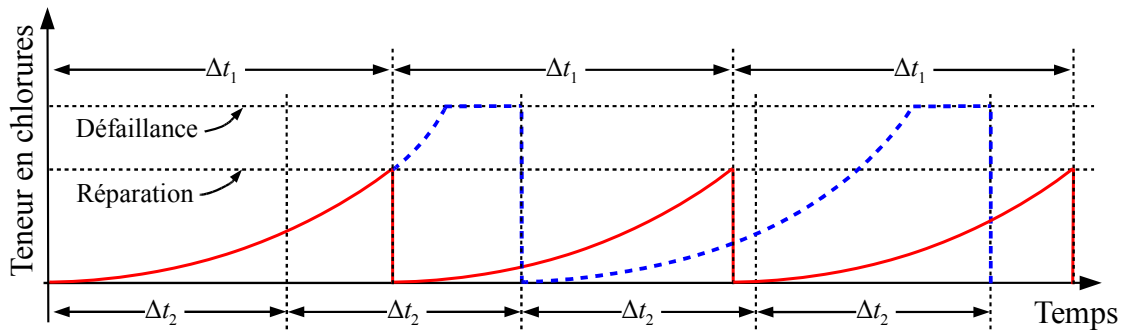


Figure 1.3 — Modélisation de l’inspection et de la maintenance.

facent la performance des structures. Pour les structures en béton armé, la corrosion induite par la pénétration des chlorures génère des dommages importants au bout de 10 ou 20 années de service (Kumar Mehta, 1997; Poupard et al., 2006; Rosquoët et al., 2006). La gestion des structures en béton armé doit donc intégrer les étapes d’inspection et de maintenance pour assurer un niveau optimal de sécurité au cours de leur vie opérationnelle. Cependant, la complexité et les incertitudes du processus de dégradation et des techniques de réparation transforment la gestion en un défi pour les propriétaires/gestionnaires où les décisions sont souvent prises sans maîtrise des conséquences.

Nous cherchons ici à développer une méthode pour optimiser la gestion des structures en béton armé soumis à la pénétration des chlorures. La gestion optimale minimise les coûts d’inspection, de réparation et de défaillance. Prenant comme point de départ les travaux de Sheils et al. (2010), une approche markovienne est utilisée pour la modélisation de la dégradation, de l’inspection et de la réparation.

1.4.1 Description de la stratégie de la maintenance

L’objectif des stratégies de maintenance est d’assurer un niveau optimal de fonctionnement et de sécurité au cours de la vie de la structure. Par conséquent, lorsque la performance structurelle est fortement affectée par la cinétique du processus de dégradation, la réparation ou le remplacement des composants structurels sont les seuls moyens d’atteindre cet objectif. Dans la stratégie de maintenance étudiée ici, les actions de réparation sont basées sur les résultats d’inspection. La figure 1.3 montre l’influence de la stratégie sur la teneur en chlorure à une profondeur donnée (par exemple la profondeur de l’enrobage). La structure est inspectée périodiquement tous les Δt années. Selon les résultats de l’inspection, la réparation est effectuée lorsque la teneur en chlorure atteint un seuil donné. $\Delta t = \Delta t_1$ représente une situation idéale où l’inspection et la réparation ont lieu au moment où la teneur en chlorure atteint le seuil de réparation. Toutefois, cette situation est rarement observée dans les structures en béton armé parce que la cinétique de la pénétration des chlorures est difficile à évaluer/prévoir en raison de l’influence de plusieurs paramètres (par exemple, les propriétés du matériau, le climat, etc.). En outre, il y a une source d’erreur et d’incertitude liée aux résultats d’inspection et au processus de dégradation qui peuvent conduire à des décisions erronées. On constate alors que, lorsque $\Delta t = \Delta t_2$, certaines inspections sont inutiles et des composants structurels peuvent tomber en défaillance entre les intervalles d’inspection. Par conséquent, une stratégie de maintenance optimale doit prendre en compte tous ces aspects pour minimiser les coûts d’inspection, de réparation et de défaillance.

La stratégie de maintenance est divisée en deux étapes : inspection et réparation. L’inspec-

tion peut être effectuée en employant des méthodes destructives et/ou non-destructives. En ce qui concerne les méthodes non-destructives, l'inspection visuelle est une technique habituellement utilisée pour évaluer l'état des structures en béton armé (Roelfstra et al., 2004). Les résultats des inspections alertent les propriétaires/gestionnaires lorsque le seuil de dégradation est atteint. La valeur seuil peut être liée à fissuration du béton ou à la perte de section transversale des armatures. Toutefois, pour l'inspection visuelle, l'évaluation de l'état de la structure demeure très incertaine lorsque l'inspection est effectuée. À l'heure actuelle, des avancées significatives voient le jour dans le développement des méthodes d'auscultation basées sur le contrôle non-destructif. Les techniques d'auscultation non-destructives ont pour but de quantifier la valeur instantanée ou l'évolution d'une variable donnée dans le temps (la résistance des matériaux, les concentrations en chlorures, le taux de corrosion, etc.), et pourtant, leurs résultats sont fortement influencés par les conditions environnementales qui réduisent alors leur précision. La précision des résultats de l'inspection est largement améliorée en utilisant des techniques de contrôle destructives. Cependant, elles sont plus coûteuses et exigent un plus grand nombre de tests quand il y a une grande variabilité des paramètres contrôlés. La sélection d'une ou la combinaison de plusieurs techniques d'inspection dépend de plusieurs aspects tels que :

- le type de phénomène inspecté –par exemple, la résistance du matériau, la concentration en chlorure, etc ;
- la taille du projet –par exemple, une structure particulière ou un réseau de structures ;
- l'usage de la structure –par exemple, nucléaire, transport, etc. Ce point est lié au risque admissible par le propriétaire/gestionnaire ;
- d'autres aspects socioéconomiques –par exemple, les priorités du pays, la disponibilité des ressources, etc.

Cette étude fait référence à des structures en béton armé soumises à la pénétration des chlorures et se concentre sur la maintenance des infrastructures (ports, ponts, etc.). Les besoins relatifs à la stratégie de maintenance ont été définis dans le cadre du projet FUI MAREO avec la collaboration des maîtres d'ouvrage, des entreprises de construction et des centres de recherche. Dans la stratégie de maintenance considérée, l'inspection est faite par l'analyse de la concentration en chlorures à la profondeur de l'enrobage sur des carottes en béton (méthode destructive). Ensuite, en fonction des résultats de l'inspection, la technique de réparation consiste à reconstituer l'épaisseur de béton pollué par diverses méthodes (figure 1.4). L'avantage de l'approche proposée est que la réparation est plus préventive que corrective. Cette caractéristique assure un niveau optimal de sécurité pendant la durée de vie du projet.

Tenant compte du fait que de nombreux facteurs influent sur le processus de dégradation et les effets de la maintenance, les modèles numériques sont indispensables pour prendre des décisions optimales. De nombreux systèmes de gestion de structures utilisent des chaînes de Markov pour simuler la dégradation et la réparation des structures au cours du temps (Cesare et al., 1992; Scherer & Glangola, 1994; Roelfstra et al., 2004). Par conséquent, cette étude utilise également une approche markovienne qui intègre les aspects suivants :

- un modèle étendu de pénétration des chlorures (section 1.2) ;
- la précision de la technique d'inspection ; et

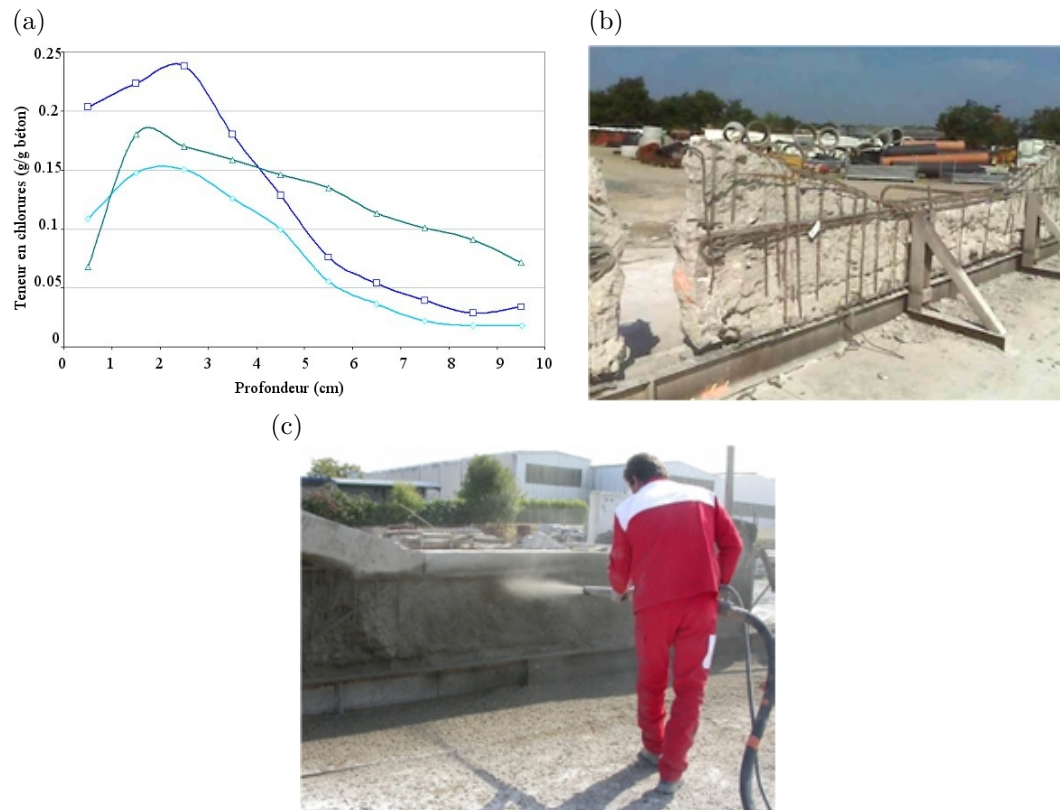


Figure 1.4 — Étapes de la stratégie de maintenance adoptée.

- l'incertitude inhérente à la pénétration des chlorures, l'initiation de la corrosion et les résultats de l'inspection.

La section suivante décrit la méthodologie proposée pour modéliser la pénétration des ions chlорure à partir des simulations de Monte-Carlo.

1.4.2 Approche Markovienne pour la modélisation de la pénétration des chlorures

Un processus de Markov à temps discret permet de prédire le futur en sachant l'état présent. Dans ce but, on discrétise l'espace de la variable d'intérêt en M états. Les processus de Markov serviront donc à déterminer la probabilité qu'un événement appartienne à un état j sachant que, pour un état précédent, il appartenait à un état i . Cette probabilité, notée $a_{ij} = P(X_{t+1} = j | X_t = i)$, est appelée la *probabilité de transition*. Cette étude considère que les probabilités de transition a_{ij} sont indépendantes de t (processus de Markov à temps discret). Les probabilités de transition sont communément regroupées dans une matrice de dimension $M \times M$ appelée matrice de transition P (Ross, 2004). D'après l'équation de Chapman-Kolmogorov, les probabilités d'appartenance aux états donnés après t transitions, $q(t)$, sont (Ross, 2004) :

$$\mathbf{q}(t) = \mathbf{q}_{ini} \mathbf{P}^t \quad (1.9)$$

où \mathbf{q}_{ini} est un vecteur contenant les probabilités d'appartenance à chaque état pour un instant initial ($t = 0$).

Dans cette étude, la quantité d'intérêt est la concentration de chlorures, C , à la profondeur

Tableau 1.5 — États utilisés pour la discrétisation du problème.

État i	1	2	3	4	5	6	7	8	9	10
minimum (kg/m^3)	0,0	0,4	0,8	1,2	1,6	2,0	2,4	2,8	3,2	3,6
moyenne, \bar{C}_i (kg/m^3)	0,2	0,6	1,0	1,4	1,8	2,2	2,6	3,0	3,4	3,8
maximum (kg/m^3)	0,4	0,8	1,2	1,6	2,0	2,4	2,8	3,2	3,6	4,0

d'enrobage qui contrôlera l'initiation de la corrosion. Les processus de Markov fournissent la probabilité que C appartienne à un état donné dans le temps. Si nous supposons qu'à l'instant initial $t = 0$ il n'y a pas de chlorure au niveau de l'enrobage, toutes les concentrations appartiendront au premier état. Par conséquent, q_{ini} deviendra $q_{ini} = [1, 0, 0, \dots, 0]$ et l'équation 1.9 donnera un vecteur contenant les probabilités d'appartenir à un état j à l'instant t .

Dans plusieurs applications des chaînes de Markov, la matrice de transition est obtenue à partir des campagnes expérimentales ou par jugement d'expert. Cependant, pour la pénétration des chlorures, l'estimation de P à partir des mesures expérimentales pose deux problèmes. D'abord, étant donné la longue durée des essais de pénétration, il est difficile d'étudier l'évolution de la concentration des chlorures avant la construction autrement que par des essais accélérés. La difficulté des essais accélérés est l'obtention des résultats équivalents à une cinétique réelle. Une alternative pour résoudre ce problème est l'utilisation des données obtenues pour des matériaux similaires. Le second problème est lié à la grande quantité de mesures nécessaires pour bien représenter le phénomène. Par conséquent, on propose ici d'estimer numériquement $\mathbf{q}(t)$ sur la base d'un modèle numérique de pénétration des ions chlorures et ensuite d'utiliser les valeurs estimées $\hat{C}(t)$ pour calculer la matrice de transition \mathbf{P} . La section suivante détaille la méthode proposée pour cette estimation.

1.4.2.1 Évaluation des matrices de transition à partir des simulations

Les matrices de transition sont obtenues à partir de simulations de Monte-Carlo du modèle de pénétration des ions chlorures en considérant les variables aléatoires décrites dans la section 1.3. Pour les simulations, on enregistre l'évolution dans le temps de la concentration des chlorures à la profondeur de l'enrobage. Après avoir réalisé un grand nombre de simulations, on dispose des résultats de cette expérimentation numérique à chaque pas de temps ; on détermine alors la fréquence pour les concentrations d'appartenir à chaque état considéré (histogramme). La probabilité d'appartenir à un état j à un instant t est estimé à partir de :

$$\hat{q}_j(t) = \frac{n_j(t)}{N} \quad (1.10)$$

où $n_j(t)$ est le nombre d'observations dans l'état j mesurées à un instant t et N le nombre de simulations. Le tableau 1.5 présente les intervalles (valeurs maximum et minimum) pour les 10 états utilisés pour discréteriser la variable d'intérêt C .

Lorsque les probabilités $\hat{q}_j(t)$ ont été estimées, on peut utiliser différentes méthodes pour calculer les probabilités de transition. La difficulté pour trouver P est liée au nombre de paramètres a_{ij} à estimer. Plusieurs études utilisent une matrice de Markov à deux paramètres dont un paramètre à

déterminer par état (Pappas et al., 2001; Roelfstra et al., 2004) :

$$\mathbf{P} = \begin{bmatrix} a_{11} & a_{12} & 0 & \cdots & 0 \\ 0 & a_{22} & a_{23} & \cdots & 0 \\ 0 & 0 & a_{33} & \cdots & 0 \\ \vdots & \vdots & \vdots & \ddots & \vdots \\ 0 & 0 & 0 & \cdots & 1 \end{bmatrix} \quad (1.11)$$

où pour un i fixe, $a_{i2} = 1 - a_{i1}$. Dans ce cas, les paramètres de \mathbf{P} peuvent être estimés à partir d'une régression non-linéaire. Cependant, ce modèle de la matrice \mathbf{P} à deux degrés de liberté par état, ne permet pas une bonne représentation de phénomènes stochastiques complexes (Roelfstra et al., 2004). Afin de résoudre cet inconvénient, nous proposons une méthode qui cherche les valeurs a_{ij} en minimisant la différence entre des probabilités provenant des simulations et celles obtenues avec le modèle de Markov (équation 1.10). Comme l'évolution dans le temps a une cinétique différente pour chaque état, il y a M fonctions à minimiser :

$$\left\{ \begin{array}{l} \min_{\mathbf{a}} \max_{\mathbf{F}} \mathbf{F}(\mathbf{a}) = (f_1(\mathbf{a}), f_2(\mathbf{a}), \dots, f_M(\mathbf{a}))^T \\ \text{s.c. } a_{ij} \geq 0 \text{ et } \sum_{j=0}^{\infty} a_{ij} = 1 \end{array} \right. \quad (1.12)$$

où \mathbf{a} est un vecteur contenant les probabilités de transition (paramètres d'optimisation) et :

$$f_j(\mathbf{a}) = \sum_{t=0}^{t_{ana}} (\hat{q}_j(t) - q_j(t, \mathbf{a}))^2 \quad (1.13)$$

où t_{ana} représente la période d'analyse considéré pour faire l'ajustement. Ce problème d'optimisation multi-objectif est résolu à l'aide du “toolbox” d'optimisation de Matlab®. La méthode d'optimisation choisie minimise la valeur maximale d'un jeu de fonctions multi-variable à partir d'une valeur initiale.

1.4.2.2 Modèle probabiliste de maintenance et de réparation

Dans l'approche proposée, on a décidé de faire des inspections périodiques de la structure tous les Δt ans. Ces inspections ont pour but de mesurer la concentration des chlorures à la profondeur de l'enrobage C qui nous donnera une idée de la probabilité d'initiation de la corrosion. En plus, ce critère nous sert aussi pour décider si la structure doit être réparée ou non. Le test expérimental pour déterminer les profils de chlorure est basée sur la procédure AFREM (Chaussadent & Arliguie, 1999; RILEM TC 178-TMC, 2002). Ce test est utilisé pour déterminer la concentration en chlorures (total ou libre) à une profondeur donnée (profils de chlorure). Bien que cette procédure soit largement utilisée pour déterminer les profils de chlorure dans plusieurs pays, Bonnet et al. (2009) ont constaté que des différences importantes existent entre les profils des chlorures théoriques et mesurés. Cette différence est liée aux facteurs suivants : erreur dans le protocole, erreur due à la variabilité des propriétés des matériaux et erreur induite par l'opérateur.

Afin de tenir compte de l'influence de l'erreur de mesure, la différence entre les valeurs mesurées \hat{d} et théoriques d est généralement modélisée par un bruit (Rouhan & Schoefs, 2003) :

$$\eta = \hat{d} - d \quad (1.14)$$

où η représente le bruit. Toutefois, d'après Bonnet et al. (2009), les mesures expérimentales de chlorure sous-estiment les concentrations réelles. Pour tenir compte de cet aspect, un biais b_η est ajouté à l'équation :

$$\hat{C} = C + \eta + b_\eta \quad (1.15)$$

où \hat{C} représente la concentration en chlorures mesurée et C est la concentration en chlorures réelle. L'erreur de mesure peut entraîner, pour une inspection donnée, une sous- ou une surestimation de la teneur en chlorures. Si la concentration en chlorures est sous-estimée, les propriétaires/exploitants décident de *ne rien faire* quand une réparation est requise. Cette décision erronée augmente la probabilité de défaillance et peut produire des sur-coûts, si une réparation excessive doit être effectuée à l'avenir. Au contraire, une surestimation génère une *mauvaise* décision où la réparation prématuée génère également des sur-coûts. La réparation est effectuée dans l'approche adoptée lorsque les résultats de l'inspection indiquent que la teneur en chlorures atteint une valeur seuil C_{rep} susceptible de déclencher la corrosion. Cette valeur peut être définie dans les normes de construction ou définie par du jugement d'experts et est liée au niveau de sécurité défini à partir d'un risque acceptable. D'un point de vue probabiliste, deux mesures doivent être définies :

- *probabilité d'une bonne évaluation*, PGA : détermine la probabilité de détecter un événement (par exemple la concentration en chlorure supérieure à la valeur seuil) étant donné que l'événement existe :

$$\text{PGA} = \text{P}(\hat{C}(\mathbf{X}) \geq C_{rep} | C(\mathbf{X}) \geq C_{rep}) \quad (1.16)$$

- *probabilité d'une évaluation erronée*, PWA : établit la probabilité de détecter un événement étant donné qu'il n'existe pas :

$$\text{PWA} = \text{P}(\hat{C}(\mathbf{X}) \geq C_{rep} | C(\mathbf{X}) < C_{rep}) \quad (1.17)$$

Le bruit est généralement modélisé par une variable aléatoire normale. Néanmoins, sur la base de mesures expérimentales, Bonnet et al. (2009) signalent qu'une distribution de valeur extrême généralisée (GEV) est plus appropriée pour représenter le bruit de la technique adoptée d'inspection. Les paramètres estimés (en kg/kg de béton) sont les suivants : forme $K = 0.016$, dispersion $\sigma_\eta = 9.3 \times 10^{-5}$ et position $\mu_\eta = -8.4 \times 10^{-5}$. Pour une masse volumique de béton de $\rho_c = 2400$ kg/m³, la dispersion et la position de η en kg de chlorures par m³ sont $\sigma_\eta = 0.2$ et $\mu_\eta = -0.2$, respectivement. En considérant que la concentration en chlorures ne peut pas être négative, et en ajustant certaines concentrations en chlorures obtenues par le modèle présenté dans les chapitres 3 et 4, on suppose ici que C suit une distribution log-normale avec moyenne μ_C et écart-type σ_C . Tenant compte que le bruit est modélisé par une variable aléatoire avec une variabilité importante, on considère que les événements $\langle \hat{C}(\mathbf{X}) \geq C_{rep} \rangle$ et $\langle C(\mathbf{X}) \geq C_{rep} \rangle$ sont faiblement corrélés. En conséquence, on suppose que ces événements sont indépendants et que la probabilité d'une bonne évaluation devient :

$$\text{PGA} = \text{P}[g(\mathbf{X}) \leq 0)] \quad (1.18)$$

où $g(\mathbf{X})$ est la fonction d'état limite. Dans ce problème, il n'y a pas de solution analytique pour

estimer la PGA à partir de l'équation 1.18. Par conséquent, le PGA est numériquement calculée en utilisant une méthode de fiabilité du premier ordre (FORM) où la fonction d'état limite est :

$$g(\mathbf{X}) = C_{rep} - C(\mathbf{X}) - \eta(\mathbf{X}) \quad (1.19)$$

On suppose dans l'équation 1.19 que, connaissant le biais, les mesures peuvent être débiaisées (c'est-à-dire, $b_\eta = 0$). Concernant PWA, en tenant compte du fait que le seuil de réparation C_{rep} est déterministe et que η suit une distribution GEV, la probabilité d'une évaluation erronée peut alors être estimée comme suit :

$$\text{PWA} = 1 - \exp \left(- \left[1 + K_\eta \left(\frac{C_{rep} - \mu_\eta}{\sigma_\eta} \right) \right]^{-1/K_\eta} \right) \quad (1.20)$$

1.4.2.3 Simulation de l'inspection, de la réparation et de la défaillance

Après inspection, les maîtres d'ouvrage peuvent prendre deux décisions :

1. réparer, auquel cas la structure revient à son état initial. Cette hypothèse est adoptée ici ; et
2. ne mener aucune réparation.

Dans le cas où aucune réparation n'est effectuée, il y a une probabilité de défaillance (initiation de la corrosion) qui augmente lorsque la teneur en chlorures est plus grande. Lorsque la défaillance se produit, la structure ou le composant sont réparés ou reconstruits à leur état initial. Ces événements sont représentés par des probabilités calculées analytiquement et intégrées dans le modèle de Markov. Par conséquent, il existe deux matrices de Markov pour la modélisation de l'ensemble du processus. La première est utilisée pour modéliser la défaillance et la réparation entre les inspections \mathbf{P}^{be} . La deuxième représente l'inspection, la réparation et la défaillance pendant les années d'inspection \mathbf{P}^{in} . Une fois que les matrices ont été déterminées, elles sont utilisées pour simuler la pénétration des chlorures, l'inspection, la réparation et la défaillance au cours du temps. Chaque état est censé avoir une population initiale de défauts. Le nombre de défauts de chaque état est calculé sur une base annuelle en utilisant la matrice de Markov concernée, et le nombre de défauts appartenant à chaque état pendant l'année précédente.

Dans la suite, la variable d'intérêt (concentration d'ions chlorure à la profondeur de l'enrobage) est discrétisée en M états. Chaque état i est donc représenté par une variable aléatoire $d_i(\mathbf{X})$ supposée suivre une loi log-normale.

La pénétration des chlorures dans le béton produit la défaillance structurale lorsqu'aucune réparation n'est effectuée. Le critère de réparation considère que le béton pollué est reconstitué lorsque la concentration en chlorures mesurée lors de l'inspection atteint une valeur seuil C_{rep} . C_{rep} est liée à la probabilité de dépassivation de l'acier ou d'initiation de la corrosion. La concentration en chlorures menant à l'initiation à la corrosion, C_{th} , est choisie dans ce travail pour calculer la probabilité de défaillance (initiation de la corrosion). En supposant que C_{th} est log-normalement distribuée, la probabilité d'initiation de la corrosion entre les intervalles d'inspection, à l'état i , peut être estimée comme suit :

$$p_{ini,i} = \text{P}(C_{th}(\mathbf{X}) - d_i(\mathbf{X}) \leq 0) = \Phi \left(\frac{\lambda_{d_i} - \lambda_{C_{th}}}{\sqrt{\xi_{d_i} + \xi_{C_{th}}}} \right) \quad (1.21)$$

où les paramètres λ et ξ représentent la moyenne et l'écart-type log-normales de C_{th} et d_i .

Les probabilités de transition $a_{i,j}$ dans la matrice de Markov pour une année entre inspections \mathbf{P}^{bet} sont calculés en fonction de celles de la croissance de la matrice de Markov \mathbf{P}^{gr} (estimées selon la méthode décrite dans la section 1.4.2.1) et la probabilité d'initiation de la corrosion de l'état correspondant (Sheils et al., 2010) :

$$a_{i,1}^{bet} = a_{i,1}^{gr} + \sum_{k=2}^M [a_{i,k}^{gr} p_{ini,k}] \quad (1.22)$$

et

$$a_{i,j}^{bet} = a_{i,j}^{gr} (1 - p_{ini,j}) \quad \text{pour } j > 1 \quad (1.23)$$

où $a_{i,j}^{bet}$ et $a_{i,j}^{gr}$ sont les probabilités de transition de \mathbf{P}^{bet} et \mathbf{P}^{gr} , respectivement.

Pendant les années d'inspection, les événements de réparation préventive R ou de défaillance F (initiation de la corrosion) peuvent survenir ($R \cup F$). Ainsi, la probabilité de réparation ou d'initiation de la corrosion à l'état i , $p_{R \cup F, i}$, peut se calculer comme suit :

$$p_{R \cup F, i} = P_i[\text{Réparation}] + P_i[\text{Défaillance} \mid \text{Non réparation}] \quad (1.24)$$

où :

$$P_i[\text{Réparation}] = P[\hat{C} \geq C_{rep}] \quad (1.25)$$

et en supposant que les événements $\langle \text{Défaillance} \rangle$ et $\langle \text{Non réparation} \rangle$ sont indépendants :

$$P_i[\text{Défaillance} \mid \text{Non réparation}] = P[\hat{C} < C_{rep}] p_{ini,i} \quad (1.26)$$

D'autre part, le paramètre γ_i représente la probabilité que la concentration en chlorures réelle à l'état i soit supérieure au seuil de réparation :

$$\gamma_i = P[d_i(\mathbf{X}) \geq C_{rep}] \quad (1.27)$$

γ_i peut se déterminer sur la base de jugement d'expert. Cependant, supposant que $d_i(\mathbf{X})$ est log-normalement distribuée, γ_i est calculé analytiquement par :

$$\gamma_i = \Phi\left(\frac{\lambda_{d_i} - \ln(C_{rep})}{\xi_{d_i}}\right) \quad (1.28)$$

où λ_{d_i} et ξ_{d_i} sont la moyenne et l'écart-type log-normales de $d_i(\mathbf{X})$. La probabilité de réparation peut donc s'écrire analytiquement en termes de γ_i , PGA_i et PWA_i :

$$P_i[\text{Réparation}] = \text{PGA}_i \gamma_i + \text{PWA}_i (1 - \gamma_i) \quad (1.29)$$

De même, la probabilité de défaillance étant donné qu'aucune réparation n'est effectuée s'écrit :

$$P_i[\text{Défaillance} \mid \text{Non réparation}] = [(1 - \text{PGA}_i) \gamma_i + (1 - \text{PWA}_i)(1 - \gamma_i)] p_{ini,i} \quad (1.30)$$

Ces valeurs sont ensuite utilisées pour calculer les probabilités de transition de la matrice de Markov pour une année d'inspection \mathbf{P}^{in} en termes de celles de la matrice de croissance \mathbf{P}^{gr} de Markov et de la probabilité d'initiation de la corrosion de l'état correspondant (Sheils et al., 2010) :

$$a_{i,1}^{in} = a_{i,1}^{gr} + \sum_{k=2}^M [a_{i,k}^{gr} p_{R \cup F,k}] \quad (1.31)$$

et

$$a_{i,j}^{in} = a_{i,j}^{gr} (1 - p_{R \cup F,j}) \quad \text{pour } j > 1 \quad (1.32)$$

où $a_{i,j}^{in}$ et $a_{i,j}^{gr}$ sont les probabilités de transition de \mathbf{P}^{in} et \mathbf{P}^{gr} , respectivement.

1.4.3 Analyse des coûts

En fonction de la cinétique du processus de dégradation et de la stratégie de réparation, le nombre de défauts de chaque état se stabilise après un certain nombre de simulations (Sheils et al., 2010). L'idée est d'obtenir un régime permanent de maintenance et non un régime transitoire à partir d'un état neuf. Ces valeurs stabilisées sont utilisées pour évaluer le coût de la stratégie de maintenance. Cette méthode distingue trois types de coûts :

- l'espérance du coût d'inspection, $E[C_I]$,
- l'espérance du coût de réparation, $E[C_R]$ et
- l'espérance du coût de défaillance, $E[C_F]$.

L'espérance du coût total de la stratégie de maintenance, $E[C_T]$, est ensuite calculée par :

$$E[C_T] = E[C_I] + E[C_R] + E[C_F] \quad (1.33)$$

Bien que les coûts susmentionnés concernent les frais directement dépensés par le maître d'ouvrage, les coûts d'utilisation peuvent également être ajoutés à l'analyse. Selon Thoft-Christensen (2009), dans certains cas, la prise en compte des coûts d'utilisation est un facteur déterminant dans la gestion des infrastructures vieillissantes. Cependant, en tenant compte du fait qu'aucune donnée n'est disponible pour quantifier avec précision le coût d'utilisation, il a été décidé de modéliser seulement les coûts des propriétaires/gestionnaires. Le développement de modèles de coûts précis est au-delà de la portée de cette étude. Néanmoins, les paramètres de coûts présentés ici ont été définis sur la base d'un jugement d'expert des opérateurs du grand port maritime de Nantes Saint-Nazaire.

Les coûts directs sont dépensés à des moments différents au cours de la durée de vie opérationnelle. Toutefois, à des fins de comparaison, les modèles de coûts décrits ci-après sont calculés sur une base annuelle. En d'autres termes, ces coûts indiquent les dépenses annuelles des maîtres d'ouvrage pour maintenir une structure.

La prise de décision fondée sur l'espérance des coûts est largement utilisée dans la pratique. Toutefois, Schoefs et al. (2009a) ont démontré que la prise de décision basée sur d'autres valeurs que l'espérance est plus pratique dans certains cas où une valeur optimale est difficile à trouver.

Tableau 1.6 — Modèles probabilistes du coefficient de diffusion des chlorures pour les matériaux de réparation.

Technique	Unité	Distribution	Moyenne	COV
matériau de construction	m^2/s	log-normale	3.0×10^{-11}	0.2
béton coffré	m^2/s	log-normale	4.5×10^{-11}	0.2
projection par voie humide	m^2/s	log-normale	2.0×10^{-11}	0.2
projection par voie sèche	m^2/s	log-normale	1.8×10^{-11}	0.1

Bien que ce point ne soit pas traité dans ce travail, il est un domaine important pour des recherches futures.

1.4.4 Exemple numérique

1.4.4.1 Description

L'objectif de cet exemple est d'illustrer la méthodologie proposée pour étudier l'influence de l'intervalle d'inspection sur l'espérance annuelle des coûts. Il est supposé que la structure en béton armé est composée de 100 éléments structuraux, qu'elle est placée dans un climat de type océanique avec une température allant de 5 à 25 °C et une humidité relative variant entre 0,6 et 0,8 par an. Le modèle stochastique de climat est décrit dans le chapitre 4. La longueur des intervalles d'inspection dépend de la variabilité spatiale de la concentration en chlorure de l'environnement. Par conséquent, deux zones d'exposition ont été incluses dans cet exemple :

- *zone de marnage* : les éléments structuraux sont en contact direct avec l'eau de mer, mais pas immersés. Dans cette zone, la concentration en chlorures de l'environnement est importante et la pénétration des chlorures est accélérée par les variations de température et d'humidité. La moyenne de la concentration en chlorures dans l'environnement de cette zone est $C_{env} = 6 \text{ kg/m}^3$.
- *zone atmosphérique* : les éléments structuraux sont situés à 0,1 km ou moins de la côte, mais sans contact direct avec l'eau de mer. La moyenne de la concentration en chlorures dans l'environnement de cette zone est $C_{env} = 3 \text{ kg/m}^3$

D'après la section 1.3, la concentration en chlorure dans l'environnement est modélisée par un processus stochastique généré par des nombres indépendants suivant une distribution log-normale (bruit log-normal) avec un coefficient de variation de 0,2. Les variables considérées comme aléatoires pour la pénétration des chlorures sont présentées dans le tableau 1.2. L'explication du choix de ces variables est donnée dans le chapitre 4. Le tableau 1.2 présente le coefficient de diffusion des chlorures pour le matériau d'origine. Pour les matériaux de réparation, les coefficients de diffusion des chlorures ont été définis en fonction des résultats expérimentaux préliminaires menés dans le cadre du projet MAREO (Villain et al., 2010). Ces coefficients sont présentés dans le tableau 1.6. Il est important de mentionner que bien que ces coefficients soient utilisés pour étudier l'influence de la qualité des techniques de réparation, les conclusions concernant les techniques de réparation ne sont pas générales.

La détermination d'un intervalle d'inspection optimal est très sensible aux modèles de coûts. Par conséquent, pour obtenir des résultats réalistes, les coefficients d'inspection, de réparation et de défaillance utilisés ont été définis en tenant compte les dépenses moyennes rapportées par le grand port maritime de Nantes Saint-Nazaire. Ces coefficients sont présentés dans le tableau 1.7.

Tableau 1.7 — Coefficients pour les modèles de coûts.

Paramètre	Technique de réparation		
	béton coffré	projection par voie sèche	projection par voie humide
Coût initial de construction, C_0	1000	1000	1000
Coefficient d'inspection, k_I	0.005	0.005	0.005
Coefficient de réparation, k_R	0.15	0.21	0.26
Coefficient de défaillance, k_F	0.30	0.42	0.52

Les coefficients de ces coûts sont référencés à un coût de construction initial de 1000 unités par élément structurel. Le coefficient de défaillance est généralement égal ou supérieur à 1 dans d'autres applications d'ingénierie qui sont basées sur les états limites ultimes. Dans ce cas, la défaillance implique le remplacement du composant affecté. Toutefois, pour l'état limite adopté, le coefficient donné dans le tableau 1.7 indique que, après la défaillance (initiation de la corrosion), le surcoût est inférieur au coût initial de construction.

1.4.4.2 Résultats

Cette section compare le rapport coût-efficacité de trois techniques de réparation qui peuvent être mises en œuvre dans la stratégie de maintenance : béton coffré, béton projeté par voie humide et béton projeté par voie sèche. La figure 1.5 présente l'espérance annuelle du coût total pour les trois techniques de réparation et les deux zones d'exposition. En comparant le coût des techniques de réparation, il est constaté que le coût du béton projeté par voie sèche est d'environ la moitié du coût des autres techniques. Ce comportement s'explique par le fait que le matériau de réparation utilisé dans cette technique a le coefficient de diffusion de chlorures le plus bas (tableau 1.6). Par conséquent, la probabilité d'initiation de la corrosion dans le temps est plus faible et les frais d'inspection, de réparation et de défaillance sont réduits.

En ce qui concerne l'effet de la zone d'exposition, il est noté dans les deux cas et pour tous les matériaux de réparation que le seuil optimal de réparation est de 1,2 kg/m³. Cela signifie qu'il existe un seuil de réparation optimal pour un problème particulier et que les décisions devraient être basées sur cette valeur optimale. Le comportement global indique que l'espérance annuelle du coût total est inférieure pour la zone atmosphérique. Étant donné que la concentration en chlorures dans l'environnement est plus faible dans la zone atmosphérique, le temps d'initiation de la corrosion est plus important. Par conséquent, les composants structuraux situés dans cette zone nécessitent moins d'entretien par rapport à ceux situés dans la zone de marnage. Ces résultats indiquent que la variabilité spatiale s'avère particulièrement importante pour améliorer la gestion des structures en béton armé sujettes à la corrosion. D'un point de vue économique, il est conclu que le béton projeté par voie sèche est la technique avec le meilleur rapport coût-efficacité.

1.5 Stratégies de maintenance dans le cadre du développement durable

Le principal défi en matière de gestion durable des structures en béton armé sujettes à la corrosion est de formuler une stratégie de maintenance techniquement et économiquement faisable, qui réduit l'impact environnemental et qui assure un niveau optimal de fonctionnement et de sécurité pendant la durée de vie opérationnelle. Les progrès récents dans la gestion visent à améliorer la performance des stratégies de réparation en optimisant les coûts directs (Frangopol, 2010). Cependant, plusieurs exigences imposées par les contraintes environnementales transforment aujourd'hui l'optimisation

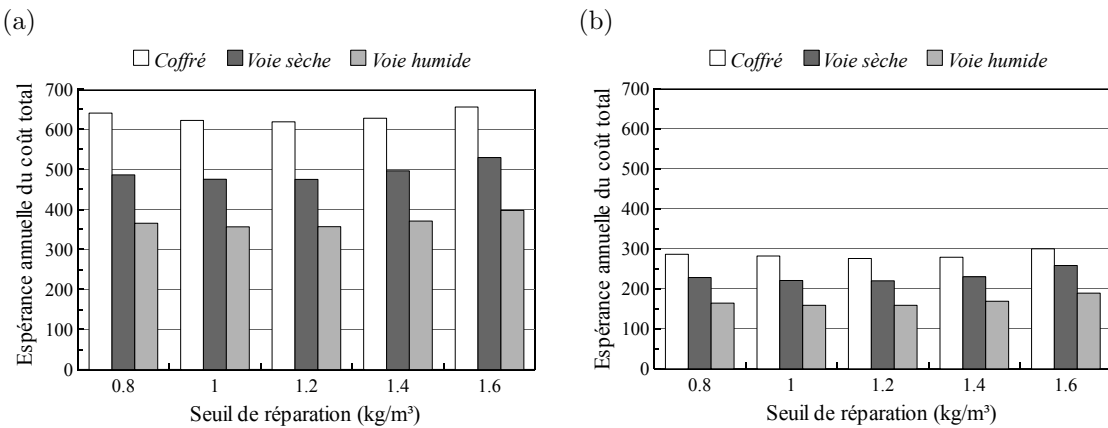


Figure 1.5 — Espérance annuelle du coût total pour plusieurs matériaux de réparation et conditions environnementales : (a) zone de marnage et (b) zone atmosphérique.

de la maintenance en un défi majeur pour les concepteurs, les propriétaires et les utilisateurs des structures.

Cette section se centre sur l'évaluation de la "durabilité" d'une stratégie de maintenance des structures en béton armé exposés aux chlorures. D'après André (1999) "...les processus et les institutions *durables* répondent à certains critères : ils n'épuisent pas les ressources nécessaires aux générations futures ; ils renforcent continuellement les capacités des individus et des institutions ; les responsabilités et les avantages sont largement partagés...". Dans ce contexte, cette étude tire partie du savoir-faire de plusieurs intervenants qui sont concernés par la gestion de ces structures : les propriétaires, les concepteurs, les entrepreneurs, les secteurs industriels, les centres de recherche, les intérêts régionaux et les organismes gouvernementaux. Les stratégies de maintenance sont destinées à garantir le bon fonctionnement et la sécurité au cours de l'exploitation et/ou d'augmenter le cycle de vie des structures. Par exemple, pour la corrosion provoquée par la pénétration des ions chlorure dans le béton, la peinture protectrice et/ou la reconstruction de l'enrobage sont des stratégies qui augmentent le temps nécessaire pour que la concentration seuil en chlorures atteigne les barres d'acier. Ces actions réduisent le temps d'initiation de la corrosion. La reconstruction de l'enrobage en utilisant différentes techniques de réparation a été choisie ici pour illustrer la méthodologie proposée.

1.5.1 Gestion durable des structures vieillissantes

Les progrès actuels dans l'optimisation des systèmes structuraux permettent la hiérarchisation des activités de maintenance des structures et des infrastructures vieillissantes lorsque la fonction d'optimisation est définie en termes de coûts ou de sécurité (Frangopol, 2010). La méthodologie proposée dans la section 1.4 combine le modèle probabiliste de pénétration des chlorures présenté dans les sections 1.2 et 1.3 avec une approche Markovienne pour déterminer une formulation optimale de la technique de maintenance. Les résultats de cette approche permettent aux décideurs de déterminer la stratégie de maintenance la plus rentable. Cependant, de nos jours, l'évaluation de l'impact environnemental doit être intégrée dans le processus de prise de décision pour déterminer une stratégie de gestion durable. La principale différence entre les solutions optimales "rentable" et "durable" réside dans la prise en compte des contraintes environnementales dans le second cas. Les aspects suivants doivent être considérés pour déterminer une stratégie de gestion durable :

- le choix d'un modèle représentatif de dégradation pour le phénomène étudié ;
- la formulation d'une stratégie de maintenance techniquement et économiquement réalisable qui assure des niveaux optimaux de fonctionnement et de sécurité pendant la durée de vie opérationnelle ;
- la mise en œuvre d'un cadre probabiliste approprié pour considérer les incertitudes liées au processus de dégradation et aux actions de maintenance ;
- l'établissement de critères appropriés pour l'évaluation de l'impact environnemental ; et
- l'adoption d'une procédure d'optimisation multi-objectifs destinée à minimiser les coûts et l'impact environnemental.

Cette section présente une méthodologie pour déterminer la durabilité des techniques de réparation ceci à différents fins. Par exemple, elle peut être utilisée pour améliorer la durabilité de la formulation d'une technique de maintenance et/ou elle peut être mise en œuvre pour comparer différentes techniques. La figure 1.6 montre les étapes pour l'obtention d'une formulation optimale ou durable d'une technique de maintenance. Les étapes suivantes sont nécessaires pour déterminer les deux résultats :

1. *Formulation de la stratégie* : il s'agit d'une étape cruciale dans le processus de gestion. La formulation doit tenir compte des caractéristiques du processus de dégradation, des étapes de l'entretien (inspection, réparation), de la philosophie de maintenance (préventive ou corrective) et de la faisabilité technique et économique de la stratégie choisie. Pour définir une stratégie appropriée, tous les acteurs concernés par la gestion de la structure au cours de son cycle de vie doivent participer à cette étape.
2. *Modélisation de la dégradation et des actions de maintenance* : l'expérimentation est le meilleur moyen de déterminer et d'améliorer les performances de ces alternatives. Toutefois, étant donné que ces tests sont coûteux et prennent du temps, la modélisation numérique de la dégradation et des actions de réparation s'avère essentielle pour étudier et/ou améliorer l'efficacité des stratégies de maintenance dans la plupart des cas. En outre, l'incertitude liée au processus de dégradation et aux actions de maintenance doit être intégrée pour améliorer le caractère prédictif des modèles. Bien que certaines entreprises spécialisées mettent actuellement en œuvre certains de ces aspects dans l'évaluation de la durée de vie, cette étape est principalement réalisée par les centres de recherche. Les prédictions réalistes requièrent également des données expérimentales et le retour d'expérience des maîtres d'ouvrages et des entrepreneurs.
3. *Amélioration de la formulation* : la performance de chaque stratégie de maintenance peut être améliorée par l'optimisation de ses paramètres les plus importants. Classiquement, la fonction d'optimisation vise à minimiser les coûts afin de fournir une *technique de maintenance optimale*. Néanmoins, afin de réduire l'impact environnemental, il est nécessaire d'inclure les contraintes environnementales dans le problème d'optimisation. En vertu de ces considérations, l'optimisation conduira à une *technique de maintenance durable*. Cette étape est dans une phase exploratoire et est donc principalement menée par les centres de recherche. Toutefois, la diffusion de ces techniques à des consultants est impérative. Encore une fois, les remarques des entrepreneurs et des maîtres d'ouvrages sont essentiels pour fournir des résultats réalisables.

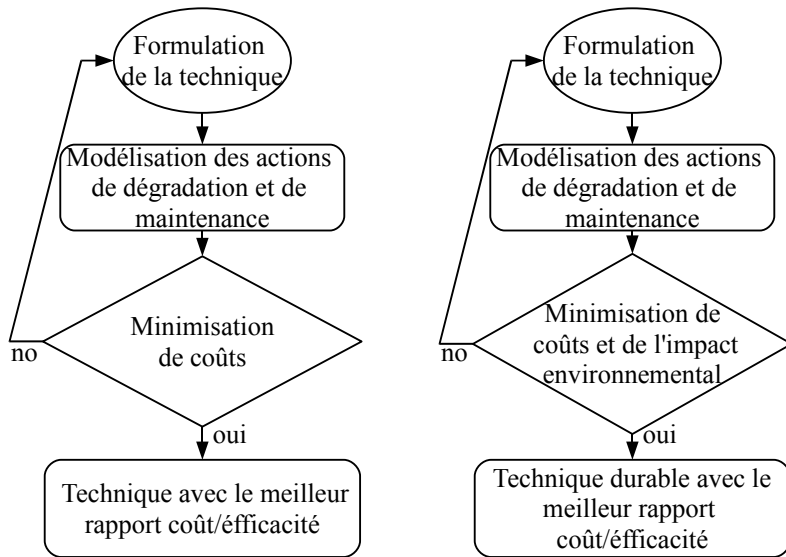


Figure 1.6 — Formulation des techniques de maintenance optimales ou durables.

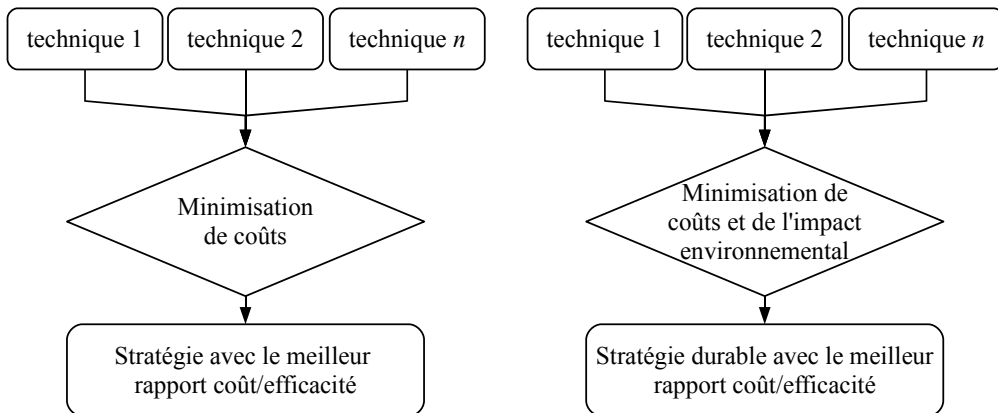


Figure 1.7 — Sélection d'une stratégie de management optimale ou durable.

En présence de différentes alternatives de maintenance, plusieurs techniques optimales/durables peuvent être formulées dans la première étape (figure 1.7). La méthode proposée peut aussi être étendue à un second niveau pour comparer la durabilité de plusieurs stratégies de maintenance.

1.5.2 Durabilité des stratégies de maintenance

Selon Struble & Godfrey (2004), les trois composantes de la durabilité sont : l'environnement, l'économie et la société. Pour atteindre son objectif, le développement durable doit assurer un équilibre entre ces éléments (Sánchez-Silva & Rosowsky, 2008). L'analyse de durabilité proposée dans cette étude considère principalement les composantes environnementales et économiques. Toutefois, la société est directement impliquée dans des décisions qui influent sur ces composants. Ainsi, l'évaluation de la durabilité des techniques de réparation est basée sur la comparaison de trois critères :

1. coûts,
2. production de déchets, et

3. émissions de dioxyde de carbone.

1.5.2.1 Coûts

Deux types de coûts sont généralement pris en compte dans l'analyse économique : les coûts des propriétaires/gestionnaires et des utilisateurs. Les coûts des propriétaires/gestionnaires sont des coûts directs dépensés au cours du cycle de vie, y compris les coûts de construction initiaux et les coûts associés à l'inspection, à la réparation, à la réhabilitation, au remplacement et à la déconstruction. Les coûts des utilisateurs représentent les frais déployés par les utilisateurs en raison des inconvénients et des perturbations de la circulation tels que les coûts des retards de voyage, les coûts d'exploitation des navires et les coûts d'accident.

Étant donné que cette étude se concentre sur la réparation des structures en béton armé, les coûts directs dépensés par l'organisme incluent les coûts liés à la maintenance (inspection, réparation et défaillance). Les coûts initiaux de construction ne sont pas inclus dans l'analyse car il est supposé qu'ils seront les mêmes pour toutes les solutions de maintenance. Comme il n'est pas possible de déterminer l'utilisation finale de la structure à la fin du cycle de vie (déconstruction ou démolition), le coût résiduel (ou de sauvetage) n'est pas considéré.

1.5.2.2 Production de déchets

Le béton a été reconnu comme le matériau le plus important et visible dans la production des déchets de construction et de démolition. Selon les estimations présentées dans le guide de ressources environnementales (American Institute of Architects, 1999), le béton produit un maximum de 67% en poids de déchets de construction et de démolition (53% en volume), avec seulement 5% actuellement recyclé. Par conséquent, la production de déchets constitue un élément majeur de la gestion de structures en béton armé.

Une évaluation exhaustive de la production de déchets devrait inclure les déchets générés pendant la production du matériau de réparation et pendant les opérations de réparation. Toutefois, compte tenu de la difficulté d'estimer les déchets générés pendant la production du béton, cette étude ne considère que les déchets produits pendant les opérations de réparation (démolition et reconstruction). La production de déchets est exprimée en m^3 de déchets générés pour réparer 1 m^3 de béton pollué. Par conséquent, les déchets produits lors de la démolition, W_d , sont égaux à 1 m^3 . Les déchets produits lors de la réparation, W_r , dépendent des caractéristiques de la technique de réparation. Connaissant W_d et W_r pour une stratégie de réparation spécifique, la production total des déchets W_T (en m^3 de déchets) est :

$$W_T = W_d + W_r \quad (1.34)$$

L'espérance totale annuelle de déchets $E[W_T]$ (en m^3 de déchets par an) est estimée en termes de l'espérance du taux annuel de réparation ν_r comme :

$$E[W_T] = \nu_r W_T \quad (1.35)$$

où l'espérance du taux annuel de réparation, exprimée en nombre de réparations par an, est déterminé par la procédure décrite dans le chapitre 5. Ce paramètre dépend principalement des caractéristiques de la technique de réparation.

1.5.2.3 Émissions de dioxyde de carbone

Selon le groupe intergouvernemental d'experts sur les changements climatiques (IPCC, 2007), les émissions de dioxyde de carbone sont identifiées comme l'une des principales causes du réchauffement climatique. Par conséquent, en tenant compte du fait que la production annuelle mondiale de 1,6 milliards de tonnes de ciment représente environ 7% des émissions mondiales de CO₂ dans l'atmosphère (Kumar Mehta, 1997), l'évaluation des émissions de dioxyde de carbone produit au cours des opérations de réparation est cruciale pour le développement durable. Cette analyse prend deux sources de dioxyde de carbone en compte :

1. les émissions produites lors du transport de matériaux, des équipements et des déchets, E_t , et
2. le CO₂ émis pendant la production du matériau de réparation, E_p .

Les émissions produites pour réparer 1 m³ de béton pollué pendant le transport sont calculées en additionnant les émissions produites lors du transport de matériaux de réparation E_m , d'équipements E_e et de l'élimination des déchets E_d :

$$E_t = E_m + E_e + E_d = \nu_t [n_m(L_m + \gamma L_d) + n_e L_e] \quad (1.36)$$

où n_m et n_e sont respectivement le nombre de voyages équivalents pour transporter les matériaux de réparation et d'équipements nécessaires pour la réparation de 1 m³ de béton pollué ; L_m , L_e et L_d sont respectivement les distances (en km) de l'approvisionnement de matériaux de réparation et d'équipements et de l'élimination des déchets ; γ est un facteur de foisonnement pour calculer le volume du béton démolî, et ν_t est le taux d'émissions de CO₂ du véhicule de transport (en grammes de CO₂ par km). Il est supposé dans l'équation 1.36 que les matériaux de réparation, les équipements et les déchets sont transportés dans le même véhicule.

Le nombre équivalent de voyages pour le transport de matériaux de réparation est calculé en fonction des déchets produits lors de la démolition et la réparation :

$$n_m = 2 \frac{W_t}{V_t} \quad (1.37)$$

où V_t représente la capacité du véhicule de transport en m³. Le nombre équivalent de voyages pour le transport des équipements est défini en tenant compte des exigences particulières d'une technique de réparation par :

$$n_e = 2 \frac{N_e}{V_r} \quad (1.38)$$

où N_e est le nombre total de voyages pour transporter les équipements nécessaires pour réparer un volume V_r de béton pollué. V_r doit être exprimé en m³. Les équations 1.37 et 1.38 sont multipliées par 2 pour prendre en compte l'aller-retour. Les distances d'approvisionnement et d'élimination sont caractéristiques d'un problème donné.

D'autre part, le CO₂ libéré pendant la production du matériau de réparation (en kg de CO₂ par an) est estimé par l'expression suivante :

$$E_p = W_T c_c \nu_p \quad (1.39)$$

où c_c est la teneur en ciment par m^3 de béton (en kg/m^3) et ν_p est le taux d'émissions de CO_2 pendant la production du matériau de réparation (en kg de CO_2/kg de matériau de réparation). Selon l'agence internationale de l'énergie (International Energy Agency, 2007), les émissions de CO_2 moyennes varient de 0,65 à 0,92 kg de CO_2 par kg de ciment pour plusieurs pays. Comme il n'existe pas d'information sur les émissions de CO_2 liées à la production des produits de réparation, une émission moyenne pondérée de $\nu_p = 0.83$ kg CO_2/kg de matériau de réparation est adoptée ici pour tous les produits de réparation.

L'espérance des émissions totales annuelles de CO_2 $E[E_T]$ (en kg de CO_2 par an) nécessaires pour réparer 1 m^3 de béton est également estimée en termes de ν_r :

$$E[E_T] = \nu_r E_T = \nu_r (E_t + E_p) \quad (1.40)$$

Cette section a présenté les trois critères qui sont considérés ici pour effectuer l'analyse de durabilité. La section suivante présentera la méthode adoptée pour la prise de décision quand le problème est régi par divers critères.

1.5.3 Prise de décision sous contraintes multi-objectifs

Un défi majeur dans la gestion des structures vieillissantes est la prise de décision satisfaisant différentes contraintes. Les propriétaires/gestionnaires sont souvent confrontés à devoir satisfaire simultanément plusieurs critères tels que : la réduction des coûts, les perturbations de la circulation, l'impact environnemental et l'amélioration de la performance, la fonctionnalité et la sécurité. Les techniques d'optimisation multi-critères ou multi-objectifs sont appropriées pour traiter ce problème. Selon Lounis (2006), les approches suivantes sont disponibles dans la littérature pour traiter ce problème :

- la théorie de l'utilité multi-attribut ;
- l'approche de la somme pondérée ;
- la programmation de compromis ;
- l'approche par contraintes ; et
- l'optimisation séquentielle.

Chaque méthode est utile en fonction des circonstances et des environnements donnés. Cependant, la programmation de compromis est plus appropriée pour les problèmes de finances ou techniques où le décideur ne peut pas se permettre de remplacer une information objective par des opinions subjectives (Ballesteros, 2007). Par conséquent, la programmation de compromis est adoptée ici pour résoudre le problème multi-objectif.

1.5.3.1 Programmation de compromis

Pour ce problème, une solution optimale doit minimiser les coûts et l'impact environnemental. La solution optimale peut être obtenue en utilisant l'optimisation multi-objectif. La programmation de compromis minimise la distance de l'ensemble des optima de Pareto à la solution "idéale". La solution idéale est définie comme celle qui donne des valeurs optimales pour tous les objectifs à la

fois. Pour m fonctions objectifs, la solution idéale peut être associée au vecteur suivant :

$$\mathbf{f}^* = [x_1^*, x_2^*, \dots x_m^*] \quad (1.41)$$

où x_i^* est la solution idéale du critère d'optimisation f_i avec $i = 1, \dots, m$. Dans ce cas particulier, il y a trois critères à évaluer : (i) les coûts, (ii) la production de déchets et (iii) les émissions de CO₂. Étant donné que chaque critère a son propre système d'unités, cette étude utilise un index multi-objectifs (MOI) pour déterminer la technique optimale (Lounis, 2006). Un MOI est défini pour chaque technique comme la déviation pondérée et normalisée de la solution idéale \mathbf{f}^* mesurée par la famille de paramètres L_p . Ainsi, la solution satisfaisante est celle qui donne un MOI minimum :

$$\text{MOI}(x) = \left[\sum_{i=1}^m w_i^p \left| \frac{x_i - x_i^*}{x_{i*} - x_i^*} \right|^p \right]^{1/p} \quad (1.42)$$

où w_i est le facteur de pondération du critère d'optimisation f_i , p est un paramètre qui indique l'importance accordée aux différentes déviations de la solution idéale, et x_{i*} est la solution avec la pire performance pour le critère f_i . La valeur de w_i varie entre 0 et 1 avec $\sum_{i=1}^m w_i = 1$. Les facteurs de pondération dépendent principalement de l'attitude des propriétaires/gestionnaires envers chaque critère. Le paramètre p varie entre 1 et ∞ . Pour $p = 1$, tous les écarts par rapport à la solution idéale sont considérés en proportion directe de leur importance, ce qui correspond à une utilité de groupe (Duckstein, 1984). Pour $p = 2$, un poids plus élevé est associé à des écarts plus importants de la solution idéale et L_2 représente la distance *euclidienne*. Pour $p = \infty$, uniquement le plus grand écart est pris en compte. L_∞ représente la distance de *Chebyshev* ou le critère mini-max qui correspond à une utilité purement individuelle (Lounis, 2006).

1.5.4 Cas d'étude : terminal agro-alimentaire

Le terminal agroalimentaire du port de Nantes Saint-Nazaire est une structure concernée par les problèmes précédemment évoqués. Ce terminal fait partie du grand port maritime de Nantes Saint-Nazaire (quatrième plus grand port en France) qui est relié à 400 ports dans le monde entier. Ce quai a été construit en 1971 et est situé à l'ouest de la France (Montoir de Bretagne) dans l'estuaire de la Loire. Les gestionnaires des activités portuaires de cette structure ont observé un problème généralisé de corrosion affectant principalement les poutres en béton armé et ont décidé d'entreprendre une réparation à grande échelle (Rosquoët et al., 2006).

1.5.4.1 Caractéristiques des techniques de réparation

La stratégie de maintenance pour le terminal agro-alimentaire consiste essentiellement en la reconstruction du béton pollué par divers techniques de réparation. Le béton contaminé est “purgé” avec des jets d'eau à haute pression (hydrodémolition) et l'enrobage est reconstruit en utilisant diverses techniques. Cette section présente les techniques utilisées pour reconstruire l'enrobage des poutres du quai qui seront comparées sur la base de la durabilité. Les exigences de base pour la sélection des techniques de réparation sont résumées comme suit :

- les techniques de réparation devront être facilement mises en œuvre pour réparer les composants de la structure situés dans les zones de marnage (par exemple, les poutres et les piles

Tableau 1.8 — Principales caractéristiques des produits sélectionnés.

Caractéristique	Technique de réparation		
	projection par voie humide	projection par voie sèche	béton coffré
Résistance initiale	20 MPa à 24 heures	11 MPa à 3 heures	4 MPa à 3 heures
Épaisseur par passe	Jusqu'à 50 mm	Jusqu'à 100 mm	Jusqu'à 100 mm
Prise	Rapide	Rapide	Rapide
Adhérence	Excellent	Excellent	Excellent

de quais).

- les techniques de réparation devront être applicables à des réparations de grande envergure ; les réparations locales sont au-delà du champ de l'étude.
- les matériaux de réparation devront avoir la même composition (composition à base de ciment) afin de centrer l'analyse sur les techniques et de faciliter les calibrations des techniques de contrôle non-destructives.

Après discussion avec les partenaires participant au projet MAREO, trois techniques de réparation ont été retenues : (1) béton projeté par voie humide ; (2) béton projeté par voie sèche et (3) béton coffré. Comme il n'y a pas d'expérience sur les performances des matériaux et des techniques de réparation, les solutions choisies ont été testées sur douze poutres qui ont été exposées à l'eau de mer pendant 80 ans puis réparées et placées en site de vieillissement naturel d'une part et plusieurs dizaines de dallettes placées en vieillissement accéléré d'autre part. Le tableau 1.8 décrit les principales caractéristiques des matériaux de réparation. En général, les matériaux ont une haute résistance initiale, une prise rapide, une excellente adhérence et une épaisseur par passe supérieure à 50 mm.

Après mise en œuvre, un retour d'expérience “chantier” a immédiatement été formalisé (Vilvoisin & Aury, 2009). Il a conduit à une comparaison selon plusieurs critères présentés dans le tableau 1.9 : coût des produits, exigence de personnel, génération de déchets et finition (pour peinture éventuelle). La génération de déchets lors de la mise en œuvre est négligeable pour la projection par voie humide et la qualité de finition est correcte et peut être améliorée par talochage. Cependant le produit utilisé pour cette réparation est le plus onéreux et exige un plus grand nombre de personnel ; le matériel doit par ailleurs être nettoyé plusieurs fois par demi-journée et des fissures de retrait peuvent être observées après 2 ou 3 jours. Bien que les déchets issus de la technique par voie sèche soient les plus importants, ils sont faciles à nettoyer si le platelage est bien confiné. Toutefois, en site maritime, les rebonds peuvent être importants et ce confinement difficile à obtenir. Enfin, cette technique implique l'utilisation d'un produit prêt à l'emploi qui est intéressant pour les opérations de grande envergure. Par son extrême fluidité (aucun besoin de vibration pour compacter le béton) et sa grande ouvrabilité, le béton coffré conduit à la meilleure finition. Son utilisation est limitée aux sites où ce coffrage peut être installé.

1.5.4.2 Évaluation des taux de réparation

Étant donné qu'il n'y a aucune information sur le temps de réparation pour chaque technique, sa performance est évaluée en termes de taux annuels de réparation, ν_r . Ces taux sont déterminés sur la base de l'approche markovienne décrite dans la section 1.4 et seront utilisés pour évaluer l'impact environnemental des stratégies de maintenance. Le principal avantage de cette méthode

Tableau 1.9 — Comparaison des différentes réparations.

Critère	Technique de réparation		
	projection par voie humide	projection par voie sèche	béton coffré
Coût du produit	17€ / 25 kg	7€ / 25 kg	5€ / 35 kg
Personnel	5 personnes	3 personnes	2 personnes
Déchets	non significatifs < 5%	importants > 30%	non significatifs < 5%
Finition	satisfaisante	rugueuse	très satisfaisante

résidé dans la prise en compte des phénomènes les plus importants qui influent sur la pénétration des chlorures et sur la maintenance y compris les incertitudes et les conséquences des décisions bonnes ou mauvaises.

Les taux de réparation seront utilisés ici pour améliorer la sélection de l'intervalle d'inspection en tenant compte des contraintes environnementales, et ensuite, pour déterminer une stratégie de gestion durable. Le taux annuel total de réparation pour un intervalle Δt d'inspection est calculé en additionnant les réparations effectuées pendant une année d'inspection avec celles produites pendant les années entre inspections. D'une manière générale, ν_r est plus élevé pour les intervalles d'inspection petits et devient constant lorsque t augmente significativement. Il est également observé que, lorsque la structure est inspectée périodiquement, ν_r est contrôlé par les réparations effectuées l'année d'inspection. Cependant, pour les grands intervalles d'inspection, ν_r dépend de la réparation induite par les défaillances entre deux inspections.

1.5.4.3 Prise de décision dans le cadre du développement durable

Comme mentionné précédemment, la méthodologie proposée peut être mise en œuvre à différents niveaux. Ainsi, la première partie de cette section illustre l'utilisation pour définir un intervalle d'inspection durable pour une technique de réparation donnée. Ensuite, la discussion s'est centrée sur la comparaison de la performance de plusieurs techniques de réparation du point de vue du développement durable.

La figure 1.8a présente un exemple qui compare les intervalles d'inspection Δt obtenus en minimisant les coûts avec ceux obtenus en ajoutant des contraintes environnementales. Ces données ont été calculées pour le béton coffré. Étant donné que le comportement est similaire pour les zones de marnage et atmosphériques, les résultats concernant la zone des marnage sont présentés. L'évaluation de la MOI utilise la distance euclidienne et suppose que la politique des maîtres d'ouvrage donne des facteurs de pondération de 0,5 pour les coûts, de 0,25 pour la génération de déchets et de 0,25 pour les émissions de CO₂. Il est observé sur la figure 1.8a que l'intervalle d'inspection qui minimise les coûts est de 8 ans, tandis que celui qui réduit les coûts et l'impact environnemental est de 14 ans. Cette différence s'explique par le fait que le taux de réparation ν_r se réduit lorsque l'intervalle d'inspection augmente. Par conséquent, l'espérance de la production totale de déchets et celle des émissions de dioxyde de carbone, qui sont directement liés à ν_r , diminuent aussi pour des grands Δt .

L'addition des contraintes environnementales dans l'évaluation de l'intervalle d'inspection génère des surcoûts. La sélection d'un intervalle donné dépend des politiques des maîtres d'ouvrage qui décident le niveau de surcoûts à dépenser pour réduire l'impact environnemental. Cette décision est régie par les aspects socio-économiques qui caractérisent une société ou un pays donné. Les priorités économiques ou environnementales sont mesurées ici par les facteurs de pondération (équation 1.42). Par conséquent, la figure 1.8b montre les surcoûts générés lorsque le facteur de pondération

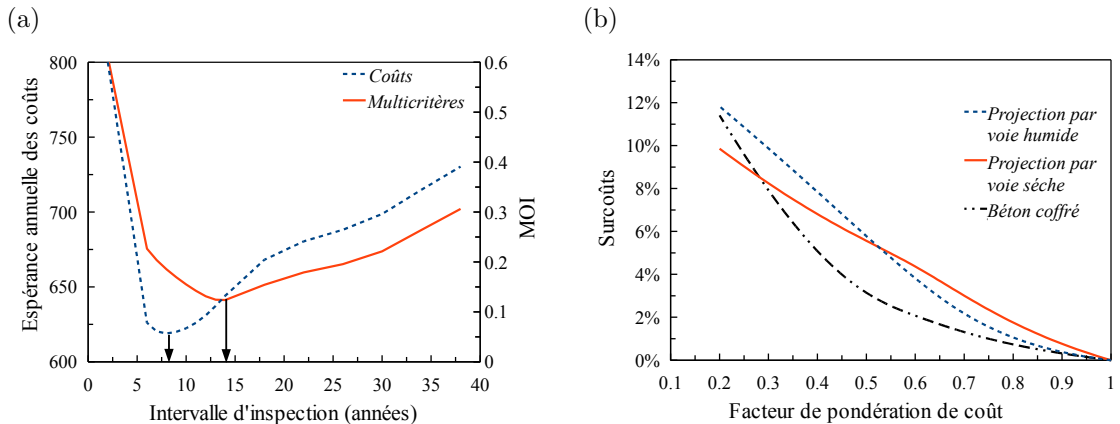


Figure 1.8 — (a) Intervalle d'inspection optimal et durable. (b) Surcoûts produits quand des contraintes environnementales sont ajoutées.

Tableau 1.10 — Coûts, génération de déchets et émissions de CO₂ pour chaque technique de réparation.

Technique	Coûts	Déchets ($\times 10^3$ m ³ /yr)	Émissions (kg CO ₂ /yr)
Projection par voie humide	468	14.59	6.82
Projection par voie sèche	362	16.44	7.85
Béton coffré	626	32.67	15.26

des coûts, w_C , varie entre 0,2 et 1. L'estimation du surcoût suppose que le facteur de pondération des déchets, w_W , et que le facteur de pondération des émissions de CO₂, w_E , sont égaux. Le facteur de pondération $w_C = 1$ implique que la décision est contrôlée uniquement par les coûts. Dans ce cas, les contraintes environnementales ne sont pas considérées et les surcoûts sont égaux à zéro. Au contraire, pour $w_C = 0$, les surcoûts convergent vers une valeur constante déterminée à un intervalle d'inspection très large où les taux de réparation sont minimums. Pour la gamme de facteurs de pondération des coûts présenté sur la figure 1.8b, les surcoûts maximaux varient de 10% à 12% en fonction des caractéristiques de chaque technique de réparation. Si les propriétaires/gestionnaires décident de donner une égale importance aux critères économiques et environnementaux ($w_C = 0.5$, $w_W = 0.25$ et $w_E = 0.25$) les surcoûts sont inférieurs à 6% pour tous les cas. Cela signifie que l'ajout des contraintes environnementales dans le processus de décision ne génère pas des surcoûts importants.

Une fois que la performance des techniques de réparation a été améliorée en considérant des critères environnementaux, un deuxième problème réside dans la comparaison de la performance de plusieurs techniques de réparation du point de vue du développement durable. Le tableau 1.10 résume les coûts, la production de déchets et les émissions de CO₂ pour chaque technique. On constate qu'il n'y a pas une alternative idéale qui minimise tous les critères. Les valeurs optimales pour chaque critère sont en gras. Le béton projeté par voie sèche est moins cher et le béton projeté par voie humide est plus respectueux de l'environnement. Par conséquent, le vecteur objectif idéal pour la zone de marnage est $\mathbf{f}^* = [362, 14.59 \times 10^3 \text{ m}^3/\text{an}, 6.82 \text{ kg CO}_2/\text{an}]$.

La figure 1.9 présente une hiérarchisation multi-critères des techniques de réparation sur la base de la minimisation du MOI (équation 1.42). Cette analyse considère l'influence des scénarios de décision 2, 3 et 4 définis dans le tableau 1.11. La comparaison de la MOI euclidienne indique que béton projeté par voie sèche est la technique de réparation la plus durable dans tous les cas. Ce com-

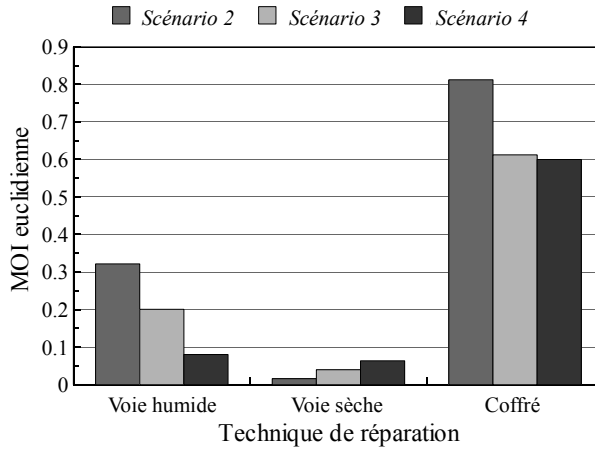


Figure 1.9 — Hiérarchisation multi-critères des techniques de réparation.

Tableau 1.11 — Scénarios pour étudier l'influence de w_i .

	Coûts, w_C	Déchets, w_W	Émissions, w_E
Scénario 1	1.00	0.00	0.00
Scénario 2	0.80	0.10	0.10
Scénario 3	0.50	0.25	0.25
Scénario 4	0.20	0.40	0.40

portement est plus évident pour le scénario 2, où les aspects économiques sont privilégiés. Il a été précédemment constaté que le béton projeté par voie humide est l'alternative la plus respectueuse de l'environnement (tableau 1.10). Cependant, cette technique n'est pas la plus durable en raison de son coût plus élevé, même pour le scénario 4 qui privilégie les contraintes environnementales. Comme prévu, compte tenu de ses coûts plus élevés et de son haut impact environnemental, le béton coffré est la solution de plus mauvaise performance. Par conséquent, ces résultats indiquent qu'une solution de maintenance durable devrait satisfaire plusieurs critères.

1.6 Conclusions et perspectives

Cette étude a mis au point une méthodologie pour la gestion durable des structures en béton armé soumises à la pénétration des chlorures. À cette fin, l'approche proposée intègre des modèles probabilistes de dégradation, d'inspection et de réparation au sein d'une méthodologie pour l'analyse de l'impact environnemental. Cette approche a été formulée et mise au point en tenant compte des recommandations des principaux acteurs qui sont liés à ce type d'ouvrages pendant sa durée de vie. Cette collaboration a joué un rôle crucial pour proposer des solutions techniquement et économiquement réalisables.

Afin d'améliorer les modèles de dégradation et d'inspection/réparation développés dans cette thèse, les recherches futures dans ce domaine doivent être dirigées vers plusieurs domaines. Par exemple, l'addition d'autres phénomènes physiques, l'amélioration de la modélisation probabiliste, la mise en œuvre d'autres techniques d'inspection ou critères de réparation, ... Les perspectives en recherche sont donc classées par rapport au type de modèle à explorer.

Modèle de pénétration des chlorures

- détermination des paramètres du modèle pour un large éventail de types de béton et matériaux de réparation à base de ciment ;
- formulation et mise en œuvre d'un modèle qui tient compte de la cinétique entre la fissuration du béton et la pénétration des chlorures ;
- étude de l'influence des variations horaires, journalières et hebdomadaires de la température et l'humidité sur la pénétration des chlorures ;
- évaluation et prise en compte de la corrélation des propriétés du matériau et des conditions climatiques à partir des données expérimentales ;
- prise en compte de la variabilité spatiale du phénomène ; et
- caractérisation et modélisation de la propagation de l'erreur dans le processus de dégradation.

Modèle d'inspection/réparation

- mise à jour des probabilités de transition à partir des données d'inspection par une approche bayésienne (i.e., Corotis et al. (2005)) et modélisation de l'inspection basée sur des techniques de contrôle non-destructifs ;
- combinaison des stratégies de réparation préventives et correctives pendant une durée de vie structurale plus importante ;
- formulation et étude de l'efficacité d'une stratégie de management qui considère les intervalles d'inspection dépendants du temps ;
- intégration des coûts d'utilisation à l'analyse et calcul de l'intervalle d'inspection optimal sur la base des grandeurs différentes de l'espérance des coûts (i.e., Schoefs et al. (2009a)) ;
- optimisation de l'efficacité des techniques et des matériaux de réparation ; et
- considération des incertitudes inhérentes à la production de déchets et aux émissions de CO₂ dans l'analyse de l'impact environnemental.

Part II

Core of the thesis

CHAPTER 2

REQUIREMENTS FOR MANAGEMENT OF CORRODING RC STRUCTURES

2.1 Introduction

Reinforced concrete (RC) structures are subjected to actions that affect performance, serviceability and safety during their operational lives (Husni et al., 2003). Depending on their origin, these actions can be external or internal and produce physical, chemical, biological and mechanical damage (Table 2.1). External actions are divided into operational and environmental actions. While operational actions result from the existence and the use of the structure (e.g., service loading, storage of chemical or biological products, etc.), environmental actions are produced by exposure to the surrounding environment (e.g., temperature, humidity, carbonation, chloride ingress, biodeterioration, etc.). On the other hand, internal actions are divided into intrinsical and induced. Intrinsical actions are related to volumetric changes that depend on material properties, construction procedures and other factors such as drying or thermal shrinkages. Induced actions are produced by changes made to improve the strength of RC or are the result of RC behavior under constant loading (i.e. prestressed or post-tensioned concrete and creep).

Under optimal conditions, the durability of RC structures is high and the variation of the structural reliability over time is not significant. However, for structures located in aggressive environments this might not be the case. Some examples of aggressive environments are those characterized by:

- high relative humidity (i.e., between 60% and 98%);
- cycles of humidification and drying, of freezing and defrosting;
- high carbon dioxide concentrations (e.g., carbonation in urban atmospheres);
- high concentration of chlorides or other salts (e.g., marine environments); or
- high concentration of sulfates and small amounts of acids (e.g., sewer pipes or residual water treatment plants).

There is a larger number of RC structures subjected to the action of chloride-induced corrosion. According to Bhide (1999), about 173,000 bridges of the interstate highway system in the United States are structurally deficient or functionally obsolete, due in part to corrosion. Other examples of structures exposed to this type of damage are ports, quays, offshore platforms, chimneys and towers situated close to the sea or exposed to the application of de-icing salts. Yunovich et al. (2001)

Table 2.1 — Actions affecting the performance of RC structures

Origin	Actions	Related damage
External	Operational	Physical, chemical and biological
	Environmental	Physical, chemical and biological
Internal	Intrinsical	Physical and mechanical
	Induced	Mechanical

reported that up to \$2.93 billion is spent annually on the repair of RC bridge decks and estimated that improved maintenance strategies can reduce this amount by up to 46%. This means that better practices of management of deteriorating RC structures will produce appreciable economic benefit.

The main objectives of this chapter are:

1. to describe the life-cycle of RC structures subjected to corrosion;
2. to present and to study the approaches for modeling deterioration and maintenance of deteriorating RC structures available in the literature and, based on this review, to select an appropriate method; and
3. to establish the research targets for modeling the deterioration process.

Section 2.2 covers the stages of the life-cycle of RC structures subjected to corrosion. Section 2.3 describes the requirements of a maintenance management system as well as the different approaches for its modeling. The conceptual framework for the proposed methodology is discussed in section 2.4. Finally, section 2.5 focuses on the needs for a comprehensive deterioration model.

2.2 Life-cycle of RC structures subjected to corrosion

Deterioration processes reduce the structural capacity of structures or structural members affecting its structural safety. In an uncertain context, the decay in structural safety produced by deterioration can be quantified in terms of a *reliability index*, β , or a *probability of failure*, p_f . Depending on the limit state, these parameters can indicate the probability of occurrence of an event such as: corrosion initiation, concrete cracking or failure. The ultimate limit state is used in this section to illustrate the effect of the deterioration process on structural safety. The event of interest for the ultimate limit state is failure and the decay in structural safety is quantified in terms of the reliability index. Taking into account the effect of deterioration on reliability, the life-cycle of corroding RC structures can be divided into three stages (Figure 2.1):

Stage 1: Immediately after construction, initial structural reliability, β_{ini} , is maximum; then, deterioration is initiated as a result of environmental actions such as: chloride ingress, carbonation, sulfate attack, biodeterioration, erosion, etc. Nevertheless, the consequences of these actions do not have significant impact on reliability until their individual or joint actions create the necessary conditions to depassivate the protective layer of the steel, e.g., low pH of concrete, specific combination of temperature and water, and oxygen availability. As a result of this new state, the reinforcement bars start to be actively corroded; the time at which this happens is called *time of corrosion initiation* (t_{ini}). If there are no cracks that accelerate the chloride ingress process, the length of this stage depends mainly on the material properties and on the surrounding environmental conditions.

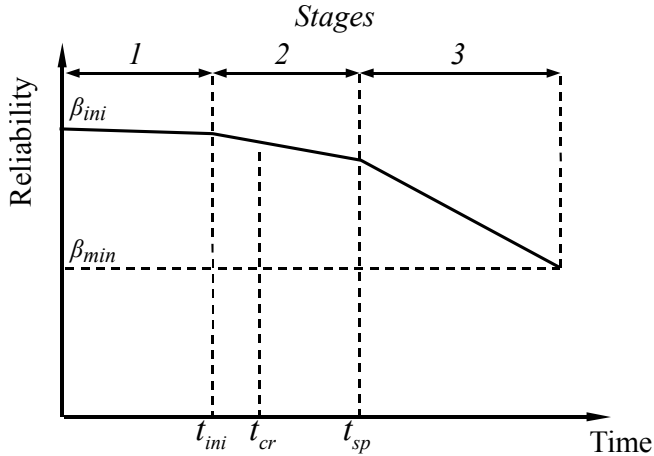


Figure 2.1 — Reliability profile for RC structures subjected to corrosion.

Stage 2: As soon as corrosion starts, corrosion products appear. Since these products have a lower density, they occupy the porous zone of the concrete surrounding the steel. When the total amount of corrosion products exceeds the amount needed to fill the porous zone, expansive pressure is induced on concrete initiating the cracking process (Liu, 1996; Liu & Weyers, 1998). In this stage, two phenomena called *crack initiation* and *crack propagation* are initiated. The former is defined as the condition for which a hairline crack of 0.05mm width appears (Vu et al., 2005). The time required to reach this point is called *time to crack initiation* (t_{cr}). The latter is measured in terms of the crack width, c_w . The time required to reach the threshold crack size, c_{wlim} (e.g., $c_{wlim} = 0.5\text{mm}$) is called *time to severe cracking*, (t_{sp}). This stage also depends on the interaction of corrosion with other deterioration processes. For example, when the structure is subjected to cyclic loading, corrosion can nucleate cracks in the reinforcement, which are in turn propagated by the loading process. This stage plays an important role in structural safety.

Stage 3: When crack width reaches a specific threshold value, there is significant increment in the corrosion rate as a result of the increase in water and oxygen availability as well as in concrete electrical conductivity (i.e., Schiessl & Raupach (1997)). This increment in the corrosion rate causes a significant decay in reliability. During this stage, the structure is more sensitive to the actions of other deterioration processes. This stage ends when reliability reaches a minimum level β_{min} after which time the serviceability and/or the safety of the structure are seriously compromised.

2.3 Deterioration and maintenance modeling

Figure 2.2 presents a conceptual description of a management system for deteriorating structures. Although Figure 2.2 focuses on one single strategy, the procedure can be used to obtain several optimal alternatives that can be after compared to find the best solution. It starts with the formulation of a maintenance strategy that should take into account:

- the kinematics of the deterioration process,
- the influence of environmental actions, and

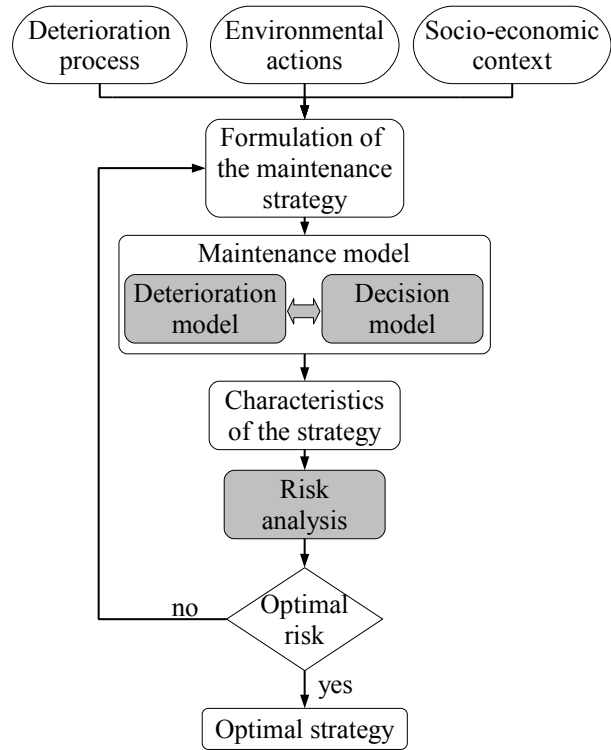


Figure 2.2 — Conceptual description of a management system.

- other socio-economic aspects proper to each problem.

The formulation includes the properties of the original and repair materials as well as the characteristics of the inspection and repair techniques –i.e., inspection interval, repair threshold, etc. The management strategy is afterwards modeled to evaluate its characteristics which are expressed in terms of repair intervals or repair rates. According to Kallen (2007), maintenance models can be roughly divided into two parts: *deterioration* and *decision* models (Figure 2.2). The deterioration model is used to assess the effect of the deterioration process on the structural performance before and after repair. The decision model is used to introduce different *decision criteria* into the deterioration model such as: inspection intervals, repair thresholds, etc. The outputs of the maintenance model ensure a given level of safety that is implicitly related to the repair threshold. A risk analysis based on costs is performed once the characteristics of the maintenance strategy (i.e., repair intervals or repair rates) have been evaluated. This cost analysis will determine if the obtained characteristics are cost-efficient or if the formulation of the maintenance strategy should be modified to optimize costs.

Management of deteriorating structures should also include the variability and uncertainties present in the deterioration process and in the maintenance actions. The main sources of uncertainty are related with properties of the construction and repair material, environmental actions (climate conditions, chloride concentrations), loading and effectiveness of inspection and repair actions. According to van Noortwijk & Frangopol (2004a) the following approaches can be used to model deterioration and maintenance actions by taking into consideration the aforementioned aspects:

- a failure rate function,

- a Markov model,
- a stochastic process, and
- a time-dependent reliability index.

The following sections describe briefly the basic principles of each approach and discuss its main advantages and shortcomings for maintenance modeling of deteriorating RC structures.

2.3.1 Failure rate function

The *failure rate function* indicates the frequency with which a structure/component fails and is computed in terms of the lifetime distribution. Maintenance based on failure rate function is useful in electrical or mechanical engineering where the states of “functioning” and “failed” are well-defined. However, depending on the use of the structure and other socio-economic aspects, the concept of structural failure in civil engineering can be related to different structural conditions such as: loss of serviceability, decrease of structural safety or even collapse. Besides, in each structural condition the structures/components can be in a range of different deterioration states. Therefore, the main disadvantage of this approach is that the failure rate cannot be measured for this problem.

2.3.2 Markov model

Nowadays, *Markov-based management systems* are widely used in management of civil engineering systems, e.g., the Arizona Management System (Golabi et al., 1982; Wang & Zaniewski, 1996), the bridge management system PONTIS (Golabi & Shepard, 1997; Thompson et al., 1998), the Swiss bridge management system KUBA-MS (Roelfstra et al., 2004), etc. Markov deterioration models discretize the structural conditions in various states. After, depending on the maintenance actions (inspection, repair or no repair) and on the kinematics of the deterioration process, the structural conditions can remain in the current state or change to other states. A stochastic process modeled by Markov chains has the Markov property that implies that the conditional probability distribution of future states depends only on the present state. In other words, the future conditions does not depend on the past.

Most part of Markov-based management systems are based on *visual inspections*. For instance, Table 2.2 presents the condition states used in the KUBA management system for management of corroding structures. It is noted that the structural condition is defined in terms of visual damages such as: cracking, spalling, spots of rust, percentage of visible reinforcement, etc. Markov models are useful to determine the condition state of structural networks and to find the critical structures that require short-term maintenance actions. However, the major limitation of this approach is that reliability is not directly incorporated in structural management (Frangopol et al., 2001).

2.3.3 Stochastic process

Time-dependent deterioration processes and maintenance actions can also be modeled by *stochastic processes*. In particular, the gamma process has been widely used to represent several deterioration processes such as: permanent erosion of dunes, longshore rock transport near berm breakwaters, loss of steel thickness due to corrosion, etc. (van Noortwijk & Frangopol, 2004a). In civil engineering problems, this approach has been implemented by the Netherlands Ministry of Transport,

Table 2.2 — Condition states defined by KUBA-MS (Roelfstra et al., 2004).

Rank	Condition state	Description
1	Good	No visible damage; only thin superficial cracks; no signs of corrosion.
2	Acceptable	Visible spots of rust and/or local spalling; thin cracks due to corrosion of the reinforcement and/or humid zones; insignificant mechanical damage.
3	Damaged	Spalling with visible reinforcement; insignificant loss of section; less than 10% of visible reinforcement; cracks and/or humid zones.
4	Bad condition	Spalling with visible reinforcement; significant loss of section; more than 10% of visible reinforcement; cracks and/or humid zones.
5	Alarming	The structure is in danger, measures are necessary before next principal inspection; immediate measures.

Public Works and Water Management (Rijkswaterstaat, van Noortwijk & Frangopol (2004b)). The Rijkswaterstaat model defines failure as the event in which the condition at time t , denoted by the resistance, drops below the failure condition due to deterioration. The main assumptions of this model are summarized as follows:

- the expected deterioration at time t is described by a power law –i.e., at^b for $a, b > 0$; and
- the coefficient of variation of the deterioration at the time at which the expected deterioration equals the failure level is unchanged.

Under these simplifications, this model offers a simplified tool for optimizing the maintenance of critical components or prioritizing maintenance of structural networks. The effect of imperfect measurements can also be added to the model (Kallen & van Noortwijk, 2003; Kuniewski et al., 2009). However, this model only focuses on one component, one failure mode and one uncertainty (coefficient of variation of the deterioration process) (van Noortwijk & Frangopol, 2004b).

2.3.4 Time-dependent reliability index

The main purpose of *reliability-based management systems* is to minimize costs by ensuring an optimal level of safety. One major advantage of this approach lies in the incorporation of the uncertainties related to material properties, environmental actions, load, inspection, repair, etc. Besides, decision-making can be based on different limit states –i.e., ultimate or serviceability and failure modes. Given that reliability is explicitly taken into account, these models represent the future generation of structure management systems. However, the main disadvantage of this approach is that the effects of maintenance are difficult to estimate (van Noortwijk & Frangopol, 2004a).

Each management approach has its advantages and shortcomings. In general, management systems are oriented to minimize costs by ensuring, implicitly or explicitly, an optimal level of safety. However, a sustainable management system should also include environmental constraints to reduce the environmental impact. It is then concluded that the selection of a given approach should take into account other aspects such as: context (civil, mechanical or electrical engineering problems), size of studied problem (network or single structures), and other socio-economic aspects (priorities of the agency, country).

2.4 Framework of the proposed management strategy

The management strategy considered in this study focuses on particular RC infrastructure (e.g., bridges, ports, etc.) subjected to chloride penetration. This strategy has been defined taking into account the needs and the feedback of the stakeholders that participate in the MAREO¹ project. The management strategy proposed in this work is mainly based on Markov modeling. This section describes the characteristics of the strategy and justifies its selection. Therefore, the discussion will turn around the following aspects:

- type and quality of inspection,
- repair criterion,
- kinematics of the deterioration process, and
- sustainability.

2.4.1 Type and quality of inspection

As mentioned before, the major weakness of Markov-based management systems is that the structural condition is defined based on the results of visual inspection. Visual inspections can be useful to prioritize maintenance actions in structural networks. However, its results depend on the subjective appreciation of the observer and cannot be used to provide a rational estimation of the decay of structural reliability produced by corrosion initiation. Another inconvenient of visual inspections is related to the fact that maintenance actions are carried out once corrosion has started. Consequently, it is difficult to know how much cross-sectional area of steel has been lost by corrosion to determine the residual structural strength.

In the proposed approach, inspection is undertaken by quantifying experimentally the chloride concentration on concrete cores. These measurements provide a rational estimate of the probability of corrosion initiation and, based on the agency's policies, are used to decide if the structure/component should be repaired. The agency defines the repair criterion that is related to the allowable risk of corrosion. When the inspection results indicate that the repair criterion has been achieved, the repair consists of rebuilding the chloride-polluted concrete by employing various techniques.

Concerning the inspection results, there are differences between *measured* and real *chloride* concentrations (Bonnet et al., 2009). These differences are related to errors in the measurement protocol, errors due to material variability and errors induced by the operator. These *imperfect inspections* can lead to erroneous management decisions. To take into account the effect of imperfect inspections this approach implements the methodology developed by Rouhan & Schoefs (2003) that combines Markov chains with decision theory.

2.4.2 Repair criterion

The repair criterion depends on the agency's policies that can perform *preventive* and/or *corrective* maintenance. Figure 2.3 presents the cross-sectional area reduction of reinforcing steel A_s and its influence on structural reliability β for both policies. In this study, preventive maintenance implies that the structure is repaired before corrosion initiation to its initial state. The advantages of preventive maintenance are:

¹MAintenance and REpair of concrete coastal structures: risk-based Optimization

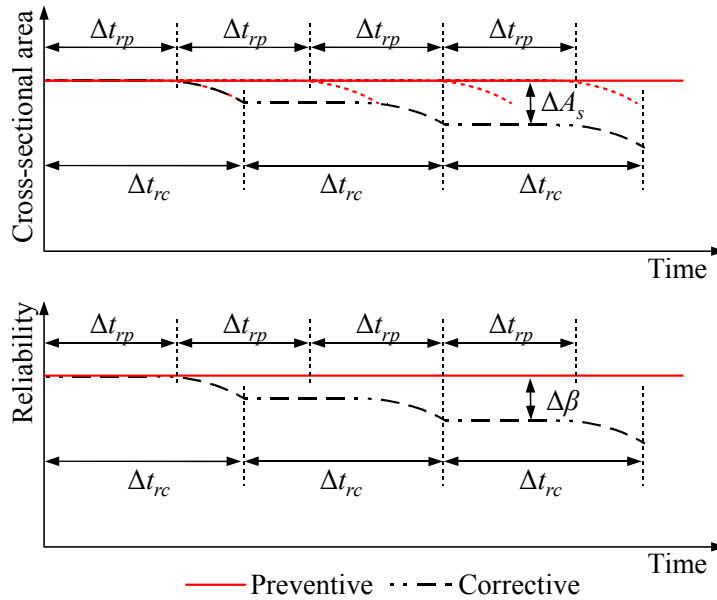


Figure 2.3 — Cross-sectional area reduction and reliability change for preventive and corrective management strategies.

1. the decrease of the residual strength produced by the loss of cross-sectional area is reduced because the corrosion initiation risks are minimized; and
2. it is possible to assume that there are no repair overcharges.

However, it can lead to overcharges produced by premature repair when the inspection/repair interval, Δt_{rp} , is not well-estimated. Corrective maintenance is undertaken after corrosion initiation. Since this repair criterion requires less interventions, the length of the repair interval computed with this criterion, Δt_{rc} , is higher than the estimated for preventive repair –i.e., $\Delta t_{rc} > \Delta t_{rp}$. However, the structural reliability is affected (reduced in $\Delta\beta$) by the loss of the effective cross-section of reinforcing steel, ΔA_s . For instance, Stewart & Val (2003) reported that the reduction in structural capacity at the time of severe cracking produced by corrosion varies between 10 and 20%. Consequently, the repair actions should include addition or replacement of reinforcing bars to ensure that the residual reliability is higher than a minimum threshold.

The selection of a given repair criterion depends on other factors such as use and/or significance of the structure or the structural member, the life-cycle length, etc. This study focuses on maintenance of transportation infrastructure (e.g., bridges, ports, etc.); more particularly on structural members located in splash and tidal zones where the probability of corrosion initiation is appreciable. After discussion with the stakeholders participating in the MAREO project, it was then decided that this study will focus on preventive maintenance.

2.4.3 Kinematics of the deterioration process

In Markov modeling, the variable of interest is discretized into M states and the kinematics of the modeled process is governed by a transition matrix. The transition matrix is then used to calculate the probability of remaining in a current state or of changing to another state. In Markov-based management systems the discretization is commonly referred to the conditions states as the presented in Table 2.2. Furthermore, the transition matrices are estimated from statistical

analysis or, in the case of lack of data, are determined from expert opinions. For instance, the KUBA management system uses expert judgment to obtain the transition probabilities between condition states 3, 4 and 5 (Table 2.2, Roelfstra et al. (2004)).

In the adopted repair strategy, decisions are taken on the basis of the inspection results that are expressed in terms of chloride concentration. Therefore, the Markov model is used herein to represent the chloride concentration at the cover depth. Chloride ingress into concrete matrix is influenced by several phenomena such as: material properties, environmental exposure, construction quality, etc. Currently, analytic models can adequately represent the influence of most part of these phenomena on chloride penetration. Consequently, this study uses a probabilistic model of chloride penetration for computing the transition probabilities. Section 2.5 presents the principles of chloride ingress and discusses the needs for a comprehensive modeling.

2.4.4 Sustainability

Design, maintenance, repair and rehabilitation of construction projects are based mainly on feasibility benefit cost analysis. However, environmental requirements demand integrated design processes directed to: (1) optimize the management of resources; (2) decrease the production of waste; and (3) reduce the environmental impact (Daigle & Lounis, 2006). These objectives can be accomplished when management is oriented to find a *sustainable* instead of a *cost-efficient* management strategy.

The availability of literature regarding evaluation of the sustainability of maintenance strategies of corroded RC structures is limited. The work of Daigle & Lounis (2006) presents a comprehensive approach to life-cycle analysis taking into account: (1) costs incurred during construction, maintenance, rehabilitation and replacement; and (2) environmental impact associated with construction and replacement. Such a study focuses on patch repair of RC bridges, uses a simplified model of chloride penetration and does not consider the randomness inherent to the phenomenon. Other research efforts have been directed to evaluate environmental impact of concrete with lower content of cementitious material (Kumar Mehta, 2004; Habert & Roussel, 2008). These studies search an optimal composition of concrete offering high structural performance and durability. Struble & Godfrey (2004) compared the sustainability of two engineering solutions used to solve the same problem (e.g., RC and steel). They found that RC requires less energy and has a lower net environmental impact than steel. Itoh & Kitagawa (2003) included carbon dioxide emissions in the life-cycle analysis of RC bridges. They compared the costs and environmental impact of a conventional bridge with those of a minimized girder bridge. They found for the same costs, the optimized solution is more environmentally friendly.

One major challenge in sustainable management of corroding RC structures lies in its multi-objective nature. A sustainable management strategy will then minimize costs and environmental impact. The problem of sustainability of management strategies can be studied at two levels. The objective, in the first one, is to optimize the environmental impact of a single maintenance strategy by maintaining reasonable costs. The second level is used to compare the performance of various maintenance strategies from a sustainability point of view. This work develops a methodology to evaluate sustainability of maintenance strategies and uses multi-objective optimization to find the solutions that minimize both criteria.

2.5 Chloride ingress into concrete

2.5.1 Chloride penetration in saturated concrete

Fick's second law of diffusion is usually used to study the flow of chlorides into concrete (Tuutti, 1982); then for the unidirectional case (flow in x -direction):

$$\frac{\partial C_{fc}}{\partial t} = D_c \frac{\partial^2 C_{fc}}{\partial x^2} \quad (2.1)$$

where C_{fc} is the concentration of chlorides dissolved in the pore solution, t is the time and D_c is the effective chloride diffusion coefficient. Assuming that concrete is an homogeneous and isotropic material with the following initial conditions: (1) the concentration is zero at $t = 0$ and (2) the chloride surface concentration is constant; the free chloride ion concentration $C(x, t)$ at depth x after time t for a semi-infinite medium is:

$$C(x, t) = C_s \left[1 - \operatorname{erf} \left(\frac{x}{2\sqrt{D_c t}} \right) \right] \quad (2.2)$$

where C_s is chloride surface concentration and $\operatorname{erf}()$ is the error function.

The closed-form solution of Fick's diffusion law can be easily used to predict the time to corrosion initiation. However, equation 2.2 is valid only when RC structures are saturated and subjected to constant concentration of chlorides on the exposed surfaces. These conditions are rarely present for real structures because concrete is a heterogeneous material that is frequently exposed to time-variant surface chloride concentrations. Besides, this solution does not consider chloride binding capacity, concrete aging and other environmental factors such as temperature and humidity (Saetta et al., 1993).

The European Union project, Duracrete (2000), proposes an expression similar to equation 2.2 which considers the influence of material properties, environment, concrete aging and concrete curing on the chloride diffusion coefficient:

$$C(x, t) = C_s \left[1 - \operatorname{erf} \left(\frac{x}{2\sqrt{k_e k_t k_c D_o \left(\frac{t_o}{t} \right)^{n_D} t}} \right) \right] \quad (2.3)$$

where k_e is an environmental factor, k_t is a factor which considers the influence of the test method to measure the diffusion coefficient D_o , k_c is an influence factor for concrete curing, D_o is the chloride migration coefficient measured at defined compaction, curing and environmental conditions, t_o is the reference period to measure D_o and n_D is the age factor. The lifetime assessment resulting from this approach is better than the one provided by equation 2.2 because it accounts for type of concrete, w/c ratio, environmental exposure (submerged, tidal, splash and atmospheric), aging and concrete curing. In addition, the strength of the Duracrete approach lies in considering the randomness related to chloride penetration. However, this method does not take into consideration: (1) chloride flow in unsaturated conditions, (2) time-variant nature and the influence of surface chloride concentration, environmental humidity and temperature; (3) chloride binding capacity; and (4) the flow of chlorides in two-dimensions. Since corrosion rates are higher in unsaturated conditions where the availability of both oxygen and water are large, a comprehensive model should include these phenomena.

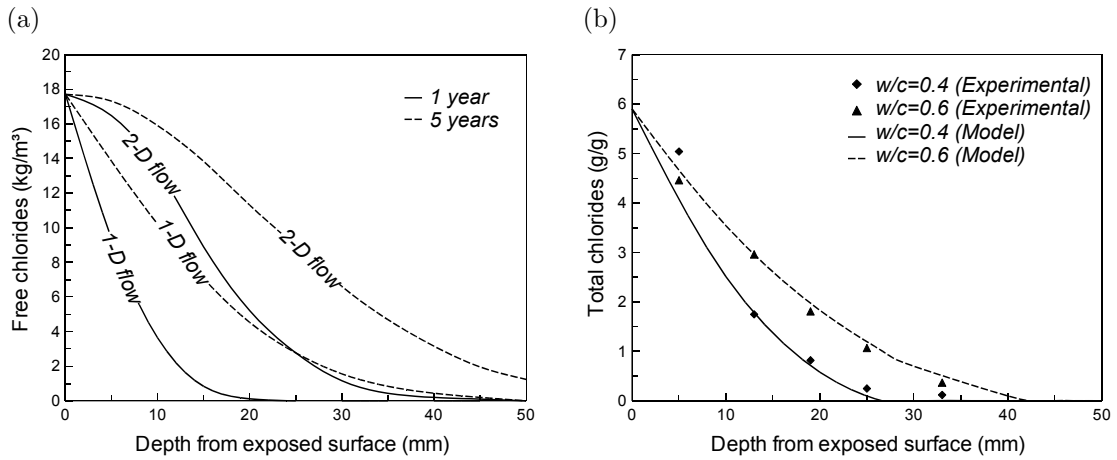


Figure 2.4 — Chloride diffusion in unsaturated environments (a) flow in one- and two-dimensions (adapted from Martín-Pérez et al., 2001); (b) comparison with experimental results (adapted from Ababneh et al., 2003).

2.5.2 Chloride penetration in unsaturated concrete

For chloride diffusion in unsaturated environments, Saetta et al. (1993) proposed a model that takes into account the effects of temperature and humidity on chloride diffusivity. This approach establishes a partial differential equation (PDE) for each physical problem (chloride transport, humidity diffusion and heat transfer) and solves the system of PDEs numerically. The model of Saetta et al. (1993) has been revised and updated by Martín-Pérez et al. (2001). The work of Martín-Pérez et al. (2001) focuses on the numerical solution and includes a corrosion rate model that takes into account the availability of oxygen at the corrosion cell. This approach allows for modeling chloride ingress in one or two dimensions (Figure 2.4a). From these results, Martín-Pérez et al. (2001) highlighted the importance of including the “corner” effects in the assessment of the time to corrosion initiation for small RC members (e.g., beams, columns). This model provides a realistic prediction of chloride penetration into concrete. However, the solution of the governing equations can only be obtained numerically and requires a larger number of parameters to find the solution.

The problem of chloride ingress into unsaturated concrete has also been addressed by Ababneh et al. (2003) who considered the interaction between the governing equations of chloride and humidity diffusion. In contrast to the model of Saetta et al. (1993), the chloride diffusion coefficient includes a factor to account for the influence of the aggregates and the cement paste. The moisture and chloride profiles were also obtained numerically by implementing an alternating-direction implicit finite-difference method. The numerical solution was compared with experimental results which in large part coincided with experimental data (Figure 2.4b). Although including a new factor to account for the effect of concrete composition may lead to a better prediction, this improvement adds more parameters which are difficult to obtain from standard laboratory tests. Furthermore, the chloride diffusion coefficient does not take into account the effect of temperature.

There are other models which, in addition to diffusion, the chloride penetration assessment includes the interaction with other mechanisms such as electrical coupling between ions, chemical activity effects and advection caused by capillarity suction flow –i.e., Samson & Marchand (2007). The multi-ionic transport model is based on the extended Nernst-Planck equation with a convective term and is valid for saturated or unsaturated conditions. Since this model needs an important

number of characterizing parameters and the methods suggested by the authors to find them are not yet widely used, it is preferable to use the model of Saetta et al. (1993) for chloride flow in unsaturated conditions.

2.6 Conclusions

1. The first part of this chapter was devoted to explain the phenomenon of chloride-induced corrosion of RC structures. This deterioration process affects the structural capacity, and consequently, reduces the structural safety. Then, taking into account the decay of the structural reliability, the life-cycle of corroding RC structures is divided into three stages. The first stage concerns the period where the initial conditions inhibit corrosion initiation. The second stage starts after corrosion initiation. Then, the reduction of the cross-sectional area of steel produced by corrosion affects the structural reliability. The third stage encompasses deterioration after severe concrete cracking where the corrosion rate, that controls the reduction of cross-sectional area of steel, is highly influenced by environmental conditions.
2. There are four approaches to model deterioration and maintenance of deteriorating structures. Each approach has advantages and disadvantages that restrict its use to specific problems. On the basis of discussions with stakeholders that are confronted to the problem of management of corroding RC structures, this study implements a Markov-based management system. Its main characteristics are summarized as follows:
 - the inspection method will be based on experimental measurements that provide an estimate of the probability of corrosion initiation;
 - decision theory will be implemented to include the effect of imperfect inspections;
 - the repair criterion will aim to preventive maintenance;
 - the kinematics of the deterioration process (chloride penetration) will be estimated from a comprehensive physical model; and
 - environmental constraints will be also added to the decision process.
3. Several models to assess chloride ingress into concrete can be found in the literature. The most common approach is based on the analytical solution to Fick's law, which can be easily implemented. However, the assumptions behind the model are difficult to justify under real exposure conditions. The Duracrete model improves the analytical solution by considering the influence of material properties, environmental exposure, aging and concrete curing. Moreover, it includes a probabilistic description of the model's governing parameters. Nevertheless, the solution is only valid for saturated conditions and does not consider the following factors:
 - the chloride binding capacity;
 - the time-dependence of temperature, humidity and surface chloride concentration; and
 - the flow of chlorides in two dimensions.

On the other hand, the models for chloride penetration in unsaturated conditions consider all the factors mentioned above leading to a more realistic assessment. Although, the solution can only be obtained numerically and requires a larger number of parameters, a model of chloride penetration in unsaturated conditions will be implemented in this work.

CHAPTER 3

MODELING CHLORIDE PENETRATION INTO CONCRETE

3.1 Introduction

In the proposed scheme of inspection/maintenance, repair is carried out when inspection results indicate that a threshold concentration of chlorides reaches the reinforcing bars. An optimal inspection interval minimizes both inspection costs and risks produced by corrosion initiation. Given that chloride penetration into concrete is a slow and complex process, numerical models are useful tools for helping owners/operators to determine an appropriate maintenance strategy. Therefore, this chapter presents a comprehensive formulation for chloride ingress modeling.

Chloride penetration is usually modeled by a simplified solution based on Fick's law. However, this solution is only valid when concrete is saturated and subjected to a constant chloride concentration in its surface. Consequently, this study implements a numerical model of chloride penetration which accounts for the following phenomena:

- chloride binding capacity of cement;
- decrease of chloride diffusivity with concrete age;
- one- and two-dimensional flow of chlorides in unsaturated concrete; and
- time-variant nature and effects of temperature, humidity and chloride concentration in the surrounding environment.

The objectives of this chapter are:

1. to describe the basic principles and the model of chloride penetration;
2. to propose and implement a numerical approach to the problem; and
3. to study the influence of time-dependence of environmental actions on chloride ingress.

Section 3.2 outlines the adopted model of chloride ingress including the effects of the surrounding environment. Section 3.3 describes the numerical solution of the governing equations and section 3.4 discusses the influence of weather on chloride ingress throughout a numerical example.

3.2 Model of chloride ingress in unsaturated conditions

The governing equations of chloride ingress consider the interaction between three phenomena (Saetta et al., 1993; Ababneh et al., 2003):

1. chloride transport;
2. moisture diffusion; and
3. heat transfer.

This section focuses on the description of each phenomenon separately. Since each phenomenon is defined by a partial differential equation (PDE), a numerical procedure is implemented to solve the nonlinear set of PDEs. It combines finite element and finite difference methods (section 3.3).

3.2.1 Chloride transport

Chloride ingress results from a complex interaction between physical and chemical processes. However, under various assumptions, this phenomenon can be simplified to a diffusion problem. Tuutti (1982) proposed modeling chloride penetration in concrete as function of time and depth using Fick's second law of diffusion:

$$\frac{\partial C_{tc}}{\partial t} = \operatorname{div} \left(D_c w_e \vec{\nabla} (C_{fc}) \right) \quad (3.1)$$

where C_{tc} is the total chloride concentration, t is the time, D_c is the effective chloride diffusion coefficient, w_e is the evaporable water content and C_{fc} is the concentration of chlorides dissolved in the pore solution –i.e., free chlorides. Equation 3.1 represents the change of the total chloride concentration as a function of the spatial gradient of free chlorides. The relationship between total and free chloride concentrations is estimated as:

$$C_{tc} = C_{bc} + w_e C_{fc} \quad (3.2)$$

where C_{bc} is the concentration of bound chlorides, i.e., chlorides chemically bound to the hydration products of cement or physically sorbed on the surfaces of gel pores (Neville, 1995). Binding isotherms relate free and bound chloride concentrations at equilibrium and are characteristic of each cementitious system. According to Tang & Nilsson (1993) and Glass & Buenfeld (2000), two common isotherms used to estimate chloride binding capacity are (1) *Langmuir isotherm*:

$$C_{bc}^L = \frac{\alpha_L C_{fc}}{1 + \beta_L C_{fc}} \quad (3.3)$$

and (2) *Freundlich isotherm*:

$$C_{bc}^F = \alpha_F C_{fc}^{\beta_F} \quad (3.4)$$

where α_L , β_L , α_F and β_F are binding constants obtained empirically from regression analyses. The values of the binding constants depend on the content of tricalcium aluminate C_3A , which affects binding capacity of cement. For instance, for a medium content of 8% of C_3A , the coefficients for the Langmuir isotherm are $\alpha_L = 0.1185$ and $\beta_L = 0.090$ (Glass & Buenfeld, 2000). For the Freundlich isotherm, Han (2007) computed the constants as functions of the content of tricalcium aluminate of cement as: $\alpha_F = 0.056 + 0.025C_3A$ and $\beta_F = 1/(1.91 + 0.076C_3A)$.

Frequently, diffusion is considered the main transport process of chlorides into concrete. However, under partially-saturated conditions, chloride ingress by convection or capillary sorption becomes an important mechanism. The proposed formulation considers chloride ingress as a com-

bination of diffusion and convection. Diffusion denotes the net motion of a substance from an area of high concentration to an area of low concentration. Convection refers to the movement of molecules (e.g., chlorides) within fluids (e.g., water). To account for both mechanisms, a convective term is added to Fick's second law of diffusion (Martín-Pérez et al., 2001):

$$\frac{\partial C_{tc}}{\partial t} = \underbrace{\text{div} \left(D_c w_e \vec{\nabla} (C_{fc}) \right)}_{\text{diffusion}} + \underbrace{\text{div} \left(D_h w_e C_{fc} \vec{\nabla} (h) \right)}_{\text{convection}} \quad (3.5)$$

where D_h is the effective humidity diffusion coefficient and h is the relative humidity. Thus, equation 3.5 can be rewritten in terms of the concentration of free chlorides. For instance, for a bi-dimensional flow of chlorides into x and y directions, equation 3.5 becomes:

$$\frac{\partial C_{fc}}{\partial t} = D_c^* \left(\frac{\partial^2 C_{fc}}{\partial x^2} + \frac{\partial^2 C_{fc}}{\partial y^2} \right) + D_h^* \left[\frac{\partial}{\partial x} \left(C_{fc} \frac{\partial h}{\partial x} \right) + \frac{\partial}{\partial y} \left(C_{fc} \frac{\partial h}{\partial y} \right) \right] \quad (3.6)$$

where D_c^* and D_h^* represent the apparent chloride and humidity diffusion coefficients, respectively:

$$D_c^* = \frac{D_c}{1 + (1/w_e) (\partial C_{bc}/\partial C_{fc})} \quad (3.7)$$

$$D_h^* = \frac{D_h}{1 + (1/w_e) (\partial C_{bc}/\partial C_{fc})} \quad (3.8)$$

where $\partial C_{bc}/\partial C_{fc}$ is the binding capacity of the cementitious system which is given by the slope of the binding isotherm (Nilsson et al., 1994).

On the other hand, experimental evidence has shown that the effective chloride diffusion coefficient depends mainly on temperature, pore relative humidity, concrete aging, cement type, porosity and curing conditions (Saetta et al., 1993). The effects of temperature, humidity and concrete aging can be estimated by correcting a reference diffusion coefficient, $D_{c,ref}$, which has been measured in standard conditions (Saetta et al., 1993; Martín-Pérez et al., 2001):

$$D_c = D_{c,ref} f_1(T) f_2(t) f_3(h) \quad (3.9)$$

where $f_1(T)$, $f_2(t)$ and $f_3(h)$ are correction expressions for temperature, aging and humidity, respectively.

The correction function for temperature is:

$$f_1(T) = \exp \left[\frac{U_c}{R} \left(\frac{1}{T_{ref}} - \frac{1}{T} \right) \right] \quad (3.10)$$

where U_c is the activation energy of the chloride diffusion process in kJ/mol, R is the gas constant ($R = 8.314 \text{ J}/(\text{mol } ^\circ\text{K})$), T_{ref} is the reference temperature in $^\circ\text{K}$ at which the reference diffusion coefficient, $D_{c,ref}$, has been evaluated ($T_{ref} = 296 \text{ }^\circ\text{K}$) and T is the actual absolute temperature in concrete in $^\circ\text{K}$. Typical values of U_c range between 32 and 44.6 kJ/mol for ordinary Portland cements (Page et al., 1981). The influence of temperature is shown in Figure 3.1a for the parameter values mentioned. It can be observed that for temperatures lower than T_{ref} chloride diffusivity is reduced. For higher values of the activation energy of the chloride diffusion process, $D_{c,ref}$ becomes

more sensitive to temperature changes. In other words, for $T > T_{ref}$ the marginal increment in temperature has more influence on $D_{c,ref}$ when U_c increases.

The correction function for aging is defined as:

$$f_2(t) = \left(\frac{t_{ref}}{t} \right)^{m_c} \quad (3.11)$$

where t_{ref} is the time of exposure at which $D_{c,ref}$ has been evaluated, t is the actual time of exposure in days and m_c is the age reduction factor. Val (2006) reported that this factor varies between 0 and 1. The relationship between $D_{c,ref}$ and f_2 for various m_c is depicted in Figure 3.1b. It can be noted that the decay of chloride diffusivity with time is slow for lower values of m_c .

The correction function for humidity is:

$$f_3(h) = \left[1 + \frac{(1-h)^4}{(1-h_c)^4} \right]^{-1} \quad (3.12)$$

where h_c is the humidity at which D_c drops halfway between its maximum and minimum values (i.e., $h_c = 0.75$ for ordinary Portland concrete (Bažant & Najjar, 1971)) and h is the actual pore relative humidity. Figure 3.1c depicts the effect of f_3 on the chloride diffusion coefficient. Since chloride diffusion depends on the amount of water in the capillary pores, the chloride diffusion coefficient is reduced for humidities lower than h_c (Bažant & Najjar, 1971).

3.2.2 Moisture diffusion

Moisture flow in concrete is also modeled by Fick's law and can be expressed in terms of pore relative humidity, h , as follows (Bažant & Najjar, 1972):

$$\frac{\partial w_e}{\partial t} = \frac{\partial w_e}{\partial h} \frac{\partial h}{\partial t} = \text{div} \left(D_h \vec{\nabla} (h) \right) \quad (3.13)$$

As well as the chloride diffusion coefficient, the humidity diffusion coefficient depends on many factors and can be estimated in terms of a reference humidity diffusion coefficient, $D_{h,ref}$ (Saetta et al., 1993):

$$D_h = D_{h,ref} g_1(h) g_2(T) g_3(t_e) \quad (3.14)$$

The function $g_1(h)$ takes into consideration the dependence on the pore relative humidity of concrete:

$$g_1(h) = \alpha_0 + \frac{1 - \alpha_0}{1 + [(1-h)/(1-h_c)]^n} \quad (3.15)$$

where α_0 is a parameter that represents the ratio of $D_{h,min}/D_{h,max}$, h_c is the value of pore relative humidity at which D_h drops halfway between its maximum and minimum values ($h_c = 0.75$ for ordinary Portland concrete) and n is a parameter that characterizes the spread of the drop in D_h . Bažant & Najjar (1971, 1972) found that the ranges for α_0 and n are [0.025, 0.1] and [6, 16], respectively. Figure 3.2a illustrates the influence of these parameters. It is noted that g_1 tends to α_0 for lower relative humidities. The parameter n controls the transition between $g_1 = \alpha_0$ and $g_1 = 1$; this transition is sudden for high values of n .

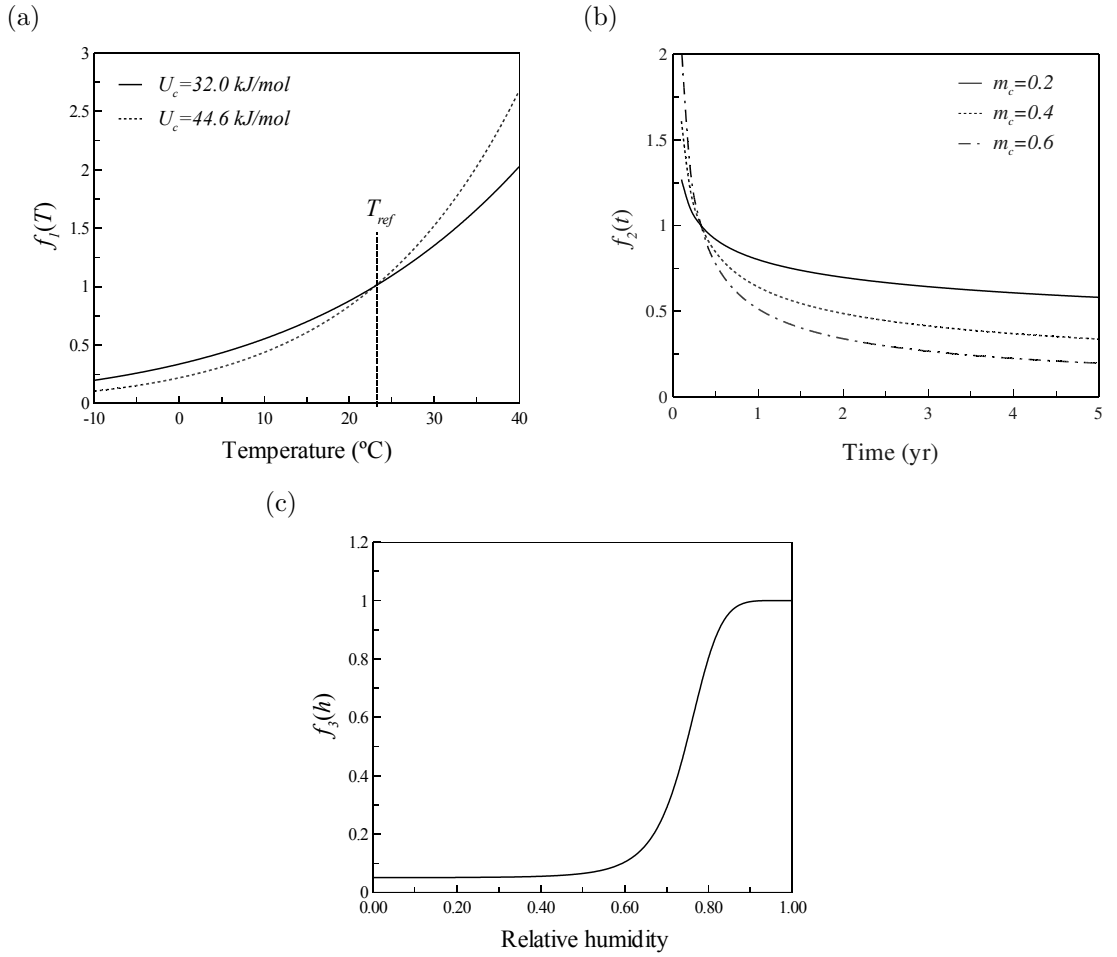


Figure 3.1 — Dependence of D_c on (a) temperature; (b) age for $t_{ref} = 120$ days; and (c) humidity for $h_c = 0.75$.

The correction function $g_2(T)$ accounts for the influence of temperature on D_h :

$$g_2(T) = \exp \left[\frac{U}{R} \left(\frac{1}{T_{ref}} - \frac{1}{T} \right) \right] \quad (3.16)$$

where U is the activation energy of the moisture diffusion process in kJ/mol and T_{ref} is the reference temperature at which $D_{h,ref}$ was measured ($T_{ref} = 276^{\circ}\text{K}$). Bažant & Thonguthai (1978) and Saetta et al. (1993) found that U ranges between 22.5 and 39 kJ/mol . The influence of temperature on D_c is presented in Figure 3.2b. As for equation 3.10, for higher values of the activation energy of the chloride diffusion process, $D_{c,ref}$ becomes more sensitive to temperature changes.

Finally, $g_3(t_e)$ considers the dependency on the degree of hydration attained in concrete:

$$g_3(t_e) = 0.3 + \sqrt{\frac{13}{t_e}} \quad (3.17)$$

where t_e represents the equivalent hydration (curing) period in days. Figure 3.2c describes the influence of g_3 on chloride diffusivity. Note that for $t_e < 28$ days the correction factor g_3 increases the chloride diffusion coefficient while for $t_e > 28$ days it tends to be constant.

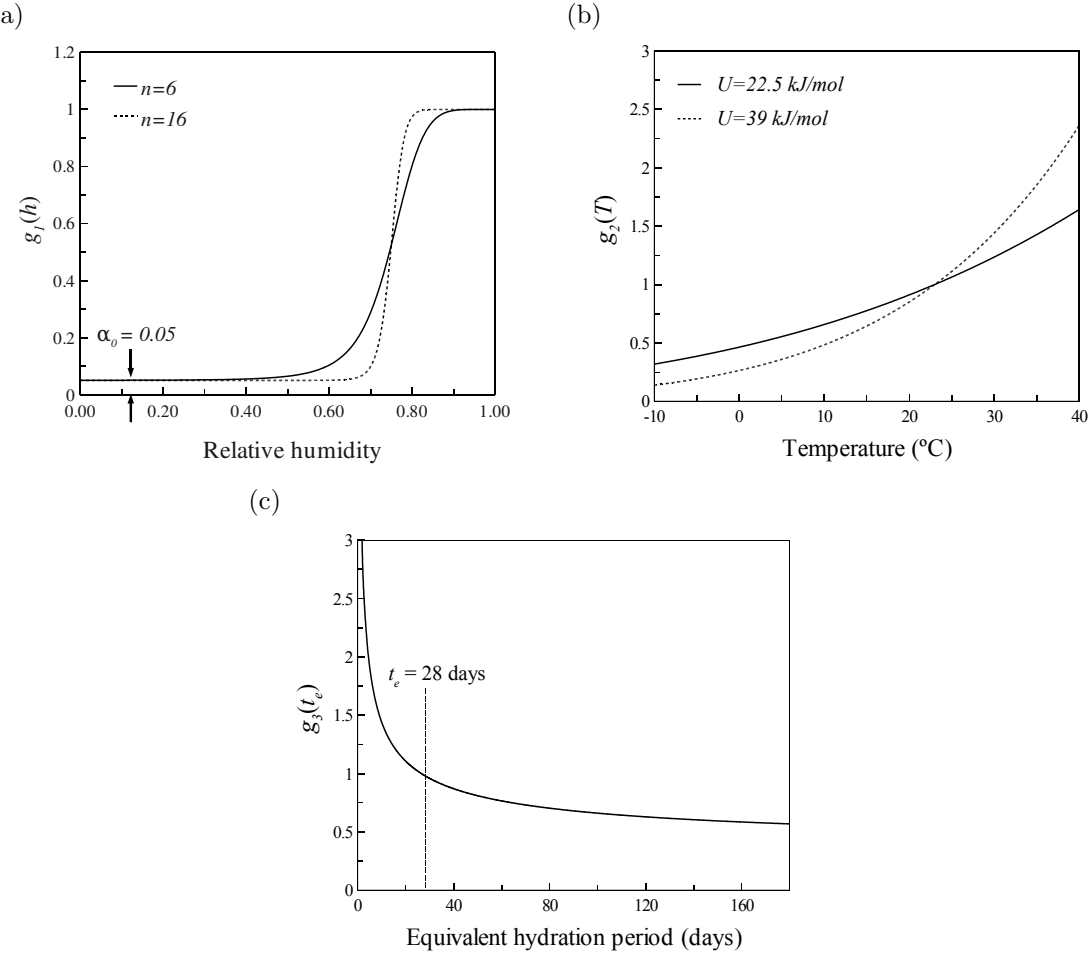


Figure 3.2 — Dependence of D_h on (a) humidity for $h_c = 0.75$ and $\alpha_0 = 0.05$; (b) temperature; and (c) equivalent hydration period.

The moisture capacity of concrete $\partial w_e / \partial h$ should also be determined to solve equation 3.13. For constant temperature, the amount of free water, w_e , and pore relative humidity, h , are related by adsorption isotherms. According to the Brunauer-Skalny-Bodor (BSB) model, the adsorption isotherm can be estimated as (Brunauer et al., 1969):

$$w_e = \frac{CkV_mh}{(1-kh)[1 + (C-1)kh]} \quad (3.18)$$

where the parameters C , k and V_m depend on temperature, water/cement ratio, w/c , and the equivalent hydration (curing) period t_e . Xi et al. (1994) developed experimental expressions for such parameters; for $t_e \geq 5$ days and $0.3 < w/c \leq 0.7$:

$$C = \exp\left(\frac{855}{T}\right) \quad (3.19)$$

$$k = \frac{(1 - 1/n_w)C - 1}{C - 1} \quad (3.20)$$

$$n_w = \left(2.5 + \frac{15}{t_e} \right) (0.33 + 2.2w/c) N_{ct} \quad (3.21)$$

$$V_m = \left(0.068 - \frac{0.22}{t_e} \right) (0.85 + 0.45w/c) V_{ct} \quad (3.22)$$

where N_{ct} and V_{ct} depend on the type of cement; e.g. for ordinary Portland cement $N_{ct} = V_{ct} = 1$. The implemented model of moisture diffusion can be used to consider several weather conditions such as drying and wetting cycles or rain. These conditions are simulated by assuming that the exposed concrete surfaces are saturated or unsaturated.

3.2.3 Heat transfer

Heat flow throughout concrete is determined by applying the energy conservation requirement to Fourier's heat conduction law (Bažant & Najjar, 1972):

$$\rho_c c_q \frac{\partial T}{\partial t} = \operatorname{div} \left(\lambda \vec{\nabla} (T) \right) \quad (3.23)$$

where ρ_c is the density of concrete (kg/m^3), c_q is the concrete specific heat capacity ($\text{J}/(\text{kg} \text{ }^\circ\text{C})$), λ is the thermal conductivity of concrete ($\text{W}/(\text{m} \text{ }^\circ\text{C})$) and T is the temperature inside concrete after time t . According to Neville (1981), the specific heat capacity for ordinary concrete ranges from 840 to 170 $\text{J}/(\text{kg} \text{ }^\circ\text{C})$. The thermal conductivity of concrete can be affected by variations in temperature and humidity. However, Bažant & Thonguthai (1978) reported that these variations are small and that λ can be assumed constant. The common range of values for thermal conductivity of concrete varies between 1.4 and 3.6 $\text{W}/(\text{m} \text{ }^\circ\text{C})$ (Neville, 1981).

3.3 Numerical solution of the governing equations

In order to study the evolution of chloride ingress into concrete, it is necessary to simultaneously solve the system of PDEs represented by equations 3.5, 3.13 and 3.23. The variation of the concentration of free chlorides, C_{fc} , humidity, h and temperature, T throughout space for a given time t is computed by using the finite element method. The evolution of spatial distribution is integrated in time by using the Crank-Nicolson method which is based on finite differences. The methodology developed by Martín-Pérez et al. (2001) to solve the system of PDEs is implemented in this study in Fortran 95. Such methodology uses linear rectangular elements and bilinear singly and doubly infinite elements to mesh the domain –i.e., Figure 3.3. Infinite elements are used to simulate the existence of material beyond the unexposed boundaries.

Fluxes of chlorides, relative humidity or heat crossing the surface define the conditions at the exposed boundaries (Robin boundary condition, Figure 3.3). The chloride flux normal to the concrete surface, J_c^s , is:

$$J_c^s = \underbrace{B_c (C_{fc}^s - C_{env})}_{\text{diffusion}} + \underbrace{C_{env} J_h^s}_{\text{convection}} \quad (3.24)$$

where B_c is the surface chloride transfer coefficient, C_{fc}^s is the concentration of free chlorides in

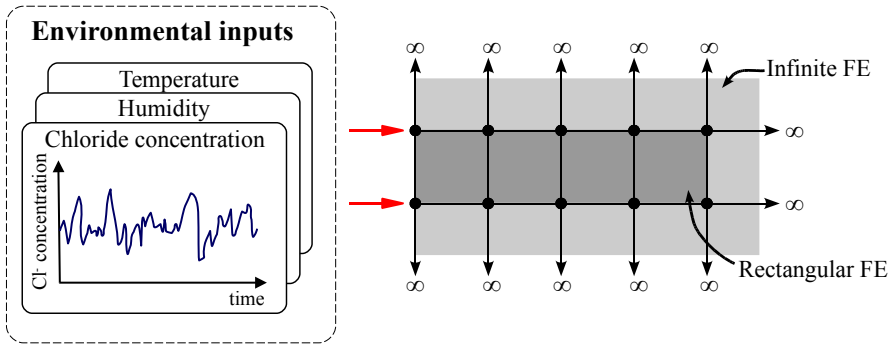


Figure 3.3 — FE mesh in one dimension.

the concrete surface, C_{env} is the concentration of chlorides in the surrounding environment and J_h^s is the humidity flux normal to the concrete surface which is defined by:

$$J_h^s = B_h (h^s - h_{env}) \quad (3.25)$$

where B_h is the surface humidity transfer coefficient, h^s is the pore relative humidity in the concrete surface and h_{env} is the relative humidity in the environment. For heat transfer, the boundary condition is given by the heat flux across the concrete surface, q^s :

$$q^s = B_T (T^s - T_{env}) \quad (3.26)$$

where B_T is the heat transfer coefficient, T^s is the temperature in the concrete surface and T_{env} is the temperature in the surrounding environment. By fitting experimental data, Saetta et al. (1993) reported that B_c varies between 1 and 6 m/s. Typical values of B_h are in the range of $2.43 - 4.17 \times 10^{-7}$ m/s (Akita et al., 1997). Finally, Khan et al. (1998) observed that B_T fluctuates between 6.2 and 9.3 W/(m²°C).

Figure 3.4 depicts the algorithm used to determine the time-dependent variation of the profiles of temperature, humidity and chlorides for one dimension –e.g., x . In the first iteration ($i = 1$), the initial values of temperature, humidity and concentration of free chlorides can be supposed constant in all points inside the mesh –e.g. T_{ini} , h_{ini} and $C_{fc,ini}$. Commonly, the concentration of free chlorides is set at zero at the beginning of the assessment. However, a given profile of chlorides can be used for existing structures. The algorithm to determine the profiles for a given time t_i can be summarized as follows:

1. the actual temperature profile is determined from equation 3.23 by considering the initial temperature profile $T(x; t = t_{i-1})$;
2. with the temperature profile estimated in the previous step $T(x; t = t_i)$ and the initial humidity profile $h(x; t = t_{i-1})$, the actual humidity profile is determined from equation 3.13; and finally;
3. equation 3.5 is solved by accounting for the actual profiles of temperature and humidity throughout the concrete and the initial values of free chlorides $C_{fc}(x; t = t_{i-1})$.

The procedure is repeated for the next step ($t_i = t_{i-1} + \Delta t$) by considering the previous profiles as initial values. The major difficulty in estimating the profiles of humidity and chlorides

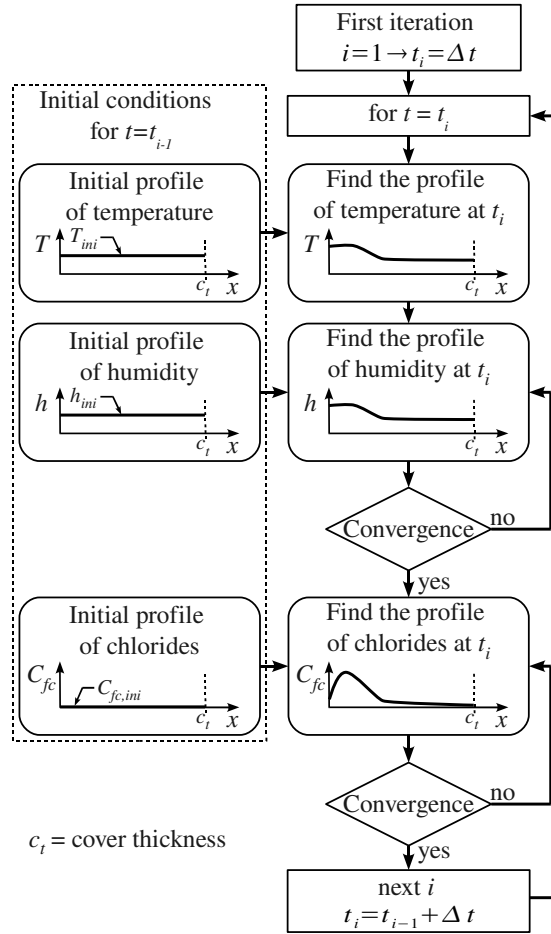


Figure 3.4 — Algorithm for estimating the profiles of temperature, humidity and chlorides.

lies in the fact that equations 3.5 and 3.13 are nonlinear because the diffusion coefficients and the isotherms depend on the actual profiles of humidity and chlorides; therefore, an iterative procedure is implemented. This procedure uses the profiles of h and C_{fc} obtained from the previous iteration, as the initial values and iterates until a given convergence criterion is reached. For example, for the profile of humidity in one dimension (i.e., x), the convergence criterion considered is:

$$\left| \frac{h(x; t_i)^{k+1} - h(x; t_i)^k}{h(x; t_i)^k} \right| \leq \varepsilon \quad (3.27)$$

where k represents the iterations to find $h(x; t_i)$, $h(x; t_i)^k$ is the humidity profile for the previous iteration, $h(x; t_i)^{k+1}$ is the humidity profile for the actual iteration and ε denotes a specified convergence parameter. A successive under-relaxation method is also implemented to increase the convergence rate. This method estimates a new humidity profile, $h^*(x; t_i)^{k+1}$, that is used as initial value for the next iteration:

$$h^*(x; t_i)^{k+1} = \omega h(x; t_i)^{k+1} + (1 - \omega)h(x; t_i)^k \quad (3.28)$$

where ω is the relaxation factor chosen in the range $[0, 1]$.

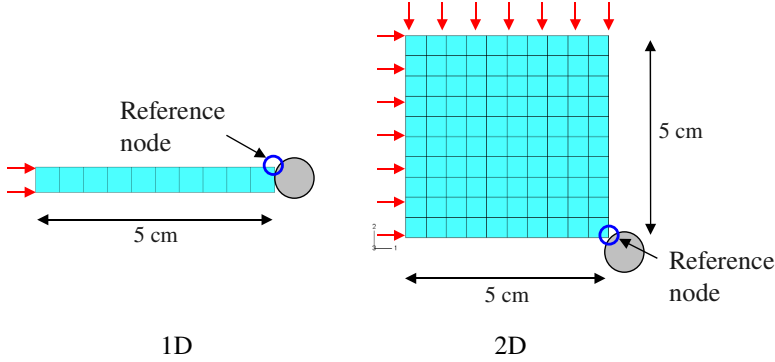


Figure 3.5 — Configuration of the calibration models.

3.3.1 Model verification

There are various commercial programs to model diffusion/convection problems (e.g., ANSYS, Abaqus, etc.). However a computer code was developed to:

- solve the non-linear PDEs –i.e., equations 3.5 and 3.13;
- implement Robin boundary conditions –i.e., equations 3.24, 3.25 and 3.26;
- use time-variant and stochastic inputs for environmental humidity, temperature, and chloride concentration; and
- consider the uncertainties involved in the problem.

This section presents a comparative study of the results obtained with: (1) the code developed, (2) commercial software (Abaqus) and (3) the analytical solution to the problem. The objective of this comparison is to validate the results.

Figure 3.5 depicts the configuration of the cases studied. The results of this analysis will focus on the reference node located at a depth of 5 cm. Taking into account the limitations of both Abaqus and the analytical solution, the following assumptions were made:

- the effective chloride diffusion coefficient is defined as constant: $D_c = 10^{-12} \text{ m}^2/\text{s}$. It means that the effects of temperature, humidity and aging are neglected;
- the chloride surface concentration is also constant: $C_s = 17 \text{ kg/m}^3$; and
- the chloride flow in one and two dimensions.

Figure 3.6 shows the chloride concentration at the reference node for one- and two-dimensional flow of chlorides. It should be noted in both cases that the solution found by Abaqus and the methodology used herein are very close. Accuracy is improved (close to the solution of Abaqus) when the time step is reduced from $\Delta t = 30$ to $\Delta t = 10$ days (Figure 3.6a). However, it can also be observed that there is a significant difference between the numerical solutions (implemented methodology and Abaqus) and the analytical solution. Given that the analytical solution remains valid in this example, it can be concluded that the numerical solution overestimates the assessment. This behavior is explained by the fact that the numerical solutions does not consider that there is material beyond the unexposed boundaries. This condition can be taken into account by adding infinite elements in such boundaries. Thus, Figure 3.7 presents a comparison between the analytical

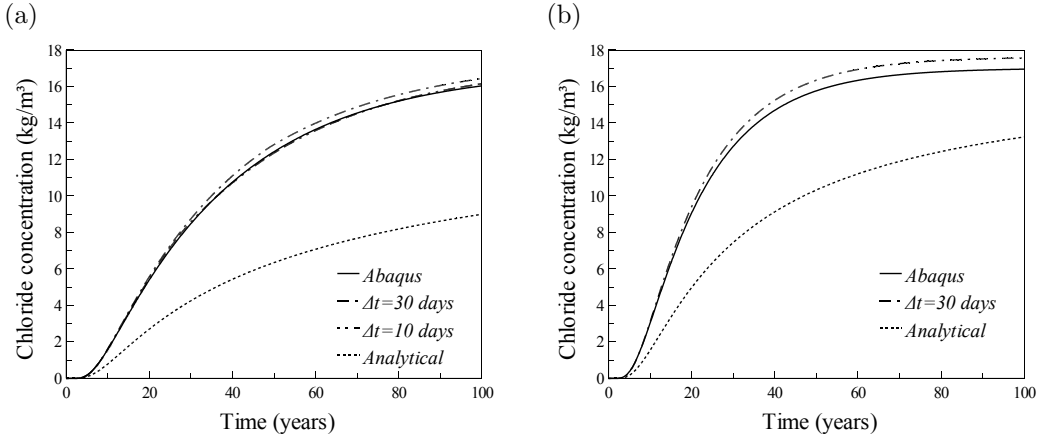


Figure 3.6 — Chloride concentration at the reference node: (a) 1D case, and (b) 2D case.

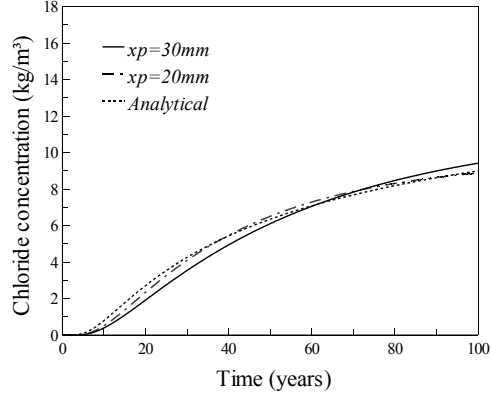


Figure 3.7 — Use of infinite elements to improve the numerical solution.

solution and the improved numerical solution by considering two lengths of infinite elements x_p . Both solutions are closer to the analytical solution. Nevertheless, the better solution corresponds to $x_p = 20\text{mm}$. From a sensitivity analysis, it has been determined that the optimal size of x_p is about 10 times the size of a finite element.

3.4 Numerical example

3.4.1 Problem description

This example studies the influence of realistic weather conditions on the kinematics of chloride penetration in RC slabs or walls. The following assumptions were considered in the analysis:

- the concentration of chlorides inside the concrete is zero at the beginning of the analysis;
- the structure is located in a partially-saturated environment;
- the flow of chlorides occurs in one-dimension (e.g., concrete slab, Figure 3.8);
- the structure is exposed to de-icing salts;
- the concrete is made with 400 kg/m^3 of Ordinary Portland Cement (OPC) with 8% of C₃A and water/cement ratio $w/c = 0.5$;

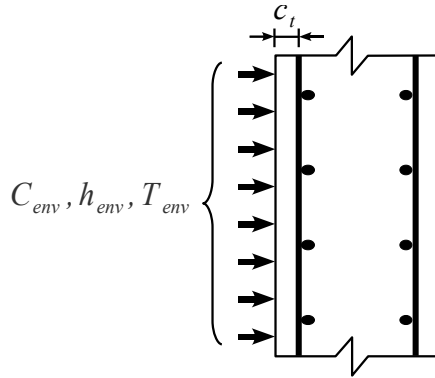


Figure 3.8 — Cross-section of the studied RC slab or wall.

- the Langmuir isotherm was used to account for the binding effect (i.e., $\alpha_L = 0.1185$, $\beta_L = 0.09$ (Tang & Nilsson, 1993; Glass & Buenfeld, 2000));
- the concrete hydration time, t_e , is 28 days; and
- the finite difference weighting factor is 0.8, and the relaxation factor ω is 0.9 for the numerical solution of the governing equations.

The evolution of environmental parameters (temperature, humidity and environmental chloride concentration) is modeled by deterministic sinusoidal functions (one year periodic) which can be considered as mean seasonal trends:

$$\phi(t) = \frac{\phi_{max} + \phi_{min}}{2} + \frac{\phi_{max} - \phi_{min}}{2} \sin(2\pi t) \quad (3.29)$$

where $\phi(t)$ is the temperature or humidity at time t , ϕ_{max} is the maximum temperature or humidity, ϕ_{min} is the minimum temperature or humidity and t is expressed in years. Figure 3.9a shows the temperature and humidity models used in this example. The values of ϕ as well as the other constants used in the example are defined in Table 3.1. In general, in chloride ingress modeling, it is assumed that the concentration of chlorides in the surrounding environment remains constant for the exposure to de-icing salts –e.g., Vu & Stewart (2000); Duracrete (2000). However, since the kinematics of chloride ingress changes as function of weather conditions, a modified model for de-icing salts exposure is adopted in this work. This model considers that during the hot seasons the chloride concentration at the surface is zero, whereas during the cold seasons it becomes time-variant (Figure 3.9b):

$$C_{env}(t) = \begin{cases} 0 & \text{for } t < t_1 \\ C_{env}^{max}(t - t_1)/(t_2 - t_1) & \text{for } t_1 \leq t < t_2 \\ C_{env}^{max}[1 - (t - t_2)/(t_2 - t_1)] & \text{for } t_2 \leq t < t_3 \end{cases} \quad (3.30)$$

where C_{env}^{max} is the maximum chloride concentration that corresponds to the minimum temperature. $C_{env}(t)$ returns to zero at the beginning of the next hot season (see Figure 3.9b). It is worthy to clarify that the value of C_{env}^{max} has been defined by considering that the quantity of chloride ions deposited during one year be the same that the average annual concentration reported in the literature, C_{env}^{ave} . For this example the value of C_{env}^{max} presented in Table 3.1 entails that $C_{env}^{ave} = 4$ kg/m³ (Vu & Stewart, 2000; Duracrete, 2000).

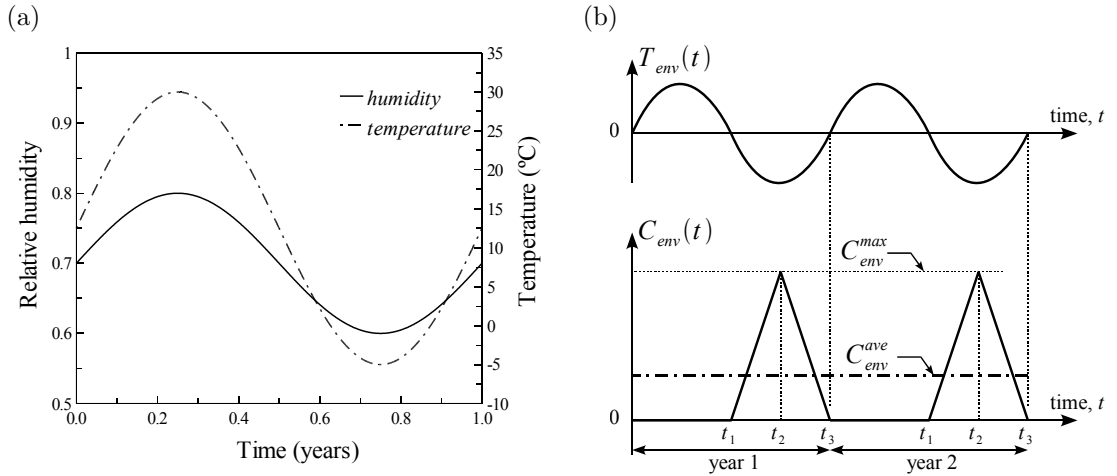


Figure 3.9 — (a) Temperature and humidity models. (b) Environmental chloride surface concentration.

Table 3.1 — Values used in the deterministic study.

Chloride transport		Moisture diffusion		Heat transfer	
Variable	Value	Variable	Value	Variable	Value
C_{env}^{max}	16 kg/m ³	h_{min}	0.6	T_{min}	-5 °C
$D_{c,ref}$	3×10^{-11} m ² /s	h_{max}	0.8	T_{max}	30 °C
U_c	41.8 kJ/mol	$D_{h,ref}$	3×10^{-10} m ² /s	λ	1.4 W/(m °C)
B_c	1 m/s	α_0	0.05	c_q	1000 J/(kg °C)
m_c	0.15	n	10	B_T	7.75 W/(m ² °C)
		U	25 kJ/mol		
		B_h	3×10^{-7} m/s		

3.4.2 Results

Figure 3.10a depicts the profiles of chlorides for different seasons after one year of exposure. The analysis begins at the end of exposure to chlorides (middle of spring) and ends when $C_{env}(t)$ is maximum (middle of winter). The *penetration front* represents the depth at which a given chloride concentration is observed. Figure 3.10a shows the advance of the penetration front for a chloride concentration of 0.20 kg/m³. Although de-icing salts are not applied during spring, summer and fall, the penetration front advances towards the reinforcement. Chloride ingress is more appreciable from spring to summer (from 7 to 16 mm) than from summer to fall (from 16 to 18.5 mm) because the chloride diffusivity increases for higher temperatures and humidities (see equations 3.10 and 3.12). It can also be observed that during winter the chloride concentration tends to C_{env}^{max} in the exposed surface.

Given that the shape of the chloride profiles depends on the season, Figure 3.10b presents the profiles after 1, 5 and 25 years of exposure at the middle of spring. These profiles were calculated for two types of environmental actions: *time-variant* and *time-invariant*. In the former, temperature, humidity and surface chloride concentration consider seasonal effects. In the latter, all the environmental variables are considered constants –i.e., $C_{env}^{ave} = 4$ kg/m³, $T_{env} = 12.5$ °C and $h_{env} = 0.7$. Note that there is a large increase in the penetration depth from 1 to 5 years in both cases. Nevertheless, the rate of chloride ingress decreases from 5 to 25 years. This reduction is due mainly to the decrease of chloride diffusivity with time –i.e., equation 3.11. If the cover thickness is $c_t = 4$ cm, the time-variant model gives larger concentrations at c_t for all exposures higher than

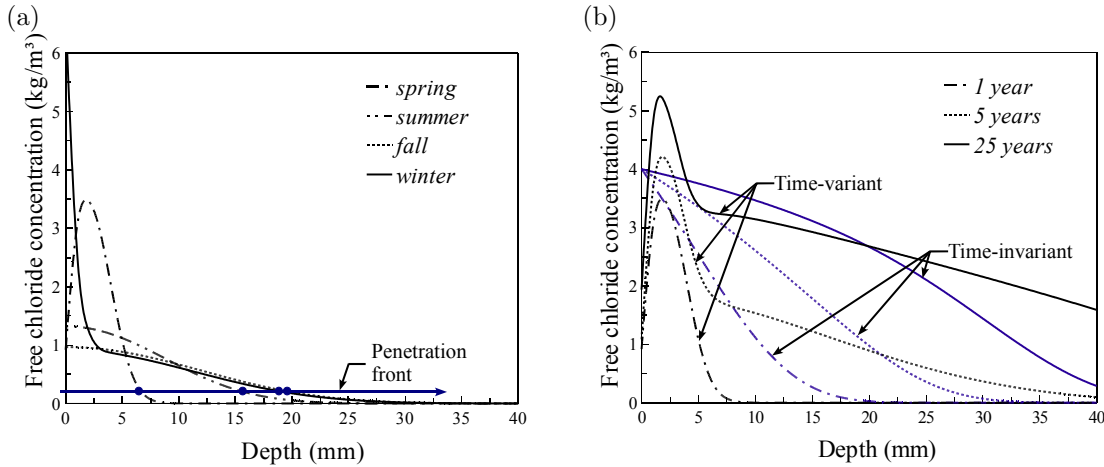


Figure 3.10 — Profiles of free chlorides for: (a) different seasons after one year of exposure, (b) the middle of spring and various times of exposure.

5 yr. This result is due to the acceleration of chloride penetration during hot and wet seasons. This analysis confirms that transfer mechanisms are very sensitive to environmental actions.

3.5 Summary and conclusions

Chloride penetration into concrete is a complex phenomenon usually modeled as a diffusion/convection process. This chapter presented a comprehensive model to assess chloride ingress into concrete considering the effects of chloride binding, temperature, humidity, concrete aging and convection. The model is represented for a system of PDEs which is numerically solved. Finally, a deterministic example is used to study the influence of environmental conditions on chloride ingress.

The conclusions of this chapter are:

1. The first part of this chapter presents the basic considerations and the model of chloride penetration. The model is based on Fick's second law of diffusion and is represented by a set of partial differential equations. The main advantage of the selected methodology is that it accounts for the following phenomena: (1) chloride binding capacity, (2) effects of concrete aging (3) two-dimensional flow of chlorides in unsaturated concrete; and (4) time-variant inputs for environmental temperature, humidity and chloride concentration. These characteristics are convenient for a realistic assessment of chloride ingress. However, the presented formulation has two main limitations: it does not consider (1) chloride ingress by capillarity sorption and (2) the effect of sun radiation on the temperature inside concrete.
2. Since the chloride penetration phenomenon is represented by a set of PDEs, a numerical approach combining finite difference and finite elements was implemented to estimate chloride penetration. The implemented model was tested by comparing its results with the results obtained for analytical and numerical solutions. In general, the results of the computer code showed significant agreement with analytical and numerical solutions.
3. A numerical example is used to evaluate the influence of time-dependence of environmental actions on chloride ingress. The results indicate that chloride diffusivity is highly influenced by changes in temperature and humidity. Therefore, a comprehensive modeling of chloride

penetration should take into account realistic models of surrounding weather conditions as well as time-variant surface chloride concentration.

CHAPTER 4

STOCHASTIC MODELING OF CHLORIDE PENETRATION

4.1 Introduction

In order to make rational predictions of structural lifetime, a comprehensive deterioration model should also take uncertainty into account. Then reliability structural analysis offers the theoretical framework for accounting uncertainties in a comprehensive decision scheme. In most engineering problems, uncertainty can be classified into the following categories (Smithson, 1989; Blockley, 1996):

1. *Randomness* is the lack of a pattern in a model or a parameter. It is present when the possible results of an experiment are known *a priori* but the result cannot be predicted with certainty.
2. *Fuzziness* is related to imprecision of definition and usually depends on the subjective interpretation of the observer. This uncertainty often results from expert appreciation of a problem. A property (e.g., cold, old, loud, etc.) is fuzzy if a precise measurement of this property can be obtained in principle.
3. *Incompleteness* refers to the quantitative insufficiency of knowledge of a problem. For this case, the information is concise, true and does not depend on the point of view of the observer. Incompleteness can be eliminated by looking for more information.

Randomness is characteristic of chloride penetration into RC structures, where there are three sources of uncertainty associated with: (1) material properties, (2) models and their parameters, and (3) environmental actions. Therefore, the purpose of this chapter is to incorporate the stochastic nature of the variables in the model of chloride penetration described in chapter 3. The specific objectives of this chapter are:

1. to present and describe the reliability problem of RC structures subjected to chloride-induced corrosion;
2. to determine the sources and the type of uncertainty related to chloride penetration;
3. to define appropriate stochastic models for all random variables;
4. to present the methodology for reliability analysis; and
5. to study the influence of probabilistic modeling and realistic weather action on corrosion initiation.

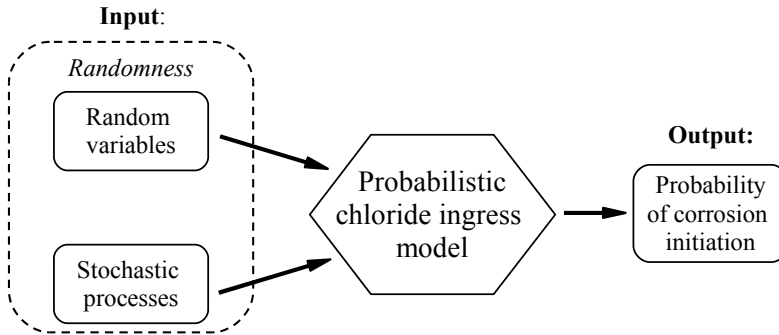


Figure 4.1 — Proposed probabilistic approach.

Figure 4.1 depicts the probabilistic approach adopted in the present study. The first part of this chapter (section 4.2) introduces some basic aspects of reliability theory and describes the limit state functions implemented in this study to compute the probability of corrosion initiation. The following sections present the inputs for the probabilistic deterioration model (Figure 4.1). The probabilistic models for the time-invariant random variables were defined on the basis of a literature review and are presented in section 4.3. Sections 4.4 an 4.5 describe the proposed stochastic models for environmental actions –i.e., humidity, temperature and environmental chloride concentrations. The weather model includes the main assumptions for modeling the effect of global warming. Sections 4.6 and 4.7 present numerical examples to illustrate the proposed probabilistic approach.

4.2 Probabilistic framework for reliability analysis

The main goal of reliability analysis is to evaluate the ability of systems or components to remain safe and operational during their life-cycle. This information can be used to define criteria for decision making, improve the management of resources, perform sensitivity studies, etc. The criterion to separate “failure” and “non failure” is defined by the so-called *limit state function* $g(\cdot)$:

$$g(\mathbf{X}) = \mathcal{R}(\mathbf{X}) - \mathcal{S}(\mathbf{X}) \quad (4.1)$$

where \mathbf{X} is the vector containing the m random variables of the problem –i.e., $\mathbf{X} = [x_1, x_2, \dots, x_m]$ and \mathcal{R} ; and \mathcal{S} represent the resistance and the demand on the system, respectively. Thus, whereas $\{\mathbf{x} : g(\mathbf{x}) > 0\}$ indicates that the system is safe (safe domain), $\{\mathbf{x} : g(\mathbf{x}) \leq 0\}$ denotes failure (failure domain), where \mathbf{x} is a realization of \mathbf{X} . The *probability of failure*, p_f , is an estimate of the safety of the system and can be evaluated as:

$$p_f = P[g(\mathbf{X}) \leq 0] = \int_{g(\mathbf{X}) \leq 0} f_{\mathbf{X}}(\mathbf{x}) dx_1 \dots dx_n \quad (4.2)$$

where $f_{\mathbf{X}}(\mathbf{x})$ is the joint probability density function of \mathbf{X} . There are several methods to evaluate equation 4.2 (Melchers, 1999; Haldar & Mahadevan, 2000). Given the complexity of the solution procedure used to estimate the evolution of chloride profiles, corrosion propagation, concrete cracking, crack nucleation and propagation, closed-form solutions for both the CDF of the time to corrosion initiation and the total corrosion-fatigue life are hard to find. Therefore, an appropriate tool to deal with this kind of problem is to use Monte Carlo simulations. This study also imple-

ments Latin Hypercube sampling to reduce the computational cost of simulations. See Appendix A for more details on these methods.

The limit state functions can be related to the following structural conditions:

- *Serviceability limit state*: this condition is satisfied when structures are still considered useful and safe although a given degree of deterioration is observed. For the problem treated in this study, the serviceability limit state is related to the *probability of corrosion initiation*.
- *Ultimate limit state*: this condition describes the state at which structural safety is highly affected and may lead to total failure or collapse. In the case of chloride-induced corrosion, the effective cross-sectional area of steel is reduced and failure occurs when the applied load exceeds the remaining resistance. The ultimate limit state is related to the *probability of failure*.

The probability of corrosion initiation and the probability of failure can be useful in lifetime assessment or maintenance/repair management of RC structures. However, the adopted strategy of maintenance is more *preventive* than *corrective*, and therefore, is based on the probability of corrosion initiation.

4.2.1 Probability of corrosion initiation

The time to corrosion initiation, t_{ini} , is defined as the time at which the chloride concentration at the steel reinforcement surface reaches a threshold value, C_{th} . This threshold concentration represents the chloride concentration for which the rust passive layer of steel is destroyed and the corrosion reaction begins. Note that this threshold is sensitive to the chemical characteristics of concrete components: sand, gravel and cement. Therefore, it is assumed herein that C_{th} is a random variable. The time to corrosion initiation is obtained by evaluating the time-dependent variation of the chloride concentration at the cover depth. This concentration is computed in the present study by solving the system of partial differential equations presented in section 3.2. The cumulative distribution function of time to corrosion initiation, $F_{t_{ini}}(t)$, is defined as:

$$F_{t_{ini}}(t) = P[t_{ini} \leq t] = \int_{t_{ini} \leq t} f_{\mathbf{X}}(\mathbf{x}) d\mathbf{x} \quad (4.3)$$

where \mathbf{X} is a vector of random variables and $f_{\mathbf{X}}(\mathbf{x})$ is the joint probability density function of \mathbf{X} . The limit state function that defines corrosion initiation can be written as:

$$g(\mathbf{X}, t) = C_{th}(\mathbf{X}) - C_{tc}(\mathbf{X}, t) \quad (4.4)$$

where $C_{tc}(\mathbf{X}, t)$ is the concentration of chlorides at the concrete cover depth c_t at time t . The probability of corrosion initiation, p_{ini} , is obtained by integrating the joint probability function over the failure domain –i.e., equation 4.2.

4.3 Time-invariant random variables

This section describes the nature and existing models that describe the random variables involved within the process of chloride penetration into concrete. The random variables considered in the proposed model are defined on the basis of previous probabilistic and deterministic studies. Before

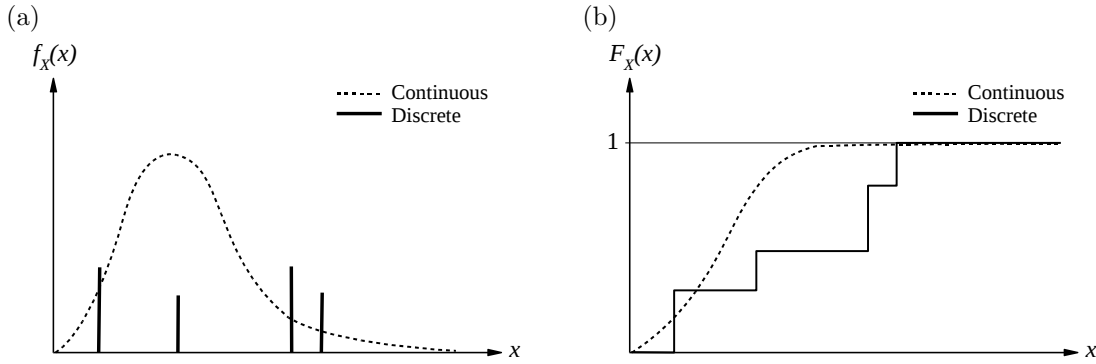


Figure 4.2 — Illustrations of (a) probability distribution function and (b) cumulative distribution function.

presenting the adopted probabilistic models, section 4.3.1 introduces some basic concepts of random variables.

4.3.1 Basic concepts of random variables

In probability theory the set of all possible outcomes for a random phenomenon defines the sample space Ω . An event E is defined as a subset of Ω containing outcomes $\omega \in \Omega$. The set of events defines the σ -algebra \mathcal{F} associated with Ω . A *probability measure* P associates numbers to events –i.e., $P : \mathcal{F} \mapsto [0, 1]$, indicating their probability of occurrence. Since the probability measures follow Kolmogorov's axioms, the *probability space* which fulfills with these characteristics is noted (Ω, \mathcal{F}, P) .

In a probability space (Ω, \mathcal{F}, P) , a *random variable* X is said to be a *measurable function* such as: $X : \Omega \rightarrow \mathcal{D}_X \subset \mathbb{R}$, where \mathcal{D}_X is a set that depends on the type of the random variable –i.e., *discrete* or *continuous*. The cumulative distribution function (CDF), $F_X(x)$, describes a random variable completely and is expressed as:

$$F_X(x) = P(X \leq x) \quad (4.5)$$

If the random variable is *discrete* (Figure 4.2), its CDF becomes:

$$F_X(x) = \sum_{i \in \mathbb{N}} p_i \mathbf{1}_{\{x^{(i)} \leq x\}}(x) \quad (4.6)$$

where p_i is the probability mass function –i.e., $p_i = P(X = x^{(i)})$ and $\mathbf{1}_{\{x^{(i)} \leq x\}}(x)$ is the indicator function of the set $\{x \in \mathbb{R} : x^{(i)} \leq x\}$, which takes the following values:

$$\mathbf{1}_{\{x^{(i)} \leq x\}}(x) = \begin{cases} 1 & \text{for } x^{(i)} \leq x \\ 0 & \text{otherwise} \end{cases} \quad (4.7)$$

If the random variable is *continuous* (Figure 4.2), the probability density function (PDF) can be computed as:

$$f_X(x) = \lim_{h \rightarrow 0, h > 0} \frac{P(x \leq X \leq x + h)}{h} = \frac{dF(x)}{dx} \quad (4.8)$$

The probability distribution of a random variable is often characterized by the n -th moments of the variable. The following moments (measures) are usually used to characterize a random variable X :

- the *expected value* or *mathematical expectation* $E[X]$ or μ_X ;
- the *variance* $\text{Var}[X]$; and
- the *coefficient of variation* $\text{COV}[X]$, which can be estimated as $\text{COV}[X] = \sigma_X / \mu_X$.

Further descriptions and details on probability theory can be found in (Gut, 2005; Ross & Pekoz, 2007).

4.3.2 Definition of the random variables

Probabilistic modeling is mainly based on robust mechanical models and on the introduction of uncertainties throughout the physical parameters involved in the phenomenon. This approach can be considered as physical modeling when each parameter has been determined experimentally (Schoefs, 2008). Nonetheless, for chloride ingress, some correction functions have been developed on the basis of the main trends of the physical phenomena –e.g., effect of aging, temperature, humidity, curing. Therefore, the choice of the random variables presented herein is mainly based on expert judgment.

This section presents the random variables used to estimate the probability of corrosion initiation from the chloride penetration model described in section 3.2. Since there are several physical phenomena involved in this deterioration problem (i.e., chloride ingress, moisture diffusion, heat transfer and corrosion initiation), the following subsections separately present the distributions and the probability measures of the random variables for each phenomenon. These random variables are valid under the following assumptions:

- The RC structures are made of ordinary Portland concrete and are subjected to unsaturated conditions.
- The COV of the random variables is independent of its mean value.
- All the random variables are independent. However, this assumption should be validated when new experimental data becomes available.

4.3.2.1 Chloride ingress

- *Reference chloride diffusion coefficient, $D_{c,\text{ref}}$* : Since the chloride diffusion coefficient is highly dependent on relative humidity, temperature and age, Saetta et al. (1993) measured this parameter under determined conditions. Although the variability induced by such variables is controlled, they reported that $D_{c,\text{ref}}$ also depends on the w/c ratio. For unsaturated conditions this coefficient is equal to $3 \times 10^{-11} \text{ m}^2/\text{s}$ for $w/c = 0.50$. This thesis takes the chloride diffusion coefficient estimated for $w/c = 0.50$ as mean value –i.e., $\mu_{D_{c,\text{ref}}} = 3 \times 10^{-11} \text{ m}^2/\text{s}$. On the basis of (Duracrete, 2000; Val & Trapper, 2008), $D_{c,\text{ref}}$ is defined as log-normally distributed with $\text{COV}[D_{c,\text{ref}}] = 0.2$.
- *Activation energy of the chloride diffusion process, U_c* : According to Collepardi et al. (1972) and Page et al. (1981), this parameter depends mainly on the porosity and the type of cement.

Based on experimental values reported by Page et al. (1981), it is supposed that U_c follows a beta distribution over the range [32,44.6] kJ/mol with a mean value $\mu_{U_c} = 41.8$ kJ/mol and $\text{COV}[U_c] = 0.1$.

- *Age reduction factor, m_c :* Mangat & Molloy (1994) report that the age reduction factor, m_c , depends on the concrete mix proportions, the type of cement, the type of curing applied to concrete and the w/c ratio. Since m_c may have values between 0 and 1, Val (2006) proposed to model m_c by a beta random variable distributed over [0,1]. Its mean corresponds to ordinary Portland cement $\mu_{m_c} = 0.15$ with $\text{COV}[m_c] = 0.3$.

4.3.2.2 Moisture diffusion

- *Reference humidity diffusion coefficient, $D_{h,\text{ref}}$:* For ordinary Portland cements and different w/c ratios, Bažant & Najjar (1971, 1972) reported that $D_{h,\text{ref}}$ ranges from 1.157×10^{-10} to 4.630×10^{-10} m²/s. In unsaturated conditions, Saetta et al. (1993) report the following values for this coefficient: 3×10^{-10} m²/s for $w/c = 0.50$ and 1×10^{-10} m²/s for $w/c = 0.75$. The chloride diffusion coefficient estimated for $w/c = 0.50$ is adopted as mean value –i.e., $\mu_{D_{h,\text{ref}}} = 3 \times 10^{-10}$ m²/s. As suggested by Val & Trapper (2008), $D_{c,\text{ref}}$ is modeled by a log-normal distribution with $\text{COV}[D_{h,\text{ref}}] = 0.2$.
- *Parameter representing the ratio $D_{h,\text{min}}/D_{h,\text{max}}$, α_0 :* Taking into account that α_0 varies between 0.025 and 0.1 (Bažant & Najjar, 1971, 1972), Val & Trapper (2008) proposed to model this parameter with a beta distribution ranging in such interval. Consequently, the mean is set as $\mu_{\alpha_0} = 0.05$ with $\text{COV}[\alpha_0] = 0.2$.
- *Parameter characterizing the spread of the drop in D_h , n :* Bažant & Najjar (1971, 1972) found that the parameter characterizing the spread of the drop in D_h , n , ranges between 6 and 16 for typical concretes. On the basis of these results, Val & Trapper (2008) recommend to model this parameter with a beta distribution ranging between 6 and 16. The suggested mean is $\mu_n = 11$ and $\text{COV}[n] = 0.1$.

4.3.2.3 Heat transfer

- *Thermal conductivity of concrete, λ :* Typical values of thermal conductivity of ordinary concrete vary between 1.4 and 3.6 W/(m·°C) (Neville, 1981). This work assumes that λ follows a beta distribution ranging between the limits established experimentally. The mean of the random variable is $\mu_\lambda = 2.5$ W/(m·°C) and $\text{COV}[\lambda] = 0.2$.
- *Concrete specific heat capacity, c_q :* Neville (1981) reported that the common range of values of the specific heat capacity for ordinary concrete, c_q , is between 840 and 1170 J/(kg·°C). On the basis of these results, it is adopted a beta distribution over [840,1170] J/(kg·°C) for c_q . The mean of this random variable is equal to $\mu_{c_q} = 1000$ J/(kg·°C) and $\text{COV}[c_q] = 0.1$.
- *Density of concrete, ρ_c :* The density of concrete depends on many factors as weight, gradation and percentage of aggregates, air content, admixtures, etc. Taking as mean a typical value for the density of normal concrete (i.e., $\mu_{\rho_c} = 2400$ kg/m³), it is assumed herein that this variable is normally distributed with $\text{COV}[\rho_c] = 0.2$.

Table 4.1 — Probabilistic models for the chloride threshold concentration (Duracrete, 2000).

Definition	w/c	Exposure conditions	Distribution	Mean (wt.-% cement)	Standard dev. (wt.-% cement)
1	— ^a	— ^a	Normal	0.48	0.15
2	0.5	Constantly water saturated	Normal	1.60	0.20
	0.4	Constantly water saturated	Normal	2.10	0.20
	0.3	Constantly water saturated	Normal	2.30	0.20
	0.5	Constantly humid	Normal	0.50	0.10
	0.4	Constantly humid	Normal	0.80	0.10
	0.3	Constantly humid	Normal	0.90	0.15

^athere is no influence of these parameters

4.3.2.4 Corrosion initiation

- *Chloride threshold concentration, C_{th} :* The sources of uncertainty affecting C_{th} are related with:
 1. structural properties and environmental conditions, and
 2. the definition of the threshold level.

Concerning structural properties and environmental conditions, the most important factors that influence the assessment of C_{th} are summarized as follows (Martín-Pérez, 1999):

- the condition of the steel/concrete interface, which influences the level of active inhibitor through its effective buffering capacity and the availability of chloride ions by restricting their mobility;
- the properties of concrete, such as binding capacity, pH of the pore solution, and barrier properties; and
- the exposure conditions, such as the source and type of chloride contamination, temperature, and moisture content.

On the other hand, based on the definition of the chloride threshold level, several values of C_{th} can be estimated for the same problem. To avoid this inconsistency, Duracrete (2000) proposes two definitions of the threshold level:

Definition 1 threshold chloride content at which depassivation of the steel surface and iron dissolution begins. C_{th} for this definition leads to visible corrosion damage on the concrete surface and does not take into account weather effects.

Definition 2 threshold chloride content which leads to deterioration or damage of RC concrete structures. For this definition, C_{th} depends also on the factors affecting the corrosion rate (e.g., on material properties and weather conditions).

From these definitions, it is expected that the threshold chloride concentrations corresponding to definition 2 be higher than those corresponding to definition 1. There are many proposals to the probabilistic modeling of C_{th} (see Duprat (2007) for a description of other models). Nevertheless, this work adopts the values presented in (Duracrete, 2000) to account for the randomness of the threshold chloride concentration.

- *Concrete cover, c_t :* The thickness of the concrete cover influences the time to corrosion initiation and the time to excessive cracking. Casciati et al. (1991) report that the mean of

the cover depth at the top and bottom steels varies within an extremely broad range from -20 to 20 mm ($-20 \text{ mm} < \mu_{c_t} \leq 20 \text{ mm}$) with a standard deviation ranging from 5 to 15 mm. These variations are attributed to construction methods and staff during execution.

Several probabilistic studies usually treat this random variable as normal or log-normal (Duracrete, 2000; Val & Stewart, 2003). However, based on the study of McGee (2000), this study models the concrete cover as a truncated normal variable (lower bound). The mean of c_t is defined by its nominal value, its coefficient of variation is assigned according to (Duracrete, 2000; McGee, 2000; Val & Stewart, 2003) –i.e., $\text{COV}[c_t] = 0.25$, and its truncation point is set at 10 mm.

4.4 Stochastic model for humidity and temperature

In order to make a good estimation of the time to corrosion initiation, it is important to implement a model that realistically reproduces environmental temperature and humidity. This section proposes a weather model that adds a stochastic perturbation to a sinusoidal mean trend representing seasonal variations. It is assumed that this model is sufficient for representing long-term variability.

A scalar stochastic process $H(\mathbf{x}, \omega)$ is a collection of random variables indexed by a continuous parameter $\mathbf{x} \in \mathcal{B}$, where \mathcal{B} is an open set of \mathbb{R}^d which describes the geometry of the physical system ($d = 1, 2$, or 3 in practice). $H(\mathbf{x}_0, \omega)$ is a *random variable* for a given $\mathbf{x}_0 \in \mathcal{B}$ or is a *realization* of the process for a given outcome $\omega_0 \in \Omega$. For the sake of simplicity, this study focuses only on scalar stochastic processes.

A stochastic process is called *Gaussian* if all its components $\{H(\mathbf{x}_1), \dots, H(\mathbf{x}_q)\}$ are Gaussian. Gaussian stochastic processes are of practical interest because they are completely defined by their mean $\mu(\mathbf{x})$ and their autocovariance function:

$$C_{HH}(\mathbf{x}, \mathbf{x}') = \text{Cov}[H(\mathbf{x}), H(\mathbf{x}')] \quad (4.9)$$

The autocorrelation function $\rho(\mathbf{x}, \mathbf{x}')$ is also used to describe the process:

$$\rho(\mathbf{x}, \mathbf{x}') = \frac{C_{HH}(\mathbf{x}, \mathbf{x}')}{\sigma(\mathbf{x})\sigma(\mathbf{x}')} \quad (4.10)$$

where the variance function $\sigma^2(\mathbf{x})$ is:

$$\sigma^2(\mathbf{x}) = C_{HH}(\mathbf{x}, \mathbf{x}). \quad (4.11)$$

According to Ghanem & Spanos (1991), there are two efficient methods to manage stochastic processes: Karhunen-Loève expansion or polynomial chaos. Taking into account the complexity of the implementation and the computational time, Karhunen-Loève expansion was selected as the most suitable method to represent the uncertainty of humidity and temperature.

4.4.1 Karhunen-Loève discretization of humidity and temperature

Analogous to Fourier series, the Karhunen-Loève expansion represents a stochastic process as a combination of orthogonal functions on a bounded interval –i.e., $[-l, l]$. The development of a stochastic process by the Karhunen-Loève method is based on the spectral decomposition of the covariance function of the process. Since the covariance function is symmetrical and positive

definite, its eigenfunctions are orthogonal and form a complete set of deterministic orthogonal functions, $f_i(t)$, which are used to represent the stochastic process. The random coefficients of the process $\xi_i(\omega)$ can also be considered orthogonal or, in other words, statistically uncorrelated.

Let $\kappa_\phi(t, \omega)$ be a stochastic process describing the humidity or temperature ϕ and defined over the domain \mathcal{B} , with ω belonging to the space of random events Ω . $\kappa_\phi(t, \omega)$ can thus be expanded as follows (Ghanem & Spanos, 1991):

$$\kappa_\phi(t, \omega) \simeq \bar{\kappa}_\phi(t) + \sum_{i=1}^{n_{KL}} \sqrt{\lambda_i} \xi_i(\omega) f_i(t) \quad (4.12)$$

where $\bar{\kappa}_\phi(t)$ is the mean of the process, $\xi_i(\omega)$ is a set of standard random variables (i.e., centered normal random variables), n_{KL} is the number of terms of the truncated discretization, t is the time and λ_i are the eigenvalues of the covariance function $C_{\kappa_\phi \kappa_\phi}(t_1, t_2)$ resulting from the evaluation of the following expression:

$$\int_{\mathcal{B}} C_{\kappa_\phi \kappa_\phi}(t_1, t_2) f_i(t_2) dt_2 = \lambda_i f_i(t) \quad (4.13)$$

The solution of equation 4.13 can be determined analytically when the covariance function is exponential or triangular (Ghanem & Spanos, 1991). This study assumes that the processes of humidity and temperature are stationary and have an exponential correlation of the form:

$$\rho_{\kappa_\phi \kappa_\phi}(t_1, t_2) = e^{-|t_1 - t_2|/b_e} \quad (4.14)$$

where b_e is the correlation length and must be expressed in the same units of t . Then, accounting for the stationarity of the process the following transcendental equations are obtained (Ghanem & Spanos, 1991):

$$\begin{cases} c_e - \varphi \tan(\varphi l) = 0 \\ \text{and} \\ \varphi + c_e \tan(\varphi l) = 0 \end{cases} \quad (4.15)$$

where $c_e = 1/b_e$. If the solution of the second equation is φ^* , the eigenfunctions are:

$$f_i(t) = \frac{\cos(\varphi_i^* t)}{\sqrt{l + \sin(2\varphi_i^* l)/2\varphi_i^*}} \text{ for even } i \quad (4.16)$$

and

$$f_i^*(t) = \frac{\sin(\varphi_i^* t)}{\sqrt{l - \sin(2\varphi_i^* l)/2\varphi_i^*}} \text{ for odd } i \quad (4.17)$$

The corresponding eigenvalues after solving equation 4.13 for these functions are:

$$\lambda_i = \frac{2c_e}{\varphi_i^2 + c_e^2} \text{ for even } i \quad (4.18)$$

and

$$\lambda_i^* = \frac{2c_e}{\varphi_i^{*2} l + c_e^2} \text{ for odd } i \quad (4.19)$$

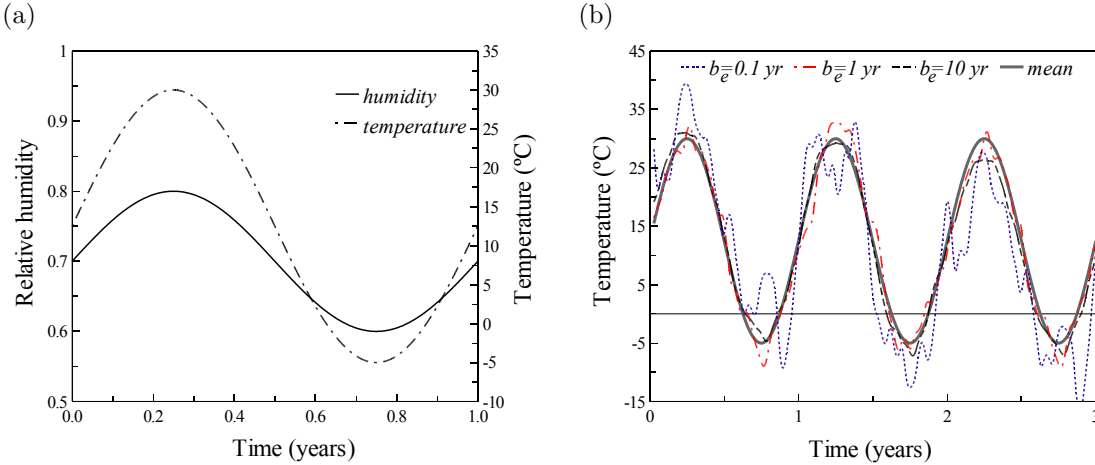


Figure 4.3 — Modeling weather: (a) mean trends of temperature and humidity and (b) stochastic realizations for temperature.

where φ_i and φ_i^* are the solutions of the transcendental equations –i.e., equation 4.15.

In order to model the effect of seasonal variations of weather, the mean of the stochastic process $\bar{\kappa}_\phi(t)$ (equation 4.12), is modeled as a sinusoidal function (Figure 4.3a):

$$\bar{\kappa}_\phi(t) = \frac{\phi_{max} + \phi_{min}}{2} + \frac{\phi_{max} - \phi_{min}}{2} \sin(2\pi t) \quad (4.20)$$

where $\bar{\kappa}_\phi(t)$ represents temperature or humidity at time t , ϕ_{max} is the maximum temperature or humidity, ϕ_{min} is the minimum temperature or humidity and t is expressed in years. Daily variations can also be considered in the model for weather as a sinusoidal function. However, this study does not take the effect of daily variations into account due to the fact that the analyses focus on long-term performance of RC structures. In this approach, both the covariance and the correlation length of weather parameters can be determined based on real measurements. Figure 4.3b shows some realizations of the stochastic process representing temperature where $\phi_{max} = 30^\circ\text{C}$ and $\phi_{min} = -5^\circ\text{C}$; the correlation lengths are 0.1, 1 and 10 years; and the truncated discretization includes 30 terms ($n_{KL} = 30$). Note that smaller correlation lengths imply that the stochastic process is less correlated, and therefore, the corresponding stochastic process is far from the mean and extreme values are frequently observed.

4.4.2 Effect of global warming on weather

Weather measurements on global warming anticipate changes in the mean temperature and humidity in the coming years (IPCC, 2007). It has been found that eleven of the twelve years during the period 1995–2006 rank among the warmest years since the beginning of the instrumental record of global surface in 1850. Besides, the linear warming trend over the last 50 years (0.13°C per decade) almost doubles the measurements during the last 100 years (0.076°C). Based on these measurements and different policies against global warming, the Intergovernmental Panel on Climate Change has announced a rise in the mean temperature from 1 to 6.4°C over the next 100 years. The basic science of weather modeling, including the greenhouse effect, is well understood and has been widely discussed. Most of these models demand large computational efforts because they integrate dynamical and physical equations to describe the complete climate system (Houghton, 2005).

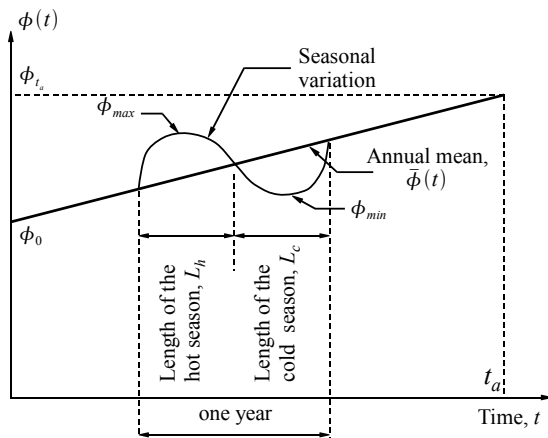


Figure 4.4 — Mean of the weather model.

Nowadays, about fifteen research centers in the world are running fully coupled models. Given the difficulties of integrating a comprehensive weather model with the chloride ingress phenomenon, a simplified model of global warming is presented in this section.

The effect of global warming is modeled by assuming that the increase or decrease of humidity and temperature over time, in the upcoming years, is a linear function. This model allows discussing the effect of climate change on chloride ingress. Nonetheless, it must be updated when comprehensive global warming models become available. By denoting ϕ as the weather parameter (humidity or temperature), the annual mean value of ϕ is equal to (Figure 4.4):

$$\bar{\phi}(t) = \phi_0 + \left(\frac{\phi_{t_a} - \phi_0}{t_a} \right) t \quad (4.21)$$

where ϕ_0 and ϕ_{t_a} are the values of the annual means of ϕ at $t = 0$ and $t = t_a$, respectively. On the other hand, to make an optimal prediction of chloride ingress, it is also important to take into consideration the seasonal variations of humidity and temperature during the year (Figure 4.4). The model divides a reference year into two seasons hot and cold for temperature, and wet and dry for humidity. Actual forecasts of global warming also indicate that droughts increase the length of hot (or wet) seasons, L_h , with respect to the length of cold (or dry) seasons, L_c (IPCC, 2007). By defining R_0 as the normalized duration of the cold (or dry) season for $t = 0$ in one year, i.e. $R_0 = L_c / 1$ year, and R_{t_a} as the normalized duration of the cold or dry season for $t = t_a$ (L_c in years); it is possible to linearly estimate the normalized duration of the cold or dry season R for a given t :

$$R(t) = R_0 + \left(\frac{R_{t_a} - R_0}{t_a} \right) t \quad (4.22)$$

Thus by using a sinusoidal formulation to simulate the seasonal variation of ϕ around the linear trend (equation 4.21), the seasonal mean of ϕ considering global warming becomes (Figure 4.4):

$$\bar{\kappa}_\phi(t) = \begin{cases} \bar{\phi}(t) + \frac{\phi_{max} - \phi_{min}}{2} \sin \left(\frac{t - |t|}{1 - R(t)} \pi \right) & \text{for hot or wet seasons} \\ \bar{\phi}(t) - \frac{\phi_{max} - \phi_{min}}{2} \sin \left(\frac{t - |t| + R(t) - 1}{R(t)} \pi \right) & \text{for cold or dry seasons} \end{cases} \quad (4.23)$$

where ϕ_{max} and ϕ_{min} are respectively the maximum and minimum values taken by ϕ during one year, t is expressed in years and $\lfloor \cdot \rfloor$ represents the floor function –i.e., $\lfloor x \rfloor = \max \{n \in \mathbb{Z} \mid n \leq x\}$. The effect of global warming is integrated into the stochastic model of weather by substituting equation 4.23 into equation 4.12.

4.5 Stochastic model for environmental chloride concentration

Chloride ions that ingress into the concrete can come from two sources: sea water or de-icing salts. This section presents the stochastic models used to simulate the chloride concentration in both environments.

4.5.1 Exposure to chlorides from sea water

In maritime environments, the environmental chloride concentration depends principally on the closeness to the sea, d . Based on a field study of 1158 bridges in Australia (McGee, 2000), the mean of the surface chloride concentration, $\mu_{C_{env}}$, can be computed as:

$$\mu_{C_{env}}(d) = \begin{cases} 2.95 & \text{for } d < 0.1 \\ 1.15 - 1.81 \log(d) & \text{for } 0.1 \leq d < 2.84 \\ 0.35 & \text{for } d > 2.84 \end{cases} \quad (4.24)$$

where d is expressed in km and $\mu_{C_{env}}$ in kg/m³. By taking equation 4.24 to define the mean, the stochastic process representing C_{env} is generated with uncorrelated log-normal fluctuations (noise). It is essential to precise that for both exposures (sea and de-icing salts) the models of surface chloride concentration represent *environmental* chloride concentrations and not *notional* surface concentrations (which appears from empirical models based on the solution of Fick's law) (Val & Trapper, 2008). Since there is no information available on the coefficient of variation (COV) for *environmental* chloride concentrations, the COV used herein is based on previous probabilistic studies which consider *notional* surface concentrations (Vu & Stewart, 2000; Duracrete, 2000). Figure 4.5a presents some realizations of C_{env} where the processes were generated by considering three mean values of $\mu_{C_{env}}$: 2.95, 1.15 and 0.35 kg/m³ which correspond to $d < 0.1$, $d = 1$ and $d = 2.84$ km, respectively (equation 4.24); a COV of 0.20 was used for all these cases.

4.5.2 Exposure to chlorides from de-icing salts

Based on experimental measurements, the probabilistic models of exposure to de-icing salts in the literature usually assume that C_{env} remains constant all the time (Vu & Stewart, 2000; Duracrete, 2000). However, since the kinematics of chloride ingress change as function of weather conditions, a modified model for de-icing salts exposure is adopted. This model considers the increase of C_{env} during cold seasons. Thus, the proposed model assumes that during hot seasons the mean of chloride concentration in the surface is zero; and during cold seasons, it grows linearly from zero to a maximum, C_{env}^{max} , that corresponds to the minimum temperature, returning to zero at the beginning of hot seasons (Figure 4.5b):

$$\mu_{C_{env}}(t) = \begin{cases} 0 & \text{for } t < t_1 \\ C_{env}^{max}(t - t_1)/(t_2 - t_1) & \text{for } t_1 \leq t < t_2 \\ C_{env}^{max} [1 - (t - t_2)/(t_2 - t_1)] & \text{for } t_2 \leq t < t_3 \end{cases} \quad (4.25)$$

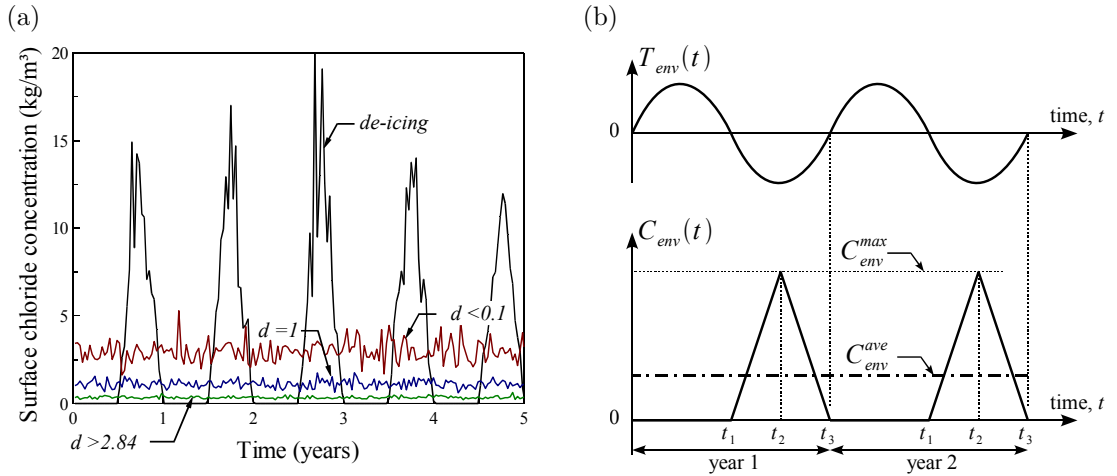


Figure 4.5 — (a) Stochastic surface chloride concentrations. (b) Mean of the concentration of de-icing salts.

where t_1 , t_2 and t_3 are shown in Figure 4.5b. The value of C_{env}^{max} has been defined by considering that the quantity of chloride ions deposited during one year is the same as the average annual concentration reported in the literature, C_{env}^{ave} .

In the stochastic model for de-icing exposure $C_{env} = 0$ during hot seasons and becomes a stochastic process during cold seasons. The stochastic process is modeled by uncorrelated log-normal fluctuations. The time-variant mean used to generate the stochastic process is computed from equation 4.25. The COV was assumed to be in the range of [0.2, 0.4] but actual data needs to be collected. An example of the stochastic modeling of C_{env} for de-icing exposure is also presented in Figure 4.5a. The maximum surface chloride concentration, C_{env}^{max} , was assumed to be 14 kg/m³. This value entails that the mean of the chloride ions deposited during a year is 3.5 kg/m³ which agrees with the data reported in (Vu & Stewart, 2000; Duracrete, 2000). A COV of 0.20 was used to generate the process shown in Figure 4.5a.

4.6 Case study 1: Probabilistic assessment of time to corrosion initiation

4.6.1 Problem description

The main goal for this example is to study the influence of chloride binding, weather conditions, concrete aging, convection, correlation length and two-dimensional chloride ingress on the probability of corrosion initiation. Figure 4.6 shows the studied RC wall and column. This application accounts for continental weather with structures placed at moderate latitudes (e.g., European countries) and far from the ocean where the source of chlorides come only from de-icing salts. Then the following values define the characteristics of weather: $h_{min} = 0.6$, $h_{max} = 0.8$, $T_{min} = -5^\circ\text{C}$ and $T_{max} = 30^\circ\text{C}$. The probabilistic models were defined based on the analysis presented in section 4.3.2 and are shown in Table 4.2. The cover thickness is modeled by a normal distribution truncated at 10 mm and its mean is set as $\mu_{ct} = 40$ mm with a COV=0.25.

Other general assumptions concerning the probabilistic model are:

- the truncated Karhunen-Loëve expansion includes 30 terms –i.e., $n_{KL} = 30$;
- the range of each random variable is divided into 10 equally probable intervals for the Latin Hypercube sampling; and

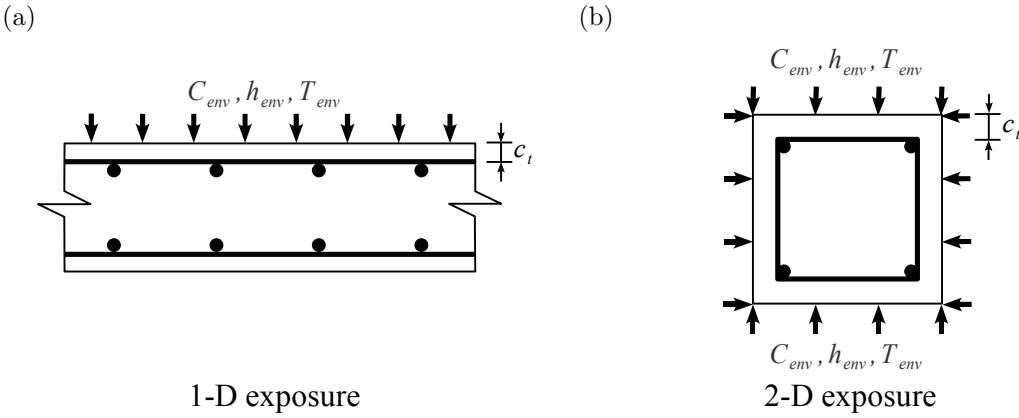


Figure 4.6 — Cross-sections of the studied RC members: (a) slab or wall and (b) column or beam.

Table 4.2 — Probabilistic models of the random variables.

Physical problem	Variable	Mean	COV	Distribution
<i>Chloride ingress</i>	$D_{c,\text{ref}}$	$3 \times 10^{-11} \text{ m}^2/\text{s}$	0.20	log-normal
	U_c	41.8 kJ/mol	0.10	beta on [32,44.6]
	m_c	0.15	0.30	beta on [0,1]
<i>Moisture diffusion</i>	$D_{h,\text{ref}}$	$3 \times 10^{-10} \text{ m}^2/\text{s}$	0.20	log-normal
	α_0	0.05	0.20	beta on [0.025,0.1]
	n	11	0.10	beta on [6,16]
<i>Heat transfer</i>	λ	2.5 W/(m °C)	0.20	beta on [1.4,3.6]
	ρ_c	2400 kg/m ³	0.20	normal
	c_q	1000 J/(kg °C)	0.10	beta on [840,1170]
<i>Corrosion initiation</i>	C_{th}	0.5 wt% cement	0.20	normal
	c_t	nominal	0.25	normal ^a

^atruncated at 10 mm (lower bound)

- the random variables are independent.

4.6.2 Results

For all the cases studied, and according to Lounis (2005), the results of Monte Carlo simulation indicate that the time to corrosion initiation is log-normally distributed. The test of Kolmogorov-Smirnov (K-S) with a significance level of 5% was used as selection criterion.

Figure 4.7 depicts the influence of the type of weather model –i.e., time-invariant, time-variant and stochastic, on the PDF of the corrosion initiation time. For the time-invariant case the annual temperature and relative humidity were set to 12.5°C and 0.7, respectively. Such values correspond to the annual mean of the time-variant model. The time-variant case accounts for the sinusoidal variation of temperature and humidity. The stochastic case considers that the mean is defined by the time-variant model with correlation length of 0.1 year for both models of temperature and humidity (sections 4.4 and 4.5). The influence of b_e on RC durability will be discussed later. It should be noted that the mean and standard deviation of the corrosion initiation time decrease when both seasonal variations and randomness of humidity and temperature are considered. Taking as a reference the mean obtained from the stochastic analysis, it is observed that the mean of the corrosion initiation time increases by 23% and 94% for the time-variant and time-invariant models, respectively. This increment is expected because, as discussed in chapter 3, accounting

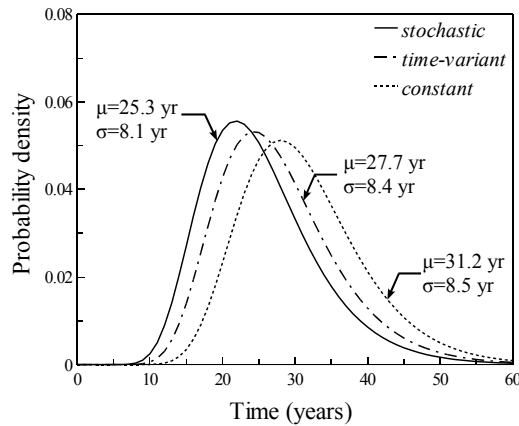


Figure 4.7 — Impact of type of weather model.

for the seasonal variation of humidity and temperature (time-variant model) reduces the corrosion initiation time. The reduction is more appreciable when the time-variant model is coupled with a stochastic process, for which there are extreme values that accelerate the chloride penetration. Given that RC structures are subjected to random environmental actions, these results highlight the importance of including comprehensive probabilistic models of weather conditions in the chloride ingress assessment.

The effects of chloride binding and the type of isotherm on the PDF of the corrosion initiation time are shown in Figure 4.8a. The constants for both isotherms were obtained for the same concrete –i.e., $\alpha_L = 0.1185$, $\beta_L = 0.09$, $\alpha_F = 0.256$ and $\beta_F = 0.397$ (Tang & Nilsson, 1993; Glass & Buenfeld, 2000). As expected, the results indicate that ignoring the effect of binding overestimates the mean of corrosion initiation time. This behavior seems reasonable because, when binding is not considered, it is assumed that all the chlorides involved in the flow (bound and free) ingress into the concrete matrix simultaneously, and therefore, the time to corrosion initiation occurs earlier. No significant difference was observed between both Langmuir and Freundlich isotherms. This similarity lies in the fact that the constants for both isotherms were determined for concrete with identical characteristics.

The impact of convection on the PDF of the corrosion initiation time is plotted in Figure 4.8b. These PDFs were obtained for Langmuir isotherm, correlation length of 0.1 year, and by modeling the environmental actions stochastically. It can be noted from Figure 4.8b that accounting for the chloride ingress by convection slightly decreases the mean of the corrosion initiation time. This reduction is due to the addition of a second mechanism of chloride ingress (i.e., convection) which augments the chloride concentration at the corrosion cell reducing the time to achieve the threshold concentration.

Figure 4.9a describes the influence of the correlation length b_e on the probability of corrosion initiation. For this study, correlation lengths of 0.1, 0.5 and 1 year, have been compared. Although this value should be determined based on real measurements of temperature and humidity, the results indicate that its influence on the mean and standard deviation of the probability of corrosion initiation is not significant. Moreover, it is noticed that smaller values of b_e lead to conservative results. This behavior is expected because small values of b_e entail the presence of extreme values that accelerate the process of chloride ingress (see Figure 4.3b).

Finally, the variation of the probability of corrosion initiation for 1-D and 2-D exposures is

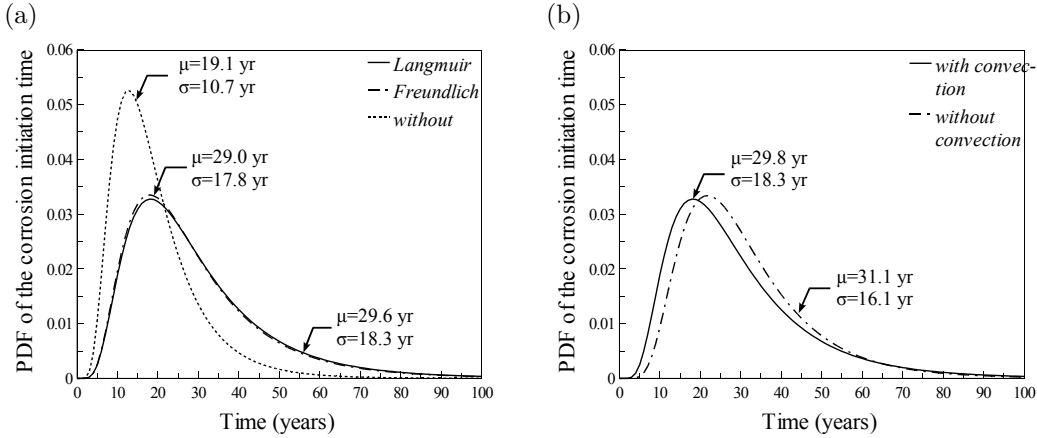


Figure 4.8 — Effect of (a) binding and type of isotherm and (b) convection.

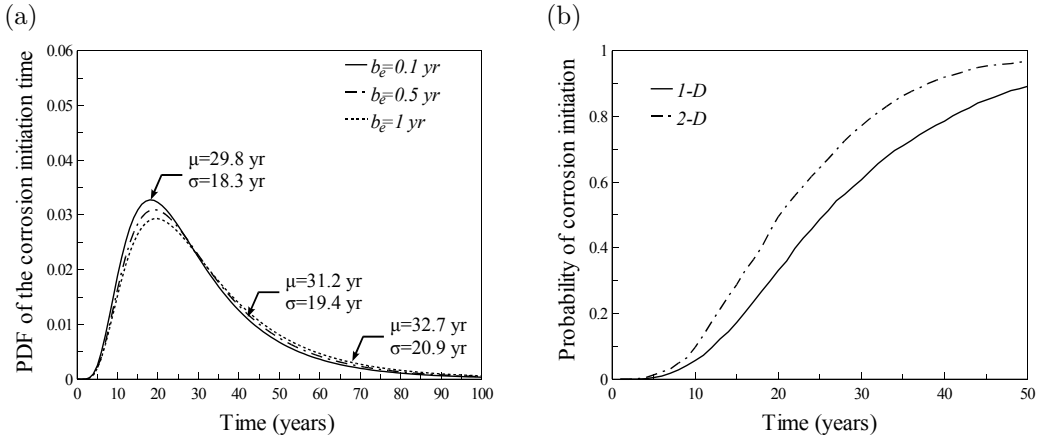


Figure 4.9 — (a) Influence of the correlation length b . (b) Probability of corrosion initiation for 1-D and 2-D exposures.

shown in Figure 4.9b. Both cases include the probabilistic nature of environmental actions, chloride ingress by convection, chloride binding and a correlation length of 0.1 years. As expected, higher probabilities correspond to 2-D exposure. The reduction of corrosion initiation time is due to the exposure to chlorides on both sides of the structural element. For instance, for 30 years of exposure the probability of corrosion initiation is increased 27% when 2-D exposure is considered. These results stress the importance of including a two-dimensional analysis for correct prediction of corrosion initiation in small RC members such as columns and beams.

4.7 Case study 2: Influence of global warming on corrosion initiation time

4.7.1 Problem description

The main goal of this example is to study the influence of real weather conditions on both the probability of corrosion initiation and lifetime reduction. Towards this aim, let us consider a RC slab or wall, with one side exposed to environmental actions (Figure 4.6a). Knowing that the depth of the RC member is much smaller than its other dimensions, the problem is reduced to

Table 4.3 — Description of the studied environments.

Climate	Description	Temperature		Humidity		$\mu_{C_{env}}$
		T_{min}	T_{max}	h_{min}	h_{max}	
<i>Continental</i>	places located at middle latitudes far from the ocean.	-10°C	20°C	0.6	0.8	Eq. 4.25
<i>Oceanic</i>	structures placed at middle latitudes close to the ocean.	5°C	25°C	0.6	0.8	Eq. 4.24
<i>Tropical</i>	sites emplaced at equatorial latitudes close to the ocean.	20°C	30°C	0.7	0.9	Eq. 4.24

one-dimensional flow of chlorides into concrete. However, it is important to highlight that for smaller members (e.g., columns or beams) the two-dimensional flow accelerates the probability of corrosion initiation for the corner bars –i.e., Figure 4.9b. The probabilistic models for the random variables are defined in Table 4.2. The cover thickness follows a normal distribution truncated at 10 mm with the following statistical parameters: $\mu c_t = 50\text{mm}$, and COV=0.25.

This application accounts for three environments with the characteristics defined by both latitude and closeness to the sea. Table 4.3 presents the values adopted for each case. For the continental environment, chloride concentration is $C_{env}^{max} = 14 \text{ kg/m}^3$, and for the marine environment, it depends on the distance from the sea.

To account for the effect of global warming, three possible scenarios were defined (Table 4.4). The characteristics of these scenarios were assigned based on the forecasts given by the Intergovernmental Panel on Climate Change IPCC (2007), which, in the author's opinion, presents the most compendious study on global warming. These predictions account for a combination of natural and anthropogenic driving forces. The action of natural forcings refers to natural climate changes due mainly to solar and volcanic activities. Anthropogenic forcings encompass the effect of human perturbations on climate. Among the anthropogenic forcings, the most important factors considered in such studies are:

- carbon dioxide, methane, nitrous oxide emissions;
- global population growth;
- introduction of new and clean technologies leading to the reduction of the impact of climatic change; and
- use of fossil sources of energy.

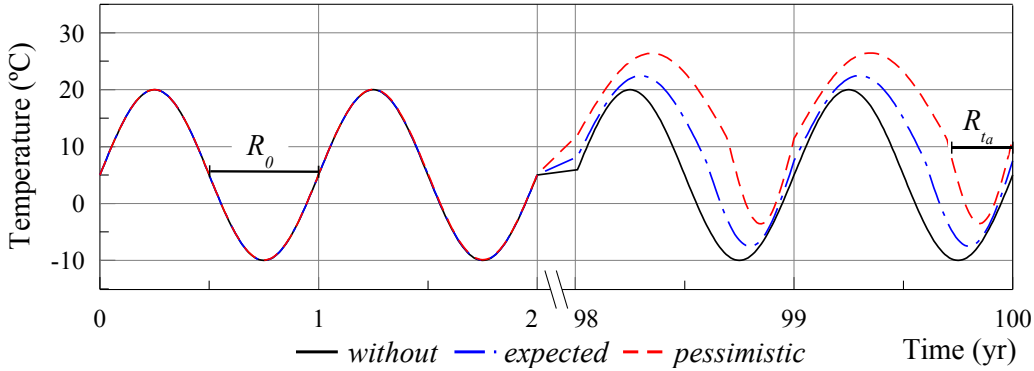
Consequently, the three possible scenarios are *without*, *expected* and *pessimistic* global warming. Each scenario is defined in terms of (section 4.4):

- the difference between the annual means of temperature for the initial year t_0 and the year of the end of the forecast t_a , $\Delta T_a = T_{t_a} - T_{t_0}$,
- the difference between the annual mean of relative humidity for t_0 and t_a , $\Delta h_a = h_{t_a} - h_{t_0}$, and
- the difference between the normalized durations of the cold seasons for t_0 and t_a , $\Delta R_a = R_{t_a} - R_{t_0}$.

By taking as reference a period of analysis of 100 years –i.e., $t_a = 100$ years, the features and the values of ΔT_a , Δh_a and ΔR_a for each scenario are presented in Table 4.4. Figure 4.10 shows an

Table 4.4 — Parameters used to simulate global warming.

Scenario	Characteristics	ΔT_a	Δh_a	ΔR_a
<i>Without</i>	climate change is neglected	0°C	0	0
<i>Expected</i>	use of alternative and fossil sources of energy, birthrates follow the current patterns and there is no extensive use of clean technologies.	2.5°C	0.05	-0.1
<i>Pessimistic</i>	vast utilization of fossil sources of energy, appreciable growth of population and there are no policies to develop and extend the use of clean technologies.	6.5°C	0.10	-0.2

**Figure 4.10** — Example of the temperature model including global warming.

example of the temperature model including the effects of global warming. For seasonal variation, the temperature fluctuates between $T_{min} = -10^\circ\text{C}$ and $T_{max} = 20^\circ\text{C}$ for a year. Taking into consideration all scenarios of global warming described in Table 4.4, the impact of climate changes at the end of the reference period is easily observable in Figure 4.10. Specifically, the length of cold seasons has decreased –i.e., $R_0 > R_{t_a}$, and temperatures during the whole year are higher. This difference is emphasized in the pessimistic scenario.

4.7.2 Results

For a better understanding of the effects of global warming on RC structures under real weather conditions, this section distinguishes between two main issues:

- the probability of corrosion initiation without climate changes, and
- the lifetime reduction induced by global warming.

The results presented herein also account for: the stochastic model of humidity and temperature, chloride binding (Langmuir isotherm) and convection.

4.7.2.1 Probability of corrosion initiation without climate changes

The aim of this analysis is to perform a comprehensive study of the influence of weather conditions without considering climate change repercussions. This study discusses the effects of:

- three different *environmental exposures* (continental, tropical and oceanic) and

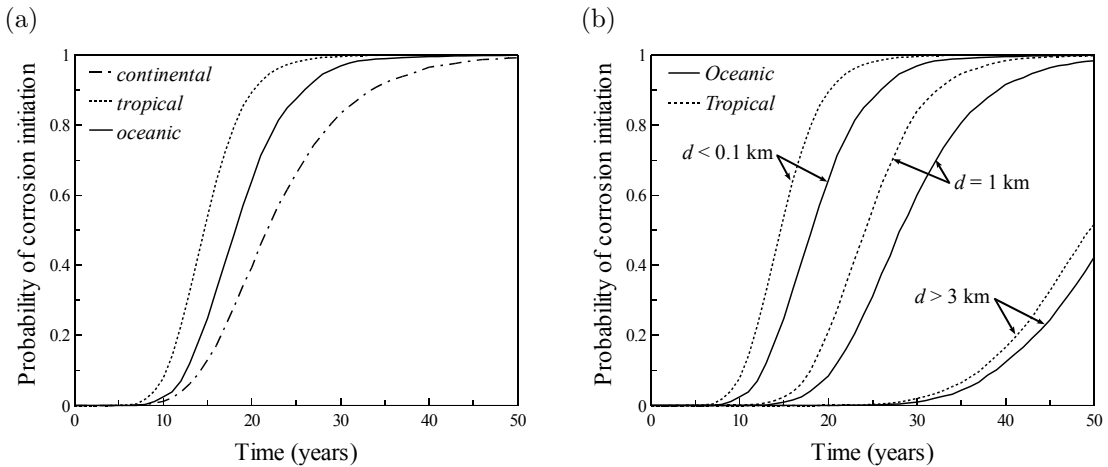


Figure 4.11 — (a) Effect of type of exposure. (b) Influence of the distance to the sea.

- the *distance to the sea* d (less than 100 m, around 1 km or more than 3 km) for marine environments.

The effect of the type of environmental exposure on the probability of corrosion initiation is plotted in Figure 4.11a. This Figure presents the probabilities of corrosion initiation for the environments described in Table 4.3. The surface chloride concentration for the marine environment (tropical or oceanic), is defined by a distance to the sea $d < 0.1 \text{ km}$. It is observed that the highest probabilities of corrosion initiation p_{corr} correspond to marine environments, in particular, for the tropical environment. These results are explained by the fact that (1) structures placed in marine environments are exposed to chlorides all the time and (2) high temperature and humidity accelerate the penetration of chloride ions inside the concrete matrix. The difference between continental and tropical environments highlights the importance of implementing a chloride penetration model that includes environmental effects. Given that the environmental chloride concentration is the same for both marine environments (e.g., tropical and oceanic), a simplified analysis would lead to the same results for both environments when climatic considerations are not taken into account.

Figure 4.11b describes the influence of the distance from the sea on the probability of corrosion initiation. These profiles were computed for oceanic and tropical environments. It is observed that the probability of corrosion initiation is higher for the locations close to the sea. This behavior is due to the increase of the environmental chloride concentration. The impact of the distance to the sea can be observed by analyzing the results for a lifespan of 30 years for the oceanic environment. In this case the probabilities of corrosion initiation change from 0.01 to 0.99 when the distance to the sea is reduced from $d = 3 \text{ km}$ to $d < 0.1 \text{ km}$, respectively. These differences justify the importance of including and measuring d in the life-cycle analysis. It can also be noted from Figure 4.11b that for all locations, the probability of corrosion initiation is higher for tropical environments. Although the chloride surface concentrations for both environments are the same, given that tropical environments are characterized by larger values of temperature and humidity, the time to corrosion initiation is reduced.

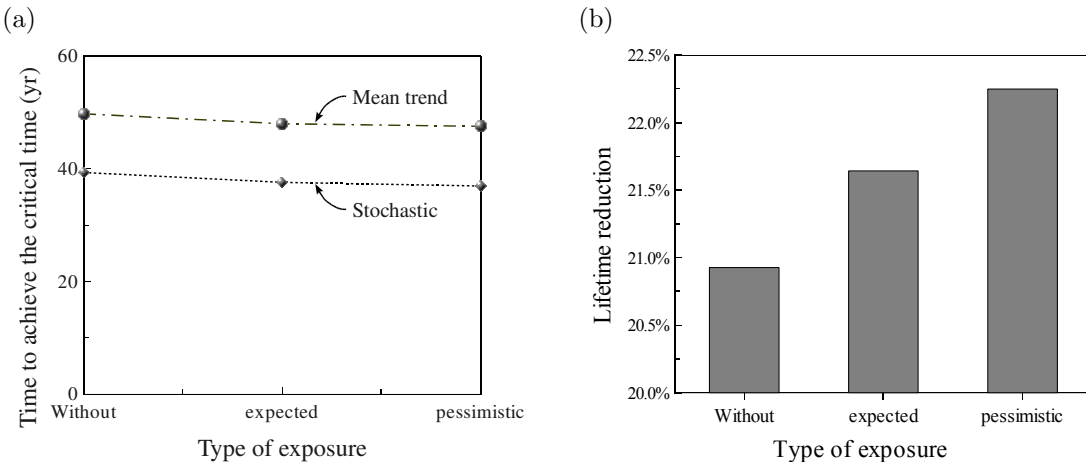


Figure 4.12 — Comparison between weather models: (a) time to achieve the 95% of p_{corr} , (b) lifetime reduction.

4.7.2.2 Lifetime reduction induced by global warming

The objective of this subsection is to study the influence of global warming on lifetime reduction under different environmental exposures and climate change scenarios. The results reported herein are expressed in terms of *critical time* which is defined as the time to reach 95% of the probability of corrosion initiation p_{corr} . The following aspects are discussed:

- the combined effect of the type of weather model (mean trend or stochastic) and climate changes on the critical times (for the continental environment and all the scenarios);
- the influence of global warming on the probability of corrosion initiation (for the oceanic environment and all the scenarios); and
- the effect of global warming on critical times and lifetime reduction (for all environments and scenarios).

Figure 4.12a shows the influence of the weather model on the critical times for the different global warming scenarios and the continental environment. The following cases of weather modeling are compared: (1) only the mean trend is considered; and (2) a stochastic variation is added. In all three scenarios accounting for the randomness associated with weather reduces the critical times. By comparing both results (stochastic and mean trend), it is observed that this reduction is about 20% for all scenarios (see Figure 4.12b). This difference is explained by the presence of extreme values of temperature and humidity for the stochastic model that influences the chloride penetration process. Since these extreme values have been observed during real exposure conditions, these results justify the consideration of the randomness inherent to the phenomenon for a better lifetime assessment. It can be also noticed that the largest lifetime reductions correspond to the expected and pessimistic scenarios (Figure 4.12b). Although the difference is not important (from 20.9 to 22.3%), this behavior is principally due to the increase of temperatures and humidities induced by global warming that reduces the time to corrosion initiation.

The effect of global warming on the probability of corrosion initiation is presented in Figure 4.13. The curves plotted in this figure correspond to the oceanic environment for all the considered locations. Overall behavior indicates that global warming increases the probability of corrosion

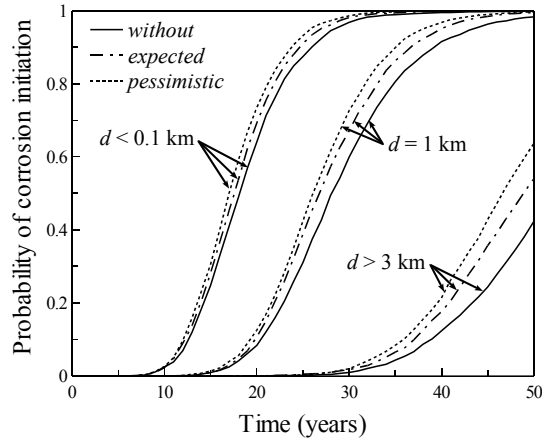


Figure 4.13 — Effect of global warming for the oceanic environment.

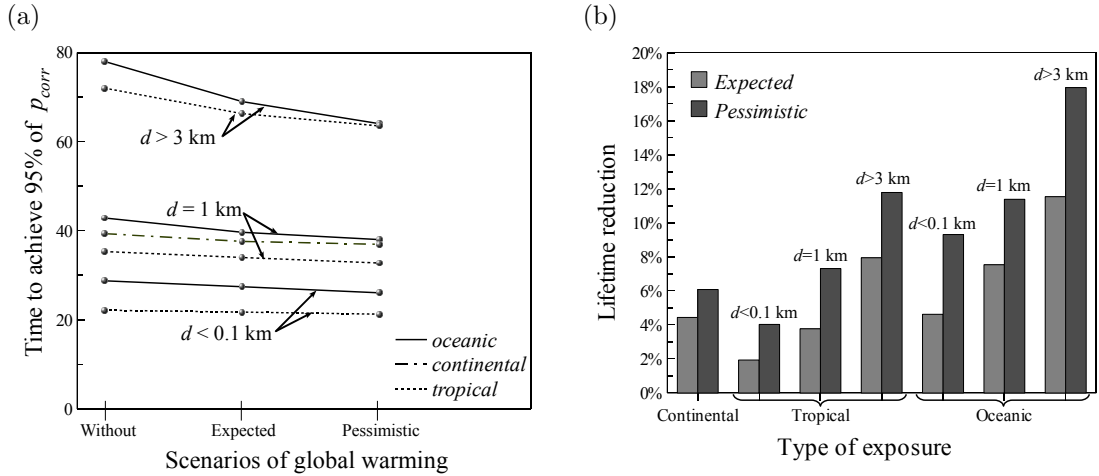


Figure 4.14 — (a) Time to achieve the 95% of p_{corr} . (b) Lifetime reduction induced by global warming.

initiation, particularly, for the pessimistic scenario. This increase is explained by the acceleration of the chloride flow induced by global warming which raises temperature and humidity as well as the length of the hot and wet periods. It can also be noted that the lifetime reduction induced by global warming is more significant for structures located far from the sea. Since the corrosion initiation time is shorter for higher surface chloride concentrations, the effect of global warming is less appreciable in this case. This means that in structures near the sea, the process is completely dominated by high chloride concentrations at the surface and rarely influenced by climatic changes.

Figure 4.14a presents the critical times for all environments considered and distances from the sea. It is observed that shorter critical times correspond to marine environments closer to the sea. The difference between critical times for scenarios without and with global warming increases when the distance to the sea is greater. These results confirm that structures far from the ocean are more susceptible to global warming in terms of reduction of critical time. For instance, global warming can reduce the critical times from 6 to 14 years for structures located at 3 km away from the seashore while this reduction is only from 1 to 3 years for $d < 0.1 \text{ km}$. By comparing both marine environments, it can also be noted that the impact of global warming is more important for oceanic environments where the chloride ingress process is more sensitive to climatic changes.

Results can also be analyzed by computing the percentage of lifetime reduction taking as reference the case without global warming (Figure 4.14b). From these results it is observed that global warming induces lifetime reductions from 2 to 12% for the *expected* scenario and from 4 to 18% for the *pessimistic* scenario. By comparing the average lifetime reduction for all the environments, the larger influence corresponds to the oceanic environment (10.4%) followed by the tropical environment (6.1%) and finally the continental environment (5.3%). These results justify the implementation of countermeasures directed at: (1) reducing and/or mitigating the action of global warming on weather and (2) minimizing the impact of climate changes on RC structures. These countermeasures should be adopted in function of specific features of the structure such as type of environment and location.

4.8 Conclusions

The conclusions of this chapter are presented as follows:

1. There are two quantities of interest in the reliability analysis of corroding RC structures: probability of corrosion initiation and probability of failure. Each quantity is estimated by evaluating the limit state functions corresponding to the serviceability and ultimate limit states, respectively. Depending on the targets of the analysis, both limit state functions can be useful for reliability assessment or for maintenance/repair management. Taking into account the adopted scheme of inspection/maintenance, this study emphasized in the probability of corrosion initiation that is related to the serviceability limit state.
2. The uncertainties for the chloride penetration process come from three sources: (1) material properties, (2) models and their parameters, and (3) environmental actions. In the uncertainty classification presented in this chapter, these uncertainties belong to the randomness category. Accordingly, they are treated by classical stochastic approaches –i.e., random variables and stochastic processes.
3. This chapter adopted and proposed models for the random variables. The time-invariant random variables were modeled by classical distributions (Normal, Log-normal, Beta, etc.), where their statistical parameters were defined based on other deterministic and probabilistic studies. The time-variant random variables were represented by stochastic processes. The weather model, for humidity and temperature, accounted for the effects of seasonal variations and global warming. For the environmental chloride concentration, the stochastic processes distinguish between exposure to de-icing salts or to the sea.
4. Taking into account the complexity of the system (deterioration model, random and fuzzy variables), Monte Carlo simulation and Latin Hypercube sampling will be used for the reliability analysis. Since the deterioration phenomenon depends on time, the chosen reliability method allows for the consideration that the input random variables and the response of the system are time-dependent.
5. The results of the numerical examples indicate that the kinematics of chloride penetration is highly influenced by the random nature of temperature, humidity, surface chloride concentration, chloride binding, convection and two-dimensional chloride ingress. Overall behavior also demonstrated that the probability of corrosion initiation is mainly influenced by the features of place such as: distance to the sea, temperature, humidity, etc. Global warming

was also identified as an important influencing factor because it produces lifetime reductions ranging from 2 to 18%. These results highlight the importance of including a comprehensive probabilistic model of chloride penetration for improving of lifetime assessment.

CHAPTER 5

OPTIMAL MANAGEMENT OF CORRODING RC STRUCTURES

5.1 Introduction

Nowadays, design and management of infrastructure must consider economic, social and environmental constraints to reduce environmental impact, to optimize resource management and to decrease waste generation. This new trend in design and management must also consider all the phenomena that affect the structural performance. For RC structures, corrosion induced by chloride ingress generates important damage after 10 or 20 years of service (Kumar Mehta, 1997; Poupard et al., 2006; Rosquoët et al., 2006). The management of corroding RC structures should therefore integrate the stages of inspection and maintenance to ensure an optimal level of safety during its operational life. However, the complexity and the uncertainties of the deterioration process and the repair techniques transform management in a challenge for owners/operators where decisions are frequently taken without being aware of the consequences of the actions.

The main purpose of this chapter is to develop a method to optimize the management of RC structures subjected to chloride penetration. Optimal management minimizes the costs of inspection, repair and failure. Taking the work by Sheils et al. (2010) as a starting point, a Markovian approach is used for modeling deterioration, inspection and repair. The specific objectives of this chapter are:

1. to define and to justify the maintenance strategy adopted in this work;
2. to integrate the probabilistic model of chloride penetration presented in chapters 3 and 4 for a comprehensive modeling of deterioration as a Markov chain;
3. to develop a model of maintenance that includes various practical problems (e.g., measurement errors and uncertainty) and realistic model parameters; and
4. to study the effect of the model parameters on the total costs and to illustrate its use for decision-making.

The description of the maintenance strategy is presented in section 5.2. Section 5.3 details the assessment of the transition matrices for modeling chloride penetration from the model presented in chapters 3 and 4. The maintenance and cost models are described in sections 5.4, 5.5 and 5.6. Section 5.7 presents a numerical example illustrating the proposed methodology.

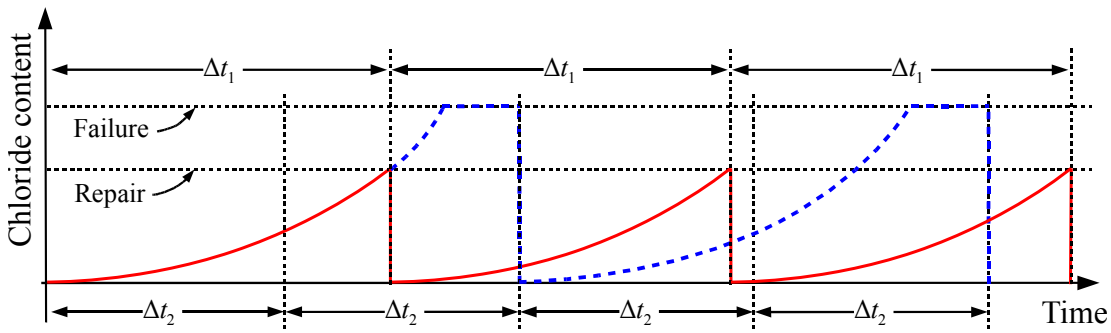


Figure 5.1 — Modeling inspection/maintenance.

5.2 Description of the strategy of maintenance

The objective of maintenance strategies is to ensure optimal levels of serviceability and safety during the structural lifetime. Therefore, when structural performance is strongly affected by the kinematics of the deterioration process, repair and/or replacement of structural components are the only ways to maintain appropriate performance levels. In the maintenance strategy considered in this chapter, repair actions are based on inspection results. Figure 5.1 shows the influence of the considered maintenance strategy on the chloride content at a given point (e.g. cover depth) inside concrete. Note that the structure is inspected periodically every Δt years, and based on the inspection results, repair is carried out when the chloride content reaches a given threshold. $\Delta t = \Delta t_1$ represents an *ideal* situation where inspection and repair takes place at the moment when the chloride content reaches the repair threshold. However, this situation is rarely observed in RC structures because the kinematics of chloride ingress is difficult to assess/predict due to the influence of several parameters (i.e., material properties, weather, etc.). Furthermore, there are errors and uncertainties related to inspection results and the deterioration process that can lead to erroneous decisions. It is then observed that, when $\Delta t = \Delta t_2$, there are either unnecessary inspections or structural components that can fail between the inspection intervals. Therefore, an optimal maintenance strategy should take all these aspects into account to minimize the costs of inspection, repair and failure.

As mentioned before, the strategy of maintenance is divided into two stages: *inspection* and *repair*. Inspection can be carried out by employing destructive and nondestructive methods. Concerning nondestructive methods, visual inspection is a technique usually used for evaluating the condition of RC structures (Roelfstra et al., 2004). Inspection results alert the owner/operator when a given deterioration threshold is reached. The threshold value can be related to concrete cracking or loss of cross-sectional area of reinforcement. However, for visual inspection, the assessment of the structural condition remains largely uncertain when inspection is undertaken. At the present time, there have been significant advances in the development of inspection methods based on nondestructive monitoring. Nondestructive techniques aim at quantifying the instant value or the evolution of a given variable during the time (material strength, chloride concentrations, corrosion rate, etc); nevertheless, their results are highly influenced by environmental conditions reducing its accuracy. The accuracy of inspection results is largely improved by using destructive inspection techniques. However, they are more expensive and require a larger number of tests when there is a larger variability of the inspected parameter. The selection of a given or a combination of inspection techniques depends on several aspects such as:

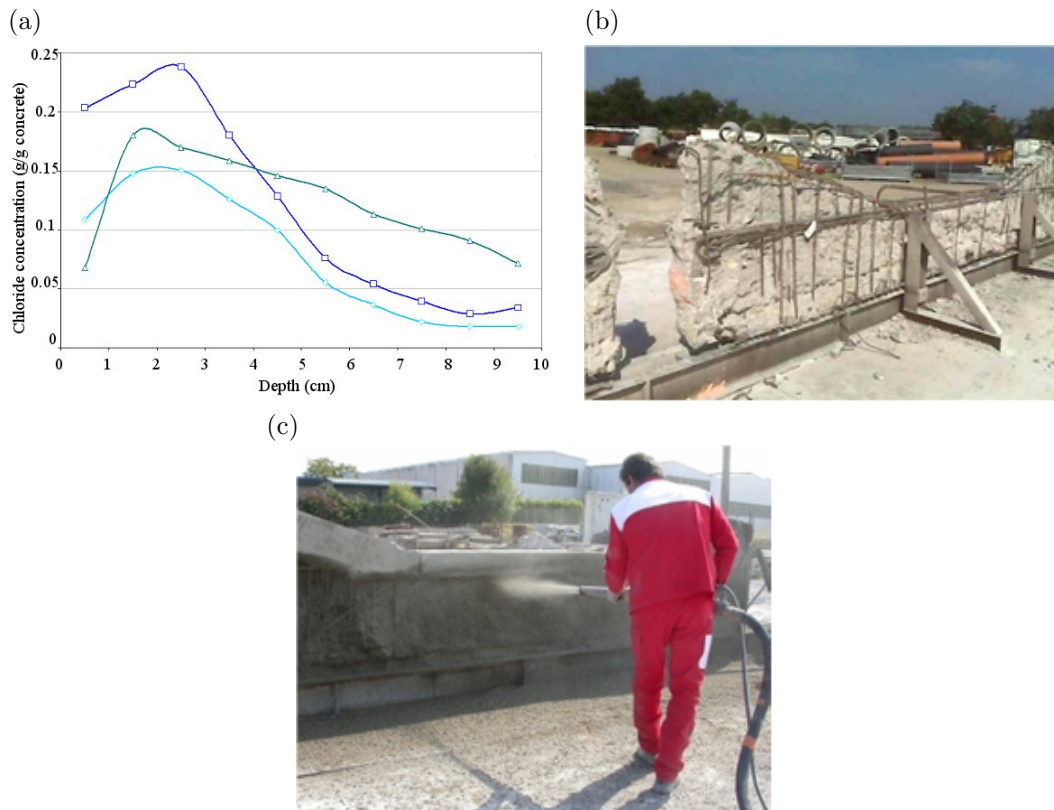


Figure 5.2 — Stages of inspection/repair for the maintenance strategy.

- the type of phenomenon inspected –e.g., material strength, chloride concentration, etc.;
- size of the project –e.g., structural network or particular structure;
- use of the structure –e.g., nuclear, transportation, etc. This point is related to the risk allowed by the agency; and
- other socio-economic aspects as priorities of the country, availability of resources, etc.

This study refers to RC structures subjected to chloride ingress and is focused on maintenance of particular infrastructure e.g., ports, bridges, etc. The requirements for the strategy of maintenance were defined within the framework of the project FUI (2007-2010) MAREO¹ with the collaboration of agencies, construction companies and research centers. In the strategy of maintenance considered herein, inspection is made by analyzing the concentration of chlorides at the cover depth on concrete cores (destructive method). Afterwards, depending on inspection results, the repair technique consists of rebuilding the polluted concrete cover by several methods (Figure 5.2). The advantage of the proposed approach is that repair is more preventive than corrective. This characteristic ensures an optimal level of safety during the lifespan of the project.

Taking into account that there are many factors that influence the deterioration process and the effects of maintenance on RC structures, numerical models are necessary to take optimal decisions. Many management systems use Markov chains to simulate the deterioration and repair of structures over the time (Cesare et al., 1992; Scherer & Glangola, 1994; Roelfstra et al., 2004). Therefore, this study also uses a Markovian approach that integrates the following aspects:

¹Maintenance and REpair of concrete coastal structures: risk-based Optimization (MAREO) Project

- a comprehensive model of chloride penetration (i.e., chapters 3 and 4);
- the accuracy of the inspection technique; and
- the uncertainty inherent to chloride penetration, corrosion initiation and inspection results.

Section 5.3 describes the methodology proposed to model chloride penetration from Monte Carlo simulations.

5.3 Markovian approach for modeling chloride ingress

A discrete-time Markov process can be used to predict the future by knowing the present state. Towards this aim, the space of the variable of interest is discretized into M states. The Markov process is thus used to determine the probability that an event belongs to a state j knowing that for a preceding time step it belonged to a state i . This probability, noted $a_{ij} = P[X_{t+1} = j | X_t = i]$, is called *transition probability*. It is considered herein that a_{ij} is independent of t (Discrete-time Markov process). The transition probabilities can be grouped in a matrix of size $M \times M$ called transition matrix \mathbf{P} (Ross, 2004). According to the Chapman-Kolmogorov equations, by knowing the initial state, the probabilities of belonging to the other states after t transitions, $\mathbf{q}(t)$, are (Ross, 2004):

$$\mathbf{q}(t) = \mathbf{q}_{ini} \mathbf{P}^t \quad (5.1)$$

where the vector \mathbf{q}_{ini} contains the probabilities of belonging to the states at an initial time –i.e., $t = 0$.

In this study, the variable of interest is the concentration of chlorides at the cover depth which controls corrosion initiation. Therefore, the Markov processes provide the probability that the concentration of chlorides at the cover depth belongs to a given state in time. If it is supposed that after construction ($t = 0$) the concentration of chlorides at the cover depth is zero, all the concentrations belong to the first state. Consequently, \mathbf{q}_{ini} will become $\mathbf{q}_{ini}[1, 0, 0, \dots, 0]$ and equation 5.1 provides a vector containing the probabilities of belonging to a state j at time t .

In several applications of Markov chains, the transition matrix is obtained from experimental data or expert judgment. However, for chloride penetration, the assessment of \mathbf{P} from experimental measurements presents two difficulties:

- Given that the rate of chloride ingress into concrete is slow, it is difficult to study the evolution of chloride ingress before construction. Accelerated tests or the use of data obtained for similar materials are alternatives to solve this problem.
- Since chloride ingress is influenced by several parameters –i.e., chapter 3, it is necessary to perform a large number of measurements to obtain a good representation of the phenomenon.

Consequently, it is proposed herein to estimate $\mathbf{q}(t)$ on the basis of a numerical model of chloride penetration, and afterwards, to use the computed values $\widehat{C}(t)$ to estimate the transition matrix \mathbf{P} . The adopted probabilistic model of chloride penetration has been described in chapters 3 and 4. Section 5.3.1 details the method proposed to estimate the transition matrix.

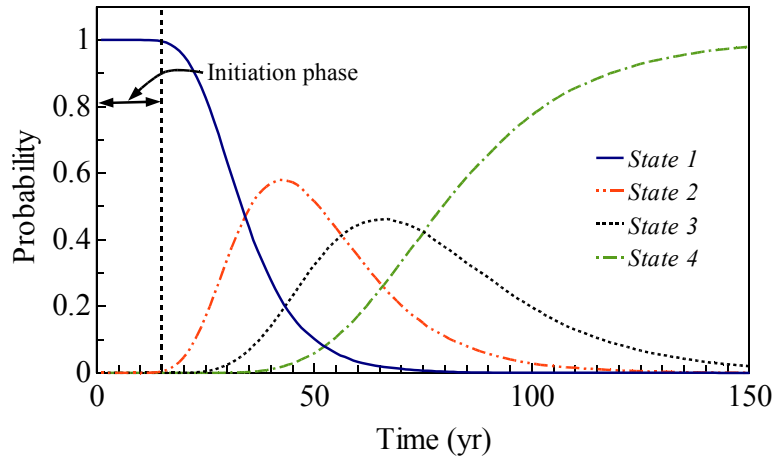


Figure 5.3 — Probabilities computed from Monte Carlo simulation for $M = 4$ states.

5.3.1 Estimation of transition matrix from simulations

Transition matrices are estimated from Monte Carlo simulations of the probabilistic model of chloride penetration by accounting for the random variables presented in chapter 4. In each simulation, the chloride concentration at cover depth during time is recorded. From all simulations, it is determined the frequency of belonging to a given state –i.e., histogram. The probability of belonging to a state j at time t is obtained from:

$$\hat{q}_j(t) = \frac{n_j(t)}{N} \quad (5.2)$$

where $n_j(t)$ is the number of observations in the state j measured at time t and N is the number of simulations. Figure 5.3 shows the variation of $\hat{q}_j(t)$ obtained from Monte Carlo simulations for $M = 4$ states.

Once the probabilities $\hat{\mathbf{q}}(t)$ have been estimated, several methods can be used to compute the transition probabilities. The major difficulty in the assessment of \mathbf{P} lies in the number of terms a_{ij} to estimate. Various studies consider a Markov matrix with two parameters for state to determine (Pappas et al., 2001; Roelfstra et al., 2004):

$$\mathbf{P} = \begin{bmatrix} a_{11} & a_{12} & 0 & \cdots & 0 \\ 0 & a_{22} & a_{23} & \cdots & 0 \\ 0 & 0 & a_{33} & \cdots & 0 \\ \vdots & \vdots & \vdots & \ddots & \vdots \\ 0 & 0 & 0 & \cdots & 1 \end{bmatrix} \quad (5.3)$$

where for a given i , $a_{i2} = 1 - a_{i1}$. In this case, the transition probabilities can be estimated from equation 5.1 by using a non-linear regression. However, complex stochastic phenomena cannot be modeled by a transition matrix with two transition probabilities per state (Roelfstra et al., 2004). To solve this problem, the proposed method searches for the probabilities a_{ij} that minimize the difference between the probabilities estimated from simulations and those obtained from the Markov model (equation 5.1). Since the kinematics of the time-dependent evolution of each state

Table 5.1 — Markov models of \mathbf{P} .

Model 1	Model 2	Model 3
$\begin{bmatrix} a_{11} & a_{12} & 0 & 0 & 0 \\ 0 & a_{22} & a_{23} & 0 & 0 \\ 0 & 0 & a_{33} & a_{34} & 0 \\ 0 & 0 & 0 & a_{44} & a_{45} \\ 0 & 0 & 0 & 0 & 1 \end{bmatrix}$	$\begin{bmatrix} a_{11} & a_{12} & a_{13} & 0 & 0 \\ 0 & a_{22} & a_{23} & a_{24} & 0 \\ 0 & 0 & a_{33} & a_{34} & a_{35} \\ 0 & 0 & 0 & a_{44} & a_{45} \\ 0 & 0 & 0 & 0 & 1 \end{bmatrix}$	$\begin{bmatrix} a_{11} & a_{12} & a_{13} & a_{14} & a_{15} \\ 0 & a_{22} & a_{23} & a_{24} & a_{25} \\ 0 & 0 & a_{33} & a_{34} & a_{35} \\ 0 & 0 & 0 & a_{44} & a_{45} \\ 0 & 0 & 0 & 0 & 1 \end{bmatrix}$

is similar, there are M functions to minimize:

$$\left\{ \begin{array}{l} \min_{\mathbf{a}} \max_{\mathbf{F}} \mathbf{F}(\mathbf{a}) = (f_1(\mathbf{a}), f_2(\mathbf{a}), \dots, f_M(\mathbf{a}))^T \\ \text{u.c. } a_{ij} \geq 0 \text{ and } \sum_{j=0}^{\infty} a_{ij} = 1 \end{array} \right. \quad (5.4)$$

where \mathbf{a} is a vector containing the transitions probabilities (optimization parameters) and $f_j(\mathbf{a})$ is the explained sum of squares (ESS) for each state j :

$$f_j(\mathbf{a}) = \sum_{t=0}^{t_{ana}} (\hat{q}_j(t) - q_j(t, \mathbf{a}))^2 \quad (5.5)$$

where t_{ana} represents the analysis period used to perform the adjustment. This problem of multi-objective optimization has been solved by using the “optimization toolbox” of Matlab®. The selected optimization method minimizes the maximum value of a set of multi-variable functions from an initial value.

5.3.2 Selection of an appropriate Markov model

An appropriate Markov model should consider the influence of the following aspects:

- length of the initiation phase,
- type of Markov model and
- quantity of states.

This section compares the efficiency of three Markov models. Table 5.1 shows the studied Markov models when $M = 5$ states. As mentioned before, the first model is the most commonly used because the assessment of the transition probability is easier. The second model considers tree transition probabilities per state and the third model estimates all transition probabilities in the upper triangular matrix.

The criterion chosen to establish an appropriate Markov consists in minimizing the total explained sum of squares:

$$\text{ESS} = \sum_{j=1}^M f_j(\mathbf{a}) = \sum_{j=1}^M \sum_{t=0}^{t_{ana}} [\hat{q}_j(t) - q_j(t, \mathbf{a})]^2 \quad (5.6)$$

As observed in Figure 5.3, there is an initiation phase during which the chloride penetration at the concrete cover is zero. Therefore, to improve the predictability of the Markov model, an initiation phase is included in the model. In the adopted methodology, for a new or repaired

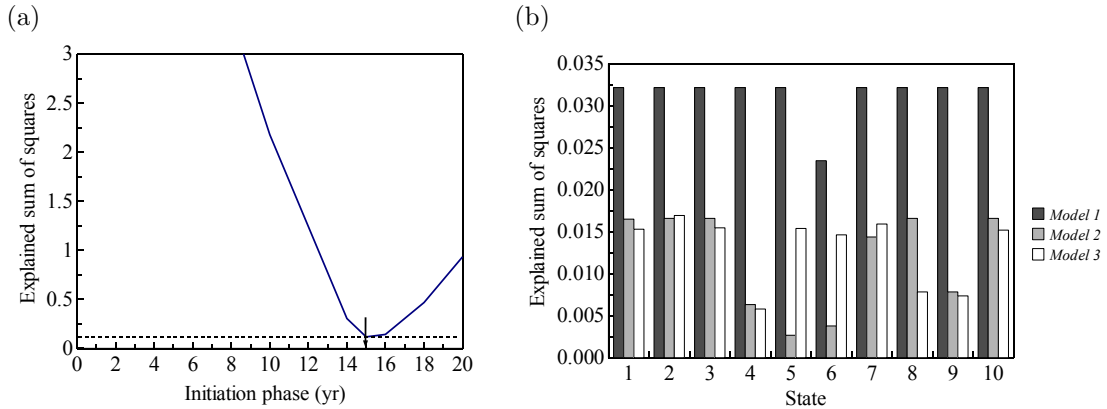


Figure 5.4 — (a) Computation of the initiation period t_m . (b) Comparison between three Markov models.

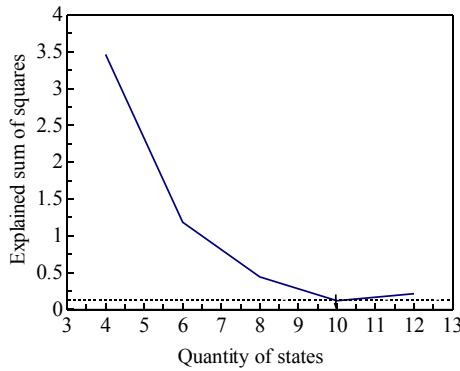


Figure 5.5 — Computation of the optimal number of states M .

structure, the defects belonging to the first state are forced to remain in such state during the initiation phase t_{ini}^M . The details of this method are found in (Sheils, 2009).

Figure 5.4a presents the ESS for the Markov model 2 (Table 5.1) and $M = 10$ states for several initiation phases. It is noted that ESS is maximum when the initiation phase is not considered and decreases until an optimal value. In this case, the optimum is found at 15 years.

The influence of the type of Markov model (Table 5.1) on the ESS for each state is presented in Figure 5.4b. These results were estimated for $M = 10$ states and an optimal t_{ini}^M . The overall behavior indicates that the ESS for the model 1 is almost the double (ESS=0.31) than the ESS for the models 2 (ESS=0.12) and 3 (ESS=0.13). This indicates that the addition of more transition probabilities to the model increases the predictability of the Markov chain. However, by comparing the total ESS obtained for the model 2 and the model 3, it is noted that although there is no larger difference between both models, ESS is higher for the model 3. The model 3 has more objective functions to optimize, and therefore, the error associated to each $f_j(\mathbf{a})$ is higher. On the other hand, by comparing the transition matrices computed with the models 2 and 3 it is observed that when a state is represented by more than four transition probabilities per state, the transition probabilities higher than four are very close to zero. Accordingly, the model 2 is adopted in this study.

Figure 5.5 presents the effect of the number of states on the ESS. This figure considers the Markov model 2 (Table 5.1) and an optimum t_{ini}^M . It is observed herein that the ESS decreases

when the number of states of the Markov models is larger until the optimal value. Therefore, this work adopts $M = 10$ states as an optimal value to model chloride ingress. Finally, taking into account the Markov model 2 and optimal values for t_{ini}^M and M Figure 5.6 presents the comparison between the probabilities computed from Monte Carlo simulations and Markov chains. It is observed that the probabilities estimated from the Markov model have a good agreement with those computed from the Monte Carlo simulations.

5.4 Probabilistic modeling of inspection/repair

In this approach, the structure is inspected periodically every Δt years. The purpose of these inspections is to establish the real chloride concentration at the cover depth, C . This parameter gives an idea on the probability of corrosion initiation, and therefore, can be used by the owner/operator to decide if the structure must be repaired. The experimental test to determine the chloride profiles is based on the AFREM procedure (Chaussadent & Arliguie, 1999; RILEM TC 178-TMC, 2002). This test is used to determine the actual chloride concentration at a given depth (chloride profiles) and can be summarized in the following steps:

1. *grinding*: the concrete specimen is ground to obtain a sample powder to be analyzed;
2. *chloride extraction*: the powder is mixed with demineralized water to produce a solution containing the total/free chlorides. In the assessment of total chloride content, nitric acid is added to the solution and after it is warmed at 80°C;
3. *filtering*: the solution is filtered to separate concrete and chlorides; and
4. *titration*: the total/free chloride content is determined from the filtered solution by titration.

Although this procedure is widely used to determine chloride profiles in several countries, Bonnet et al. (2009) found that there are significant differences between *theoretical* and *measured* chloride profiles –e.g., Figure 5.7. Theoretical profiles are computed from analytical functions knowing the porosity and the chloride concentration in water. This difference has been related to the following factors: error in the *protocol*, error due to *material variability* and error induced by the *operator*.

In order to take into account the influence of error in measurement, the difference between measured \hat{d} and theoretical d values is usually modeled by a noise (Rouhan & Schoefs, 2003):

$$\eta = \hat{d} - d \quad (5.7)$$

where η represents the noise. However, as observed in Figure 5.7 and as reported by Bonnet et al. (2009), chloride measurements underestimate real chloride concentrations. To account for this aspect, a bias b_η is added to equation 5.7:

$$\hat{C} = C + \eta + b_\eta \quad (5.8)$$

where \hat{C} represents the measured chloride concentration and C corresponds to the real chloride concentration. Errors in measurement can lead, for a given inspection, to under- or overestimations of chloride content. If chloride content is underestimated, the owner/operator decides to “do nothing” when repair is required. This erroneous decision increases the probability of failure and can produce overcharges if excessive repair should be carried out in the future. On the contrary, an

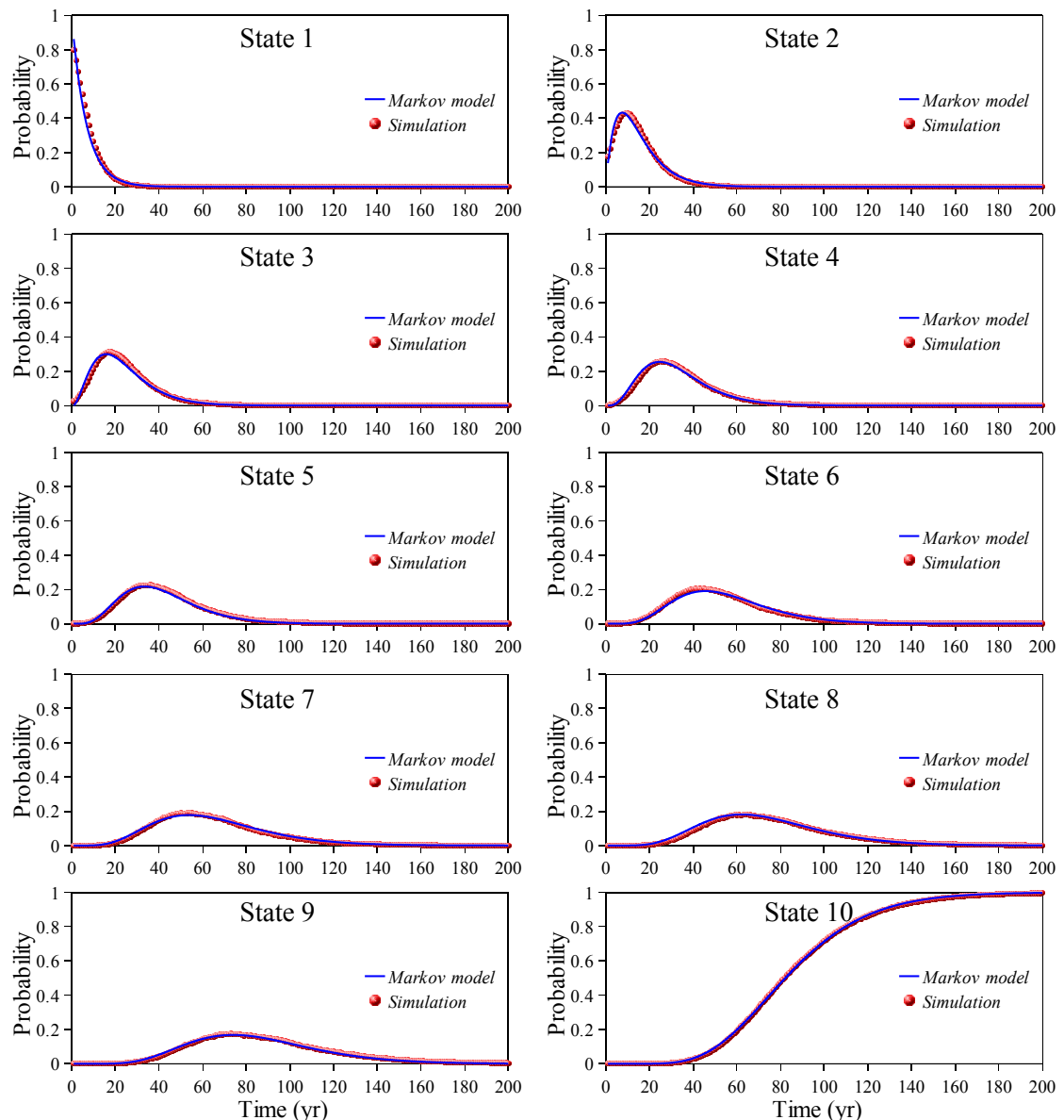


Figure 5.6 — Comparison between the probabilities computed from Monte Carlo simulations and Markov chains.

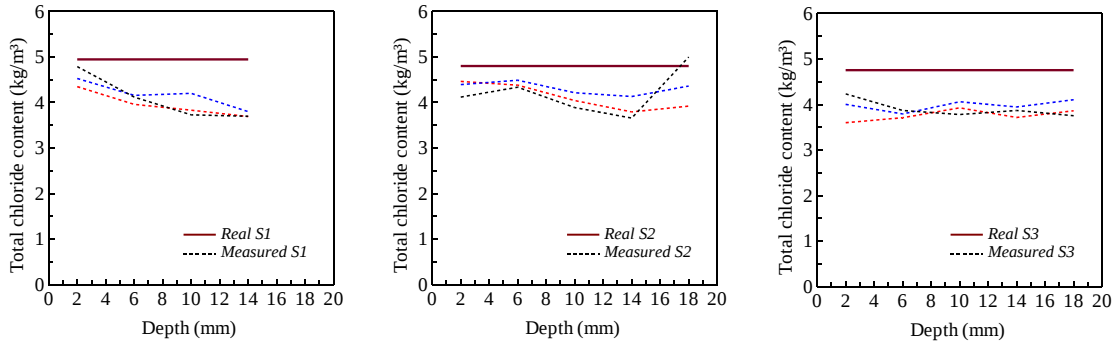


Figure 5.7 — Differences between theoretical and measured chloride profiles for three specimens (with the values reported by Bonnet et al. (2009)).

overestimation generates a “wrong” decision where the early repair generates overcharges. Repair is undertaken in the adopted approach when inspection indicates that the chloride content at the corrosion cell reaches a threshold value C_{rep} . This value can be defined in the construction standards or based on expert judgment and is related to the required safety level itself linked to the acceptable risk. From a probabilistic point of view, two measures can be defined:

- *probability of good assessment*, PGA: determines the probability of detecting an event (e.g. chloride concentration higher than the repair threshold) given that the event exists:

$$\text{PGA} = \text{P}(\hat{C}(\mathbf{X}) \geq C_{rep} | C(\mathbf{X}) \geq C_{rep}) \quad (5.9)$$

- *probability of wrong assessment*, PWA: establishes the probability of detecting an event given that it does not exist:

$$\text{PWA} = \text{P}(\hat{C}(\mathbf{X}) \geq C_{rep} | C(\mathbf{X}) < C_{rep}) \quad (5.10)$$

5.4.1 Assessment of PGA and PWA

Figure 5.8 presents the probability density functions used to compute PGA and PWA for a given repair threshold. It is noted that the distributions of noise and signal (chloride concentration) and the repair threshold should be determined for a particular problem. It is supposed herein that the noise is independent of the real chloride concentration because there are several sources of error influencing the results of the inspection. This assumption has been validated from a series of measurements on metallic harbor structures (Schoefs et al., 2009b). It is also assumed that the noise and the detection threshold are constant for each inspection.

The noise is usually modeled by a normal random variable. Nonetheless, on the basis of experimental measurements, Bonnet et al. (2009) report that a generalized extreme value distribution (GEV) is more appropriate to represent the noise for the adopted technique of inspection. The parameters estimated (in kg/kg of concrete) are: scale $K_\eta = 0.016$, shape $\sigma_\eta = 9.3 \times 10^{-5}$ and location $\mu_\eta = -8.4 \times 10^{-5}$. For a density of concrete of $\rho_c = 2400 \text{ kg/m}^3$, the shape and location of η in kg of chlorides per m^3 are $\sigma_\eta = 0.2$ and $\mu_\eta = -0.2$, respectively. By considering that the chloride concentration cannot be negative, and by fitting some chloride concentrations obtained from the model presented in chapters 3 and 4, it is assumed herein that C is log-normally distributed with mean μ_C and standard deviation σ_C . Taking into account that, for this problem, the noise

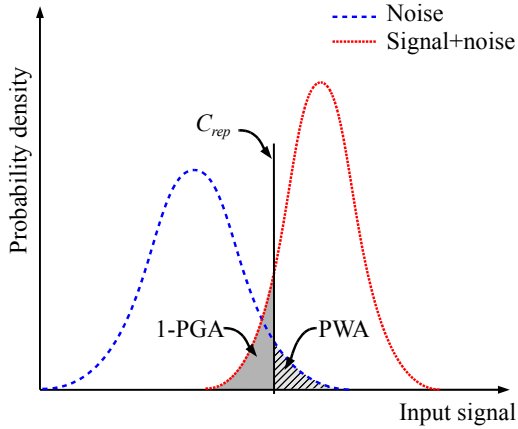


Figure 5.8 — Illustration of PGA and PWA.

is modeled as a random variable with an important variability, it is possible to consider that the events $\langle \hat{C}(\mathbf{X}) \geq C_{rep} \rangle$ and $\langle C(\mathbf{X}) \geq C_{rep} \rangle$ are weakly correlated. Consequently, it is assumed that both events are independent and that the probability of good assessment becomes:

$$\text{PGA} = P[g(\mathbf{X}) \leq 0] \quad (5.11)$$

where $g(\mathbf{X})$ is the limit state function. In this problem, there is no analytical solution to estimate PGA from equation 5.11. Therefore, PGA is numerically computed by using a first order reliability method (FORM) where the limit state function is:

$$g(\mathbf{X}) = C_{rep} - C(\mathbf{X}) - \eta(\mathbf{X}) \quad (5.12)$$

It is assumed in equation 5.12 that, knowing the bias, the measurements can be unbiased –i.e., $b_\eta = 0$. By taking into account that the repair threshold C_{rep} is deterministic and that η follows a GEV distribution, the probability of wrong assessment can be estimated as:

$$\text{PWA} = 1 - \exp \left(- \left[1 + K_\eta \left(\frac{C_{rep} - \mu_\eta}{\sigma_\eta} \right) \right]^{-1/K_\eta} \right) \quad (5.13)$$

It is observed from equation 5.12 that PGA depends on the chloride content C , the repair threshold C_{rep} , and the characteristics of the noise. From the probabilistic model of chloride penetration presented in chapters 3 and 4, it has been determined that the standard deviation of C for ordinary Portland concrete is about $\sigma_C = 0.10 \text{ kg/m}^3$. However, this parameter should be determined for a particular problem. Figure 5.9a plots the influence of σ_C on PGA when $\mu_\eta = -0.2 \text{ kg/m}^3$, $\sigma_\eta = 0.2 \text{ kg/m}^3$ and $C_{rep} = 1.6 \text{ kg/m}^3$. Overall behavior indicates that PGA increases for higher total chloride contents. Note that small variations of σ_C from the estimated value do not produce appreciable changes in PGA. Then, this study adopts the value estimated from simulations –i.e., $\sigma_C = 0.10$. These results indicate that the precision of the inspection technique is not suitable for measuring small chloride concentrations. However, it can be used to determine concentrations higher than 0.3 kg/m^3 which are compared with the threshold chloride concentration for corrosion initiation, that varies between 1 and 2.5 kg/m^3 , to determine if the structure should be repaired. Further research should be addressed to improve the precision of the inspection technique.

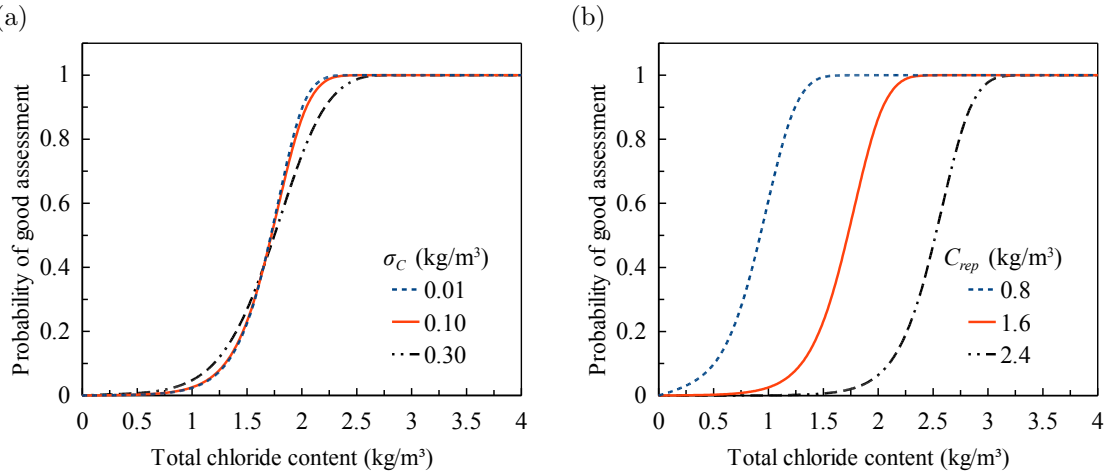


Figure 5.9 — Factors influencing PGA: (a) σ_C and (b) C_{rep} .

Figure 5.9b describes the interaction between the repair threshold C_{rep} and PGA. These values were obtained for the following conditions: $\sigma_C = 0.10 \text{ kg}/\text{m}^3$, $\mu_\eta = -0.2 \text{ kg}/\text{m}^3$ and $\sigma_\eta = 0.10 \text{ kg}/\text{m}^3$. It is noted that PGA is very sensitive to this parameter diminishing when the detection threshold increases. The repair threshold indicates a limit after which the structure is repaired. This value can be defined according to the construction standards or based on expert judgment. The French standard (NF EN-206, 2004) establishes that the maximum allowable chloride content is 0.4% wt. cem. ($\approx 1.6 \text{ kg}/\text{m}^3$ for a cement content of 400 kg per m^3 of concrete and $\rho_c = 2400 \text{ kg}/\text{m}^3$) whereas the Spanish standard (EHE, 2008) recommends a higher value (i.e., 0.6% wt. cem. $\approx 2.4 \text{ kg}/\text{m}^3$). Taking into account the higher influence of this parameter on PGA, the considerations for selecting a representative value will be discussed in section 5.7.

The influence of the mean and standard deviation of noise on PGA is presented in Figure 5.10. The PGAs presented in this figure were computed with the following parameters: $\sigma_C = 0.10 \text{ kg}/\text{m}^3$ and $C_{rep} = 1.6 \text{ kg}/\text{m}^3$. As expected, the PGAs are larger when μ_η tends to zero and the change in PGA from 0 to 1 is more pronounced when σ_C increases. This indicates that the precision of the inspection technique is improved for smaller μ_η and σ_C . For the value reported by Bonnet et al. (2009), the PGAs vary from 2% to 100% for chloride contents between 1 and 2.2 kg/m^3 which are in the interval of interest.

Given that the probability of wrong assessment is only influenced by the characteristics of the noise and the detection threshold –i.e., equation 5.13, Figure 5.11a presents the influence of the detection threshold on PWA for $\mu_\eta = -0.2 \text{ kg}/\text{m}^3$ and $\sigma_\eta = 0.2 \text{ kg}/\text{m}^3$. Note that although PWA is sensitive to changes in C_{rep} , their values are low ($< 10^{-3}$) for C_{rep} varying between 0.8 and 2.4 kg/m^3 . The higher PWA correspond to small repair thresholds. This indicates that the area below the PDF of the noise after C_{rep} (PWA) increases when C_{rep} is reduced (Figure 5.11b). This behavior is expected because this inspection technique always underestimates the real chloride content. Then, the decisions are principally based on the probability of good assessment in this particular problem.

5.5 Simulation of inspection, repair and failure

After inspection, there can be two decision outcomes:

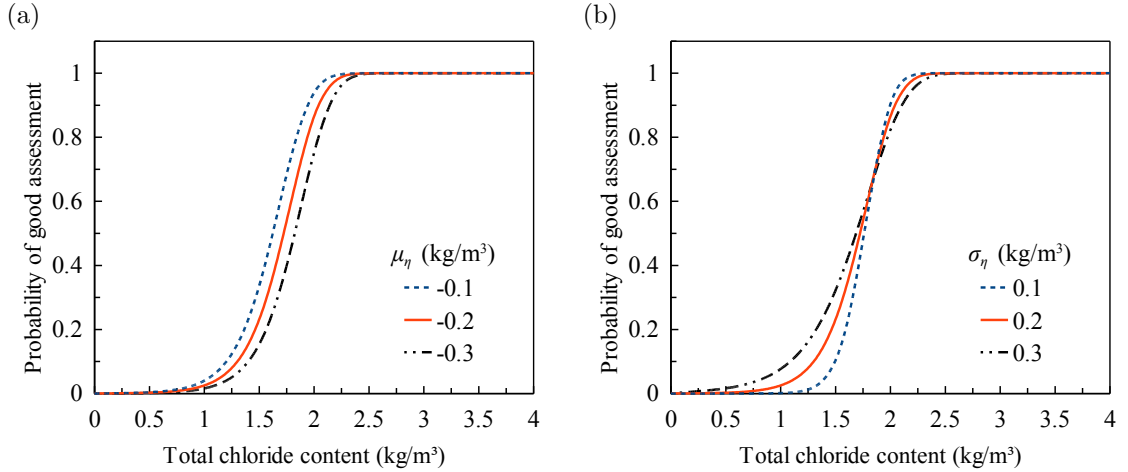


Figure 5.10 — Factors influencing PGA: (a) μ_η and (b) σ_η .

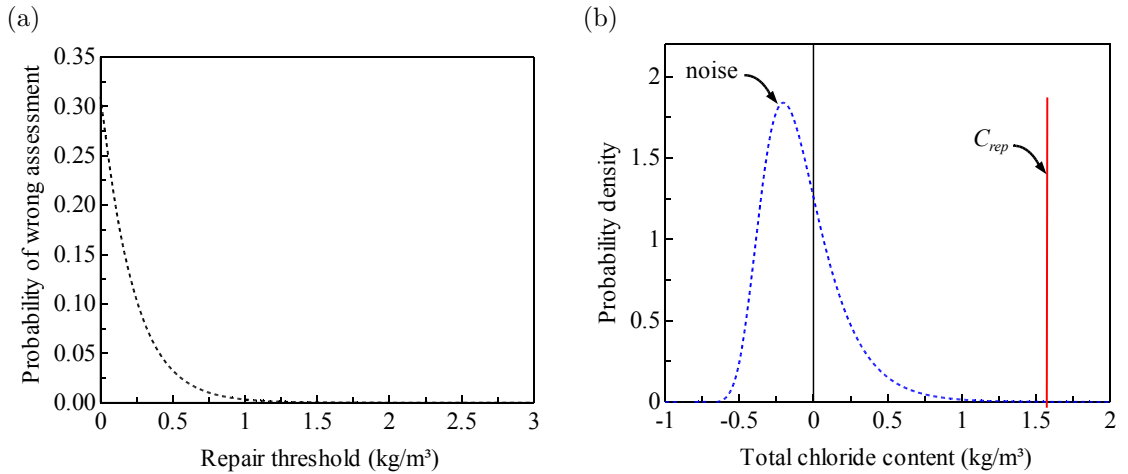


Figure 5.11 — (a) Effect of C_{rep} on PWA. (b) PDF of noise.

1. To repair, in which case the structure/component returns to its initial state. This assumption is adopted herein but it can be changed without lack of generality of the method.
2. To carry out no repair.

When no repair is decided, there is a remaining probability of failure (corrosion initiation) that increases when the chloride content is larger. When failure occurs the structure/component is repaired or rebuilt to its initial state. These events are represented by probabilities that are calculated analytically and integrated in the Markov model. Therefore, there are two Markov matrices for modeling the whole process. The former is used to model failure and repair between inspections \mathbf{P}^{be} . The latter represents inspection, repair and failure at inspection years \mathbf{P}^{in} .

Once both matrices have been formulated they are used to simulate chloride ingress, inspection, repair and failure over time. Each state is assumed to have an initial population of defects. The number of defects in each state is then calculated on a yearly basis using the relevant Markov matrix, and the number of defects in each state from the previous year. This section presents the methodology for determining \mathbf{P}^{be} and \mathbf{P}^{in} .

The variable of interest (i.e., chloride concentration at the cover depth) is discretized into M states in the following formulation. Each state i is therefore characterized by a random variable $d_i(\mathbf{X})$ which is assumed log-normally distributed.

5.5.1 Failure between inspections

Chloride penetration into concrete produces structural failure when no repair is carried out. The repair criterion considers that the polluted concrete is rebuilt when the chloride concentration measured during the inspection reaches a threshold value C_{rep} , which is related to a probability of steel depassivation or corrosion initiation. The chloride concentration leading to corrosion initiation, C_{th} , is chosen in this work to compute the probability of failure (corrosion initiation). By assuming that C_{th} is log-normally distributed, the probability of corrosion initiation between the inspection intervals for a state i can be estimated as:

$$p_{ini,i} = P(C_{th}(\mathbf{X}) - d_i(\mathbf{X}) \leq 0) = \Phi\left(\frac{\lambda_{d_i} - \lambda_{C_{th}}}{\sqrt{\xi_{d_i} + \xi_{C_{th}}}}\right) \quad (5.14)$$

where λ and ξ are the log-normal location and scale of C_{th} and d_i .

The transition probabilities $a_{i,j}$ in the complete Markov matrix for a year between inspections \mathbf{P}^{bet} are computed in terms of those of the Markov growth matrix \mathbf{P}^{gr} (estimated according to the methodology described in section 5.3) and the probability of corrosion initiation for the corresponding state as (Sheils et al., 2010):

$$a_{i,1}^{bet} = a_{i,1}^{gr} + \sum_{k=2}^M [a_{i,k}^{gr} p_{ini,k}] \quad (5.15)$$

and

$$a_{i,j}^{bet} = a_{i,j}^{gr}(1 - p_{ini,j}) \quad \text{for } j > 1 \quad (5.16)$$

where $a_{i,j}^{bet}$ and $a_{i,j}^{gr}$ are the transition probabilities of \mathbf{P}^{bet} and \mathbf{P}^{gr} , respectively.

5.5.1.1 Repair criterion

The owners/operators define the schedule of repair actions on the basis of a given criterion related to an allowable damage threshold. The selection of the repair criterion is an important topic in maintenance because it should consider several aspects that differ for particular problems – i.e., economic, environmental, practical, etc. This study establishes a repair criterion where the structure is repaired before corrosion initiation. As discussed in chapter 4, the probability of corrosion initiation computed with equation 5.14 corresponds to a serviceability limit state where the consequences of failure remain moderate in terms of economy, safety and functionality.

This criterion can be considered as conservative in comparison to other criteria found in the literature where repair is carried out after initial or several concrete cracking occurs (e.g., Mullard & Stewart (2009)). However, the criterion proposed herein has been defined after discussion with the stakeholders participating in the MAREO project. The reasons to define this criterion are summarized as follows:

- When the repair criterion is based on the structural condition after corrosion initiation (e.g.,

concrete cracking), structural safety is affected by the loss of reinforcing steel. Therefore, the assessment of the next repair time should consider the initial structural condition as well as the replacement of the corroded reinforcing steel at a given time. These considerations make the repair scheme complex because (1) repair times are time-dependent and (2) replacement or reinforcement actions should be included in the analysis. Since for the selected criterion repair is carried out before corrosion initiation, it is possible to assume that the repair action is perfect. This means that after each repair the RC member is “as good as new”. Under this assumption, the repair intervals are constant.

- From a practical point of view, the contractors manifest that the replacement of reinforcing bars in existing structures is complicated. Therefore, another advantage of the proposed criterion is that, since repair takes place before corrosion initiation, the replacement of corroded bars is few. However, the condition of reinforcement should be checked before cover rebuilding.
- Finally, this criterion is convenient to combine the maintenance strategy with inspections because it is based on a measurable variable (chloride concentration at the reinforcement depth). Consequently, the owner/operator can evaluate the condition of the structure before repair to calibrate the maintenance schedule.

5.5.1.2 Threshold chloride concentration

Since the repair criterion is based on the probability of corrosion initiation, the determination of an appropriate threshold chloride concentration becomes a major challenge for the owner/operator. It is not feasible to define a representative value for this parameter because there is a wide range of threshold chloride concentrations suggested in the literature. This larger variability can be attributed to the number of variables influencing C_{th} : type and content of cement, exposure conditions, time and type of exposure, distance to the sea, oxygen availability at the bar depth, type of steel, electrical potential of the bar surface, presence of air voids, etc. In addition, the following aspects add more variability to the problem (Alonso & Sánchez, 2009; Angst et al., 2009):

- *Definition of corrosion initiation:* As discussed in section 4.3.1, there are two ways to define corrosion initiation:
 - Definition 1: depassivation occurs when a certain shift in the corrosion potential or rate is produced.
 - Definition 2: depassivation is associated with “visible” or “acceptable” deterioration of the RC structure.

In the adopted scheme of inspection/maintenance, repair is carried out before corrosion initiation. Therefore, definition 1 is used to determine C_{th} . According to Alonso et al. (2000), depassivation occurs when, in a surface of steel of 1 cm^2 , the corrosion rate is higher than $0.1 \mu\text{A}$.

- *Technique used to determine active corrosion:* The method used to determine the depassivation period also influence the measurement of C_{th} . A certain decay of corrosion potential E_{corr} or an increase of corrosion rate i_{corr} can be used as indicators of corrosion initiation.

However, taking into account that there is no direct relationship between E_{corr} and i_{corr} (Geocisa & the Torroja Institute, 2002), the assessment of C_{th} for each technique would lead to different values. As mentioned before, an increase in corrosion rate is considered herein to define C_{th} .

- *Testing methods for chloride threshold determination:* Alonso & Sánchez (2009) classified these testing methods into two categories:

- Natural methods: This category considers that the electrochemical changes occurring at the surface of the reinforcement during depassivation are not affected by any electrical action.
- Accelerated methods: These methods take into account any external action that affects the electrochemical conditions of the surface of the reinforcement from that of the natural state and which even can accelerate chloride penetration.

As expected, threshold chloride concentrations for accelerated methods are lower than those for natural methods. Depending on the technique for the accelerated methods (potentiostatic and migration), the mean of the total threshold chloride concentration measured by natural methods can be reduced from 25 to 92%. Accordingly, the threshold chloride concentrations measured by natural methods are considered in this approach because they are more representative of real exposure conditions.

Table 5.2 presents the values of C_{th} reported by Alonso & Sánchez (2009) for natural methods. For comparative purposes, a widely used probabilistic model of the threshold chloride concentration is added to Table 5.2 (Duracrete, 2000). To compute C_{th} in kg/m³, it is assumed that the concrete contains 400 kg of cement per m³. From equation 5.14, Figure 5.12 presents the probability of corrosion initiation for the models presented in Table 5.2 by assuming that C_{th} is log-normally distributed in all the cases. In general, the probability of corrosion initiation is larger when the mean of the threshold chloride concentration is small. This behavior is expected because a lower value of the mean of C_{th} implies that the quantity of chlorides required to initiate the corrosion reaction is small. It is also noted that the probability of corrosion initiation is highly dependent on concrete cracking and the exposure conditions (immersed or in air). The adversest condition corresponds to cracked structures exposed to the air above the splash zone. In this case, since the availability of oxygen and water at the corrosion cell is larger, the quantity of chlorides required for corrosion initiation decreases. The Duracrete model gives a mean trend and the “cracked immersed” and “in field” conditions are more conservative. It is also important to note that the larger variability for “in field” case is explained by the fact that this category groups measurements for several environmental conditions.

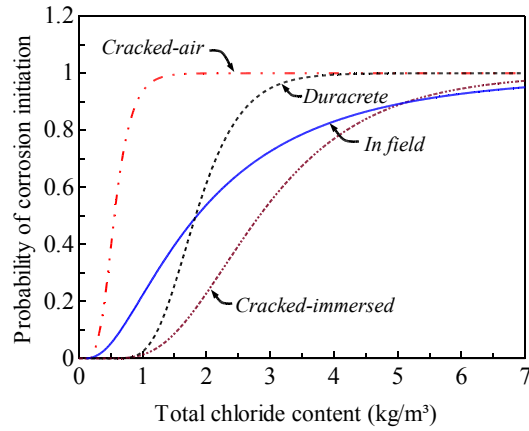
5.5.2 Failure and repair at inspection years

At an inspection year, the events of preventive repair R or failure F (corrosion initiation) can occur (i.e., $R \cup F$). Therefore, the probability of repair or corrosion initiation for a state i , $p_{R \cup F, i}$, can be computed as follows:

$$p_{R \cup F, i} = P_i[\text{Repair}] + P_i[\text{Failure} \mid \text{No repair}] \quad (5.17)$$

Table 5.2 — Total threshold chloride concentrations.

Source	Exposure conditions	Mean % wt. cem.	Standard dev. % wt. cem.
Alonso & Sánchez (2009)	<i>Cracked-air</i> : cracks > 0.4 mm and exposed to the air above the splash zone	0.15 (0.60 kg/m ³)	0.06 (0.24 kg/m ³)
Alonso & Sánchez (2009)	<i>Cracked-immersed</i> : cracks > 0.4 mm and immersed in seawater	0.79 (3.16 kg/m ³)	0.39 (1.56 kg/m ³)
Alonso & Sánchez (2009)	<i>In field</i> : it groups measurements for cracked, uncracked, immersed and non-immersed conditions	0.64 (2.56 kg/m ³)	0.61 (2.44 kg/m ³)
Duracrete (2000)		0.48 (1.92 kg/m ³)	0.15 (0.60 kg/m ³)

**Figure 5.12** — Probability of corrosion initiation for various models of C_{th} .

where:

$$P_i[\text{Repair}] = P[\hat{C} \geq C_{rep}] \quad (5.18)$$

and assuming that the events $\langle\text{Failure}\rangle$ and $\langle\text{No repair}\rangle$ are independent:

$$P_i[\text{Failure} \mid \text{No repair}] = P[\hat{C} < C_{rep}]p_{ini,i} \quad (5.19)$$

On the other hand, the parameter γ_i represents the probability that for the state i the actual chloride concentration is greater than the repair threshold:

$$\gamma_i = P[d_i(\mathbf{X}) \geq C_{rep}] \quad (5.20)$$

γ_i can be determined based on expert judgment. However, as mentioned previously, by assuming that $d_i(\mathbf{X})$ is log-normally distributed, γ_i is calculated analytically as:

$$\gamma_i = \Phi\left(\frac{\lambda_{d_i} - \ln(C_{rep})}{\xi_{d_i}}\right) \quad (5.21)$$

The probability of repair can be written analytically in terms of γ_i , PGA _{i} and PWA _{i} :

$$P_i[\text{Repair}] = \text{PGA}_i \gamma_i + \text{PWA}_i (1 - \gamma_i) \quad (5.22)$$

Similarly, the probability of failure given that no repair is carried out writes:

$$P_i[\text{Failure} \mid \text{No repair}] = [(1 - \text{PGA}_i)\gamma_i + (1 - \text{PWA}_i)(1 - \gamma_i)]p_{ini,i} \quad (5.23)$$

These values are then used to calculate the transition probabilities in the complete Markov matrix for an inspection year \mathbf{P}^{in} in terms of those of the Markov growth matrix \mathbf{P}^{gr} and the probability of corrosion initiation for the corresponding state as (Sheils et al., 2010):

$$a_{i,1}^{in} = a_{i,1}^{gr} + \sum_{k=2}^M [a_{i,k}^{gr} p_{R\cup F,k}] \quad (5.24)$$

and

$$a_{i,j}^{in} = a_{i,j}^{gr}(1 - p_{R\cup F,j}) \quad \text{for } j > 1 \quad (5.25)$$

where $a_{i,j}^{in}$ and $a_{i,j}^{gr}$ are the transition probabilities of \mathbf{P}^{in} and \mathbf{P}^{gr} , respectively.

5.6 Cost analysis

Depending on both the kinematics of the deterioration process and the repair strategy, the number of defects in each state stabilizes after a given number of simulations (Sheils et al., 2010). These stabilized values are used to evaluate the cost of the maintenance strategy. This methodology distinguishes among three costs:

- the expected inspection cost, $E[C_I]$,
- the expected repair cost, $E[C_R]$ and
- the expected failure cost, $E[C_F]$.

The expected total cost of the maintenance strategy, $E[C_T]$, is then computed as:

$$E[C_T] = E[C_I] + E[C_R] + E[C_F] \quad (5.26)$$

Although the aforementioned costs are agency (direct) costs, user costs can also be added to the analysis. According to Thoft-Christensen (2009), in certain cases, the consideration of user costs is an influencing factor in management of deteriorating infrastructure. However, taking into account that no data is available to accurately quantify the user cost, it was decided to model only the agency costs. The development of accurate costing models for agency costs is beyond the scope of this study. Nonetheless, the cost parameters presented herein were defined on the basis of expert judgment of the operators of the port of Nantes-St. Nazaire.

Direct costs are incurred at different times during the operational life. However, for comparative purposes, the costing models described herein are computed on an annual basis. In other words, these costs indicate the annual expenditures of the agency to maintain a structure.

Decision-making based on expected costs is widely used in the practice. However, Schoefs et al. (2009a) demonstrated that decisions that take other values different to the expected one are more convenient in some cases where an optimal value is hard to find. Although this point is not explored in this work, it is an important area for further research.

5.6.1 Inspection cost

The expected inspection cost is calculated by assuming that all structures/components are inspected. Then expected annual number of inspections n_I is equal to the total number of structures/components to inspect n_t divided by the length of the inspection interval Δt :

$$E[n_I] = \frac{n_t}{\Delta t} \quad (5.27)$$

Thus, the expected annual inspection cost $E[C_I]$ is evaluated as a fraction of the initial cost of construction C_0 as:

$$E[C_I] = E[n_I]C_0k_I \quad (5.28)$$

where k_I is a coefficient used to compute the inspection cost of as a fraction of C_0 . The value of this coefficient takes into account all the stages of the inspection process: preparation of the access to the inspected area, extraction of concrete cores, laboratory tests, data analysis, etc. Therefore, for a particular problem, this coefficient can be considered as constant.

5.6.2 Repair cost

Repair costs depend on deterioration mechanisms, labor costs, material costs, site setup costs etc. The deterioration mechanism defines the expected number of repairs which is computed from the results of the Markov model. The costs are defined in function of the characteristics of the repair technique.

As mentioned before, repair is carried out when the inspection indicates that chloride concentration is larger than the repair threshold. Therefore, the number of repairs n_R depends on the probability of repair (equation 5.22) and the stabilized number of structures/components in each state $n_d(i)$ (Sheils et al., 2010):

$$E[n_R(i)] = \frac{n_d(i)}{\Delta t} P_i[\text{Repair}] \quad (5.29)$$

Then the expected annual repair cost $E[C_R]$ becomes:

$$E[C_R] = C_0 k_R \sum_{i=1}^M E[n_R(i)] \quad (5.30)$$

where k_R is a coefficient used to compute the repair cost of as a fraction of C_0 . It is observed from equation 5.30 that the cost of repair is constant and only depends on the initial construction cost, C_0 and the repair cost coefficient k_R . When corrective maintenance is undertaken, repair costs depend mainly on the extent of damage. However, in the proposed approach the structure is repaired at a given damage threshold where the repair actions, and therefore the expected value of repair costs, are known and can be assumed as constant.

5.6.3 Failure cost

The assessment of the expected annual total failure cost should consider the failures occurred between inspections and at inspection years. The expected annual total failure cost of the structure $E[C_F]$ is then calculated by summing the expected cost of failure between inspections $E[C_{F1}]$ and

the expected cost of failure at inspection year $E[C_{F2}]$:

$$E[C_F] = E[C_{F1}] + E[C_{F2}] \quad (5.31)$$

5.6.3.1 Failure cost between inspections

According to equation 5.14, there is a probability of corrosion initiation that depends on the actual chloride concentration for each state. Therefore, the expected number of failures in each state between inspections, $E[n_{F1}]$, is computed by multiplying the number of failures in each state i each time between inspections j , $n_f(i, j)$, by its corresponding probability of corrosion initiation. At each year between inspections, there will be a different number of failures in each state. Therefore, the expected number of failures in each state must be calculated and summed together (assuming that they are non-correlated):

$$E[n_{F1}(i)] = \frac{p_{ini}(i)}{\Delta t} \sum_{j=1}^{\Delta t - 1} n_f(i, j) \quad (5.32)$$

Then the expected annual cost of failure between inspections writes:

$$E[C_{F1}] = C_0 k_F \sum_{i=1}^M E[n_{F1}(i)] \quad (5.33)$$

where k_F is a coefficient used to compute the failure cost as a fraction of C_0 . This failure coefficient should be defined taking the impact of failure into account. The impact of failure depends on many factors such as the importance of the structure and/or structural component and the limit state being considered. In the proposed maintenance strategy, this coefficient is related to the overcharges of repair costs that are incurred when corrosion has started –e.g., replacement of corroded bars, removal of more chloride-polluted concrete, etc.

5.6.3.2 Failure cost at inspection year

Since repairs are carried out at inspection years, the probability of failure given no repair (equation 5.23) is used to compute the expected number of failures, $E[n_{F2}(i)]$, at inspection year:

$$E[n_{F2}(i)] = \frac{n_d(i)}{\Delta t} P_i[\text{Failure}|\text{No repair}] \quad (5.34)$$

where $n_d(i)$ is the number of structures/components in each state. Then the expected annual cost of failure at inspection year becomes:

$$E[C_{F2}] = C_0 k_F \sum_{i=1}^M E[n_{F2}(i)] \quad (5.35)$$

5.7 Illustrative example

5.7.1 Problem description

The objective of this example is to illustrate the proposed methodology studying the influence of the inspection interval on expected annual costs. It is supposed that the RC structure is composed

Table 5.3 — Random variables for modeling chloride ingress.

Variable	Units	Distribution	Mean	COV
$D_{c,ref}$ (original material)	m^2/s	log-normal	3.0×10^{-11}	0.2
$D_{c,ref}$ (formed concrete)	m^2/s	log-normal	4.5×10^{-11}	0.2
$D_{c,ref}$ (wet shotcrete)	m^2/s	log-normal	2.0×10^{-11}	0.2
$D_{c,ref}$ (dry shotcrete)	m^2/s	log-normal	1.8×10^{-11}	0.1
U_c	kJ/mol	beta on [32;44.6]	41.8	0.1
m		beta on [0;1]	0.15	0.3
$D_{h,ref}$	m^2/s	log-normal	3×10^{-10}	0.2
α_0		beta on [0.025;0.1]	0.05	0.2
n		beta on [6;16]	11	0.1
λ	$\text{W}/(\text{m}^\circ\text{C})$	beta on [1.4;3.6]	2.5	0.2
c_q	$\text{J}/(\text{kg}^\circ\text{C})$	beta on [840;1170]	1000	0.1
ρ_c	kg/m^3	Normal	2400	0.2

by 100 structural components placed in an oceanic climate with temperature ranging from 5 to 25 °C and with relative humidity between 0.6 and 0.8 for each year. The stochastic climate model has been described in chapter 4. The length of inspection intervals depends on the spatial variability of the environmental chloride concentration. Therefore, two exposure zones have been included in this example:

- *Splash and tidal zone*: the structural components are in direct contact with seawater but not immersed. In this zone there exists a larger environmental chloride concentration and chlorides ingress is accelerated by the variations in temperature and humidity. The average environmental chloride concentration for this zone is $C_{env} = 6 \text{ kg}/\text{m}^3$.
- *Atmospheric zone*: the structural components are situated to 0.1 km or less from the coast but without direct contact with seawater. The average environmental chloride concentration for this zone is $C_{env} = 3 \text{ kg}/\text{m}^3$.

As discussed in chapter 4, the environmental chloride concentration is modeled as a stochastic process generated by independent numbers following a log-normal distribution (log-normal noise) with a coefficient of variation of 0.2. The considered random variables for chloride penetration are presented in Table 5.3. The explanation of the choice of such variables is given in chapter 4. Table 5.3 includes chloride diffusion coefficients for four materials. The first one corresponds to the original material which is supposed to be ordinary Portland concrete with a chloride diffusivity appropriated for chloride-contaminated environments. The following three materials correspond to repair materials that are being tested in the framework of the MAREO project by accelerated and normal tests. The chloride diffusion coefficients for these repair materials were defined based on preliminary results (Villain et al., 2010). It is important to mention that although these coefficients are used to study the influence of the quality of the repair techniques, the conclusions concerning the repair techniques are not general.

Other assumptions in this example are:

- the concentration of chlorides inside the concrete is zero at the beginning of the analysis;
- the considered concrete contains 400 kg/m^3 of ordinary Portland cement, 8% of C₃A and $w/c = 0.5$;
- the hydration period, t_e , is 28 days; and

Table 5.4 — States used for discretizing the problem.

State	Splash and tidal zone			Atmospheric zone			σ_C
	From	To	\bar{C}	From	To	\bar{C}	
1	0	0.4	0.2	0	0.2	0.1	0.1
2	0.4	0.8	0.6	0.2	0.4	0.3	0.1
3	0.8	1.2	1	0.4	0.6	0.5	0.1
4	1.2	1.6	1.4	0.6	0.8	0.7	0.1
5	1.6	2	1.8	0.8	1	0.9	0.1
6	2	2.4	2.2	1	1.2	1.1	0.1
7	2.4	2.8	2.6	1.2	1.4	1.3	0.1
8	2.8	3.2	3	1.4	1.6	1.5	0.1
9	3.2	3.6	3.4	1.6	1.8	1.7	0.1
10	3.6	4	3.8	1.8	2	1.9	0.1

Table 5.5 — Initiation phase for the original and repair materials.

Exposure zone	Initiation phase (yr)			
	Original	Wet shotcrete	Dry shotcrete	Formed concrete
Splash and tidal	15	24	31	10
Atmospheric	18	27	34	11

- the random variables are independent.

Following the procedure presented in section 5.3, the Markov matrices of deterioration were obtained for the four materials (original and repair materials) and the two exposure zones. To estimate these Markov matrices, the problem is discretized into $M = 10$ states. Table 5.4 details the discretization for both zones. These ranges differ for both zones because higher chloride concentrations are computed when the environmental chloride concentration increases. The transition probabilities were obtained from 10,000 simulations for a concrete cover of 5 cm. The length of the initiation phase for all the materials is presented in Table 5.5. It is noted for both zones that, excepting formed concrete, the repair materials have initiation phases larger than the original material. This behavior is expected because according to the material specifications, these materials have lower chloride diffusivity. Unfortunately, it was impossible to obtain the material composition to study in depth its influence on chloride diffusivity.

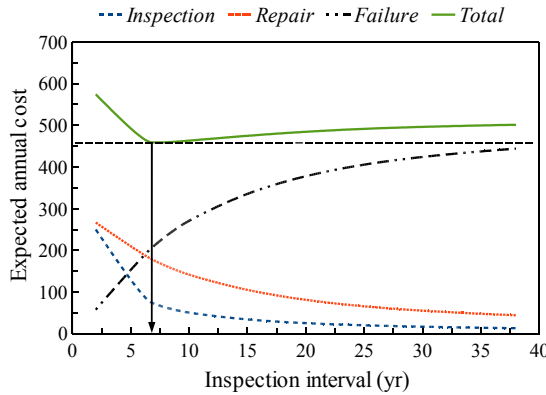
The determination of an optimal inspection interval is very sensitive to the cost models. Therefore, to obtain realistic results, the inspection, repair and failure coefficients (i.e., k_I , k_R and k_F) were defined taking into account the average expenditures for these items incurred by the port of Nantes-Saint Nazaire. These coefficients are presented in Table 5.6. Note that these costs coefficients are refereed to an initial construction cost of 1000 units per structural element. The coefficient of failure is usually equal to or greater than 1 in engineering applications based on ultimate limit states. In such cases failure implies the replacement of the affected component. However, for the adopted limit state, the coefficient given in Table 5.6 indicates that after failure (corrosion initiation) the overcharges are lower than the initial cost of construction.

5.7.2 Results

The first part of the results is devoted to study the influence of the length of the inspection interval on the total costs and its governing parameters. After, the discussion focuses on the use of the proposed approach as a decision-making tool.

Table 5.6 — Coefficients for cost models.

Parameter	Repair technique		
	Formed concrete	Dry shotcrete	Wet shotcrete
Initial cost of construction, C_0	1000	1000	1000
Inspection coefficient, k_I	0.005	0.005	0.005
Repair coefficient, k_R	0.15	0.21	0.26
Failure coefficient, k_F	0.30	0.42	0.52

**Figure 5.13** — Effect of the inspection interval on expected annual costs

5.7.2.1 Total costs and influence of the governing parameters

To simplify the study, it is assumed in this work that the repair material has the same characteristics as the construction material and that the structure is located in the splash and tidal zone.

Figure 5.13 depicts the influence of the length of the inspection intervals on the expected annual cost. This analysis considers that the repair threshold is $C_{rep} = 1.6 \text{ kg/m}^3$ which corresponds to the limit established in (NF EN-206, 2004). The total cost is discriminated into the costs of inspection, repair and failure. It is observed that the costs of inspection and repair decrease and the cost of failure increases for larger inspection intervals. This behavior is explained by the fact that when the inspection interval is greater, most part of inspections detect that the components failed. On the contrary, when the structure is inspected regularly, repair is preventive, and therefore, the cost of failure decreases. By varying the length of the inspection interval, it can be concluded, in this case, that total costs are optimal when the structure is inspected every 7 years.

Figure 5.14a shows the influence of the repair threshold C_{rep} on the expected total costs. For comparative purposes, two values of C_{rep} defined in the French (NF EN-206, 2004) and Spanish (EHE, 2008) standards are also included –i.e., $C_{rep} = 1.6$ and $C_{rep} = 2.4 \text{ kg/m}^3$, respectively. The overall behavior indicates that total expected annual cost is sensitive to this parameter. For $C_{rep} < 1.6 \text{ kg/m}^3$, the optimal inspection intervals decrease when C_{rep} is larger. It is also noted that there is no a minimum value when the repair limit is $C_{rep} = 2.4 \text{ kg/m}^3$. This behavior indicates that C_{rep} should be defined for a particular problem and not defined according to a given standard.

The assessment of an optimal C_{rep} is presented in Figure 5.14b. This figure also includes the discrimination of costs, for the optimal inspection interval, in each case. Given that there is no optimum for $C_{rep} = 2.4 \text{ kg/m}^3$, the presented values are the costs at 38 years. Excepting $C_{rep} = 2.4 \text{ kg/m}^3$, the inspection costs increase when C_{rep} is greater. This indicates that since

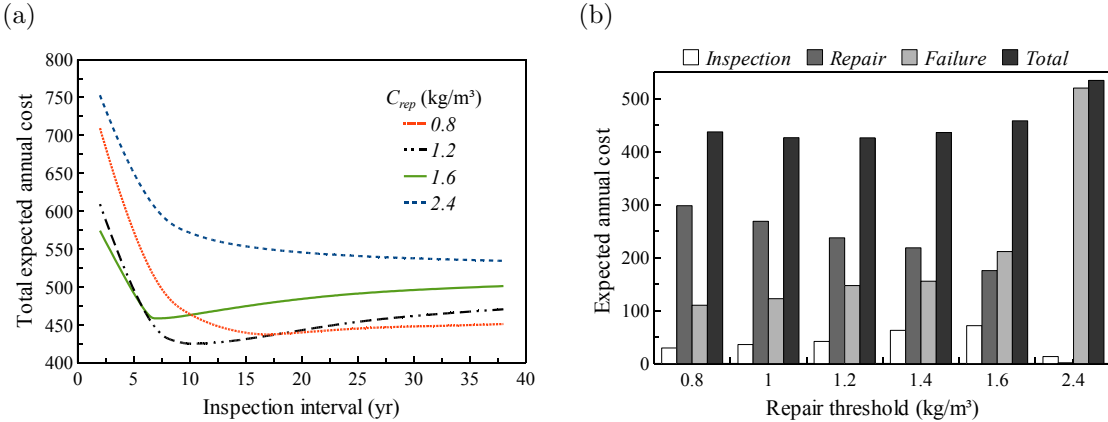


Figure 5.14 — (a) Influence of C_{rep} on total cost. (b) Assessment of an optimal C_{rep} .

for larger values of C_{rep} there are more corrosion risks, and consequently, the structure should be inspected more periodically (Figure 5.14a). On the contrary, repair cost decreases and failure cost increases for larger values of C_{rep} . When the repair threshold increases there are more corrosion risks. Therefore, the components are repaired once they have failed increasing failure costs. For $C_{rep} = 2.4$, inspection is undertaken every 38 years decreasing the inspection cost. Nonetheless, at this time, almost all the components are corroded, and then, the failure cost is the more important item. These results show that the optimal inspection interval should be determined for a $C_{rep} = 1.2 \text{ kg/m}^3$. In such case, the optimal inspection interval is 10 years.

The effect of the mean of the corrosion initiation threshold, C_{th} , on the total expected annual costs is presented in Figure 5.15. These values were obtained for a repair threshold of $C_{rep} = 1.2 \text{ kg/m}^3$. The compared means were defined based on the values presented in Table 5.2. Then, $C_{th} = 1.92 \text{ kg/m}^3$ corresponds to the mean reported by Duracrete (2000) and $C_{th} = 2.56 \text{ kg/m}^3$ and $C_{th} = 3.16 \text{ kg/m}^3$ are the values found by Alonso & Sánchez (2009) for “in field” and “cracked immersed” cases, respectively. Taking into account that the standard deviation reported in (Alonso & Sánchez, 2009) gathers information of several studies under different conditions, it is assumed in this example that for one single structure the variability is reduced. Therefore, all threshold chloride contents have the same coefficient of variation (i.e., $\text{COV}[C_{th}] = 0.20$). As expected, the total expected annual cost decreases when the mean of C_{th} increases. This means that a higher chloride concentration is necessary to start the corrosion reaction, and then, the number of inspections, repairs and failures will be reduced. As mentioned in section 5.5.1.2, a comprehensive assessment of this parameter is crucial for an optimal management of structures.

Figure 5.16 shows the influence of the quality of the inspection technique on the expected total annual costs. To simulate inspection quality, it is assumed that an improvement of the quality decreases the values of the parameters μ_η and σ_η . Then, Figure 5.16a shows that a decrease of μ_η and σ_η reduces the dispersion of the measurement leading to more precise results. It is noted from Figure 5.16b that the expected optimal total annual cost is lower when the quality of the inspection technique increases. Furthermore, it is observed that for the same problem the structure should be inspected every 11 years for high quality instead of 10 years for low quality. These results indicate that further research is required to improve the quality of the inspection techniques, and consequently, to reduce the total costs.

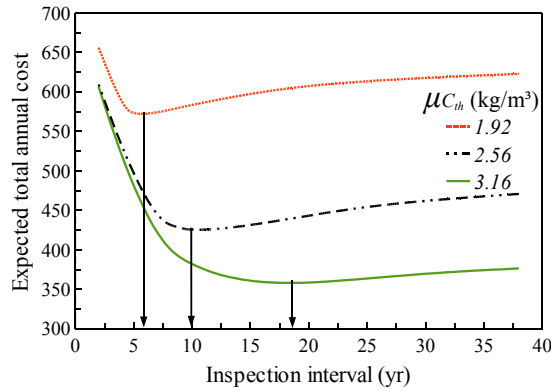


Figure 5.15 — Impact of the mean of C_{th} on the total expected annual costs

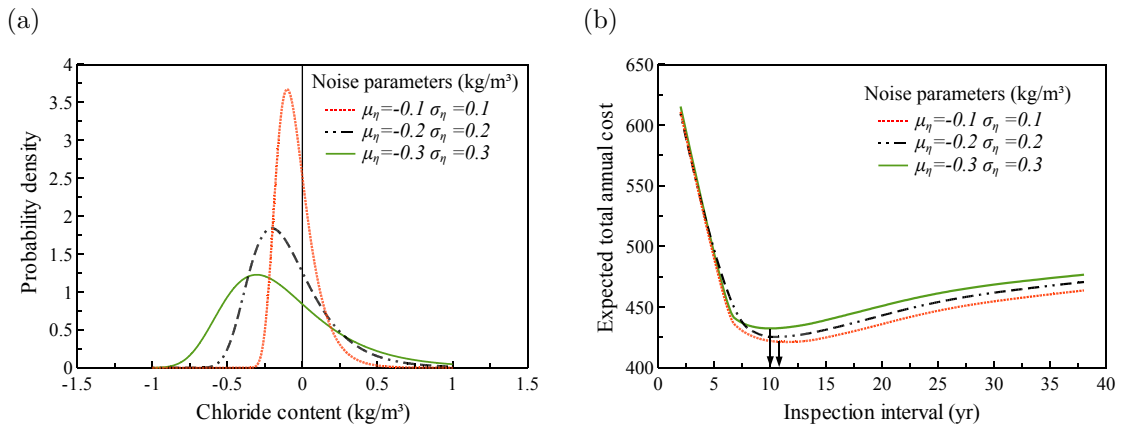


Figure 5.16 — Influence of the quality of the inspection technique on the total expected annual costs.

5.7.2.2 Use of the model for decision-making

This section compares the cost-efficiency of three repair techniques that can be implemented in the maintenance strategy: formed concrete, wet shotcrete and dry shotcrete. Figure 5.17 presents the expected total annual cost for the three repair techniques and both exposure zones. Comparing the cost of the repair techniques, it is observed that the cost of dry shotcrete is about a half of the other techniques. This behavior is explained by the fact that the repair material used in this technique has the lowest chloride diffusion coefficient (Table 5.3). Therefore the probability of corrosion initiation throughout time is lower and the costs of inspection, repair and failure are reduced. For instance, according to Table 5.7, the largest inspection intervals correspond to this technique.

Concerning the effect of the exposition zone, it is noted in both cases and for all the repair materials that the optimal repair threshold is 1.2 kg/m³. This means that there is an optimal repair threshold for a particular problem and that decisions should be based on this optimal value. The overall behavior indicates that the expected total annual costs are lower for the atmospheric zone. Given that the environmental chloride concentration is lower in the atmospheric zone the time to corrosion initiation is larger. Therefore, structural components located in this zone require less maintenance compared with those located in the splash and tidal zone. These results indicate that spatial variability is particularly important for improving the management of corroding RC

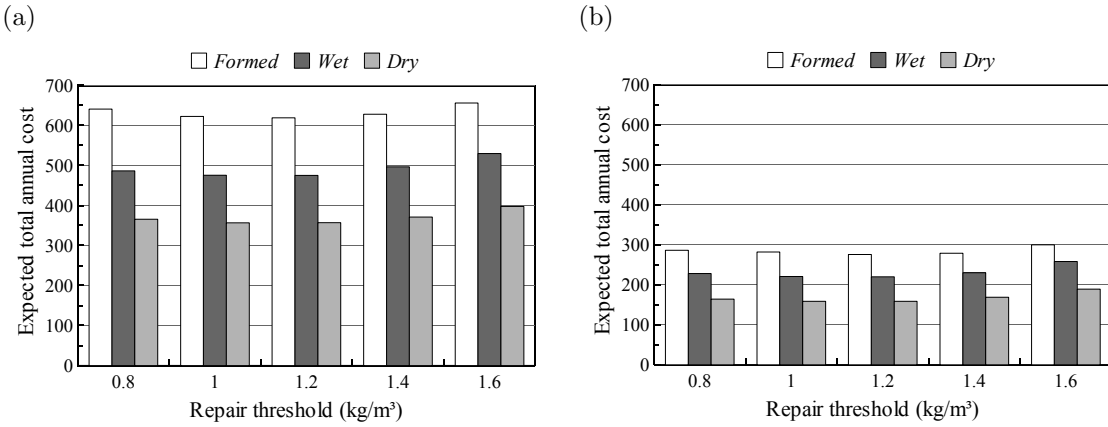


Figure 5.17 — Expected total annual cost for various repair materials and to environmental conditions:
(a) Splash and tidal zone and (b) atmospheric zone.

Table 5.7 — Optimal inspection intervals for various repair materials and exposure conditions.

Repair technique	Splash and tidal	Atmospheric
Formed concrete	8 yr	24 yr
Wet shotcrete	10 yr	27 yr
Dry shotcrete	13 yr	30 yr

structures. From an economic point of view, it is concluded that dry shotcrete is the more cost-efficient technique.

5.8 Conclusions

The main conclusions of this chapter are summarized as follows:

1. This chapter presented a preventive maintenance strategy where repair is carried out before corrosion initiation. This strategy was developed after discussion with the stakeholders that are confronted to this problem. The inspection technique measures the concentration of chlorides at the cover depth. Afterwards, based on the inspection results, the structure is repaired by replacing the polluted concrete with new material. This maintenance strategy ensures an optimal level of serviceability and safety during the structural lifetime.
2. Given that Markov chains are more appropriate for modeling all the stages of the life-cycle (i.e., deterioration process, inspection, maintenance, failure), this chapter proposed a methodology for determining the transition matrix from Monte Carlo simulations of a chloride penetration model. The Markovian approach included an initiation phase and several transition probabilities per state for improving the accuracy of the model.
3. The inspection/maintenance strategy chosen is modeled using decision theory and Markov processes. This approach is convenient to take into account the “good” or “wrong” decisions resulting from imprecise inspection measurement as well as the uncertainties involved in the process. In addition this chapter included data determined from experimental measurements or expert judgment to give more representative results.
4. The proposed method was illustrated with an example where it was showed that there is an inspection interval that minimizes the costs of inspection, repair and failure. This example

discussed the effect of the main influencing parameters as well as an application of the model for decision-making when various repair techniques can be applied. It is concluded that optimal management of maintenance requires:

- to optimize the repair threshold C_{rep} for a particular problem;
- to determine an appropriate probabilistic model for the threshold chloride concentration C_{th} ; and
- to improve the quality of the inspection technique.

This analysis has been performed by assuming that random variables are sufficient for characterizing uncertainty in material behavior of structural components and that destructive tests are the best alternative for inspection. However, the proposed approach should be improved in the future in two directions:

- Consideration of the spatial variability of the material in a given component and estimation of the length and the costs of the repaired surface. Expert judgment and non-destructive tests could be used to accomplish this aim.
- Combination of preventive and corrective repair strategies during the structural lifetime to find an optimal solution in a larger time-window. This requires to introduce ultimate limit states in lifetime assessment.

CHAPTER 6

SUSTAINABLE DECISION-MAKING FOR MAINTENANCE STRATEGIES

6.1 Introduction

The main challenge in sustainable management of corroding RC structures is to formulate a maintenance strategy technically and economically feasible, that reduces the environmental impact and that ensures optimal levels of serviceability and safety during the operational life. Recent advances in management aim to improve the performance of repair strategies by optimizing agency costs (Frangopol, 2010). However, multiple requirements imposed nowadays by environmental constraints undergo maintenance planning optimization into a major challenge to designers, owners and users of structures.

This chapter focuses on the evaluation of the sustainability of a maintenance strategy for RC structures exposed to chlorides. Towards this aim, this study takes advantage of the know-how of several stakeholders that are connected to the structure during its life-cycle –i.e., owners, designers, contractors, industry sectors, research centers, regional interests and government agencies. Maintenance strategies are directed to ensure serviceability and safety during operational life and/or to extend the life-cycle of structures. For instance, for chloride-induced corrosion, protective painting and cover rebuilding are strategies that increase the time at which the chloride concentration reaches the steel bars, reducing the time to corrosion initiation. The maintenance strategy of cover rebuilding by using different repair techniques has been chosen herein to formulate and to illustrate the proposed methodology.

The objectives of this chapter are:

1. to formulate the problem of sustainability in management of RC structures subjected to chloride penetration and to propose a methodology for its quantification;
2. to propose a methodology for decision-making when environmental constraints are added to the problem; and
3. to illustrate the proposed approach through application to real structure.

The conceptual formulation proposed herein for sustainable management is described in section 6.2. Section 6.3 presents the criteria taken into account in the sustainability analysis. Since these criteria are different in nature, section 6.4 depicts the approach adopted for decision-making under multi-objective constraints. Finally, section 6.5 illustrates the proposed approach with an application to large-scale maintenance of a real structure (Agri-foodstuffs terminal wharf). Although the

analysis focuses on a particular problem, the proposed methodology can be adapted for evaluating sustainability of other structures or materials subjected to different deterioration processes.

6.2 Sustainable management of deteriorating structures

Current advances in optimization of structural systems enable powerful prioritization of maintenance activities of deteriorating structures and infrastructures when the optimization function is defined in terms of costs or safety (Frangopol, 2010). The methodology proposed in chapter 5 combined the probabilistic model of chloride ingress presented in chapters 3 and 4 with a Markovian approach to determine an optimal *cost-effective management strategy*. However, nowadays the evaluation of the environmental impact should be integrated in the decision-making process to determine an optimal *sustainable management strategy*. The main difference between “cost-effective” and “sustainable” solutions lies in the consideration of environmental constraints in the second case. The following aspects should be considered to determine a sustainable management strategy:

- the implementation of a deterioration model representative of the considered phenomenon;
- the formulation of a maintenance strategy technically and economically feasible and that ensures optimal levels of serviceability and safety during the operational life;
- the implementation of an appropriate probabilistic framework for considering the uncertainties related to both the deterioration process and the inspection/maintenance actions;
- the establishment of criteria for the evaluation of the environmental impact; and
- the adoption of a multi-objective optimization procedure oriented to minimize costs and environmental impact.

This section presents a methodology to consider sustainability of repair techniques at different levels. For instance, it can be used to improve the sustainability of the formulation of a single maintenance technique and/or it can be implemented to compare different techniques. Figure 6.1 depicts the stages for obtaining a cost-effective/sustainable formulation of the maintenance technique. The following stages are required to determine both results:

1. *Formulation of the technique*: this is a crucial stage in the management process. The formulation should consider: the characteristics of the deterioration process, the stages of the maintenance (i.e., inspection, repair), the maintenance philosophy (i.e., preventive or corrective) and the technical and economic feasibility of the selected technique. To define an appropriate technique, all the stakeholders that are connected to the structure during its life-cycle should participate in this stage.
2. *Modeling of deterioration and maintenance actions*: experimental testing is the best way to determine and to improve the performance of repair techniques. However, given that these tests are expensive and time-consuming, numerical modeling of deterioration and repair actions is essential to study and/or to improve the efficiency of maintenance techniques in most cases. Furthermore, the uncertainty related to the deterioration process and the maintenance actions should be considered to improve the predictability of the models. Although some specialized companies currently implement some of these aspects in lifetime

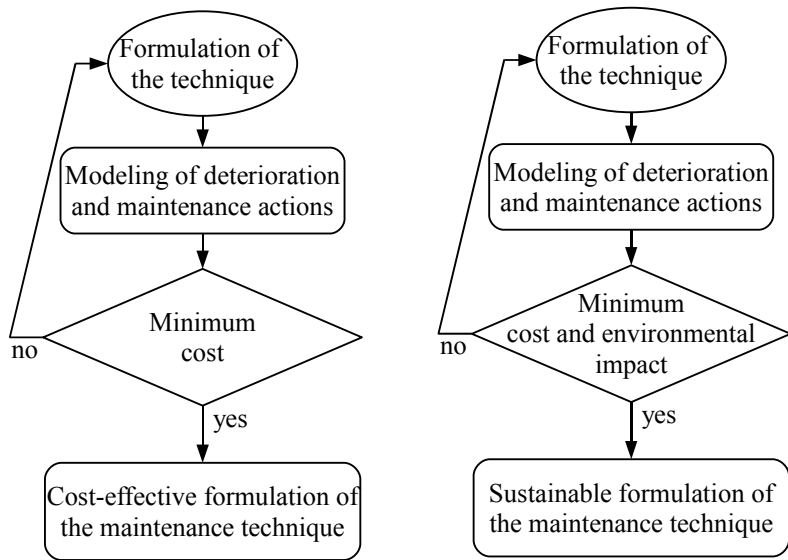


Figure 6.1 — Cost-effective and sustainable formulation of repair techniques.

assessment, this stage is mainly carried out by research centers. Realistic predictions also require experimental data in addition to the feedback of contractors and agencies.

3. *Improvement of the formulation:* the performance of each maintenance technique can be improved by optimizing its governing parameters. Classically, the optimization function aims to minimize costs and will provide an *optimal cost-effective formulation of the maintenance technique*. Nevertheless, to reduce the environmental impact, it is necessary to include environmental constraints in the optimization problem. Under these considerations, the optimization will lead to an *optimal sustainable formulation of the maintenance technique*. This stage is in an exploratory phase and is therefore carried out mainly by research centers. However, the diffusion of these techniques to consultants is imperative. Again, the feedback of contractors and agencies are essential to provide feasible results.

When there are various management techniques to solve the management problem, several cost-effective/sustainable formulations can be established in the first stage (Figure 6.2). Therefore, the proposed methodology can also be extended to a second level to compare the sustainability of different maintenance options. In the classical approach, the selection of an optimal management strategy is focused on minimizing costs. In the proposed approach, the comparison between several management alternatives also includes environmental criteria. The definition and the assessment of these criteria for corroding RC structures are described in the following section.

6.3 Sustainability of repair strategies

The World Commission on Environment and Development (1987) defines sustainable development as: *development that meets the needs of the present without compromising the ability of future generations to meet their own needs*. According to Struble & Godfrey (2004), there are three components of sustainability: environment, economy and society (Figure 6.3). To meet its goal, sustainable development must provide a balance between these components (Sánchez-Silva & Rosowsky, 2008).

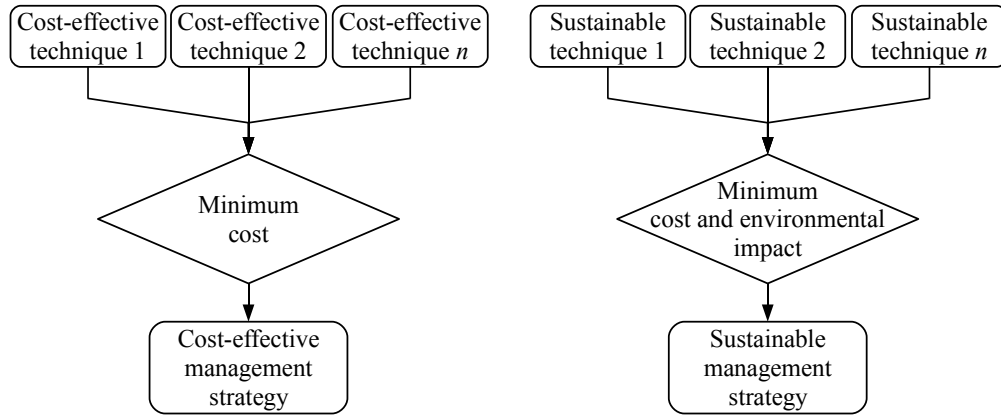


Figure 6.2 — Selection of an cost-effective/sustainable management strategy.

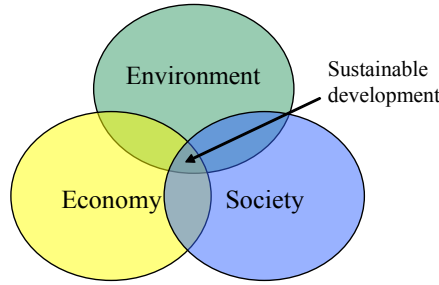


Figure 6.3 — Components of sustainable development.

The sustainability analysis proposed in this study accounts principally for environmental and economic components. However, society is directly implied in decisions affecting these components. Thus, the evaluation of the sustainability of the repair techniques is based on the comparison of three criteria:

1. cost,
2. waste generation, and
3. carbon dioxide emissions.

Additional criteria can also be considered. For instance, given that NOx emissions cause respiratory diseases, its effect should be included in urban environments.

6.3.1 Cost

Two kinds of costs are usually considered in cost analysis: *agency* and *user* costs. Agency costs encompass the direct costs incurred by the owner/operator during the life-cycle including initial construction costs and costs associated with inspection, repair, rehabilitation, replacement and disposal. User costs represent the inconvenience and expenses incurred by users due to traffic disruption such as travel delay costs, ship operating costs and accident costs. According to Thoft-Christensen (2009), user costs should be included in the analysis to formulate a comprehensive strategy of maintenance management of infrastructure. However, given that the information to estimate user costs is hard to find, this work is only based on agency costs.

Given that this study focuses on repair of RC structures, the direct costs incurred by the agency include only costs associated with maintenance (inspection, repair and failure). The initial construction costs are not included in the analysis because it is assumed that it would be the same for all maintenance alternatives. Since it is not possible to determine the final use of the structure at the end of the life-cycle (deconstruction or demolition), the residual (or salvage) value is also not considered.

The procedure to calculate total costs is described in chapter 5. Basically, these costs depend on the properties of the original and repair material; and on the characteristics of the maintenance strategy (i.e., inspection interval, inspection quality, repair threshold, etc.).

6.3.2 Waste generation

Concrete has been recognized as the largest and most visible component of construction and demolition waste. According to estimates presented in the Environmental Resource Guide (American Institute of Architects, 1999), concrete accounts for up to 67% by weight of construction and demolition waste (53% by volume), with only 5% currently recycled. Therefore, waste generation should be included as a selection criterion for sustainable management.

A comprehensive assessment of waste generation should include waste generated during the production of the repair material and the repair operations. However, taking into account the difficulties in estimating the waste generated during the production of concrete, this study only considers waste produced during repair operations (demolition and rebuilding). Waste generation is expressed in m^3 of waste generated to repair 1 m^3 of polluted concrete. Then the waste produced during demolition, W_d , is equal to 1 m^3 . The waste produced during the repair, W_r , depends on the characteristics of the repair technique. By knowing W_d and W_r for a specific repair strategy, the total waste W_T (in m^3 of waste) is:

$$W_T = W_d + W_r \quad (6.1)$$

The expected annual total waste $E[W_T]$ (in m^3 of waste per year) is computed in terms of the expected annual repair rate ν_r as:

$$E[W_T] = \nu_r W_T \quad (6.2)$$

where the expected annual repair rate, expressed in number of repairs per year, is determined from the procedure described in chapter 5. This parameter depends mainly on the characteristics of the repair technique.

6.3.3 Carbon dioxide emissions

According to the International Panel on Climate Change (IPCC, 2007), carbon dioxide emissions are identified as one of the major causes of global warming. Therefore, taking into account that the world's yearly production of 1.6 billion tons of cement accounts for about 7% of the global emissions of CO_2 into the atmosphere (Kumar Mehta, 1997), the assessment of carbon dioxide emissions produced during repair operations is crucial for sustainable development. This analysis takes two sources of carbon dioxide into account:

1. emissions produced during transportation of materials, equipments and waste, E_t , and

2. CO₂ released during production of the repair material, E_p .

The emissions produced to repair 1 m³ of polluted concrete during transportation are calculated by summing the emissions released during provision of repair materials E_m , provision of equipments E_e and those generated during disposal of waste E_d :

$$E_t = E_m + E_e + E_d = \nu_t [n_m(L_m + \gamma L_d) + n_e L_e] \quad (6.3)$$

where n_m and n_e are the equivalent number of travels to transport the repair materials and equipments required to repair 1 m³ of polluted concrete, respectively; L_m , L_e and L_d are the distances (in km) of provisioning of repair materials and equipments and of disposal of waste, respectively; γ is an expansion factor to compute the volume of the demolished concrete; and ν_t is the rate of CO₂ emissions of the transportation vehicle (in grams of CO₂ per km). For the sake of simplicity, it is supposed in equation 6.3 that:

- repair materials, equipments and waste are transported in the same vehicle, and
- L_m is the distance from the building supplies store or the concrete plant to the repair site. In other words, emissions released during transportation from the cement plant to the store or the concrete plant are not considered.

The equivalent number of travels to transport repair materials is calculated in function of the waste produced during demolition and repair:

$$n_m = 2 \frac{W_T}{V_t} \quad (6.4)$$

where V_t represents the capacity of the transportation vehicle in m³. The equivalent number of travels to transport equipments is defined by considering the particular requirements of a repair technique as:

$$n_e = 2 \frac{N_e}{V_r} \quad (6.5)$$

where N_e is the total number of travels to transport the equipments required to repair a volume V_r of polluted concrete. V_r should be expressed in m³. Note that equations 6.4 and 6.5 are multiplied by 2 to take the round trip into account. The distances of provisioning and disposal are characteristic of a given problem.

On the other hand, the CO₂ released during production of the repair material (in kg CO₂ per year) is estimated as:

$$E_p = W_T c_c \nu_p \quad (6.6)$$

where c_c is the cement content per m³ of concrete (in kg/m³) and ν_p is the rate of emissions of CO₂ during the production of the repair material (in kg CO₂/kg of repair material). According to the International Energy Agency (2007), the average CO₂ emissions range from 0.65 to 0.92 kg of CO₂ per kg of cement across several countries. Since there is no information about the CO₂ emissions related to the production of the repair products, a weighted average emission of $\nu_p = 0.83$ kg CO₂/kg of repair material is adopted herein for all the repair products.

The expected annual total CO₂ emissions E[E_T] (in kg of CO₂ per year) required to repair 1 m³ of concrete is also estimated in terms of the expected annual repair rate ν_r as:

$$E[E_T] = \nu_r E_T = \nu_r (E_t + E_p) \quad (6.7)$$

This section presented the three criteria that are considered herein to perform the sustainability analysis. The following section presents the method adopted for decision-making when the problem is governed by various criteria.

6.4 Decision-making under multi-objective constraints

The challenge in management of deteriorating structures lies in its multi-objective nature. Owners/operators are confronted to simultaneously satisfy several criteria such as: minimization of cost, traffic disruptions and environmental impact on the one hand, and improvement of serviceability, functionality and safety on the other hand. The techniques of multi-criteria or multi-objective optimization are appropriate to deal with this problem. According to Lounis (2006), the following approaches are available in the literature:

- multi-attribute utility theory;
- weighted sum approach;
- compromise programming;
- constraint approach; and
- sequential optimization.

Each method is useful depending on the considered environments and circumstances. However, compromise programming is more appropriate for finance/engineering problem where the decision maker cannot afford to replace objective information by subjective points of view, although the principle of bounded rationality is still accepted in a moderate way (Ballesteros, 2007). Therefore, compromise programming is adopted herein to solve the multi-objective problem.

6.4.1 Compromise programming

For this problem, an optimal solution should minimize the costs and the environmental impact. The optimal solution can be found by using multi-objective optimization. Compromise programming minimizes the distance from the set of Pareto optima to the so-called *ideal solution*. The ideal solution is defined as the solution that yields simultaneously optimal values for all objectives. For m objective functions, the ideal solution can be associated with the following ideal objective vector:

$$\mathbf{f}^* = [x_1^*, x_2^*, \dots x_m^*] \quad (6.8)$$

where x_i^* is the ideal solution of the optimization criterion f_i with $i = 1, \dots, m$. In this particular case there are three criteria to evaluate: (1) costs, (2) waste generation and (3) CO₂ emissions. Since each criterion has its own system of units, this study uses a multi-objective index (MOI) to determine the optimal technique (Lounis, 2006). A MOI is defined for each technique as the value

of the weighted and normalized deviation from the ideal solution \mathbf{f}^* measured by the family of L_p metrics. Thus, the “satisfying” solution is the one that yields a minimum MOI:

$$\text{MOI}(x) = \left[\sum_{i=1}^m w_i^p \left| \frac{x_i - x_i^*}{x_{i*} - x_i^*} \right|^p \right]^{1/p} \quad (6.9)$$

where w_i is the weighting factor of the optimization criterion f_i , p is a parameter indicating the importance given to deviations from the ideal solution, and x_{i*} is the anti-ideal solution of f_i . The value of w_i varies between 0 and 1 with $\sum_{i=1}^m w_i = 1$. The weighting factors depend mainly on the attitude of the owner/operator towards each criterion. The parameter p varies between 1 and ∞ . For $p = 1$, all deviations from the ideal solution are considered in direct proportion to their magnitudes, which corresponds to a group utility (Duckstein, 1984). For $p = 2$, a greater weight is associated with the larger deviations from the ideal solution and L_2 represents the *Euclidian* metric. For $p = \infty$, the largest deviation is the only one taken into account and is referred to as the *Chebyshev* metric or mini-max criterion and L_∞ corresponds to a purely individual utility (Lounis, 2006).

Once the framework for sustainability analysis has been defined, the following section illustrates its application to a real problem.

6.5 Case study: Agri-foodstuffs terminal

The Agri-foodstuffs terminal of the port of Nantes Saint-Nazaire (Figure 6.4a) is a structure subjected to chloride-induced corrosion and will be used in this study to illustrate the proposed methodology. The Port of Nantes Saint-Nazaire is the government agency managing the harbor activities of this structure. This agency observed a generalized problem of corrosion affecting mainly the RC beams (Figure 6.4b) and decided to perform a large-scale repair (Rosquoët et al., 2006).

This terminal is part of the port of Nantes Saint-Nazaire (fourth largest port in France) which is linked to 400 ports worldwide. With a maximal draught of 14 m, the Agri-foodstuffs terminal plans to receive big tonnage ships as container carriers (50,000 Ton). The Port of Nantes Saint-Nazaire is the French market leader for cattle feed imports with nearly 60% market share. There are four berths at the Agri-foodstuffs terminal, which also handles fertilizers, peat, cement and other miscellaneous industrial bulk products. This wharf was built in 1971 and is located at the west of France (Montoir de Bretagne) in the estuary of the Loire River.

Figure 6.5 presents the zone of the Agri-foodstuffs terminal to be repaired. This zone has a triangular form, is 68 m long and 37 m wide. The structure is composed by a RC deck of 0.32 m thick, put down on a triangular network of RC beams of 1.00 m side. The beams are supported by steel piles filled with concrete in the upper side. The piles have external diameters of 711, 813 and 914 mm.

6.5.1 Characteristics of the repair techniques

The maintenance strategy for the Agri-foodstuffs terminal consists basically of rebuilding the polluted concrete cover by various repair techniques. The deteriorated and contaminated concrete is removed using high velocity water jets (hydrodemolition) and the cover is rebuilt by using various techniques. This section presents the techniques used to rebuild the cover of the wharf and that

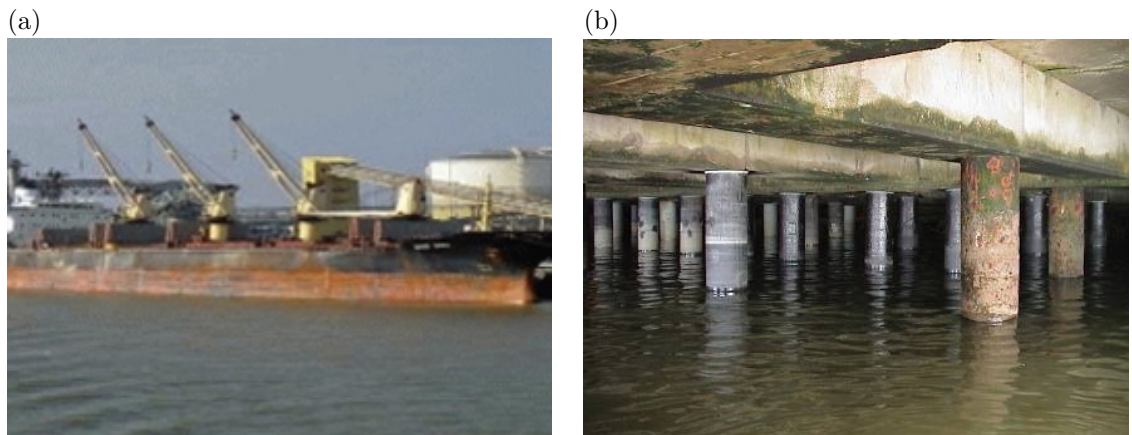


Figure 6.4 — (a) Agri-foodstuffs terminal. (b) Corroded beams.

Table 6.1 — Features of the selected repair materials.

Features	Wet shotcrete	Dry shotcrete	Formed concrete
Initial strength	20 MPa in 24 hours	11 MPa in 3 hours	4 MPa in 3 hours
Thickness per coat	up to 50 mm	up to 100 mm	up to 100 mm
setting	Rapid	Rapid	Rapid
bonding	Excellent	Excellent	Excellent

will be compared on the basis of the sustainability. The basic requirements for the selection of the repair techniques are summarized as follows:

- The repair techniques should be easily implemented to repair structural components located in the splash and tidal zones (e.g., beams and piles of wharfs).
- The repair techniques should be applicable to large-scale repairs; local or patch repairs are beyond the scope of the study.
- The repair materials should have similar composition (i.e., cement-based composition) to focus the analysis on the techniques.

After discussion with the stakeholders participating in the MAREO project, three repair techniques were chosen: (1) wet shotcrete; (2) dry shotcrete and (3) formed concrete. Since there is no previous experience about the performance of the repair materials and techniques, the alternatives selected were tested on twelve chloride-contaminated beams which have been exposed to seawater during 80 years. The beams were part of the structural system of a port built in 1927 at Lorient, France, and demolished in 2006. Figure 6.6 presents the beams before repair. An important degree of corrosion including cover spalling is observed in all of them. Furthermore, accelerated tests on slabs are being performed in laboratory to characterize the repair materials. Table 6.1 describes the main characteristics of the repair materials. In general, the materials have a high initial strength, rapid setting, excellent bonding, and a thickness per coat higher than 50 mm.

Based on the data reported by Vilvoisin & Aury (2009) after repair, a comparison among all repair techniques is presented in Table 6.2. This comparison focuses on: product cost, staff requirements, waste generation and finishing. The staff requirements reported herein correspond to the repair of the testing specimens. Some practical aspects of the repair process showed that the waste production of wet shotcrete is almost negligible, finishing is satisfactory and it can be

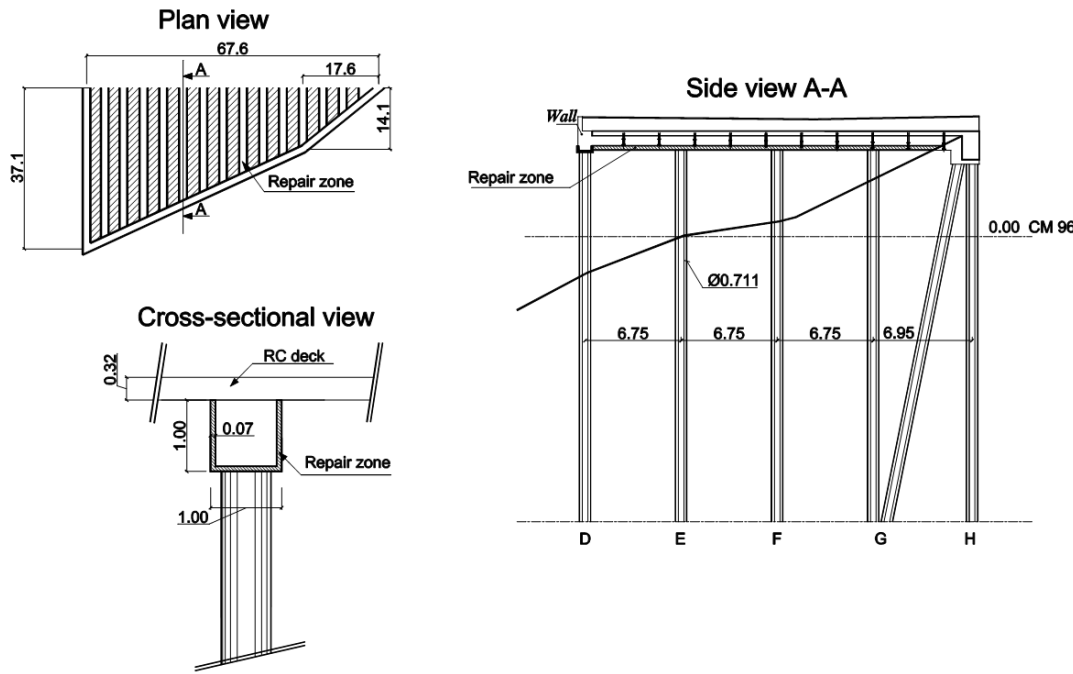


Figure 6.5 — Zone of the Agri-foodstuffs terminal to be repaired.



Figure 6.6 — Beams after 80 years of exposure.

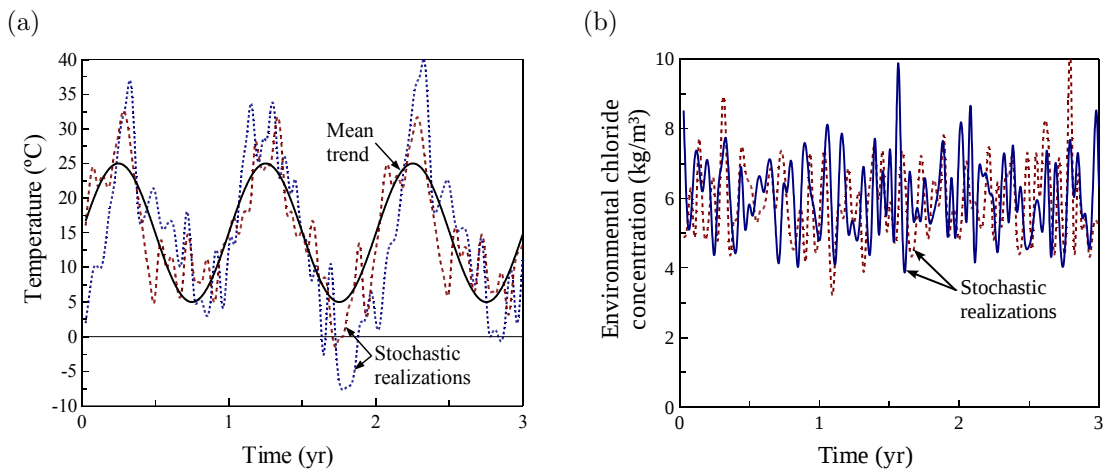
enhanced by polishing. However, wet shotcrete is the most expensive repair technique, requires the highest number of staff and some cracks were observed after 2-3 days (shrinkage). Although the waste produced by dry shotcrete is the largest, the work area is easily cleaned and the product is ready-to-use, which is convenient for large-scale projects. Given both, its extreme fluidity (no need for vibrators to compact the concrete) and its high workability, the best finished surface corresponds to formed concrete. Yet, the use of such technique is limited to places where the formwork can be placed.

6.5.2 Assessment of the repair rates

Given that there is no information about the repair times for each technique, its performance is evaluated in terms of its annual repair rates, ν_r . These rates are determined on the basis of the Markovian approach described in chapter 5 and will be used to evaluate the environmental impact of maintenance strategies (i.e., equation 6.2 and 6.7). The main advantage of this methodology lies in the consideration of the most important phenomena influencing chloride ingress and maintenance

Table 6.2 — Comparison between products and repair techniques.

Criteria	Wet shotcrete	Dry shotcrete	Formed concrete
product cost	17€ / 25 kg	7€ / 25 kg	5€ / 35 kg
staff	5 people	3 people	2 people
waste generation	not significant < 5%	important > 30%	not significant < 5%
finished	satisfactory	rough	very satisfactory

**Figure 6.7** — Stochastic inputs of: (a) weather, (b) environmental chloride concentration.

including uncertainties and consequences of “good” or “wrong” decisions.

6.5.2.1 Basic considerations

The influence of weather on chloride ingress is considered by assuming that the structure is placed in an oceanic climate where the mean temperature varies between 5 and 25 °C, and the mean relative humidity ranges from 0.6 to 0.8. The stochastic nature of weather and environmental chloride concentration is integrated by using the methodology presented in chapter 4. Figure 6.7 presents some realizations of temperature and environmental chloride concentrations. To model temperature, a stochastic perturbation is added to a sinusoidal mean trend by using Karhunen-Loève expansion (Ghanem & Spanos, 1991). The truncated expansion series in this model includes 30 terms, the autocorrelation is exponential and the correlation length is 0.1 years. Since several studies indicate that the environmental chloride concentration C_{env} follows a log-normal distribution (Vu & Stewart, 2000; Duracrete, 2000), this work models this variable as a stochastic process generated by independent log-normal numbers (log-normal noise). A coefficient of variation of 0.2 was assumed to model C_{env} . Although the maintenance strategy has been formulated for structural members located in the splash and tidal zone, its influence on the atmospheric zone is studied for illustrative purposes. The means of C_{env} for the “splash and tidal” and “atmospheric” zones are 6 and 3 kg/m³, respectively.

The probabilistic models of the random variables used in this example are shown in Table 6.3. The mean of the reference chloride diffusion coefficient depends on the characteristics of the material. Whereas the chloride diffusion coefficient for the original material was assigned according to the experimental values reported by Saetta et al. (1993), the chloride diffusion coefficients were defined based on preliminary results obtained in the framework of the MAREO project (Villain et

Table 6.3 — Random variables for modeling chloride ingress.

Variable	Units	Distribution	Mean	COV
$D_{c,ref}$ (original material)	m^2/s	log-normal	3.0×10^{-11}	0.2
$D_{c,ref}$ (formed concrete)	m^2/s	log-normal	4.5×10^{-11}	0.2
$D_{c,ref}$ (wet shotcrete)	m^2/s	log-normal	2.0×10^{-11}	0.2
$D_{c,ref}$ (dry shotcrete)	m^2/s	log-normal	1.8×10^{-11}	0.1
U_c	kJ/mol	beta on [32;44.6]	41.8	0.1
m		beta on [0;1]	0.15	0.3
$D_{h,ref}$	m^2/s	log-normal	3×10^{-10}	0.2
α_0		beta on [0.025;0.1]	0.05	0.2
n		beta on [6;16]	11	0.1
λ	$\text{W}/(\text{m}^\circ\text{C})$	beta on [1.4;3.6]	2.5	0.2
c_q	$\text{J}/(\text{kg}^\circ\text{C})$	beta on [840;1170]	1000	0.1
ρ_c	kg/m^3	Normal	2400	0.2

al., 2010). For the sake of simplicity, it is assumed that the other model parameters are similar for all materials. The considerations for choosing the random variables are presented in chapter 4.

The assessment of the repair rates for the problem studied in this chapter takes the following assumptions into account:

- the Langmuir isotherm is used to consider chloride binding which coefficients for this case are $\alpha_L = 0.1185$ and $\beta_L = 0.09$;
- the repair times are established by assuming chloride penetration in one dimension; and
- the random variables are independent and do not vary in the space.

It is important to highlight that the assumptions mentioned previously are used in this work only for illustrative purposes. The hypothesis of chloride diffusion in one dimension should be carefully validated for particular cases. According to Val & Trapper (2008), chloride penetration in two dimensions is an influencing mechanism that should be considered when estimating chloride ingress in small structural members as columns and beams. On the other hand, the influence of spatial variability should be also included to improve the assessment of chloride penetration. Stewart (2004) presents a comprehensive approach to account for the spatial variability of corroding RC beams in flexure and studies its influence on reliability. An application of this methodology to the stochastic assessment of repair times and the evaluation of efficiency of maintenance is presented in (Mullard & Stewart, 2009).

6.5.2.2 Repair rates

The repair rate ν_r was defined in chapter 5 by minimizing costs of inspection, repair and failure. This parameter will be used herein to improve the selection of the inspection interval by accounting for environmental constraints, and afterwards, to determine a sustainable management strategy.

Figure 6.8 presents the influence of the inspection interval on inspection and failure repair rates for dry shotcrete and the splash and tidal zone. These rates are expressed in percentage of repairs per year and were computed by following the procedure described in chapter 5. The following parameters were used in the assessment: $M = 10$ states, $C_{rep} = 1.2 \text{ kg}/\text{m}^3$, $\mu_{C_{th}} = 2.56 \text{ kg}/\text{m}^3$ and $\text{COV}[C_{th}] = 0.20$. A complete description of the considerations of the Markov model is presented in section 5.7.

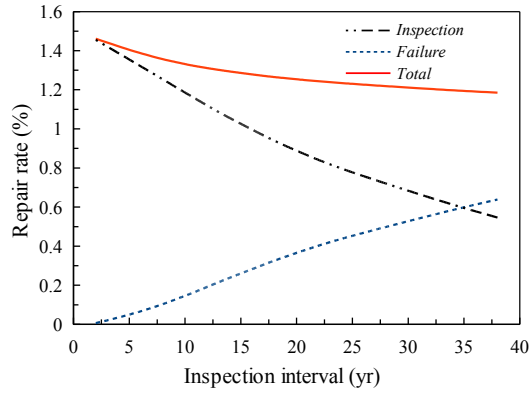


Figure 6.8 — Influence of the inspection interval on inspection and failure repair rates for dry shotcrete and the splash and tidal zone.

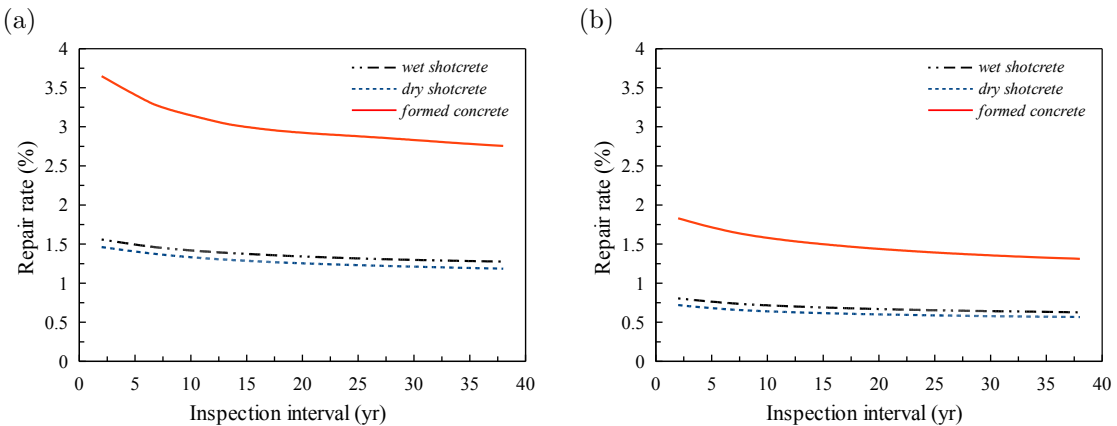


Figure 6.9 — Repair rates for all the repair techniques and: (a) splash and tidal zone and (b) atmospheric zone.

The expected annual total repair rate ν_r for a given inspection interval Δt is calculated by summing the repairs carried out at an inspection year with those produced by failure between two inspection years. In general terms, ν_r is higher for small inspection intervals and leads to a constant value when Δt increases. It is also observed that when the structure is inspected periodically ν_r is controlled by the repairs carried out at inspection years whereas for larger inspection intervals it depends on the repairs produced by failures between inspections.

Figure 6.9 shows the expected annual total repair rates for all the repair techniques and zones. As expected, for both zones the larger ν_r corresponds to techniques whose repair materials have larger chloride diffusivity (i.e., formed concrete and dry shotcrete). By comparing ν_r for splash and tidal (Figure 6.9a) and atmospheric (Figure 6.9b) zones, it is noted that structures or structural members located in the last zone require less repair. This behavior is expected because the low environmental chloride concentration in atmospheric zones decreases corrosion risk. It is paramount to clarify that the repair rates reported herein are illustrative. Since the coefficients of diffusion were defined on the basis of previous experimental results (Villain et al., 2010), these rates only show the tendency of the overall behavior.

Table 6.4 — Computed agency costs.

Item	Wet shotcrete €	Dry shotcrete €	Formed concrete €
Hydrodemolition	1500	1500	1500
Recovery, treatment and disposal of waste	172	172	172
Materials	1309	828	250
Labor	685	418	192
Equipments	183	210	94
Total	3848	3128	2208

Table 6.5 — Coefficients for cost models.

Parameter	Repair technique		
	Formed concrete	Dry shotcrete	Wet shotcrete
Initial cost of construction, C_0	1000	1000	1000
Inspection coefficient, k_I	0.005	0.005	0.005
Repair coefficient, k_R	0.15	0.21	0.26
Failure coefficient, k_F	0.30	0.42	0.52

6.5.3 Criteria for sustainability analysis

This section describes the evaluation of the criteria considered for sustainability analysis for a single repair operation. These values will be used latter to establish a sustainable inspection interval and to compare the performance of the three repair techniques from economic and environmental points of view.

6.5.3.1 Total cost

Table 6.4 presents the agency costs estimated to repair 1 m³ of polluted concrete. Such costs were estimated based on the repair experience reported in section 6.5.1 (e.g., Table 6.2) and include costs related to hydrodemolition of the polluted concrete, cover rebuilding, labor, equipments (rental), form, transport and waste disposal. It is noted, for a single repair operation, that wet shotcrete is the most expensive alternative. Wet shotcrete uses the most expensive material and requires more labor (Table 6.2). On the contrary, formed concrete is the cheapest option.

The costs presented in Table 6.4 cannot be used directly for decision-making because they do not consider the effectiveness and the environmental impact of the repair technique. They are used herein to estimate the repair and failure cost coefficients (i.e., k_R and k_F) defined in section 5.6. Taking into account the average expenditures for construction, inspection and failure incurred by the port of Nantes-Saint Nazaire and the costs presented in Table 6.4, the coefficients for the cost models are presented in Table 6.5. These cost coefficients are referred to an initial construction cost of 1000 units per structural element.

6.5.3.2 Waste generation

Figure 6.10a shows the waste produced to repair 1 m³ of concrete by discriminating for repair operations (i.e., demolition W_d and repair W_r). The waste generation is expressed in m³ of waste. Then, the waste produced by hydrodemolition is equal to 1 m³. For cover rebuilding, waste production is estimated by taking the values measured during the repairs into account –i.e., Table 6.2. Although the highest production of waste corresponds to the demolition phase, there is a large

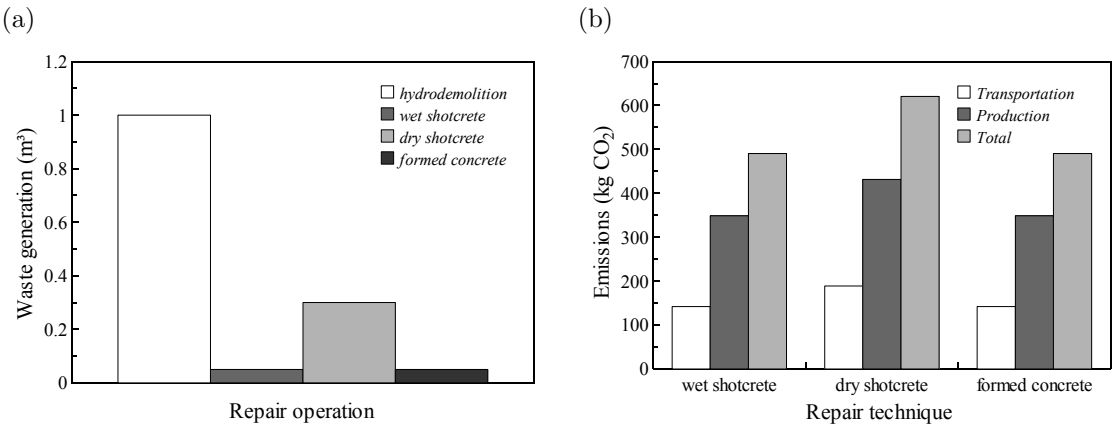


Figure 6.10 — (a) Waste and (b) emissions generated to repair 1 m^3 of polluted concrete.

Table 6.6 — Parameters used in the estimation of CO_2 emissions.

Variable	Value
Capacity of the transportation vehicle, V_t (m^3)	8
Volume of concrete to repair, V_r (m^3)	65.7
Expansion factor, γ	1.3
Distance of provisioning of repair materials, L_m (km)	100
Distance of disposal of waste, L_d (km)	150
Distance of provisioning of equipments, L_e (km)	100
CO_2 emissions of the transportation vehicle, ν_t (kg CO_2 per km)	1.7
CO_2 emissions for production of cement, ν_p (kg CO_2 / kg of repair material)	0.83
Content of cement per m^3 of concrete, c_c (kg/m^3)	400

loss of material for the dry shotcrete technique.

6.5.3.3 Carbon dioxide emissions

Table 6.6 summarizes the values used in the assessment of carbon dioxide emissions. According to Norton et al. (1998), it is assumed in this study that the average emission of CO_2 for a truck is 1.7 kg of CO_2 per km. This estimation also supposes that all transportation of materials and waste is carried out in a standard truck with a capacity of 8 m^3 . The distances of provisioning of materials and equipments and disposal of waste are 100 and 150 km, respectively.

Figure 6.10b depicts the emissions of CO_2 per 1 m^3 of concrete repaired (in kg CO_2) for source and repair technique. These results were obtained for a single repair operation. For all the techniques, it is observed that the emissions released during the production correspond to about 75% of the total. Therefore, current research efforts should be addressed to reduce the production emissions. For a single repair operation, the emissions released for wet shotcrete and formed concrete are the same, whereas dry shotcrete is more contaminant. This behavior is explained by the fact that for the same volume of repaired concrete, dry shotcrete requires a higher quantity of material (30% of waste generation –i.e., Table 6.2) increasing the emissions of transportation and production.

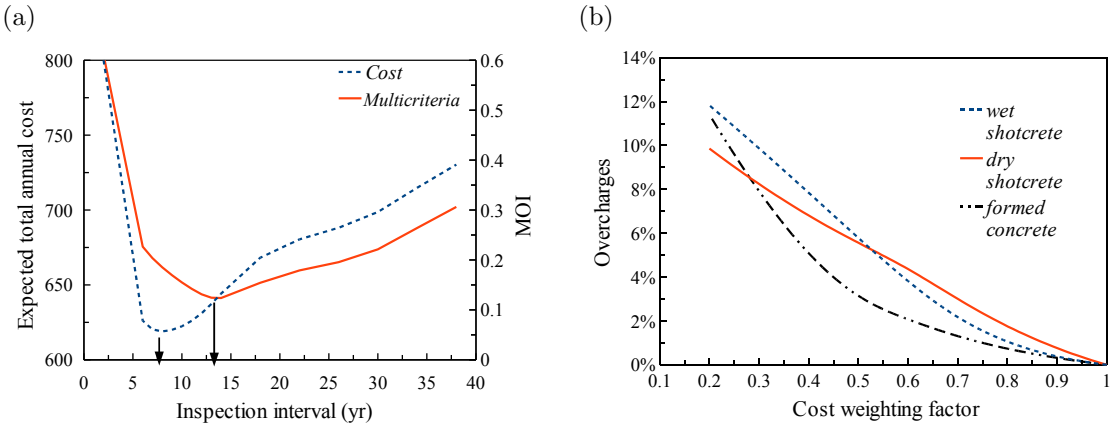


Figure 6.11 — (a) Cost-effective and sustainable inspection interval. (b) Overcharges produced when environmental criteria are considered.

6.5.4 Sustainable decision-making

As mentioned before, the proposed methodology can be implemented at different levels. Thus, the first part of this section illustrates its use to define a sustainable inspection interval for a given repair technique. Then, the discussion focuses on the comparison of the performance of different repair techniques from a sustainable point of view.

6.5.4.1 Sustainable inspection interval

This section compares the inspection intervals computed by considering only economic aspects (chapter 5) with those obtained by adding environmental constraints. Figure 6.11a presents an example where the inspection interval Δt is obtained for both cases. These data were computed for the formed concrete alternative and the aforementioned considerations. Given that the procedure for determining sustainable inspection intervals is similar for splash and tidal and atmospheric zones, only the results concerning the splash and tidal zone are illustrated. The assessment of the MOI considers the Euclidean metrics and assumes that the agency's policy gives weighting factors of 0.5 for costs, 0.25 for waste and 0.25 for CO₂ emissions. The procedure to compute the MOI was described in section 6.4. The Euclidean metric will be adopted herein for the following analyses. It is observed in Figure 6.11a that whereas the inspection interval that minimizes costs is 8 years, the inspection interval that reduces costs and environmental impact is 14 years. This difference is explained by the fact that the repair rate ν_r is reduced when the inspection interval increases (Figure 6.9). Therefore, the expected total waste generation and carbon dioxide emissions, that are directly related to ν_r (equations 6.2 and 6.7), also decrease for larger Δt .

The consideration of environmental constraints in the assessment of the inspection interval generates overcharges. The selection of a given interval depends on the agency's policies which could decide how much overcharges can be expended to reduce environmental impact. This decision is governed by socio-economic aspects that are characteristic of a given company or country. Economic or environmental priorities are measured herein by the weighting factors (equation 6.9). Consequently, Figure 6.11b shows the overcharges generated when the cost weighting factor, w_C , varies between 0.2 and 1. The estimation of the overcharges supposes that the waste weighting factor, w_W , and the CO₂ emission weighting factor, w_E , are equal. The cost weighting factor $w_C = 1$ implies that the decision is controlled only by costs. In this case, environmental constraints are

Table 6.7 — Scenarios for studying the influence of w_i .

	Cost, w_C	Waste, w_W	Emissions, w_E
Scenario 1	1.00	0.00	0.00
Scenario 2	0.80	0.10	0.10
Scenario 3	0.50	0.25	0.25
Scenario 4	0.20	0.40	0.40

Table 6.8 — Inspection interval and expected total annual costs for the studied scenarios.

Scenario	wet shotcrete		dry shotcrete		formed concrete	
	Δt (yr)	Total cost	Δt (yr)	Total cost	Δt (yr)	Total cost
1	11	465.51	13	357.1	8	618.97
2	13	468.07	18	361.91	11	626.04
3	22	493.79	26	375.23	14	644.16
4	34	527.97	38	396.16	22	680.45

not considered, and then, the overcharges are zero. On the contrary, for $w_C = 0$, the overcharges lead to a constant value determined at a larger inspection interval where the repair rate is minimum (i.e., Figure 6.9). For the range of cost weighting factors presented in Figure 6.11b, the maximum overcharges vary from 10% to 12% depending on the characteristics of each the repair technique. If the agency decides to give equal importance to economic and environmental criteria (i.e., $w_C = 0.50$, $w_W = 0.25$ and $w_E = 0.25$) the overcharges are lower than 6% for all the cases. This means that including environmental constraints in decision-making does not generate larger overcharges.

In order to study the influence of agency policies, Table 6.7 defines four different scenarios. The first scenario does not consider environmental impact. Although some environmental considerations are accounted for in the second scenario, it remains dominated by economic constraints. In the third scenario, economic and environmental constraints have the same weight. The latter scenario is mainly governed by environmental constraints.

Table 6.8 shows the inspection intervals and the expected total annual costs for the scenarios defined in Table 6.7. These values were obtained by minimizing the Euclidean MOI for the splash and tidal zone. It is observed that the expected total annual costs increase for the scenarios where the agency decides to give more weight to environmental impact. In these cases, the repair rate decreases (i.e., Figure 6.9) and repair is more corrective than preventive increasing failure costs. The adoption of the scenarios 3 or 4 has a positive effect on the environment. However, given that the corrosion risks increase for these scenarios, an analysis based on the ultimate limit state should be carried out to ensure that structural safety is not affected.

6.5.4.2 Criteria for the selection of a sustainable repair technique

Based on the repair rate computed in section 6.5.2.2 and the agency costs presented in Table 6.4, the expected annual costs to repair 1 m³ of polluted concrete for all the techniques and scenarios are presented in Figure 6.12. By comparing total costs, these results indicate that dry shotcrete is the cheapest alternative for all scenarios. The overall behavior indicates that total costs increase when the weight of environmental constraints is larger. According to Table 6.8, the length of inspection intervals is higher for scenarios 3 and 4. Therefore, the consideration of environmental constraints reduces inspection and repair costs and increases failure and total costs.

Figure 6.13a presents the waste generation and CO₂ emissions generated annually for each

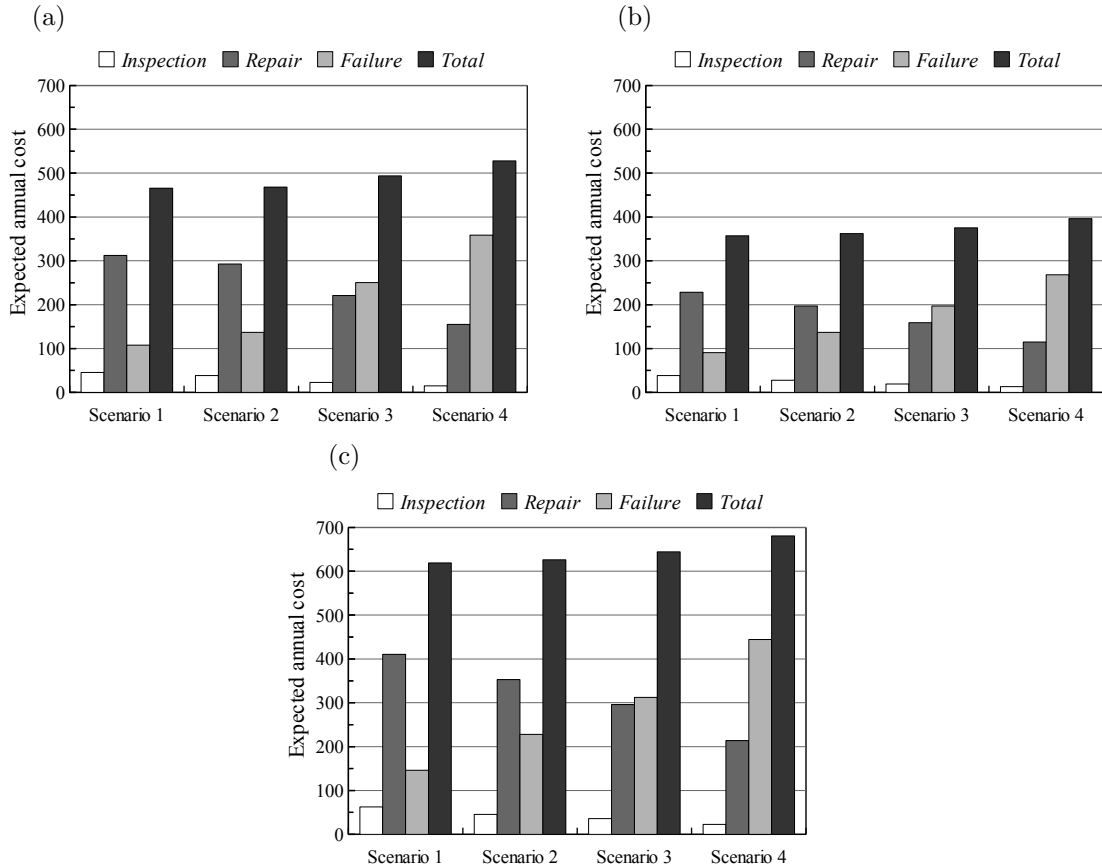


Figure 6.12 — Expected annual cost for (a) wet shotcrete, (b) dry shotcrete and (c) formed concrete.

alternative to repair 1 m³ of polluted concrete. Waste generation and CO₂ emissions are related because they are both dependent on the repair rate (i.e., equations 6.2 and 6.7). According to Figure 6.10, the higher loss of material and CO₂ emissions during the repair process corresponds to dry shotcrete. Nevertheless, formed concrete is the less environmentally friendly alternative given its higher repair rate. By comparing wet shotcrete and formed concrete in all the considered cases, it is noted that the environmental impact of wet shotcrete is about the half of the corresponding to formed concrete. For a structural lifetime of 50 yr, a volume of concrete to repair $V_r = 65.7 \text{ m}^3$ and the scenario 2, the choice of wet shotcrete instead of formed concrete will reduce the waste generation by 59.4 m³ and CO₂ emissions by 27.7 ton of CO₂. Consequently, given its low repair rate, waste generation and CO₂ emissions, it is concluded that wet shotcrete has the most positive effect on the environment.

From a comparison of the environmental impact of the different scenarios, it is noted that waste generation and CO₂ emissions decrease when the agency policies are more environmentally friendly. The reduction of environmental impact for different scenarios and repair techniques is depicted in Figure 6.13b. These reductions were calculated taking as reference the scenario 1 where environmental constraints are not considered. As expected, an increase of the weights of the environmental constraints reduces the environmental impact. These reductions range from 1.4% to 9.9% and are more important for formed concrete.

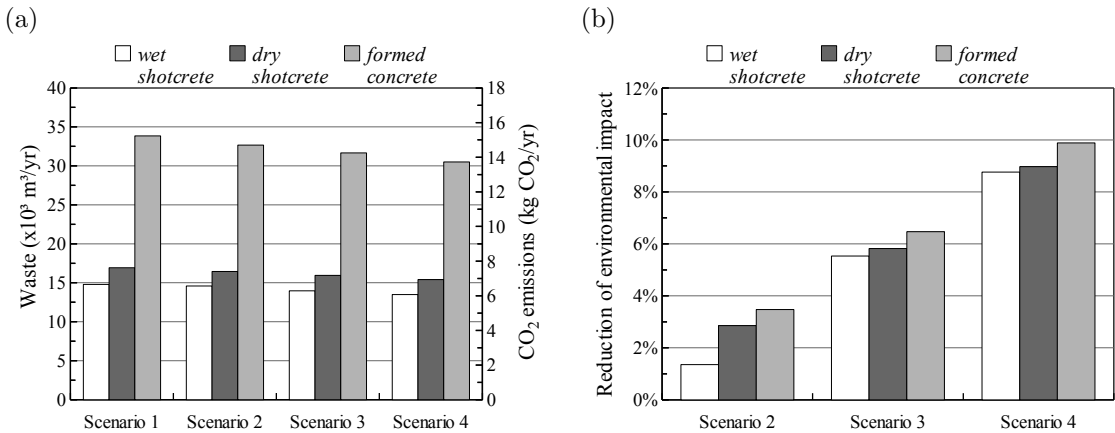


Figure 6.13 — (a) Waste generation and emissions of CO₂. (b) Reduction of environmental impact.

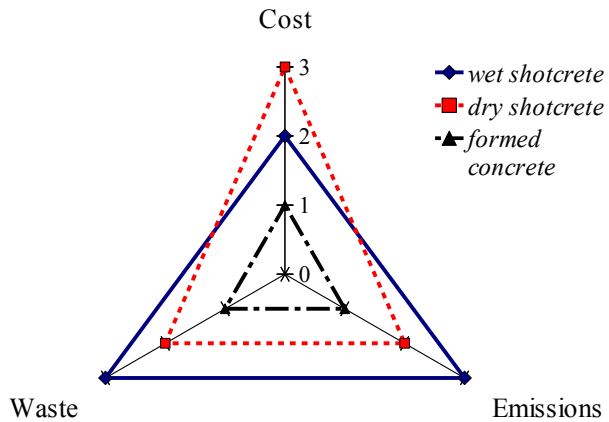


Figure 6.14 — Multi-criteria comparison.

6.5.4.3 Selection of a sustainable repair technique

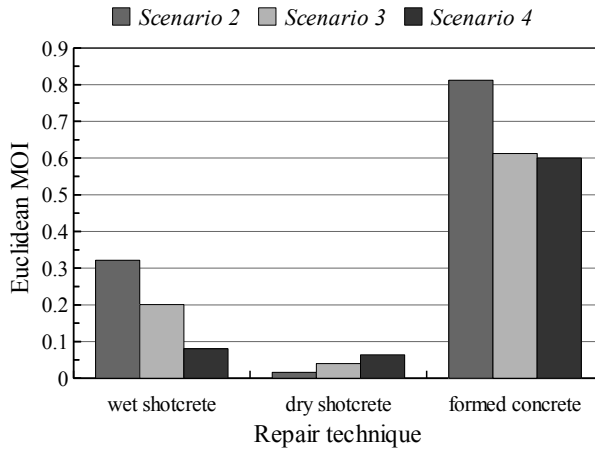
This section presents a decision-making scheme oriented to compare the performance of the repair techniques from economic and environmental points of view. It is assumed herein that the criteria to select the sustainable inspection interval correspond to the scenario 3 –i.e., the decision-maker gives the same priorities to economic and environmental aspects. Therefore, the expected total annual cost and repair rate reported in this section correspond to this case.

The comparative analysis also includes the three criteria described previously: (1) expected total annual cost, (2) waste production, and (3) CO₂ emissions. Since these criteria are quantified in their own type of units, for comparative purposes, the results are classified as 1, 2 or 3 based on its performance. Therefore, 1 is given to the alternative with the worst performance and 3 to the repair technique with best performance per criterion. For instance, 1 indicates that such alternative is more pollutant in terms of both waste generation and CO₂ emissions.

On the basis of this new classification, Figure 6.14 presents a multi-criteria comparison for the studied repair techniques. These results indicate that there is no a repair technique that satisfies all the criteria. Economically speaking, dry shotcrete is the cheapest alternative followed by wet shotcrete and formed concrete. From an environmental point of view, wet shotcrete generates less waste and carbon dioxide followed by dry shotcrete and formed concrete. The formed concrete option becomes unattractive due to its high environmental impact and costs. Figure 6.14 presents

Table 6.9 — Costs, waste generation and CO₂ emissions for each technique.

Technique	Cost	Waste ($\times 10^3$ m ³ /yr)	Emissions (kg CO ₂ /yr)
wet shotcrete	468	14.59	6.82
dry shotcrete	362	16.44	7.85
formed concrete	626	32.67	15.26

**Figure 6.15** — Multi-criteria prioritization of the repair techniques.

a useful scheme oriented to increase owners' awareness concerning to environmental problems. However, it illustrates the conflicting nature of these criteria and the difficulty in prioritizing.

Table 6.9 summarizes the costs, the waste generation and the CO₂ emissions for each technique. It is observed that there is no "ideal" alternative that minimizes the three criteria. The optimal values for each criterion are bold. As mentioned before, dry shotcrete is less expensive and wet shotcrete is more environmentally friendly. Consequently, the ideal objective vector for the splash and tidal zone is $\mathbf{f}^*=[362, 14.59 \times 10^3 \text{ m}^3/\text{yr}, 6.82 \text{ kg CO}_2/\text{yr}]$.

Figure 6.15 presents a multi-criteria prioritization of the repair techniques based on the MOI minimization –i.e., equation 6.9. This analysis considers the influence of the scenarios 2, 3 and 4 defined in Table 6.7. The comparison of the Euclidean MOI indicates that dry shotcrete is the most sustainable repair technique in all the cases. This behavior is most evident for the scenario 2 where economic aspects are privileged. It was found previously that wet shotcrete was the more environmentally friendly alternative. However, this technique is not the most sustainable because of its higher costs even for the scenario 4 that benefits environmental constraints. As expected, given its higher costs and environmental impact, formed concrete is the option with the worst performance. Accordingly, these results indicate that a sustainable alternative should satisfy all the different criteria.

6.6 Conclusions

- Chloride-induced corrosion has been recognized as one of the major factors affecting durability of RC structures and infrastructure. Therefore, management of RC structures should include maintenance to ensure optimal levels of safety and serviceability during the operational life. Recent studies are oriented to optimize the effectiveness and cost of maintenance

strategies. However, taking into account the higher waste generated during repair operations and the CO₂ emissions released during cement production, environmental constraints should be included in the formulation and choice of the management strategies. In this context, this chapter proposed an approach for evaluating the sustainability of repair strategies for chloride-contaminated RC structures. Sustainable development should provide a balance between economic, social and environmental aspects. Although this study focused on economic and environmental constraints, society is directly beneficed by sustainable solutions that minimize costs and environmental impact. Therefore, the proposed approach considers three criteria: (1) costs, (2) waste production and (3) CO₂ emissions.

2. The multi-objective nature of management is a major challenge for decision-making. The owner/operator is frequently confronted to problems where several criteria must be satisfied –i.e., minimization of costs, traffic disruptions, environmental impact, etc. The decision-making scheme proposed herein is based on compromise programming and aims to minimize the distance from the set of Pareto optima to an ideal solution. This decision-making tool can be used to improve the performance of a repair technique from economic and environmental points of view or to compare the sustainability of various repair techniques.
3. The final part of the chapter was devoted to illustrate the proposed methodology evaluating the sustainability of large-scale maintenance techniques of a real structure. The maintenance strategy consists of the replacement of the chloride-polluted concrete with new concrete. Three repair techniques for rebuilding of cover (wet shotcrete, dry shotcrete and formed concrete) were considered in the study. These techniques were tested on beams exposed to chlorides during 80 years to introduce real input data in the models. The proposed approach was firstly used to define a sustainable inspection interval for each repair technique. It was then implemented to compare the sustainability of the three repair techniques.

CLOSURE

Conclusions

In accordance with the main objectives of this thesis, the following conclusions have been drawn:

1. Chapter 2 presented and discussed the stages of the life-cycle of corroding RC structures as well as the methods most used in the literature to model deterioration and maintenance actions. Accordingly, there are four approaches available in the literature for management of corroding RC structures that are based on: (1) failure rate functions, (2) Markov models, (3) stochastic processes and (4) time-dependent reliability indexes. Each method has advantages and shortcomings and can be useful for a particular problem.

Taking into account the requirements defined in collaboration with stakeholders that are linked to the structure during its life-cycle in the framework of the MAREO project, this study adopts a modified Markovian approach. In such an approach, inspections are carried out by experimental measurements and aim to determine the chloride concentration at the concrete cover. Based on inspection results, the owner/operator decides whether preventive repair should be done or not. The effect of “imperfect inspections”, that can lead to “good” or “wrong” decisions, is also considered by using the decision theory.

In Markovian modeling of deterioration, the variable of interest is discretized into M states. Besides, the transitions between the M states are controlled by transition probabilities. In this problem, Markov processes are used to model chloride ingress. Therefore, the transition probabilities are computed from a physical model of chloride ingress. Chloride penetration into concrete is a complex process that can be represented by diffusion/convection principles modeled by analytical or numerical solutions of Fick’s law. Analytical solutions are useful for sensitivity analyses and use few parameters. However, its assumptions are not valid for real exposure conditions. Numerical solutions consider the effects of: (1) chloride penetration in unsaturated conditions; (2) chloride binding capacity; (3) time-dependence of temperature, humidity and surface chloride concentration; and (4) flow of chlorides in two dimensions. Although they require several parameters and are time-consuming, they are adopted herein to estimate the transition probabilities.

2. Based on the needs for deterioration modeling defined in chapter 2, this study implemented analytical and numerical solutions of the second Fick’s diffusion law. While the analytical solutions are based on error function, the numerical solution combines finite difference and finite element methods to solve the governing equations of the problem.

The model presented in this thesis is based on and combines extensive experimental studies at the different stages of the process. Moreover, the modularity of the proposed scheme has the advantage of being able to take account of new information and/or observations, either

by updating the behavior parameters, or by introducing more refined and accurate models and components.

3. As in all phenomena in nature, the chloride-induced corrosion is a random phenomenon. The main sources of uncertainty are related to: (1) material properties, (2) models and associated parameters and (3) environmental actions. The uncertainties were treated by random variables and stochastic processes. Time-invariant random variables represented the uncertainties of the material properties and the model parameters. The probabilistic models of time-invariant random variables were defined based on a literature survey. Stochastic processes described the environmental actions; thus, this study proposed stochastic models for:

- temperature and humidity (including the effect of global warming) and
- environmental chloride concentration (distinguishing between exposure to de-icing salts or sea).

The proposed model of chloride penetration was illustrated by various numerical applications. The conclusions of these examples are summarized as follows:

Factors controlling chloride ingress: the results indicate that the mean of corrosion initiation time decreases when the randomness and the seasonal variations of humidity, temperature and chloride concentration, as well as convection are considered; and increases when chloride binding is taken into account. By comparing chloride penetration in one- and two-dimensions, it has been found that high probabilities of failure correspond to 2-D exposure. These results stress on the importance of including the effects and the random nature of temperature, humidity, surface chloride concentration, chloride binding, convection and two-dimensional chloride ingress for a comprehensive lifetime assessment.

Impact of weather: the examples considered three environments –i.e., continental, oceanic and tropical. It was observed that the highest probabilities of corrosion initiation correspond to marine environments, in particular, for tropical environments. These results are explained by the facts that (1) structures placed in marine environments are exposed to chlorides all the time and (2) higher temperatures and humidities accelerate the penetration of chloride ions into the concrete matrix. The probability of corrosion initiation increases in structures close to the sea. This effect is more appreciable for the tropical environment because greater values of temperature and humidity reduce the time to corrosion initiation.

Effect of global warming: the results indicate that the lifetime reduction induced by global warming is more significant for structures located in chloride-contaminated environments far from the sea. The climate change effect is high for structures located in oceanic environments and leads to lifetime reductions ranging from 2 to 18%. These observations justify the implementation of countermeasures directed to (1) reduce and/or mitigate the action of global warming on weather and (2) minimize the impact of climate change on RC structures.

4. This study presented a stochastic method to optimize the management of RC structures subjected to chloride penetration. The selected optimization strategy is oriented to find an

interval between two consecutive inspections that (1) minimizes the costs of inspection, repair and failure and (2) ensures a given level of safety. The optimal interval is therefore determined by using stochastic processes and decision theory. The chloride penetration phenomenon is integrated into the management process by computing the transition matrix for chloride penetration from simulations.

Concerning chloride penetration model using Markov chains, it was found that to have a good representation of the phenomenon, the following consideration should be taken:

- at least three parameters per state;
- an initiation phase; and
- a discretization of ten states.

The formulated methodology was illustrated by a numerical example. The results indicate that the optimization of the performance of maintenance strategies requires:

- to optimize the repair threshold C_{rep} for a particular problem;
 - to determine an appropriate probabilistic model for the threshold chloride concentration C_{th} ; and
 - to improve the quality of the inspection technique.
5. This study presented a methodology to evaluate the sustainability of maintenance strategies used in RC structures exposed to chlorides. Three criteria are used to evaluate the sustainability of the repair techniques: costs, waste production and CO₂ emissions. Decision-making under multiple constraints is a major challenge for owners/users. Therefore, a simplified decision-making scheme based on compromise programming is proposed herein. The proposed approach is illustrated with an application to large-scale maintenance of a real structure (Agri-foodstuffs terminal wharf). The repair strategy consists of demolition of the polluted concrete and rebuilding of cover by using three techniques (wet shotcrete, dry shotcrete and formed concrete).

The proposed approach can be implemented at two levels. Namely, it can be used to improve the sustainability of the formulation of a single maintenance technique and/or it can be implemented to compare different techniques. In the first case, it was found that the consideration of environmental constraints increases the expected total annual costs is about 6% when the decision-maker gives the same weight to economical and environmental constraints. This means that including environmental constraints in decision-making does not generate larger overcharges.

By comparing the different repair techniques from the economical point of view, wet shotcrete was the cheapest alternative in all the cases. The environmental consequences of the selection of a given maintenance technique are surprising. For instance by comparing the alternatives with the best and worst environmental performance for a structural lifetime of 50 yr, it was found that the choice of wet shotcrete instead of formed concrete will reduce the waste generation by 59.4 m³ and the CO₂ emissions by 27.7 ton of CO₂. These values correspond to a volume of concrete to repair of $V_r = 65.7$ m³. Consequently, it is concluded that wet shotcrete has the most positive effect on the environment.

The comparison of the Euclidean MOI of the repair techniques indicates that dry shotcrete is most sustainable in all the cases. It was demonstrated that although wet shotcrete was the most environmentally friendly alternative, it is not the most sustainable because of its higher costs. Given its higher costs and environmental impact, formed concrete is the option with the worst performance. These results indicate that a sustainable alternative should satisfy all the different criteria.

Recommendations for future research

There are many areas in which further research is needed to improve the models of deterioration and inspection/repair developed in this thesis. These improvements include addition of other physical phenomena, improvements of the probabilistic model and use of other inspection techniques or repair criteria. The following paragraphs classify these recommendations for the *deterioration* and the *inspection/maintenance* model.

Chloride penetration model

- determination of model parameters for a wide range of concrete types and cement-based repair materials;
- formulation and implementation of a model that considers the kinematics between concrete cracking and chloride penetration;
- study of the influence of hourly, daily and weekly variations of temperature and humidity on chloride ingress;
- assessment and consideration of the correlation of material properties and climatic conditions from experimental data;
- consideration of the spatial variability of the phenomenon; and
- characterization and modeling of error propagation in the whole deterioration process.

Inspection/repair model

- updating of transition probabilities from inspection data (Bayesian approach Corotis et al. (2005)) and modeling of inspection based on NDT-tools;
- combination of preventive and corrective repair strategies during the structural lifetime to find an optimal solution in a larger time-window;
- formulation and study of the effectiveness of a management strategy that considers time-variant inspection intervals;
- integration of user costs to the analysis and computation of the optimal inspection intervals on the basis of values other than the expected costs (i.e., Schoefs et al. (2009a));
- optimization of the efficiency of the repair techniques and the repair materials; and
- consideration of the uncertainty inherent to waste generation and CO₂ emissions in the assessment of environmental impact.

APPENDIX A

RELIABILITY ANALYSIS

A.1 Time-invariant reliability analysis

Reliability methods have been conceived to take into account the uncertainty of the parameters of a given problem in terms of the failure probability of a structure. In this approach the governing parameters of the problem are modeled as random variables. Random variables can be grouped in a random vector \mathbf{X} which joint PDF of \mathbf{X} is equal to $f_{\mathbf{X}}(\mathbf{x})$. For reliability analysis, the domain of the problem \mathcal{D} is divided into the *failure domain* and the *safe domain* (Figure A.1). The failure domain \mathcal{D}_f is defined by:

$$\mathcal{D}_f = \{\mathbf{X} | g(\mathcal{M}(\mathbf{X})) \leq 0\} \quad (\text{A.1})$$

where $\mathcal{M}(\mathbf{X})$ represents the response of the system and $g(\mathcal{M}(\mathbf{X}))$ the *limit state function* of the problem. In the simplest case, $\mathcal{M}(\mathbf{X})$ is expressed as the subtraction between the resistance $\mathcal{R}(\mathbf{X})$ and the demand on the system $\mathcal{S}(\mathbf{X})$:

$$\mathcal{M}(\mathbf{X}) = \mathcal{R}(\mathbf{X}) - \mathcal{S}(\mathbf{X}) \quad (\text{A.2})$$

In reliability engineering analysis, $\mathcal{M}(\mathbf{X})$ is usually expressed in terms of displacement, strain, stress, etc. The *safety domain*, \mathcal{D}_s , is defined by:

$$\mathcal{D}_s = \{\mathbf{X} | g(\mathcal{M}(\mathbf{X})) > 0\} \quad (\text{A.3})$$

The boundary between these two domains constitutes the limit state surface –i.e., $\{g(\mathbf{X}, \mathcal{M}(\mathbf{X})) = 0\}$. By accounting for these definitions, the failure probability, p_f , is determined by:

$$p_f = P[g(\mathcal{M}(\mathbf{X})) \leq 0] = \int_{g(\mathcal{M}(\mathbf{X})) \leq 0} f_{\mathbf{X}}(\mathbf{x}) dx_1 \dots dx_n \quad (\text{A.4})$$

A.2 Time-dependent reliability analysis

In some cases, the input random variables or the response of the system can be time-dependent. Structures subjected to deterioration processes such as corrosion and fatigue are two examples of time-dependent problems. In both cases, the resistance of the material is reduced and/or there are stochastic inputs during the life cycle of the structure. Examples of these actions are:

- *Environmental actions*: wind, temperature, humidity, chloride concentration, etc.

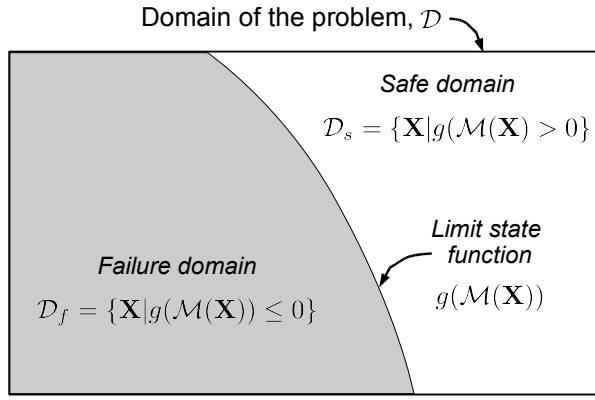


Figure A.1 — Domain of the problem for reliability analysis.

- *Operational actions:* cyclic loading induced by traffic, etc.

In these cases, the random variables become time-dependent $X(t, \omega)$ and are known as scalar random or stochastic processes. Then, at a given time t_0 , $X(t_0, \omega) \equiv X_{t_0}(\omega)$ represents a random variable. Where ω describes the *outcome*; all possible outcomes constitute the sample space Ω . Conversely, for a fixed outcome ω_0 , a sample function or trajectory is noted $x(t, \omega_0)$ or simply $x(t)$. A stochastic process is also characterized by a joint PDF of finite sets of variables $\{X_{t_1}, \dots, X_{t_n}\}$ for $t_1 < \dots < t_n \in \mathbb{R}^n$.

Time-dependent reliability analysis studies the evolution of failure probability over time. Towards this aim, the domain and sub-domains of the problem also depend on time, i.e., $\mathcal{D}(t)$. Thus, the *failure domain*, $\mathcal{D}_f(t)$ is written:

$$\mathcal{D}_f(t) = \{\mathbf{X} | g(\mathcal{M}(\mathbf{X}, t)) \leq 0\} \quad (\text{A.5})$$

where $\mathcal{M}(\mathbf{X}, t)$ and $g(\mathcal{M}(\mathbf{X}, t))$ represent the response of the system and the limit state function in time, respectively. Therefore, the time-dependent failure probability, $p_f(t)$, is computed as:

$$p_f(t) = P[g(\mathcal{M}(\mathbf{X}, t)) \leq 0] = \int_{g(\mathcal{M}(\mathbf{X}, t)) \leq 0} f_{\mathbf{X}}(\mathbf{x}, t) dx_1 \dots dx_n \quad (\text{A.6})$$

where $f_{\mathbf{X}}(\mathbf{x}, t)$ represents the time-dependent joint PDF of the problem.

A.3 Methods for reliability assessment

Explicit solutions of equations A.4 or A.6 are difficult to find in most cases. Therefore, several methods have been proposed to evaluate failure probability. Sudret & Der Kiureghian (2000) classify these methods as function of the quantities of interest as:

1. when the mean value and the standard deviation are the quantities of interest, second moment analysis methods are used. This category includes: the *perturbation method*, the *weighted integral method* and the *quadrature method*.
2. when the region of interest is situated at the tails of the joint PDF, methods of structural reliability analysis should be implemented. The most commonly used methods in this category are: FORM/SORM, *importance sampling* and *directional simulation*.

3. when analysis is focused on the whole domain, *Monte Carlo simulation* is the basic approach to solve the problem.

Given the nature of the problem and the complexity of the system (chapters 3 and 4), this study has implemented Monte Carlo simulation and Latin Hypercube sampling.

A.3.1 Monte Carlo simulation

The Monte Carlo method is based on the *law of large numbers* and is a simple technique to estimate the expected value I of a given function, G :

$$I = \int_{\mathcal{D}} G(\mathbf{x}) f_{\mathbf{x}}(\mathbf{x}) dx_1 \dots dx_M \quad (\text{A.7})$$

where \mathbf{X} is a random vector of dimension M –i.e. $\mathbf{X} = (X_1, \dots, X_M)$; $f_{\mathbf{x}}(\mathbf{x})$ is the joint PDF of \mathbf{X} ; and \mathcal{D} the domain of integration. Equation A.7 can also be expressed in terms of the expected value $E[\cdot]$:

$$I = E[\mathbf{1}_{\mathcal{D}}(\mathbf{X})G(\mathbf{X})] \quad (\text{A.8})$$

where $\mathbf{1}_{\mathcal{D}}(\mathbf{X})$ is the characteristic function of \mathcal{D} which is equal to 1 if $\mathbf{X} \in \mathcal{D}$ and 0 otherwise. The law of large numbers establishes that the mean of independent realizations converges very likely to the mathematical expectation. Based on this definition, an unbiased estimator of I , Θ , gives an approximation to the expected value of $G(\mathbf{X})$ (i.e., $\Theta \approx E[G(\mathbf{X})]$):

$$\Theta = \frac{1}{N} \sum_{i=1}^N \mathbf{1}_{\mathcal{D}}(\mathbf{X}^{(i)}) G(\mathbf{X}^{(i)}) \quad (\text{A.9})$$

where N is the number of realizations. Its variance σ^2 is defined as:

$$\sigma^2 = \frac{1}{N-1} \left[\frac{1}{N} \sum_{i=1}^N \mathbf{1}_{\mathcal{D}}(\mathbf{X}^{(i)}) G(\mathbf{X}^{(i)})^2 - \Theta^2 \right] \quad (\text{A.10})$$

It can be observed from equation A.10 that the variance tends to zero for a large number of realizations –i.e., $N \rightarrow \infty$. This means that the estimator Θ is more accurate when the number of simulations increases.

Figure A.2a shows an example where the quantity of interest is the probability of failure. In this case, the characteristic function $\mathbf{1}_{\mathcal{D}_f}(\mathbf{X})$ indicates if a simulation belongs to the failure domain and p_f is estimated from equation A.9. It can also be noted that the distribution of the points is widely spread. While there are some empty areas, several points are concentrated in other areas. Hence, it is necessary to perform a large number of simulations to ensure that the estimator is representative of the problem.

A.3.2 Latin Hypercube sampling

Latin Hypercube sampling is a method used to reduce the variance of the estimator, and consequently, the number of simulations. This technique divides the domain of each random variable into K non-overlapping sub-domains on the basis of equal probability. For each sub-domain, a value is selected randomly with respect to its probability density. This operation is repeated N/K

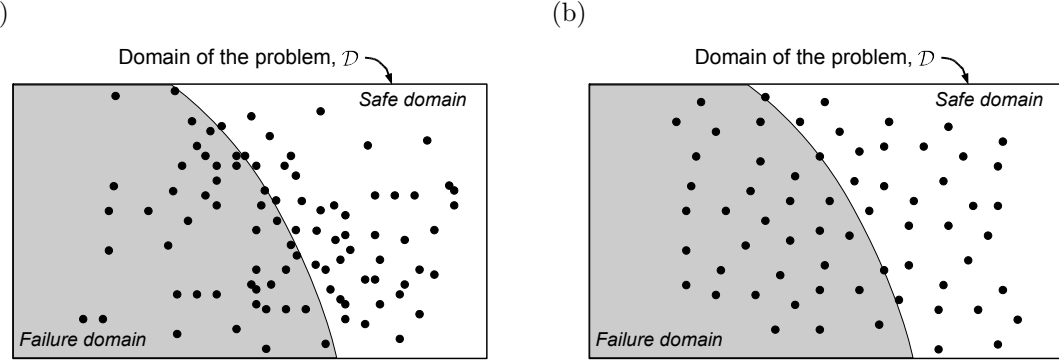


Figure A.2 — Illustration of (a) Monte Carlo simulation and (b) Latin hypercube sampling.

times. This method reduces variance by ensuring that there are realizations in each sub-domain. Thus for N simulations and K sub-domains, the estimator given by equation A.9 becomes:

$$\Theta^{LH} = \frac{1}{N} \sum_{i=1}^{N/K} \sum_{j=1}^K \mathbf{1}_{\mathcal{D}}(\mathbf{X}_j^{(i)}) G(\mathbf{X}_j^{(i)}). \quad (\text{A.11})$$

Figure A.2 compares simulations using Monte Carlo crude and Latin Hypercube sampling. Note that when Latin Hypercube sampling is implemented, the points are distributed more uniformly over the domain of the problem. Therefore, the evaluation of the expected value of the quantity of interest requires less simulations to estimate the solution.

BIBLIOGRAPHY

- A.N. Ababneh, F. Benboudjema, & Y. Xi. Chloride penetration in unsaturated concrete. *Journal of Materials in Civil Engineering ASCE*, 15:183–191, 2003.
- H. Akita, T. Fujiwara, & Y. Ozaka. A practical procedure for the analysis of moisture transfer within concrete due to drying. *Magazine of Concrete Research*, 49(179):129–137., 1997.
- C. Alonso, C. Andrade, M. Castellote, & P. Castro. Chloride threshold values to depassivate reinforcing bars embedded in a standardized OPC mortar. *Cement and Concrete Research*, 30:1047–1055, 2000.
- M.C. Alonso & M. Sánchez. Analysis of the variability of chloride threshold values in the literature. *Materials and Corrosion*, 60:631–637, 2009.
- American Institute of Architects. *Environmental Resource Guide*. Wiley, 1999.
- P. André. *L'évaluation des impacts sur l'environnement - Processus, acteurs et pratiques*. Presses internationales polytechniques, Canada, 1999.
- U. Angst, R. Elsener, C.K. Larsen, & O. Vennesland. Critical chloride content in reinforced concrete – a review. *Cement and Concrete Research*, 39:1122–1138, 2009.
- E. Ballesteros. Compromise programming: A utility-based linear-quadratic composite metric from the trade-off between achievement and balanced (non-corner) solutions. *European Journal of Operational Research*, 182:1369–1382, 2007.
- Z. Bažant & L. Najjar. Drying of concrete as a nonlinear diffusion problem. *Cement and Concrete Research*, 1:461–473, 1971.
- Z. Bažant & L. Najjar. Nonlinear water diffusion in nonsaturated concrete. *Materials and Structures*, 5(25):3–20, 1972.
- Z. Bažant & W. Thonguthai. Pore pressure and drying of concrete at high temperature. *Journal of the Engineering Mechanics Division ASCE*, 104:1059–1079, 1978.
- S. Bhide. Material usage and condition of existing bridges in the U.S. Technical Report SR342, Portland Cement Association, Skokie, Ill, 1999.
- D. Blockley. *Process re-engineering for safety*, pages 51–66. Telford, 1996.
- S. Bonnet, F. Schoefs, J. Ricardo, & M. Salta. Effect of error measurements of chloride profiles on reliability assessment. In H. Furuta, D.M. Frangopol, & M. Shinozuka, editors, *10th International Conference on Structural Safety and Reliability*, Osaka, Japan, 2009.

- S. Brunauer, J. Skalny, & E. Bodor. Adsorption in nonporous solids. *Journal of Colloid Interface Science*, 30:546–552, 1969.
- F. Casciati, I. Negri, & R. Rackwitz. Geometrical variability in structural members and systems, a critical review of available data on buildings. Technical report, JCSS working document, 1991.
- CC Technologies Laboratories Inc. Corrosion costs and preventive strategies in the United States. Technical Report FHWA-RD-01-156, Federal Highway Administration (FHWA), Office of Infrastructure Research and Development, September 2001.
- M.A. Cesare, C. Santamarina, C. Turkstra, & E.H. Vanmarcke. Modelling bridge deterioration with markov chains. *Journal of Transportation Engineering, ASCE*, 118:820–833, 1992.
- T. Chaussadent & G. Arliguie. AFREM test procedures concerning chlorides in concrete: extraction and titration methods. *Material and Structures*, 32:230—234, 1999.
- J.R. Clifton. Predicting the service life of concrete. *ACI Materials Journal*, (90):611–617, 1993.
- M. Collepardi, A. Marciallis, & R. Turriziani. Penetration of chloride ions in cement pastes and in concretes. *Journal of the American Ceramic Society*, 55(10):534–535, 1972.
- R.B. Corotis, J.H. Ellis, & M. Jiang. Modeling of risk-based inspection, maintenance and life-cycle cost with partially observable Markov decision processes. *Structure and Infrastructure Engineering*, 1:75–84, 2005.
- L. Daigle & Z. A. Lounis. Life-cycle cost analysis of high performance concrete bridges considering their environmental impacts. Technical Report NRCC-48696, Institute for Research in Construction, 2006.
- L. Duckstein. *New directions in optimum structural design*, chapter Multi-objective optimization in structural design: The model choice problem, pages 459–481. Wiley, 1984.
- F. Duprat. Reliability of rc beams under chloride-ingress. *Construction and Building Materials*, 21:1605–1616, 2007.
- Duracrete. Statistical quantification of the variables in the limit state functions. Technical report, The European Union - Brite EuRam III - Contract BRPR-CT95-0132 - Project BE95-1347/R9, 2000.
- EHE. Instrucción española del hormigón estructural, 2008.
- D.M. Frangopol. Life-cycle performance, management, and optimization of structural systems under uncertainty: Accomplishments and challenges. In H. Furuta, D.M. Frangopol, & M. Shinozuka, editors, *Safety, Reliability and Risk of Structures, Infrastructures and Engineering Systems*, pages 38–60, 2010.
- D.M. Frangopol, J.S. Kong, & E.S. Gharaibeh. Reliability-based life-cycle management of highway bridges. *Journal of Computing in Civil Engineering ASCE*, 15:27–34, 2001.
- Geocisa & the Torroja Institute. Contecvet: A validated users manual for assessing the residual service life of concrete structures. manual for assessing corrosion-affected concrete structures. annex C calculation of a representative corrosion rate. Technical Report EC Innovation Program IN309021, Geocisa and Torroja Institute, 2002.

- R.G. Ghanem & P.D. Spanos. *Stochastic Finite Elements: A Spectral Approach*. Springer, New York, USA, 1991.
- G. Glass & N. Buenfeld. The influence of the chloride binding on the chloride induced corrosion risk in reinforced concrete. *Corrosion Science*, 42(2):329–344, 2000.
- K. Golabi & R. Shepard. Pontis: A system for maintenance optimization and improvement of US bridge networks. *Interfaces*, 27:71–88, 1997.
- K. Golabi, R.B. Kulkarni, & G.B. Way. A state-wise pavement management system. *Interfaces*, 12:5–21, 1982.
- J. Grata. Road salt, hits from trucks likely led to bridge collapse. *Pittsburgh Post-Gazette*, 2005.
- A. Gut. *Probability: A Graduate Course*. Springer Texts in Statistics, 2005.
- G. Habert & N. Roussel. Comment concevoir un béton ayant un faible impact environnemental? In *XXVIème Rencontres Universitaires de Génie Civil*, Nancy, France, 2008.
- A. Haldar & S. Mahadevan. *Probability, Reliability, and Statistical Methods in Engineering Design*. John Wiley and Sons, 2000.
- S.H. Han. Influence of diffusion coefficient on chloride ion penetration of concrete structures. *Construction and Building Materials*, 21(2):370–378, 2007.
- J. Houghton. Global warming. *Reports on Progress in Physics*, 68:1343–1403, 2005.
- Husni et al. *Acciones sobre las estructuras de hormigón*, pages 39–108. Red Rehabilitar CYTED, Guarulhos, 2003.
- International Energy Agency. *Tracking Industrial Energy Efficiency and CO₂ Emissions - Energy Indicators*. OECD., Paris, 2007.
- IPCC. Climate change 2007: The physical science basis. Contribution of working group I to the fourth assessment report of the intergovernmental panel on climate change. Technical report, Intergovernmental Panel on Climate Change, Cambridge, United Kingdom and New York, NY, USA, 2007.
- Y. Itoh & T. Kitagawa. Using CO₂ emission quantities in bridge lifecycle analysis. *Engineering Structures*, 25:565–577, 2003.
- M.J. Kallen. *Markov processes for maintenance optimization of civil infrastructure in the Netherlands*. PhD thesis, Delft University of Technology, Delft, Netherlands, 2007.
- M.J. Kallen & J.M. van Noortwijk. Inspection and maintenance decisions based on imperfect inspections. In *Proceedings of the European Safety and Reliability Conference*, Maastricht, The Netherlands, 2003.
- A. Khan, W. Cook, & D. Mitchell. Thermal properties and transient thermal analysis of structural members during hydration. *ACI Materials Journal*, 95(3):293–303, 1998.
- P Kumar Mehta. Durability – critical issues for the future. *Concrete International*, 19:27–33, 1997.

- P. Kumar Mehta. High-performance, high-volume fly ash concrete for sustainable development. In *International Workshop on Sustainable Development and Concrete Technology*, pages 3–14, Beijing, 2004.
- S.P. Kuniewski, J.A.M van der Weide, & J.M. van Noortwijk. Sampling inspection for the evaluation of time-dependent reliability of deteriorating systems under imperfect defect detection. *Reliability Engineering and System Safety*, 94:1480–1490, 2009.
- Y. Liu. *Modeling the Time-to-Corrosion Cracking of the Cover Concrete in Chloride Contaminated Reinforced Concrete Structures*. PhD thesis, Virginia Polytechnic Institute and State University, Blacksburg, Virginia, 1996.
- Y. Liu & R.E. Weyers. Modeling the time-to-corrosion cracking of the cover concrete in chloride contaminated reinforced concrete structures. *ACI Materials Journal*, 95:675–681, 1998.
- Z. Lounis. *Uncertainty modeling of chloride contamination and corrosion of concrete bridges*, pages 491–511. Springer, USA, 2005.
- Z. Lounis. Risk-based maintenance optimization of aging highway bridge decks. *Advances in Engineering Structures, Mechanics and Construction*, 140:723–734, 2006.
- P. Mangat & B. Molloy. Prediction of long term chloride concentration in concrete. *Materials and Structures*, 27:338–346, 1994.
- B. Martín-Pérez. *Service life modelling of RC highway structures exposed to chlorides*. PhD thesis, University of Toronto, 1999.
- B. Martín-Pérez, S.J. Pantazopoulou, & M.D.A. Thomas. Numerical solution of mass transport equations in concrete structures. *Computers and Structures*, 79:1251–1264, 2001.
- R. McGee. Modelling of durability performance of Tasmanian bridges. In R.E. Melchers & M.G. Stewart, editors, *Applications of statistics and probability in civil engineering*, pages 297–306, Rotterdam, 2000. Balkema.
- R.E. Melchers. *Structural reliability-analysis and prediction*. Ellis Horwood Series in Civil Engineering, Chichester, 1999.
- Y. Mori & B.R. Ellingwood. Reliability-based life prediction of structures degrading due to environment and repeated loading. In M Lemaire, JL Favre, & A Mébarki, editors, *Applications of Statistics and Probability: Civil Engineering Reliability and Risk Analysis*, pages 971–976, Paris, France, 1995. Balkema.
- J.A. Mullard & M.G. Stewart. Stochastic assessment of timing and efficiency of maintenance of corroding RC structures. *Journal of Structural Engineering ASCE*, 135:887–895, 2009.
- A. Neville. *Properties of Concrete (3rd ed.)*. Longman Scientific & Technical, 1981.
- A. Neville. Chloride attack of reinforced concrete: an overview. *Materials and Structures*, 28: 63–70, 1995.
- NF EN-206. Béton—partie 1 : Spécification, performances, production et conformité, 2004.

- L.-O. Nilsson, M. Massat, & L. Tang. The effect of non-linear chloride binding on the prediction of chloride penetration into concrete structure. In V. Malhotra, editor, *Durability of Concrete, ACI SP-145*, pages 469–486, Detroit, USA, 1994. ACI.
- P. Norton, K. Vertin, B. Bailey, N.N. Clark, D.W. Lyons, S. Goguen, & J. Eberhardt. Emissions from trucks using fischer-tropsch diesel fuel. *SAE technical paper series*, 982526 SP 1391:1–10, 1998.
- C. Page, N. Short, & A. E. Tarras. Diffusion of chloride ions in hardened cement pastes. *Cement and Concrete Research*, 11(3):395–406, 1981.
- Y.Z. Pappas, P.D. Spanos, & V. Kostopoulos. Markov chains for accumulation of organic and ceramic composites. *Journal of Engineering Mechanics*, 127:915–926, 2001.
- O. Poupart, V. L'Hostis, S. Catinaud, & I. Petre-Lazar. Corrosion damage diagnosis of a reinforced concrete beam after 40 years natural exposure in marine environment. *Cement and Concrete Research*, 36:504–520, 2006.
- RILEM TC 178-TMC. Analysis of chloride content in concrete. *Material and Structures*, 35: 583–585, 2002.
- G. Roelfstra, R. Hajdin, B. Adey, & E. Brühwiler. Corrosion evolution in bridge management systems and corrosion-induced deterioration. *Journal of Bridge Engineering ASCE*, 9:268–277, 2004.
- F. Rosquoët, S. Bonnet, F Schoefs, & A. Khelidj. Chloride propagation in concrete harbor. In J. Marchand, B. Bissonnette, R. Gagné, M. Jolin, & F. Paradis, editors, *2nd International RILEM Symposium on Advances in Concrete through Science and Engineering*, Quebec, Canada, 2006. RILEM Publications.
- S.M. Ross & E.A. Pekoz. *A Second Course in Probability*. Pekozbooks, Boston, MA, 2007.
- T.J. Ross. *Fuzzy Logic with Engineering Applications*. Wiley, Chinchester, 2 edition, 2004.
- A. Rouhan & F. Schoefs. Probabilistic modeling of inspection results for offshore structures. *Structural Safety*, 25:379–399, 2003.
- A. Saetta, R. Scotta, & R. Vitaliani. Analysis of chloride diffusion into partially saturated concrete. *ACI Materials Journal*, 90(5):441–451, 1993.
- E. Samson & J. Marchand. Modeling the transport of ions in unsaturated cement-based materials. *Computers and Structures*, 85:1740–1756, 2007.
- WT Scherer & DM Glangola. Markovian models for bridge maintenance management. *Journal of Transportation Engineering*, 120:37–51, 1994.
- P. Schiessl & M. Raupach. Laboratory studies and calculations on the influence of crack width on chloride-induced corrosion of steel in concrete. *ACI Materials Journal*, 94:56–62, 1997.
- F. Schoefs. Sensitivity approach for modelling the environmental loading of marine structures through a matrix response surface. *Reliability Engineering and Systems Safety*, 93:1004–1017, 2008.

- F. Schoefs, X. Aduriz, O. Bernard, & B. Capra. Comparison of additional costs for several replacement strategies of randomly ageing reinforced concrete pipes. *Computer-Aided Civil and Infrastructure Engineering*, 24:492–508, 2009a.
- F. Schoefs, A. Clément, & A. Nouy. Assessment of spatially dependent ROC curves for inspection of random fields of defects. *Structural Safety*, 31:409–419, 2009b.
- E. Sheils. *Optimisation of inspection planning for structures*. Ph.D. Thesis, University of Dublin, Trinity College, January 2009.
- E. Sheils, A. O'Connor, D. Breysse, F. Schoefs, & S. Yotte. Development of a two stage inspection process for the assessment of deteriorating infrastructure. *Reliability Engineering and System Safety*, 95:182–194, 2010.
- M. Smithson. *Ignorance and uncertainty: emerging paradigms*. Springer-Verlag, New York, 1989.
- M. Sánchez-Silva & D.V. Rosowsky. Structural reliability and risk in the developing world and its relationship with sustainability. *ICE -- Structures*, 161:189–198, 2008.
- M.G. Stewart. Spatial variability of pitting corrosion and its influence on structural fragility and reliability of RC beams in flexure. *Structural Safety*, 26:453–470, 2004.
- M.G. Stewart & D.V. Val. Multiple limit states and expected failure costs for deteriorating RC bridges. *Journal of Bridge Engineering*, 8:405–415, 2003.
- L. Struble & J. Godfrey. How sustainable is concrete? In *International Workshop on Sustainable Development and Concrete Technology*, pages 201–211, Beijing, 2004.
- B. Sudret & A. Der Kiureghian. Stochastic finite elements and reliability – a state-of-the-art report. Technical Report UCB/SEMM-2000/08, 2000.
- L. Tang & L.O. Nilsson. Chloride binding capacity and binding isotherms of OPC pastes and mortars. *Cement and Concrete Research*, 23:247–253, 1993.
- P. Thoft-Christensen. Life-cycle cost-benefit (LCCB) analysis of bridges from a user and social point of view. *Structure and Infrastructure Engineering*, 5:49–57, 2009.
- P.D. Thompson, E.P. Small, M. Johnson, & A.R. Marshall. The pontis bridge management system. *Structural Engineering International IABSE*, 8:303–308, 1998.
- K. Tuutti. Corrosion of steel in concrete. *Swedish Cement and Concrete Institute*, 1982.
- D.V. Val. Service-life performance of RC structures made with supplementary cementitious materials in chloride-contaminated environments. In *Proceedings of the international RILEM-JCI seminar on concrete durability and service life planning*, pages 363–373, Ein-Bokek, Israel, 2006.
- D.V. Val & M.G. Stewart. Life-cycle analysis of reinforced concrete structures in marine environments. *Structural safety*, 25:343–362, 2003.
- D.V. Val & P.A. Trapper. Probabilistic evaluation of initiation time of chloride-induced corrosion. *Reliability Engineering and System Safety*, 93:364–372, 2008.

- J.M. van Noortwijk & D.M. Frangopol. *Life-Cycle Performance of Deteriorating Structures: Assessment, Design and Management*, chapter Deterioration and maintenance models for insuring safety of civil infrastructures at lowest life-cycle cost, pages 384–391. ASCE, 2004a.
- J.M. van Noortwijk & D.M. Frangopol. Two probabilistic life-cycle maintenance models for deteriorating civil infrastructures. *Probabilistic Engineering Mechanics*, 19:345–359, 2004b.
- Villain et al. Protocoles de mesures non destructives et profils en chlorure – premiers résultats de marnage accéléré sur dalles en laboratoire. Technical report, projet FUI (2007-2010) MAREO, 2010. Number 9, version 1.
- P. Vilvoisin & F. Aury. Retour d’expérience chantier de l’utilisation des produits de réparation. Technical report, projet FUI (2007-2010) MAREO, 2009. Number 4, version 1.
- K.A.T. Vu & M.G. Stewart. Structural reliability of concrete bridges including improved chloride-induced corrosion. *Structural Safety*, 22:313–333, 2000.
- K.A.T. Vu, M.G. Stewart, & J. Mullard. Corrosion-induced cracking: Experimental data and predictive models. *ACI Structural Journal*, 102:719–726, 2005.
- K.C.P. Wang & J.P. Zaniewski. 20/30 hindsight: The new pavement optimization in the Arizona state highway network. *Interfaces*, 26:77–89, 1996.
- World Commission on Environment and Development. *Our common future*. Oxford University Press, Oxford, 1987.
- Y. Xi, Z. Bažant, & H. Jennings. Moisture diffusion in cementitious materials – adsorption isotherms. *Advanced Cement Based Materials*, 1(6):248–257, 1994.
- M. Yunovich, N.G. Thompson, T. Balvanyos, & L. Lave. Corrosion costs and preventive strategies in the United States. Technical report, Office of Infrastructure Research and Development, Washington, D.C., 2001.